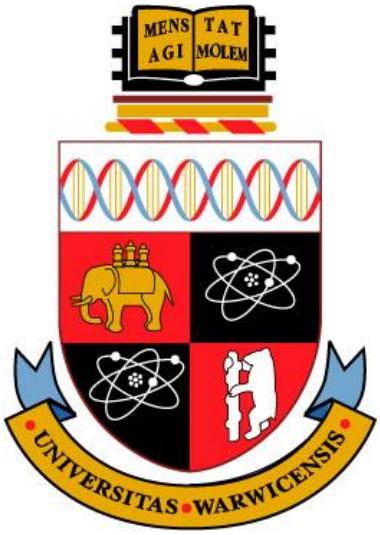

SHAPE VARIATION MODELLING, ANALYSIS AND STATISTICAL CONTROL FOR ASSEMBLY SYSTEM WITH COMPLIANT PARTS

By

Abhishek Das

A thesis submitted in partial fulfilment of the requirements for the degree of Doctor of Philosophy in Engineering

Warwick Manufacturing Group, University of Warwick,
United Kingdom, CV4 7AL

February 2016

TABLE OF CONTENTS

TABLE OF CONTENTS ..... **ii**

DEDICATION ..... **vii**

ACKNOWLEDGEMENTS ..... **viii**

DECLARATION ..... **ix**

LIST OF TABLES ..... **x**

LIST OF FIGURES ..... **xi**

LIST OF PUBLICATIONS ..... **xvii**

ABSTRACT ..... **xviii**

LIST OF SYMBOLS AND ACRONYMS ..... **xx**

CHAPTER 1 INTRODUCTION **1**

1.1 Motivation 1

1.2 Current Limitations and the Proposed Research Framework for Shape Variation Modelling, Analysis and Statistical Control 7

1.2.1 Current Limitations for Shape Variation Modelling, Analysis and Statistical Control 8

1.2.2 Proposed Research Framework for Shape Variation Modelling, Analysis and Statistical Control 11

1.3 Research Contributions 18

1.4 Organisation of the Thesis 21

CHAPTER 2 BACKGROUND **23**

2.1 Assembly Station with Compliant Parts 23

2.1.1 Assembly Key Characteristics 24

2.1.2 Input: Compliant Parts 25

2.1.3 Assembly Process Fixturing 27

2.1.4 Assembly Process Joining: Remote Laser Welding (RLW) as Case-in-Point Application 31

2.2 Measurement of Compliant Parts 33
2.2.1 Measurement Data for Quality Inspection and Reverse Engineering of Compliant Parts 36
2.2.2 Measurement Data for Monitoring and Control of Compliant Parts 38
2.2.3 Part and Assembly Measurement to Demonstrate Case Studies 42
2.3 Summary 43
CHAPTER 3 LITERATURE REVIEW 45
3.1 Introduction 45
3.2 Related Work on Shape Error Modelling of Compliant Part 47
3.2.1 Shape Error Representation 51
3.2.2 Shape Error Decomposition 53
3.3 Related Work on Shape Variation Modelling of Compliant Parts 59
3.4 Related Work on Shape Variation Monitoring and Control of Compliant Parts 65
3.5 Related Work on Assembly Fixture Layout Optimisation Considering Production Batch 71
3.6 Summary 75
CHAPTER 4 SHAPE ERROR MODELLING OF COMPLIANT PART 78
4.1 Introduction 78
4.2 Limitations of Current Decomposition Approaches 82
4.3 Geometric Modal Analysis (GMA) Methodology 85
4.3.1 Data Pre-processing 88
4.3.2 GMA-based Shape Error Decomposition 88
4.3.2.1 Voxelisation of Mesh Nodes 88
4.3.2.2 Voxel Smoothing by Laplace Interpolation 90
4.3.2.3 3D DCT Decomposition 91
4.3.3 GMA Modes Identification 91

4.3.3.1 Modes Selection or Truncation Criteria 92
4.3.3.2 Modes Magnitude Correction 94
4.4 Results of GMA with Industrial Case Studies 97
4.4.1 GMA Based Mode Decomposition 97
4.4.2 Comparison with Other Models 104
4.4.2.1 Comparison with SMA Model 104
4.4.2.2 Comparison with Natural Mode Decomposition 105
4.5 Summary 108
CHAPTER 5 SHAPE VARIATION MODELLING OF BATCH OF COMPLIANT PARTS 110
5.1 Introduction 110
5.2 Limitations of Current Approaches 113
5.3 Statistical Geometric Modal Analysis (SGMA) Methodology 115
5.3.1 GMA Based Modal Matrix 116
5.3.2 Variational Virtual Parts 119
5.3.2.1 Statistical Characterisation of Preserved Modes 119
5.3.2.2 Generation of Virtual Batch of Parts 122
5.3.3 Synthesis of Composite Parts 124
5.3.3.1 Energy Compaction Criteria (ECC) for Composite Part 125
5.3.3.2 Root Sum of Squares (RSS) Criterion for Composite Part .. 126
5.4 Results of SGMA with Industrial Case Study 128
5.4.1 Variational Virtual Door Inner Panel Generation 130
5.4.2 Synthesis of Composite Parts 131
5.5 Summary 134
CHAPTER 6 CONTROL CHARTS TO MONITOR PROCESS AND PRODUCT QUALITY SHAPES 137
6.1 Introduction 137
6.2 Problem Identification 139

6.3 Shape Monitoring Methodology 141
6.3.1 Determine T^2 and Q Statistics using GMA 142
6.3.1.1 T^2 Statistic 145
6.3.1.2 Q Statistic 145
6.3.1.3 Orthogonality of T^2 and Q Statistics 145
6.3.1.4 Estimate Confidence Region of GMA based T^2-Q Integrated Statistics 148
6.3.1.5 GMA based T^2-Q Control Chart for Shape Monitoring 149
6.4 Industrial Case Study 151
6.4.1 GMA-based T^2-Q Control Chart Development 152
6.4.2 Detection of Faulty Conditions 154
6.4.3 Comparative Analysis of GMA-Based T^2-Q Control Chart vs. PCA-Based T^2-Q Control Chart 159
6.4.3.1 In-Control Mean Shift and Variance Change Detection 160
6.4.3.2 Average Run Length (ARL) Comparison 162
6.5 Summary 163
CHAPTER 7 FIXTURE LAYOUT OPTIMISATION CONSIDERING PRODUCTION BATCH 166
7.1 Introduction 166
7.2 Problem Formulation 170
7.3 Fixture Layout Optimisation Methodology 172
7.3.1 SGMA based Composite Assembly Selection 175
7.3.1.1 Correlation Criteria Based Clustering 177
7.3.1.2 Entropy Based Assembly Selection 178
7.3.2 SGMA Based Optimisation Strategy Formulation 180
7.4 Results of Fixture Layout Optimisation with Industrial Case Study 181
7.4.1 SGMA based Composite Assembly Selection 182
7.4.1.1 Correlation Criteria Based Clustering 187

7.4.1.2 Entropy Based Assembly Selection 188
7.4.2 SGMA Based Optimisation 189
7.5 Summary 195
CHAPTER 8 CONCLUSIONS, CRITICAL REVIEW AND FUTURE SCOPE 197
8.1 Conclusions 197
8.2 Critical Review 209
8.2.1 Advantages of Proposed Methodologies 209
8.2.2 Limitations of Proposed Methodologies 212
8.3 Future Scope 213
8.4 Broader Impact 215
REFERENCES 217

DEDICATION

To my parents for their endless wishes and blessings

ACKNOWLEDGEMENTS

I would like to express my earnest gratitude to Professor Dariusz Ceglarek, for providing the opportunity to work with him for my doctoral studies. His guidance and mentoring to the right pathway of conducting research have played a significant role in my graduate life.

I would like to thank Dr. Pasquale Franciosa for his unconditional support for both technical and personal along with sharing his unbounded experience in numerous areas throughout my doctoral work. My gratitude also goes to all the past and current members of the Digital Lifecycle Management (DLM) lab of Warwick Manufacturing Group (WMG), University of Warwick, who made my stay at the DLM lab an enjoyable one.

I would like to acknowledge the support received from the European Commission funded research project ─ EU-FP7 FoF-ICT-2011.7.4: "Remote Laser Welding System Navigator for Eco &Resilient Automotive Factories" (grant agreement number 285051). I would like to thank all RLW navigator project partners for their valuable information about industrial trend and suggestions to carry out my research. I convey my sincere thanks to Mr. Charles Marine at Stadco Automotive Ltd., Mr. Anil Mistry at Jaguar & Land Rover and Mr. David Moseley at EnginSoft UK for supporting with industrial case studies, measurement data and suggestions. In addition, the co-operation and support from Mr. Selim Yilmazer, Mr. David Williams, Dr. Sumit Hazra and Dr. Iain Masters for arranging software, fixturing elements and measurement equipment, deserve special mention. I acknowledge the supports received from WMG, University of Warwick to carry out my doctoral research.

I express my warm gratitude for the care and concern, during my doctoral studies, of Arnab, Anup, Debajyoti, Debasmita, Nilanjan, Paranjayee, Supratik, Nisia, Hillol, Bramha & Manoj and for making my stay at UK delightful.

Last but not the least, I would like to mention the generous wishes and blessings of my parents, which made it possible to pursue doctoral studies and provided more that support throughout my years of education. My uncle and aunt, Brajendranath Dhar and Pali Dhar, need special mention for their unwavering support.

DECLARATION

This thesis is presented in accordance with the regulations for the degree of Doctor of Philosophy. It has been written by myself and has not been submitted in any previous application for any degree. The work in this thesis has been undertaken by me, except otherwise stated.

LIST OF TABLES

Table 3.1 Literature review of part shape error modelling approaches with identified research gap 50

Table 3.2 Major shape error decomposition approaches with applications and limitations.....58

Table 3.3 Literature review of shape variation modelling approaches with identified research gap 61

Table 3.4 Multivariate statistical process monitoring approaches and research gap for shape error related defects monitoring 68

Table 3.5 Literature review of fixture layout optimisation approaches with identified research gap 72

Table 4.1 Comparison of SMA method and proposed GMA method 83

Table 4.2 Diversified application of 2.5D DCT vs. proposed GMA (based on 3D DCT) application.....84

Table 5.1 Current shape variation modelling approaches with their applications and limitations.....114

Table 5.2 Comparative analysis between the generated composite parts and original part deviation by quantifying the average residue surface 134

Table 7.1 Composite assembly clustering and entropy based assembly selection.....188

LIST OF FIGURES

Figure 1.1 Shape variation modelling, analysis and statistical control: (a) ideal CAD model based current approach, and (b) shape variation model (non-ideal parts) based proposed research framework 12

Figure 1.2 Pictorial representation of modelling and application requirements for shape variation modelling, analysis and statistical control 17

Figure 1.3 Organisation of this thesis and research areas 21

Figure 2.1 Variation propagation from KCC to KPC in an assembly process by Ding *et al.* (2002).....25

Figure 2.2 Automotive sheet metal assembly locator types (Shiu *et al.*, 1996).....30

Figure 2.3 'N-2-1' (N=4) locating scheme for sheet metal parts (Camelio and Hu, 2004) 30

Figure 2.4 RLW requirements for tight part-to-part gap control (Ceglarek, 2011).....32

Figure 2.5 Compliant part measurement (a) using CMM at few specific sampled points, and (b) using 3D non-contact optical scanners to capture entire product surface information (i.e. CoP data).....34

Figure 2.6 Current applications vs proposed applications of CoP measurement data 35

Figure 2.7 Use of CoPs measurement data for shape error modelling, shape variation modelling and statistical process control.....40

Figure 3.1 Current PCA- or PLS-based approaches vs. the proposed GMA-based decomposition approach 67

Figure 4.1 Normal deviation calculations from nominal features to CoP.....86

Figure 4.2 Overview of GMA based shape error decomposition methodology 87

Figure 4.3 Voxelisation process: (a) nominal mesh model and deviation calculation at mesh node, and (b) bounding box computation and voxel grid mapping ($L \times M \times N$).....89

Figure 4.4 GMA-based shape error modelling steps using top hat part: (a) data pre-processing, (b) pictorial representation, and (c) actual representation.....96

Figure 4.5 Automotive door components hinge reinforcement and door inner panel as in assembly configuration.....97

Figure 4.6 Voxel grid size selection.....99

Figure 4.7 Hinge reinforcement part: (a) mesh model of hinge reinforcement (b) measured shape error from CoP, (c) voxelisation of error data (Voxel grid size = 20×20×40, used for visualization only), and (d) voxel elements containing error data only (Voxel grid size = 60×60×100) 99

Figure 4.8 GMA decomposed major shape error modes of the hinge reinforcement part.....100

Figure 4.9 Shape error (i.e. deviation plot) of the hinge reinforcement: (a) original shape error plot, (b) GMA reconstructed shape error plot, and (c) error plot between original shape error and GMA reconstructed shape error. 101

Figure 4.10 Door inner panel of automotive door: (a) nominal door part, and (b) mesh model of the part.....102

Figure 4.11 GMA decomposition of door inner panel into significant shape error modes 102

Figure 4.12 Few main shape error modes with their interpretation 103

Figure 4.13 Numerically developed rectangular shape error: (a) original shape error, and (b) reconstructed shape error using SMA and GMA methods.....105

Figure 4.14 Hinge surface deviation: (a) Original shape error, (b) Rebuild shape error using natural mode decomposition (200 modes), and (c) Rebuild shape error using GMA decomposition (200 modes).....106

Figure 4.15 Comparison of natural modes and GMA modes: (a) root sum of squares of the shape error of residue surface, and (b) standard deviation of the shape errors of residue surface 107

Figure 5.1 Overview of Statistical Geometric Modal Analysis (SGMA) method for shape variation modelling 116

Figure 5.2 GMA based modal matrix creation by using a batch of top hat parts.....119

Figure 5.3 Statistical characterisation of modal parameters using top hat parts ...121

Figure 5.4 Statistical characterisation of modal parameters using KDE 122

Figure 5.5 Generation of variational virtual parts based on statistical characterisation of modal parameters 122

Figure 5.6 Synthesis of maximum and minimum energy compacted composite parts based on top hat parts 126

Figure 5.7 Door inner panel of automotive door: (a) nominal CAD model, and (b) mesh model of the part 128

Figure 5.8 Main shape error modes identification of a batch of parts using GMA decomposition 129

Figure 5.9 Statistical characterisation of modal parameters of door inner panel by determining the probability density function (PDF) using KDE 130

Figure 5.10 Silhouettes graph plot for (a) 2 clusters; (b) 3 clusters; (c) 4 clusters; and (d) 5 clusters 131

Figure 5.11 Synthesis of composite parts (deviation in mm) for three clusters based on (a) maximum energy compaction, (b) minimum energy compaction, and (c) root sum of squares criterion 132

Figure 5.12 Average residue surface plot by using maximum, minimum and RSS based composite parts (deviation in mm) 133

Figure 6.1 Overview of shape monitoring methodology driven by GMA method 142

Figure 6.2 Increased sensitivity of control chart by joint T^2- Q statistics 150

Figure 6.3 Hinge reinforcement part of automotive door: (a) original shape error computed from CoP, and (b) decomposed shape error modes (LVs) 152

Figure 6.4 Joint probability density function (PDF) of integrated T^2-Q statistics for hinge reinforcement part 153

Figure 6.5 2D plot of confidence regions estimation with 95% and 99% confidence intervals of integrated T^2-Q statistics 153

Figure 6.6 Control chart operating characteristics behaviour with changing global mean shift 155

Figure 6.7 Product data with global mean shifts of (a) 0.1 mm, and (b) 0.15 mm at 95% and 99% confidence interval 156

Figure 6.8 Univariate chart (log scale) on joint analysis of T^2 and Q statistics for global mean shift of hinge reinforcement parts 157

Figure 6.9 Product shape error with localised part deformation by 1.0 mm 158

Figure 6.10 T^2-Q control chart for locally deformed hinge reinforcement parts 158

Figure 6.11 Univariate chart (log scale) on joint analysis of T^2 - Q statistics for locally deformed hinge reinforcement parts 159

Figure 6.12 GMA-based T^2-Q control chart plot considering mean shift and variance induced data sets 161

Figure 6.13 PCA-based T^2-Q control chart plot considering mean shift and variance induced data sets 161

Figure 6.14 ARL comparison between PCA-based and GMA-based T^2-Q control chart: (a) global mean shift, and (b) local deformation 162

Figure 7.1 Schematic representation of the KPC and KCC locations: (a) the KCC (clamp) movement from start to end point in the design space, (b) cross sectional view of part-to-part interactions along with KPC and KCC, and (c) KPC lengthwise part-to-part gap distribution with upper specification limit to satisfy the KPC quality criteria 172

Figure 7.2 Overview of fixture design optimisation considering production batch of sheet metal parts 174

Figure 7.3 Overview of optimisation framework with objective function.....181

Figure 7.4 Door inner panel and hinge reinforcement assembly configuration....182

Figure 7.5 Synthesis of composite parts (deviation in mm) for hinge reinforcement component using SGMA methodology.....183

Figure 7.6 Map Index (*MI*) for composite parts of hinge cluster 2 and individual hinge parts belong to the cluster assembled with nominal door inner component.....184

Figure 7.7 Synthesis of composite parts (deviation in mm) for door inner component using SGMA methodology 185

Figure 7.8 Map Index (*MI*) for composite parts of door inner cluster 1 and individual door inner parts belong to the cluster assembled with nominal hinge component.....186

Figure 7.9 Map Index (*MI*) for composite assemblies of inner cluster 1 and hinge cluster 2 with 30 randomly generated variation hinge-inner assemblies 186

Figure 7.10 Probability of joining feasibility index plot (surrogate model) for selected composite assemblies (a) with respect to KCC_1 and KCC_2, and (b) with respect to KCC_4 and KCC_5.....191

Figure 7.11 Hinge reinforcement and door inner panel composite assembly: (a) initial clamp layout, (b) optimised clamp layout, (c) clamp movement, and (d) optimised clamp location values 192

Figure 7.12 Map Index (*MI*) at optimised clamp location for selected composite assemblies (*SCA*).....193

Figure 7.13 Map index (*MI*) for 50 Monte-Carlo based assemblies at optimised clamp location.....194

LIST OF PUBLICATIONS

1. Das, A., Franciosa, P., Prakash, P.K.S., Ceglarek, D., 2014, "Transfer Function of Assembly Process with Compliant Non-ideal Parts", *Procedia CIRP*, 21**,** 177-182.
2. Franciosa, P., Das, A., Ceglarek, D., Bolognese, L., Marine, C., Mistry, A., 2014, "Design Synthesis Methodology for Dimensional Management of Assembly Process with Compliant non-Ideal Parts", *2014 International Joint Conference on Mechanical, Design Engineering & Advanced Manufacturing*, June 18-20, Toulouse, France.

   This paper received ***BEST PAPER AWARD*** at the *2014 International Joint Conference on Mechanical, Design Engineering and Advanced Manufacturin*g held in Toulouse, France. A total of 95 papers were presented during the conference.

   The Best Student Poster award at the 2013 British Computer Society (BCS) University Challenge for poster titled: "RLW Navigator: Software Architecture and Multidisciplinary Optimisation for Embedding New Production Processes."
3. Das, A., Franciosa, P., & Ceglarek, D., 2016, "Geometric Modal Analysis (GMA) for Shape Error Modeling and Analysis in Manufacturing", to be submitted to *IEEE Transaction on Industrial Informatics*.
4. Das, A., Franciosa, P., & Ceglarek, D., 2016, "Statistical Geometric Modal Analysis (SGMA) for Shape Variation Modeling and Analysis in Manufacturing", to be submitted to *IEEE Transaction on Industrial Informatics*.
5. Das, A., Franciosa, P., & Ceglarek, D., 2016, "Using Control Charts to Monitor Process and Product Quality Shapes", to be submitted to *IEEE Transaction on Industrial Informatics*.
6. Das, A., Franciosa, P., & Ceglarek, D., 2015, "Fixture Layout Optimisation Considering Production Batch of Compliant Non-Ideal Sheet Metal Parts", *Procedia Manufacturing*, 1**,** 157-168.

   This conference paper has been extended to journal version for submission to the *Journal of Manufacturing Systems*.

ABSTRACT

Modern competitive market demands frequent change in product variety, increased production volume and shorten product/process change over time. These market requirements point towards development of key enabling technologies (KETs) to shorten product and process development cycle, improved production quality and reduced time-to-launch. One of the critical prerequisite to develop the aforementioned KETs is efficient and accurate modelling of product and process dimensional errors. It is especially critical for assembly processes with compliant parts as used in automotive body, appliance or wing and fuselage assemblies. Currently, the assembly process is designed under the assumption of ideal (nominal) products and then check by using variation simulation analysis (VSA). However, the VSA simulations are oversimplified as they are unable to accurately model or predict the effects of geometric and dimensional variations of compliant parts, as well as variations of key characteristics related to fixturing and joining process.

This results in product failures and/or reduced quality due to un-modelled interactions in assembly process. Therefore, modelling and prediction of the geometric *shape errors* of complex sheet metal parts are of tremendous importance for many industrial applications. Further, as production yield and product quality are determined for production volume of real parts, thus not only shape errors but also *shape variation* model is required for robust assembly system development. Currently, parts shape variation can be measured during production by using recently introduced non-contact gauges which are fast, in-line and can capture entire part surface information. However, current applications of non-contact scanners are limited to single part inspection or reverse engineering applications and cannot be used for monitoring and statistical process control of shape variation. Further, the product shape variation can be reduced through appropriate assembly fixture design. Current approaches for assembly fixture design seldom consider shape variation of production parts during assembly process which result in poor quality and yield.

To address the aforementioned challenges, this thesis proposes the following two enablers focused on modelling of *shape errors* and *shape variation* of compliant parts applicable during assembly process design phase as well as production phase: (i) modelling and characterisation of *shape errors* of individual compliant part with capabilities to quantify fabrication errors at *part level*; and (ii) modelling and characterisation of *shape variation* of a batch of compliant parts with capabilities to quantify the shape variation at *production level*.

The *first* enabler focuses on *shape errors* modelling and characterisation which includes developing a *functional data analysis* model for identification and characterisation of real part shape errors that can link design (CAD model) with manufacturing (shape errors). A new functional data analysis model, named Geometric Modal Analysis (GMA), is proposed to extract dominant shape error

modes from the fabricated part measurement data. This model is used to decompose shape errors of 3D sheet metal part into orthogonal shape error modes which can be used for product and process interactions. Further, the enabler can be used for statistical process control to monitor shape quality; fabrication process mapping and diagnosis; geometric dimensioning and tolerancing simulation with free form shape errors; or compact storage of shape information.

The *second* enabler aims to model and characterise *shape variation* of a batch of compliant parts by extending the GMA approach. The developed functional model called Statistical Geometric Modal Analysis (SGMA) represents the statistical shape variation through modal characteristics and quantifies shape variation of a batch of sheet metal parts a single or a few composite parts. The composite part(s) represent major error modes induced by the production process. The SGMA model, further, can be utilised for assembly fixture optimisation, tolerance analysis and synthesis.

Further, these two enablers can be applied for monitoring and reduction of shape variation from assembly process by developing: (a) efficient statistical process control technique (based on enabler 'i') to monitor part shape variation utilising the surface information captured using non-contact scanners; and (b) efficient assembly fixture layout optimisation technique (based on enabler 'ii') to obtain improved quality products considering shape variation of production parts. Therefore, this thesis proposes the following two applications:

The *first* application focuses on statistical process control of part shape variation using surface data captured by in-process or off-line scanners as Cloud-of-Points (CoPs). The methodology involves obtaining reduced set of statistically uncorrelated and independent variables from CoPs (utilising GMA method) which are then used to develop integrated single bivariate T^2-Q monitoring chart. The joint probability density estimation using non-parametric Kernel Density Estimator (KDE) has enhanced sensitivity to detect part shape variation. The control chart helps speedy detection of part shape errors including global or local shape defects.

The *second* application determines optimal fixture layout considering production batch of compliant sheet metal parts. Fixtures control the position and orientation of parts in an assembly process and thus significantly contribute to process capability that determines production yield and product quality. A new approach is proposed to improve the probability of joining feasibility index by determining an N-2-1 fixture layout optimised for a production batch. The SGMA method has been utilised for fixture layout optimisation considering a batch of compliant sheet metal parts.

All the above developed methodologies have been validated and verified with industrial case studies of automotive sheet metal door assembly process. Further, they are compared with state-of-the-art methodologies to highlight the boarder impact of the research work to meet the increasing market requirements such as improved in-line quality and increased productivity.

LIST OF SYMBOLS AND ACRONYMS

GD&T	Geometric Dimensioning and Tolerancing
CAD	Computer-Aided Design
CoP	Cloud-of-Points
KPCs	Key Product Characteristics
KCCs	Key Control Characteristics
RLW	Remote Laser Welding
FEM	Finite Element Method
GMA	Geometric Modal Analysis
SGMA	Statistical Geometric Modal Analysis
3D DCT	Three-Dimensional Discrete Cosine Transform
3D IDCT	Three-Dimensional Inverse Discrete Cosine Transform
SMA	Statistical Modal Analysis
FEA	Finite Element Analysis
RSS	Root Sum of Squares
SD	Standard Deviation
SPC	Statistical Process Control
KDE	Kernel Density Estimator
PDF	Probability Density Function
CMM	Coordinate Measuring Machine
RE	Reverse Engineering
LVs	Latent Variables
PCA	Principal Component Analysis
ARL	Average Run Length
VRM	Variation Response Method

$f(x,y,z)$	Deviation at a coordinate of *(x,y,z)*
$g(x,y,z,u,v,w)$	A forward transformation kernel
$h(x,y,z,u,v,w)$	An inverse transformation kernel
$T(u,v,w)$	A transformation coefficient
N_n	Number of mesh node coordinates *(x,y,z)*
D_n	Deviation vector at mesh node N_n
$L \times M \times N$	Voxel grid size
f(i,j,k)	Voxel element deviation in voxel space at *(i,j,k)*
$C(u,v,w)$	3D DCT coefficient vector
E	Energy compaction threshold
Ω_e	Coefficient index set after energy compaction
ρ_q	Correlation coefficient of q^{th} coefficient
T_q	Mesh node deviations associated with q^{th} coefficient
α	Threshold for correlation criteria based coefficient selection
Ω_c	Coefficient index set after correlation threshold
Ω	Truncated coefficient index set
wt_q	Least squares based weightage associated with q^{th} coefficient
ε	Residue error vector
$\tilde{C}(u,v,w)$	Truncated coefficient vector
$\tilde{f}(i,j,k)$	Deviation after reconstruction of surface
X	Set of orthogonal shape vectors
b	Magnitudes of truncated coefficients
m	Sample size of a batch of parts
β	Modal parameters set

p	Number of preserved modes
wt	Weightage vector for modes
N_v	Number of virtual parts generated
K	Kernel function
$\hat{F}(\tilde{C},h)$	Kernel density estimator function
h	Bandwidth or smoothing parameter of KDE
R	Number of cluster
$E_{\tilde{C}_{pr}}$	Energy compaction index
$(E_{\tilde{C}_p})_{\max}$	Maximum energy compaction index
$(E_{\tilde{C}_p})_{\min}$	Minimum energy compaction index
$\beta_{\max}$	Modal parameters set for maximum energy compacted part
$\beta_{\min}$	Modal parameters set for minimum energy compacted part
D_{RSS}	Optimal mesh node deviation after root sum of squares error
β_{LS}	Modal parameters set for RSS criteria based composite part
q	Number of modes selected per part
T_k^2	T^2 statistic for k^{th} instance
Q_k	Residual statistic for k^{th} instance
C_L, C_M, C_N	Cosine basis transform matrices
$\times_L, \times_M, \times_N$	Matrix product operator
N	Number of primary datum plane locators
N_{st}	Number of stitches (i.e. KPCs)
p	Probability of joining feasibility index
PT_m	Number of different types of parts in assembly

$CPT_{m,max}$	Maximum energy compacted composite part of part id m
$CPT_{m,min}$	Minimum energy compacted composite part of part id m
$CPT_{m,avg}$	Average energy compacted composite part of part id m
CPT_{MAX}	Set of maximum composite parts in the assembly
CPT_{MIN}	Set of minimum composite parts in the assembly
CPT_{AVG}	Set of average composite parts in the assembly
CA	Set of Composite Assembly
$MI_{i,j}$	Map Index of i^{th} KPC of j^{th} composite assembly
TMI_j	Total Map Index of j^{th} composite assembly
$\rho_{j,k}$	Correlation coefficient between j^{th} and k^{th} assemblies
N_{cl}	Number of clusters of composite assemblies
$I_{i,j}$	Information (I) contained on the i^{th} MI of j^{th} assembly
$p_{i,j}$	Probability of satisfying the joining requirements of $MI_{i,j}$
H_j	Entropy of j^{th} complete assembly
SCA	Selected Composite Assembly

CHAPTER 1 **INTRODUCTION**

1.1 MOTIVATION

Global competitive market with increasing customer preferences requires newly designed quality products with enhanced features and functionality. Faster design, manufacturing or quality checks of these products are not trivial tasks; especially with higher product quality and shorter lead time to develop the product. For example, manufacturers need to introduce product variety with increased production volume, reduction in cost, and time-to-launch (or time-to-market). These market requirements lead to key technological challenges, such as, in-process production quality improvement, reduction in product and process development cycle, and early detection of detects etc. These key technological challenges are to be satisfied. The fabrication and assembly of compliant/deformable sheet metal parts are one of the key areas where the technological challenges are to be addressed. Sheet metal parts are prone to various dimensional and geometric quality defects due to their intrinsic nature. As a consequence, assembly processes involving sheet metal parts are critical to avoid product defects or part fit-ups errors during assembly. To facilitate ease of assembly and achieve better product quality, there are needs for simulation models which can depict the product and process behaviours considering uncertainties (i.e. process variation) associated with the manufacturing process. Therefore, assembly process requires attention to develop such simulation models to reduce product/process variation.

Three dimensional compliant sheet metal parts [also under the category of '*freeform shaped parts*' (Savio *et al.*, 2007)] are extensively used for many industrial applications such as automotive body, aerospace wing /fuselage or home appliances. One of the key challenges to deal with compliant sheet metal parts is conforming to the dimensional and geometric quality as defined by geometric dimensioning and tolerancing (GD&T) during design phase. Further, dimensional and geometric/shape variations of sheet metal assemblies play a vital role to achieve final product quality. Previous studies have reported that the presence of shape variation in sheet metal parts contributes up to two third of the engineering changes in automotive body and aircraft fuselage assembly (Ceglarek and Shi, 1995; Shalon *et al.*, 1992). Therefore, part shape management and shape variation control through modelling are inevitable prerequisite for assembly process simulation with compliant parts. The assembly process simulation with shape variation reduces the occurrence of defects during manufacturing and product usage. Therefore, shape variation modelling, analysis and control could be the key enabling technologies (KETs) to put manufacturer at the forefront of the competitive market by improving product quality, shortening product development time and detecting failures at early stage of assembly process.

Currently, assembly process is designed under the assumption of ideal part which is being assembled under ideal process conditions. Thereafter, variation simulations are performed by using variation simulation analysis (VSA) which are oversimplified and are unable to depict the real production scenario. Further, they fail to model or predict the effects of geometric and dimensional variations of compliant sheet metal parts during joining or assembly processes. To understand the product and process variations and their characteristics, it is necessary to understand the geometric and dimensional errors associated with the real production parts which are far from the

ideal part assumption. Therefore, there is an urgent need for geometric *shape errors* modelling of compliant sheet metal parts for many industrial applications. Further, a batch of sheet metal parts, produced by forming processes (such as stamping), are not geometrically and dimensionally identical. As a result, their characteristics also vary during fixturing or joining processes and produce lower quality product and reduced production yield. Therefore, for robust assembly system development with compliant sheet metal parts, not only shape error modelling is important but also *shape variation* modelling is equally important. Thus, modelling and characterisation of shape variation help to identify the process behaviours for better production quality and yield.

However, traditional assembly process simulation exhibits shortcomings to address the aforementioned *shape errors* and *shape variation* modelling requirements in the following way:

i. *Shape errors modelling of real part (real part also called in this thesis as non-ideal or non-nominal part)*: The assembly process simulation must be supported with real part model where dimensional and geometric shape errors are taken into consideration. Most of the works related to sheet metal part modelling and tolerance synthesis are based on the assumption of ideal rigid parts/sub-assemblies (Shen *et al.*, 2005). On the contrary, sheet metal parts are compliant in nature which cannot be modelled as rigid body as it poses substantial limitations towards the analysis and output results. It has been reported that one third of automotive body parts and subassemblies cannot be modelled as rigid parts (Shiu *et al.*, 1997). Camelio *et al.* (2004a) demonstrated that part error, tooling error, and assembly spring-back have significant impact on the quality of assembly. Therefore, part shape error

embedded compliant sheet metal modelling is necessary to reveal the un-modelled interactions with fixture and joining processes during assembly for more accurate assembly process simulation. Hence, many industrial applications have tremendous need for efficient modelling of *shape errors* of 3D freeform shaped part.

ii. *Shape variation modelling of a batch of real parts (batch of real parts also called in this thesis as non-ideal production parts)*: Sheet metal parts, produced by plastic deformation during forming processes such as stamping, consist of shape errors which are varying from part-to-part (i.e. production parts consist of *shape variation)*. The main causes of shape variation are due to variation in fabrication process, tooling and material. For example, sheet metal stamping process shows variation of key control characteristics such as press tonnage, shut height, press parallelism (Zhou and Cao, 1994) as well as spring back problem, tool wear, material thickness variation, uneven load distribution or variation caused by part handling, etc. (Ceglarek *et al.*, 2001). Further, a batch of sheet metal parts consists of various shape error patterns with changing magnitude of those shape error patterns. Subsequently, modelling and prediction of *shape errors* associated with individual non-ideal part is not sufficient to meet current industrial needs. It emphasises to quantify the *shape variation* engraved within a batch of parts. Therefore, shape variation modelling of batch of parts is required to quantify accurately the *non-ideal production parts* during assembly process simulation.

As evident from the aforementioned discussions, the assembly process must be supported with the two key enablers: *(i) shape error model*, and *(ii) shape variation model*. These models are particularly important not only for increasing product

performance and functionality, but also for manufacturability and ease of assembly. Shape variation also directly impacts on the perceived product quality, and is a critical quality measure of the final product. Further, these two enablers can be utilised for shape variation monitoring and reduction from the assembly process by developing: (a) statistical process control chart (based on enabler *'i'*) to monitor part shape variation and detect part shape errors related faults from the assembly process; and (b) efficient assembly fixture layout optimisation technique (based on enabler *'ii'*) to obtain improved quality products considering shape variation of production parts. However, traditional statistical process control charts and assembly process simulation with batch of non-ideal compliant parts exhibits shortcomings to address the aforementioned application requirements in the following way:

a. *Statistical process control of part shape errors and detection of shape errors related faults to improve assembly process quality*: As shape errors of manufactured parts or assembled products represent the important aspect of quality, the shape errors related defects must be monitored and detected. Currently, shape errors related faults can be quickly inspected by measurement scanners which have capability to conduct non-contact measurement of entire part surface and generate measurement information in the form of Cloud-of-Points (CoPs). These surface based non-contact measurement scanners based on white light or laser are also frequently used in industries. It has been demonstrated that these scanners are very efficient in capturing part surface data and also have potential to be utilised for both off-line (i.e. gauge is in separate measurement area away from production line) as well as in-line (i.e. gauge being embedded directly as part of production line) applications (Reinhart and Tekouo, 2009). However, current

use of the non-contact scanners is limited to: (a) part inspection, i.e. comparing the measured part with Computer Aided Design (CAD) model of the part (ideal part); or (b) reverse engineering applications, i.e. generating CAD model of a given part by using the measurement data (Son *et al.*, 2002). However, recent advances in fast speed of capturing part surface data during off-line or in-line measurement expand the opportunities of surface scanner to be used for part surface quality monitoring and shape defects detection. To monitor the pre- and post- assembly product quality, there is a strong need for statistical process control method to efficiently and effectively monitor quality of non-linear shapes using CoP data.

b. *Assembly process simulation for assembly fixture layout optimisation considering production shape variation to improve production yield*: Shape variation of production parts coupled with compliant nature exhibits variation in output assembly quality and it is not trivial to obtain uniform quality during assembly operation. As a consequence, the individual part shape error model is not sufficient to predict production quality. In order to reduce production quality variation, it is important to simulate the assembly process taking into consideration of batch of parts *shape variation*. Further, to satisfy the product GD&T requirements during the assembly process, shape variation needs to be taken into consideration upfront during jig or fixture design. As production yield and product quality are determined based on a production volume of real (non-ideal) parts, shape variation model is required to be considered during assembly process simulation. Therefore, assembly process must be supported with design of production fixtures considering production shape variation.

1.2 CURRENT LIMITATIONS AND THE PROPOSED RESEARCH FRAMEWORK FOR SHAPE VARIATION MODELLING, ANALYSIS AND STATISTICAL CONTROL

Modelling, Analysis and statistical control of shape variation of compliant sheet metal parts are not trivial tasks as they involve freeform 3D shapes (i.e. 3D shapes having irregular contours, edges, holes, slots etc.), non-functional data (i.e. CoP measurement can be categorised as non-functional data as it cannot be used directly), extraction of shape error patterns from the CoP data (i.e. functional data analysis based approach is required to extract useful information from the CoP measurement). For efficient modelling and analysis of assembly system with compliant parts, compact and accurate functional data analysis based approaches are required to model and characterise (i) *the shape errors of individual compliant part, and* (ii) *the shape variation of a batch of compliant parts.* Further, these two enablers help to extend the current application of 3D non-contact scanners from (a) *part inspection to statistical process control* - to overcome the limitation associated with the use of 3D non-contact scanners for shape monitoring, and (b) *reverse engineering to design optimisation* - to extend the current practice of design optimisation from individual part shape errors based approach to production shape variation based approach. Therefore, modelling and characterisation of part shape errors and production shape variation as mentioned in (i) and (ii) are crucial to monitor process behaviour as in (a) and optimise the process with batch of compliant parts as in (b).

To address the modelling requirements, this thesis, *firstly*, identifies the current limitations associated with shape variation modelling, analysis and statistical control (in Section 1.2.1); and, *secondly*, proposes research framework for shape variation modelling, analysis and statistical control (in Section 1.2.2).

1.2.1 Current Limitations for Shape Variation Modelling, Analysis and Statistical Control

Attempts have been made to model the shape error of compliant sheet metal part and shape variation of batch of compliant sheet metal parts. However, the current available techniques raise major limitations, to address the *shape error* and *shape variation* modelling requirements, and subsequently, shape variation monitoring by using statistical process control charts and shape variation reduction by assembly fixture layout optimisation, in the following way:

(i) Limitations to model shape error of compliant sheet metal part: Current shape error modelling approaches can be categorised into: (a) shape error representation – the measured CoP data is mapped with nominal CAD data to represent shape error by obtaining the deviation field (Gupta and Turner, 1993; Sorkine, 2006; Franciosa *et al.*, 2011; Wagersten *et al.*, 2014); and (b) shape error decomposition – to understand and establish the relationship between part shape error and the source of variation, the shape error is required to be decomposed into a series of independent shape error modes (Tonks, 2002; Huang and Ceglarek, 2002; Samper and Formosa, 2006; Huang *et al.*, 2014). To address shape error modelling as an enabler for shape variation monitoring or shape variation reduction, the current available techniques have the following limitations:

- To provide a generic model with capabilities to extract underlying process information from measured CoP data.
- To support assembly process simulation related tasks (such as design synthesis, tolerance allocation or root cause analysis based faults identification, or statistical process control with CoP data) which can

provide a parametric relation between nominal data (i.e. CAD data) and measured data (i.e. CoP data).

- To provide an approach to decompose shape error (measured CoP data) of 3D freeform shaped part into orthogonal shape error modes.

Due to these limitations, a universal functional data analysis based model is required to express shape error of 3D freeform shaped part in a coherent manner by integrating nominal features (ideal/nominal shape information) with manufacturing variability (real shape information).

(ii) Limitations to model shape variation of batch of compliant sheet metal parts:

In assembly process, production shape variation plays significant role to achieve quality results. To address the production shape variation, current methods have following assumptions and limitations:

- The extracted shape error modes based on shape error decomposition approaches (Samper *et al.*, 2009; Huang *et al.*, 2014) are normally distributed. However, real complex process, such as sheet metal stamping, seldom adheres with it as stamping process exhibits variance shift or mean shift during within batch or batch-to-batch production.
- Data-driven approach, such as Principle Component Analysis (Camelio *et al.*, 2004b), used for shape variation modelling ignores the underlying production behaviour of identifying process mean shift or variance shift in measured data set (Matuszyk *et al.*, 2010).
- These methods are limited to virtual generation of production parts and there is no specific approach available which can quantify shape variation of a batch of parts.

Due to the aforementioned assumptions and limitations, an effective shape variation characterisation and quantification technique is necessary.

(iii) Limitations to monitor part shape variation and fast detection of shape error related faults: Available monitoring techniques are mainly limited to point feature based control (Chen *et al.*, 2004; Antory, 2007; Phaladiganon *et al.*, 2013) or profile feature based control (Jin and Shi, 2001; Woodall *et al.*, 2004; Colosimo and Pacella, 2007) and they are not able to cope with high dimensional CoP data to monitor non-linear shapes. Current monitoring and statistical control techniques are mainly suffering from:

- Monitoring of shape variation, as point feature or profile feature based control charts do not reveal all types of shape related errors.
- Extracting all the underlying shape error related information from the captured CoP data as currently used data dimensionality reduction techniques, such as Principal Component Analysis (PCA) or Partial Least Squares (PLS) are not suitable for shape error characterisation.
- Normality assumption of the measurement data which is a strong assumption for real fabrication process and it might cause problem for fast detection of faults.

Due to the aforementioned limitations, a proactive shape monitoring technique is necessary which can detect shape related faults using CoP data.

(iv) Limitations to reduce product shape variation by using assembly fixture to improve production yield and product quality: The production yield and product quality are affected by shape variation and large number of *Key Control Characteristics* (*KCCs* - such as clamps, NC blocks, locators). The

current assembly fixture design does not consider production shape variation during assembly process simulation and exhibits lack of capability to model *Key Product Characteristics* (*KPCs*- such as part-to-part gap, joining requirements) with respect to large number of KCCs. They are mainly lacking the following:

- Assembly fixture layout optimisation considering production shape variation to improve product quality and production yield.
- Consideration of high dimensional design space, due to number of parts to be assembled in an assembly station and large number of KCCs, to achieve required product quality.
- Identifying the highly non-linear relationship between KPCs and KCCs to improve fixture design.

Due to the aforementioned issues and limitations, an assembly fixture layout optimisation technique is required considering production shape variation in order to improve joining quality and eventually the production yield.

As evident from the abovementioned limitations presented in this section, new models and methods are required for modelling shape error and shape variation, and subsequently, statistical process control to monitor shape variation and process design to reduce shape variation.

1.2.2 Proposed Research Framework for Shape Variation Modelling, Analysis and Statistical Control

Ideal CAD model based simulation is not sufficient as it represents the ideal features and geometry of the part. The ideal part model is essential during designing of assembly system as it provides vital information about ideal characteristics of the

system. On the contrary, real fabricated parts are not ideal and their behaviour varies with the type of errors contained within it. Therefore, CAD based ideal part is not sufficient to represent the shape errors associated with the real parts (i.e. *non-ideal parts*). Figure 1.1(a) depicts the current approach for statistical process control and fixture analysis which are mainly based on the ideal CAD model. Further, ideal part based process control fails to monitor part shape variation and fast detection of shape errors related faults. Similarly, ideal part based variation simulation analysis has limited capability to reduce product shape variation during assembly operation.

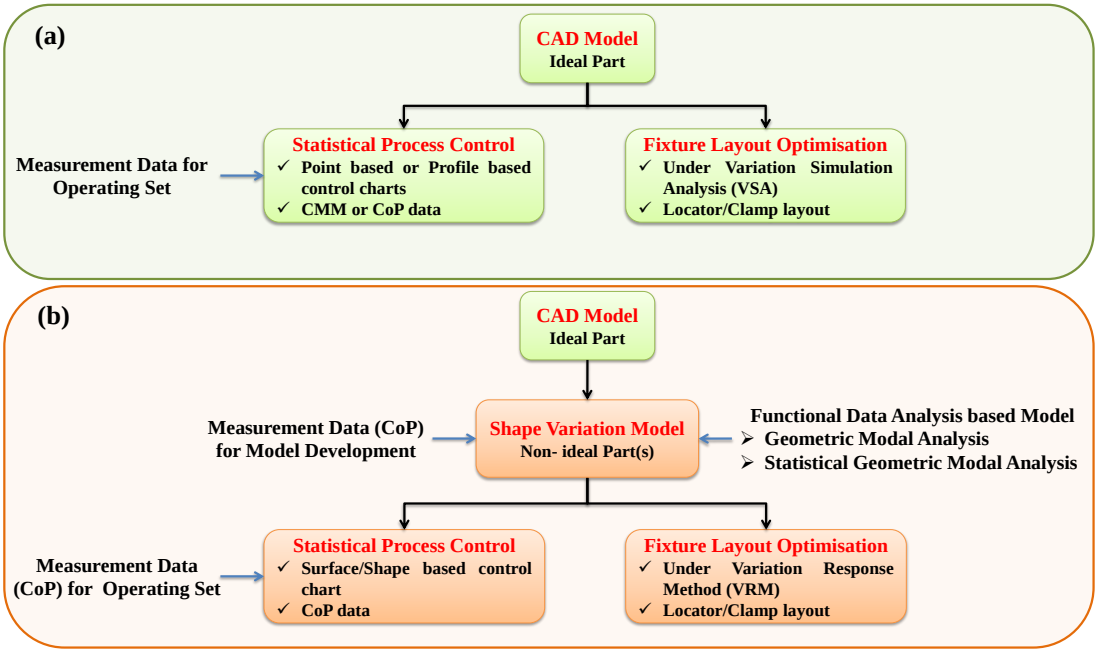

Figure 1.1 Shape variation modelling, analysis and statistical control: (a) ideal CAD model based current approach, and (b) shape variation model (non-ideal parts) based proposed research framework

The proposed research framework for shape variation modelling, analysis and statistical control is shown in Figure 1.1(b) where, *firstly*, shape variation models are developed to represent non-ideal part(s), *thereafter*, statistical process control and fixture analysis are carried out to monitor and reduce shape variation from the assembly process.

In the context of shape variation modelling, analysis and statistical control, this thesis defines the following research objectives:

(i) *To model and characterise shape errors of individual compliant part:* a functional data analysis based shape error model which characterises and quantifies the measured 3D free-form shape error of sheet metal part by decomposing into significant shape error modes.

(ii) *To model and characterise shape variation of a batch of compliant parts:* an extension of the part shape error model, to characterise shape variation of a batch of parts by identifying the significant shape error modes [*research objective (i)*] and quantifying them by means of its identified magnitude.

(iii) *To detect the shape error related defects from assembly process:* an application based extension of shape error model [*research objective (i)*] to develop a Multivariate Statistical Process Control (MSPC) approach for detecting shape error related faults which has ability to process multi-dimensional CoP data for monitoring non-linear shapes.

(iv) *To optimise assembly fixture layout considering production batch:* an application based extension of shape variation model [*research objective (ii)*] to develop a robust fixture layout optimisation method considering shape variation which improves the product quality and production yield.

To meet the aforementioned research objectives, this thesis develops research methodologies for 'Shape Variation Modelling, Analysis and Statistical Control' to provide the following capabilities:

(i) *Shape error characterisation and extraction of shape error modes from measured CoP data:* To extract the shape error modes from part

measurement data (CoP as non-functional data), a novel *functional data analysis* based shape error decomposition method is proposed. The extracted shape error modes have mathematical representation which can be further used for: (a) design synthesis to identify the KCCs through optimisation and indicates towards the possible failure of the system through root cause analysis; (b) monitoring and diagnosis of assembly process to identify shape related defects; (c) statistical tolerance simulation with shape error for compliant sheet metal parts; and (d) storage of real part shape error information as historical data for future design and manufacturing.

The proposed shape error model, named *Geometric Modal Analysis (GMA),* aims to develop a universal functional model which expresses shape error in a coherent manner by integrating design features (CAD information) with manufacturing variability (CoP information). The GMA model is presented in Chapter 4.

In this thesis, a *functional data analysis* based shape error modelling approach, named *Geometric Modal Analysis (GMA),* is proposed which allows to emulate part shape error of individual compliant part. The *GMA* method is able to *identify orthogonal shape error modes* from measurement data of *3D freeform shaped part.*

(ii) *Shape variation characterisation and quantification of batch of complaint parts:* To characterise and quantify the shape variation, *GMA* model has been extended to *Statistical Geometric Modal Analysis (SGMA).* The shape variation model provide the capability to: (1) generate virtual production parts to represent the production shape variation, and (2) quantify the shape

variation by synthesising *'composite part'* which is composed of all major shape error modes associated with a batch of parts. The generated virtual parts and composite parts can be further used for: (a) assembly process optimisation considering batch of parts which is pointing towards the robust fixture layout optimisation, such as, jig and fixture design; (b) statistical characterisation of the production process to predict the process capability aiming to produce quality products; and, (c) statistical tolerance synthesis of assembly system with non-ideal compliant parts. The SGMA model is presented in Chapter 5.

> In this thesis, a GMA- based shape variation modelling approach, named *Statistical Geometric Modal Analysis (SGMA),* is proposed which allows statistical characterisation of shape variation and quantifies the shape variation of a batch of compliant parts.

(iii) <u>*Monitoring and detection of shape related faults of compliant parts:*</u> Current control charts cannot be used for shape-monitoring using high dimensional data (CoPs) captured by in-process or off-line sensors. To detect shape related faults and abnormal process behaviour, a novel control chart based monitoring approach has been developed using GMA model. The control chart has ability to: (a) detect global shape faults such as unwanted variance change or mean shift, a common occurrence for within batch or batch-to-batch production of stamping process; (b) detect local shape defects such as local shift or variance change; and, (c) classify the shape faults to predict manufacturing quality and yield. Chapter 6 develops the control chart to monitor and detect shape related faults of compliant part.

In this thesis, a *GMA-based integrated bivariate monitoring chart* is proposed for statistical process monitoring of non-linear shapes. The control chart uses high dimensional data (CoPs) captured by in-process or off-line sensors with ability to fast detection of shape error related defects.

(iv) *Assembly fixture layout optimisation considering production batch:* To develop robust fixture invariant to shape variation, a fixture layout optimisation method has been proposed considering production batch of parts. It is an extension of current application of non-contact scanners from reverse engineering of a single part (obtaining CAD model from the measurement data) to design optimisation of assembly process with batch of compliant parts. It provides significant improvements which are reflected in (a) less fixture tuning quality loop and adjustments; (b) shorter product development time; and (c) enhanced product quality. Chapter 7 proposes the assembly fixture layout optimisation method by improving the fixture capability to produce quality product. This work has been disseminated as a conference paper (Das *et al.*, 2015).

In this thesis, a novel *SGMA-based fixture layout optimisation* methodology is proposed for assembly fixture simulation considering shape variation, high dimensional design space and non-linear product - process interactions.

This section describes the methodologies required for shape variation modelling, analysis and control with their capabilities. Figure 1.2 shows the modelling and application requirements for shape variation modelling, analysis and statistical control with emerging technologies.

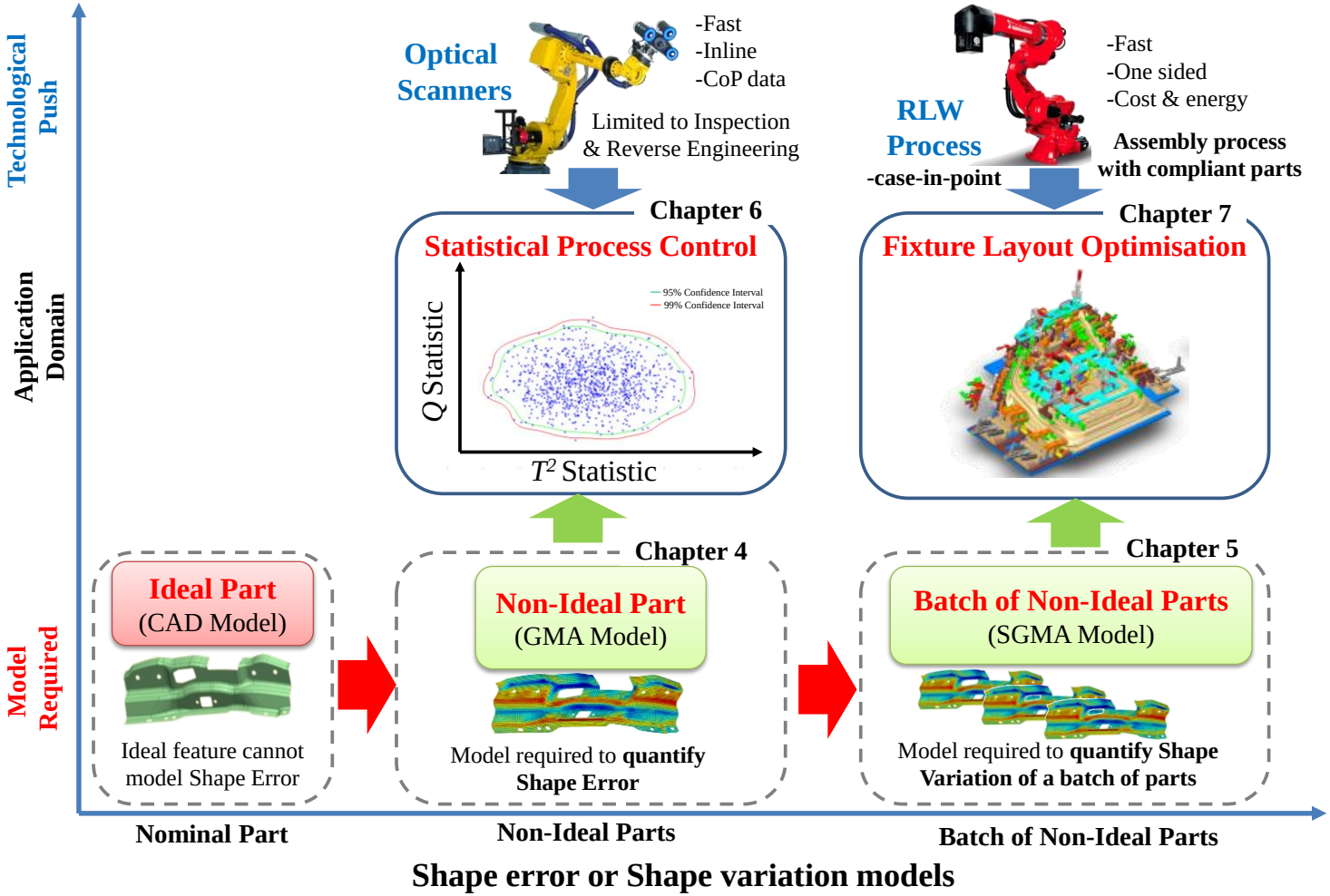

Figure 1.2 Pictorial representation of modelling and application requirements for shape variation modelling, analysis and statistical control

1.3 RESEARCH CONTRIBUTIONS

This thesis proposes a research framework for 'Shape Variation Modelling, Analysis and Statistical Control'. The proposed methodologies are motivated by the requirements of assembly system modelling with compliant sheet metal parts, especially for automotive and aerospace applications. The research contributions of the proposed methodologies are as follows:

(i) Modelling and characterisation of shape error -GMA Method

- *Development of a functional data model bridging design and manufacturing:* The functional data analysis based approach helps to bridge the gap between design characteristics (CAD data) and manufacturing characteristics (CoP measured data) and identifies major shape error modes produced by the fabrication process.
- *Measurement data (CoPs) based shape error decomposition:* The proposed GMA method extracts orthogonal shape error modes from measured CoP data (i.e. from real fabricated part). Further, GMA decomposes shape error of 3D freeform shaped part where the previous measured data decomposition methods are limited to 1D or 2D cases.
- *Compact model representation:* It is always preferable to develop a tractable model with mathematical representation which can be utilised for further applications, such as design optimisation, tolerance analysis, statistical process control or storage of shape error information.

(ii) Modelling and characterisation of shape variation – SGMA Method

- *Generalisation of the obtained shape error modes by determining statistical characteristics:* The main normality assumption of shape error

modes has been overcome by using Kernel Density Estimation (KDE). The statistical characterisation of shape error modes depicts real scenario of production parts by generating *variational virtual parts*.

- *Quantification of shape variation of a batch of parts by synthesising composite part(s):* The quantification of shape variation of a batch of parts is not available in literature. The SGMA method develops a novel technique to quantify the shape variation into single or few *composite part(s)* which is composed of major shape error modes present in a batch of parts. The SGMA method acts as enabler to optimise the fixture design process considering not only the individual part but also a batch of parts.

(iii) Control charts to monitor process and product quality shapes – GMA-based integrated bivariate monitoring chart

- *New direction to obtain the reduced variable set to synthesise multivariate statistics:* a new direction of obtaining reduced set of statistically uncorrelated and independent process variables by decomposing the data set within a single sample (GMA decomposition) instead of PCA- or PLS-based decomposition which is done across the samples. This emphasises the enhanced granularity of decomposition which then leads towards enhanced shape fault detectability.
- *Use of high dimensional CoP data for shape monitoring:* The control chart has the ability to process the high dimensional CoP data captured by modern 3D non-contact scanners. Therefore, the proposed control chart can be used for shape monitoring and defects detection using CoP data.
- *Fast detection of shape error related defects:* The control chart has the ability to detect the global mean shift or variance change. During sheet

metal stamping, variance change may be observed for within-batch production or mean shift may present for batch-to-batch production. The localised mean shift or variance change can also be detected using the proposed control chart. Further, the proposed GMA-based control chart has the ability to detect shape defects quickly as average run length reduces faster than the state-of-the-art PCA-based control chart.

(iv) Optimisation of assembly fixture layout considering production batch – SGMA-based fixture layout optimisation

- *Part shape variation based fixture layout optimisation:* The fixture layout optimisation considering shape variation significantly goes beyond the current state-of-the-art and practice as the fixture can be designed and optimised not only for individual part shape errors based but a batch of parts shape variation based. The composite parts based optimisation reduces the design space and it helps to eliminate thousands of variational assembly instances based Monte-Carlo simulation.
- *Assembled product quality improvement:* As production yield and product quality are determined based on production volume of real parts, fixture simulation considering shape variation improves the product quality and production yield.
- *Analytical surrogate model linking KPCs and KCCs:* The analytical relationship between the KPCs and KCCs reveals the effect of shape variation on product quality. The analytical surrogate model has been developed by linking SGMA based assembly and fixture locators, then, utilised to maximise the probability of satisfactory joints.

1.4 ORGANISATION OF THE THESIS

The organisation of this thesis is depicted in Figure 1.3 with addressed research areas for shape variation modelling, analysis and statistical control. This thesis is organised into eight chapters with introduction being the first.

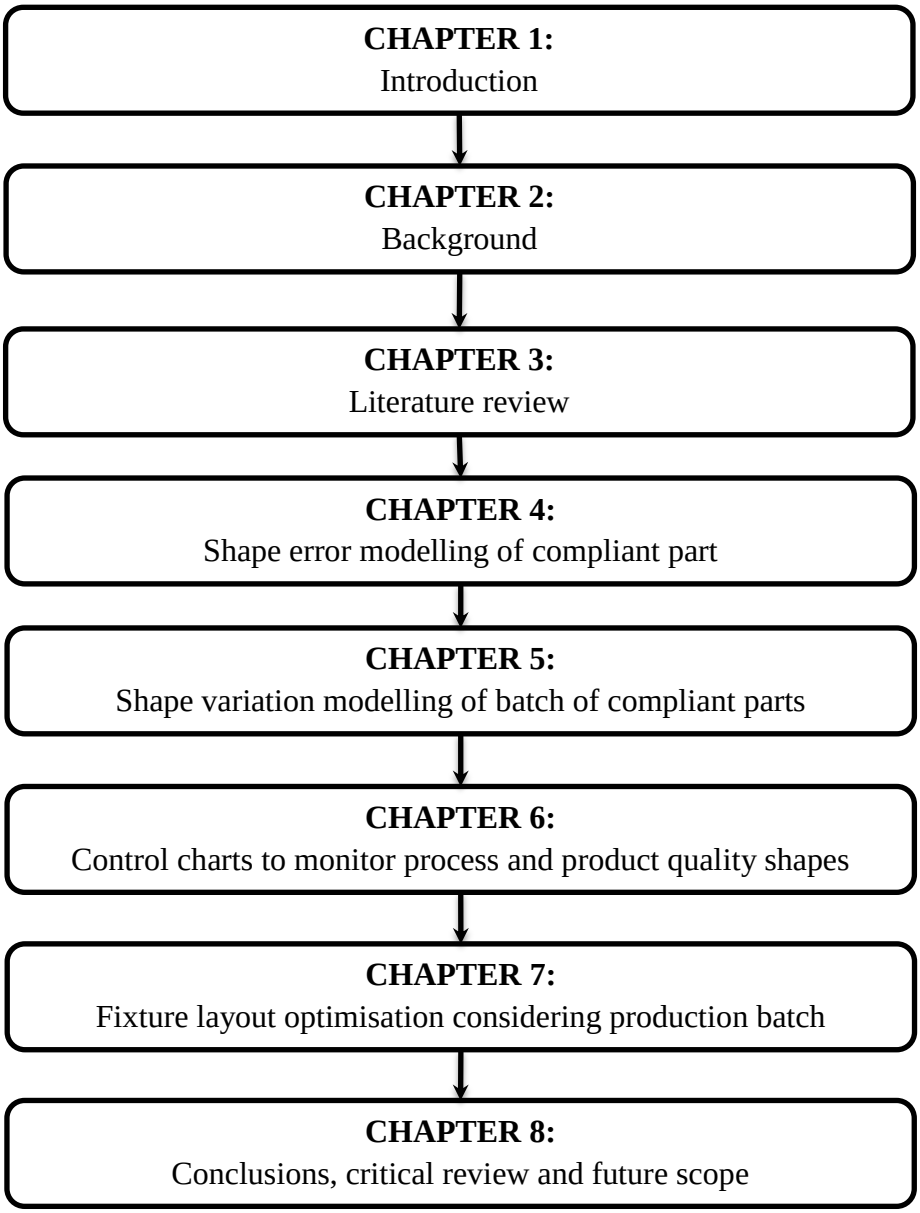

Figure 1.3 Organisation of this thesis and research areas

Chapter 2 introduces the background knowledge about the major terminologies, basic concepts of assembly station and measurement station for compliant parts, and case-in-point used in this thesis.

Chapter 3 reviews the literature related to modelling and characterisation of shape error and shape variation. Further, it reviews the reported work on statistical process control and fixture design optimisation considering the non-ideal compliant parts.

Chapter 4 describes in details the methodology used for modelling and characterisation of shape error of individual compliant part. It also demonstrates the results with other state-of-the-art methods available in literature.

Chapter 5 details the methodology used for modelling and characterisation of shape variation of a batch compliant parts by using statistical characterisation and synthesising composite parts.

Chapter 6 develops a new methodology to detect shape related faults by introducing new multivariate statistical process control charts to take advantage from measured CoP data. The methodology developed in Chapter 4 has been used as base kernel to develop the control chart.

Chapter 7 uses the obtained results from Chapter 5 to demonstrate the usability of shape variation quantification model to conduct fixture layout optimisation. It optimises the key control characteristics to obtain satisfied key product characteristics.

Chapter 8 lists the major conclusions of the research study along with critical review, and future direction of research work.

CHAPTER 2 **BACKGROUND**

This chapter focuses on the background information related to the proposed work, with a brief introduction to the assembly process with compliant parts, measurement of compliant parts/subassemblies. As this thesis develops the research framework for 'Shape variation modelling, analysis and statistical control', where *(i) shape error model* and *(ii) shape variation model* act as enablers to (a) monitor shape variation with capabilities to detect shape defects, and, (b) reduce shape variation with proper fixture design to improve product quality. The research framework involves compliant sheet metal parts which are assembled at assembly station and measured at measurement station to support many assembly related tasks and inspection checks. Starting with an overview of assembly station with compliant parts, special focus has been drawn on variation modelling of rigid ideal part modelling, compliant part modelling, and non-ideal (i.e. shape error) compliant part modelling for assembly system. Further, this chapter outlines the current industrial usage of 3D non-contact scanners based measurement data for quality inspection and reverse engineering followed by extended usage of these scanners for compliant part monitoring and shape defects detection. As case-in-point, this thesis uses Remote Laser Welding joining application for validation and verification of the developed methodologies.

2.1 ASSEMBLY STATION WITH COMPLIANT PARTS

An assembly station involves assembly process in manufacturing which can be simply defined as a method of assembling two or more parts together using various temporary or permanent assembly techniques. In case of compliant sheet metal assembly, two or more sheet metal parts are joined together using various joining

techniques which result in sub-assembled or final assembled product (Camelio *et al.*, 2003). The following subsections describe the basic concepts of assembly key characteristics to inspect product quality, management of assembly variation associated with compliant parts, assembly fixturing with complaint parts and assembly joining of sheet metal parts with emerging remote laser welding.

2.1.1 Assembly Key Characteristics

In an assembly operation, one of the most important challenges is to manage dimensional and geometric quality as it has direct impact on product functionality and performance (Camelio *et al.*, 2003). In assembly process, dimensional and geometric qualities are defined with important dimensional and geometric relations which are referred as *key characteristics* (KC) (Whitney, 2004). A comprehensive definition of key characteristics is proposed by Thornton (1999) as 'Key Characteristics are the product, subassembly, part, and process features that significantly impact the final cost, performance, or safety of a product when the KCs vary from nominal'. To obtain a good assembled product quality, KCs are to be achieved accurately through product and process design, monitoring and control. In an automotive assembly process, hundreds of sheet metal parts or subassemblies are joined together to obtain functional product. For example, a typical autobody assembly consists of 200-250 sheet metal parts assembled at 60-100 assembly stations with 1,700 to 2,100 fixture locators (Ceglarek and Shi, 1995; Shiu *et al.*, 1996). Therefore, it is of upmost requirement that the KCs should lie within the defined tolerance limit in order to achieve good quality functional product, especially for managing sheet metal assemblies such as autobody frame, closure panels etc. Further, assembly fixture plays a dominant role to achieve dimensional and geometric quality during assembly operation. These dimensional and geometric

qualities of a product are determined through *Key Product Characteristics* (KPCs) and *Key Control Characteristics* (KCCs). KPCs are the identified crucial features which are needed to be controlled to achieve the functionality of the product and KCCs are the controlling elements such as position of fixture elements, clamps, pins and NC blocks (Ding *et al.*, 2002). Ding *et al.* (2002) also mentioned that an assembly system can be broken into several layers corresponding to the process-KC, part-KC and product-KC where Figure 2.1 illustrates the variation propagation from KCC to KPC for assembly station with compliant parts.

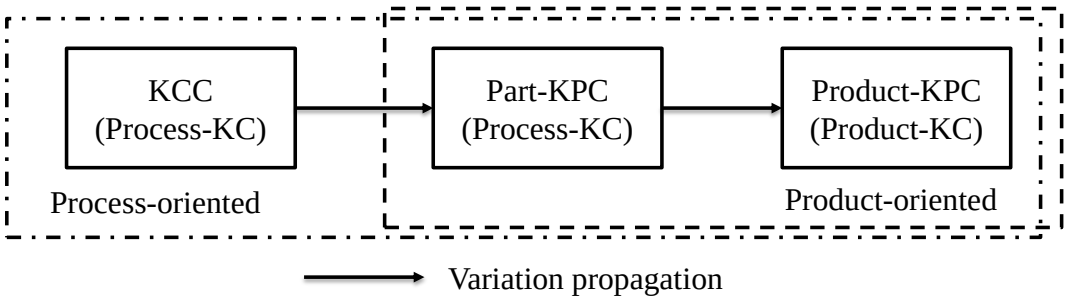

Figure 2.1 Variation propagation from KCC to KPC in an assembly process by Ding *et al.* (2002)

2.1.2 Input: Compliant Parts

One of the major challenges associated with compliant sheet metal assembly is the proper characterisation of *variation* in the assembly process. Due to intrinsic flexible nature of compliant sheet metal parts, variation occurs during assembly process interactions among parts, holding fixtures or joining processes.

In general, *variation* in manufacturing and assembly can be defined as physical deviation from the nominal characteristics of a part due to manufacturing, fabrication or assembly process errors. To quantify, analyse and tolerate the amount of variation, tolerance analysis and synthesis is well known in literature. Internationally

recognised standards, such as ISO-Geometrical Product Specification (ISO-17450-1, 2011) or ANSI-GD&T (ASME, 2004), have been developed for tolerance specification which defines general terms for geometrical features of part. Many works related to variation modelling of part are directly linked with the tolerance analysis and synthesis. The variation modelling can be broadly classified into two categories: (i) rigid body modelling, and (ii) flexible/deformable body modelling. In the first category, parts are assumed to be rigid where no part deformation has been allowed. This is suitable for machined component modelling, jig or fixture components modelling. In later case, parts are deformed with additional force, assembly variation such as sheet metal parts. Similarly, depending on the presence of dimensional and geometric error components in the part model, it can be either ideal part model or non-ideal part model. In case of ideal part modelling, the part is modelled to its nominal geometry which consists of ideal features, ideal dimensions and ideally placed with ideal orientation. On the contrary, non-ideal part modelling considers the error components associated with different features in addition to the ideal features such as size and orientation errors, geometrical shape errors etc. As per the modelling trend observed in the literature, the compliant part modelling approaches can be divided into three categories: (i) ideal rigid part modelling, (ii) ideal compliant part modelling, and (iii) non-ideal compliant part modelling. Different approaches have been adapted in literature to model the aforementioned three categories.

In the area of tolerance analysis and synthesis, the initial step is to assign variational features for modelling. The main efforts are given to mathematise the variational features to keep the features within the defined tolerance zone. Traditionally, the variational features are modelled by introducing small translational and rotational

parameters where shape errors or form errors are normally neglected. Therefore, these parameters mainly deal with rigid body motion to determine various configurations within the tolerance zone. Mainly two well-known modelling approaches have been identified in the literature which are based on the mathematical modelling of the variational features, (i) the small displacement torsor proposed by Clement and Bourdet (1988); and (ii) the 4×4 transformation matrix method proposed by Whitney *et al.* (1994). Using a set of parameters, these methods parameterise the variational features which are used for tolerance analysis mainly for rigid body motions. However, the shape errors are neglected in those aforementioned approaches of variational feature modelling. Therefore, to model shape errors, more sophisticated models were proposed by Samper and Formosa (2006), Huang *et al.* (2014) where shape errors were also accounted by using a modal decomposition analysis based on real measurement data.

2.1.3 Assembly Process Fixturing

Assembly fixtures are mainly used for various type of joining operations, especially in automotive and aerospace industries. The role of the assembly fixture is to provide the accurate locating scheme for alignment of parts to be assembled during the joining operations. Due to the compliant nature of sheet metal parts, assembly fixturing with compliant parts is recognised as one of the major challenges as the non-ideal variational features coupled with intrinsic flexibility of part can cause part deformation and quality variation (Liu and Hu, 1997). Therefore, another important role of assembly fixture is to control the assembly variation especially during the sheet metal assembly operation. A number of modelling techniques has been developed to analyse the assembly variation with non-ideal compliant parts in single assembly station (Liu and Hu, 1997; Long and Hu, 1998; Liu *et al.*, 1996; Cai *et al.*,

2005; Hu *et al.*, 2001). Typically, assembly system modelling with compliant parts in a single station involves four major steps (Liu and Hu, 1997):

(i) Parts loading in the fixture: The parts to be assembled are loaded in the fixture. Due to fabrication errors and process variation, individual part errors contribute to initial part-to-part deviation or gap.

(ii) Parts clamping in fixture: The initial part-to-part gap between loaded components or subassemblies is closed with clamping force to the nominal position.

(iii) Joining operation: The clamped parts or subassemblies are joined using the joining methods such as riveting, welding and result in further deformation due to joining operation.

(iv) Releasing clamps and springback: After the joining operation, the clamps are released. The joined components take final shape due to assembly spring back after releasing the stored strain energy induced during clamping and joining operation.

In assembly process with compliant parts, fixture plays a significant role to achieve desired dimensional and joining qualities (KPCs) of assembled product where fixture design parameters act as KCCs. Therefore, fixture has significant impact on productivity and product quality as a well-designed fixture reduces variation within assembly process. Typically, a basic fixture consists of four different components (i) locators, (ii) clamps, (iii) supporting blocks, and (iv) main fixture body (Nee *et al.*, 2004). In case of sheet metal assembly, locators are used to position the parts within the fixture at correct position and orientation whereas clamps and support blocks are used to securely hold the part by preventing deformations during assembly operation.

Part locating scheme is an important feature to load part(s) on the fixture by restricting the DoFs of the part(s). The well-known locating principle '3-2-1' is widely used in industries to locate rigid body parts quite uniquely without creating locator interferences (Lowell, 1982; Shirinzadeh, 2002). Beyond the basic requirement of part placement and constraining the rigid body motion, the fixture should also be able to stop part geometrical deformation. Unfortunately, compliant parts like sheet metal parts cannot be controlled through '3-2-1' scheme which require increase the number of locators to 'N-2-1' to minimise geometric deviation (N>3). For compliant part fixturing, Cai *et al.* (1996) proposed 'N-2-1' locating principle which allows to prevent excessive deformation of sheet metal parts and developed an optimal fixture design method, which can reconfigure the N locators on the primary datum to minimize total part deformation.

Locator pins, clamps and NC Blocks are used as fixture elements in sheet metal assembly process. Locator pins are used in '2-1' locating scheme by using one 4-way pin and one 2-way pin. The 4-way pin restricts translation in X and Y directions and 2-way pin restricts translation in Y direction. NC blocks are usually used to support the flexible part against clamping force. Hence, at each clamp location one NC block is stationed. NC blocks restrict translation in –Z direction by surface contact when they are used without clamps and +Z translation is restricted by clamps (Shiu *et al.*, 1996). Figure 2.2 represents the types of locating elements used for sheet metal assembly. The 'N-2-1' (N=4) fixturing scheme for sheet metal part has been demonstrated in Figure 2.3 considering the locator pins, clamps and NC blocks as fixturing elements.

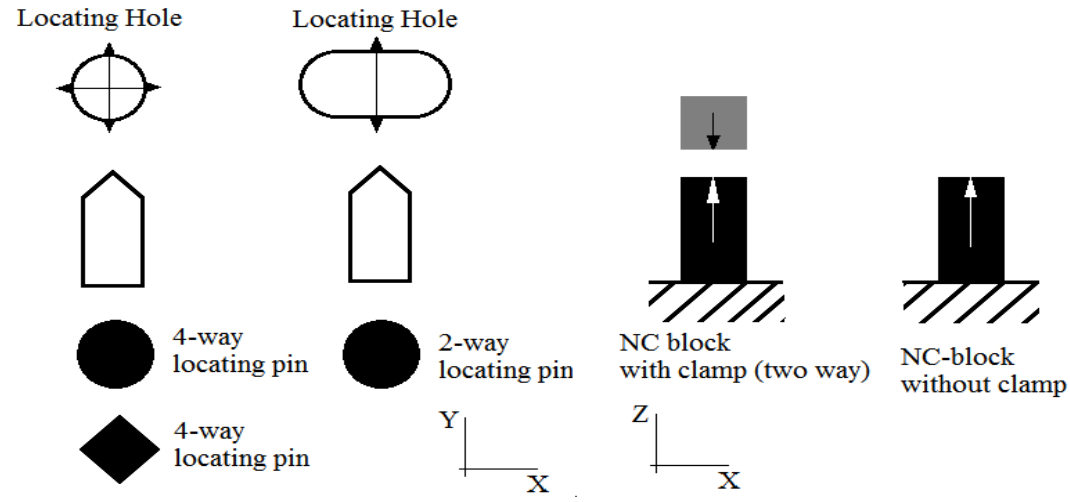

Figure 2.2 Automotive sheet metal assembly locator types (Shiu *et al.*, 1996)

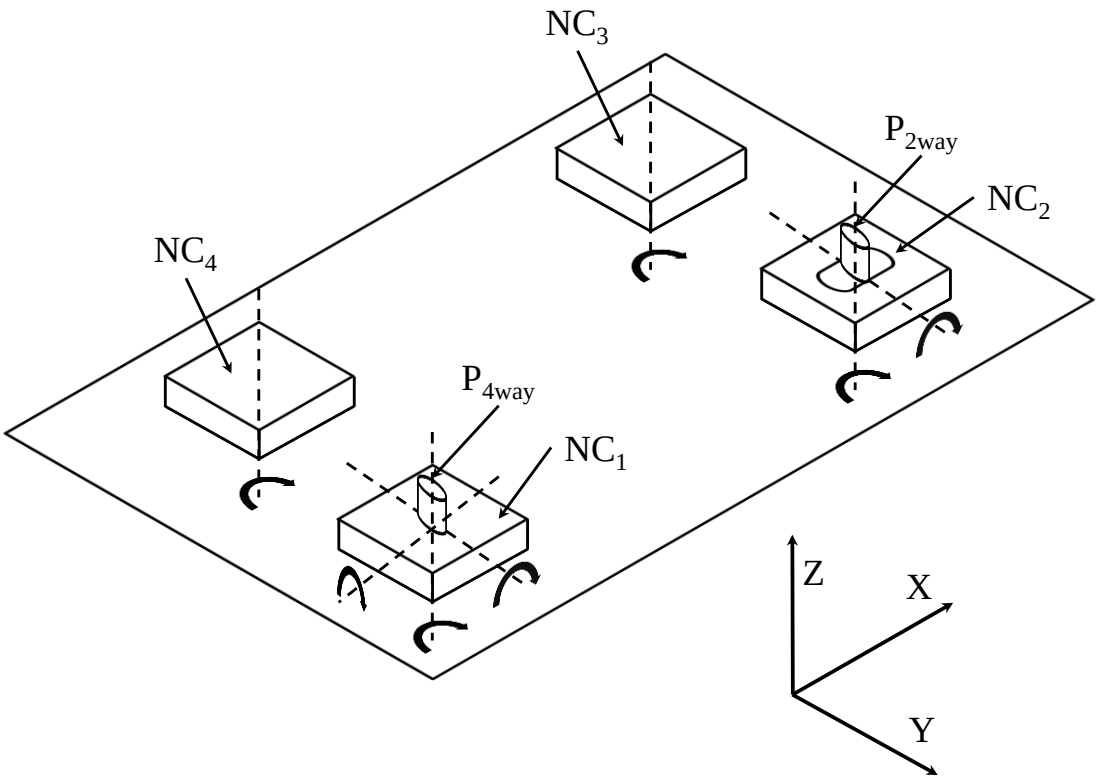

Figure 2.3 'N-2-1' (N=4) locating scheme for sheet metal parts (Camelio and Hu, 2004)

2.1.4 Assembly Process Joining: Remote Laser Welding (RLW) as Case-in-Point Application

Joining is an important step of assembly operation in which clamped parts or subassemblies are joined using the joining methods such as riveting or welding. Further, the joining operation contributes to assembly variation as it introduces further deformation to the assembly. The most commonly used joining operations for sheet metal parts are self-piercing riveting, resistance spot welding, brazing or laser welding.

Recently, remote laser welding (RLW) is gaining significant industrial interests as a substitute to conventional joining processes such as self-piercing riveting, resistance spot welding. RLW is a non-contact joining process using laser beam and it has emerged as a response to sheet metal assembly industries where high efficiency and flexibility of the joining systems are required. RLW provides several benefits which are of great interest for sheet metal assembly process, such as, one sided non-contact joining, high welding speed, less floor space, less number of robots, less energy or lower investment and operating costs (Mori *et al.*, 2010; Reinhart *et al.*, 2008; Vaamonde Couso and Vázquez Gómez, 2012; Shibata, 2008; Ceglarek, 2011).

Despite of having the aforementioned benefits of RLW process over the traditional joining processes, the main challenge to implement RLW system in vast scale is the part-to-part fit up problem. The part to part gap control requirement has been illustrated in Figure 2.4. Dimensional and geometric shape variations of part during their fabrication process, such as, sheet metal forming, result in gaps between them after they are mounted on the assembly fixture. For example, to join two galvanised steel parts successfully, RLW requires maintaining a gap between 0.05 mm to 0.3

mm and for aluminium, between 0 mm to 0.05 mm. Failure to meet the aforementioned part-to-part fit-up requirements, RLW results in welding defects, such as under-cut, porous weld, poor finishing and corrosion prone. For example, lower gap causes the undercut, porosity and spatter when welding galvanised steel as coated zinc gets vaporised and unable to find path to escape causing inclusion in the weld pool. Similarly, higher gap (more than 0.3 mm for steel) results in shrinkage, undercut and lower interface width due to excess material flow in the gap. As a consequence, it requires tight control of the gap which is much lower than the individual part shape error. This emphasises to model the randomness of the individual part shape error for proper understanding of part behaviour and gap analysis. Subsequently, as product quality and production yield depend on production parts, it triggers proper designing of fixture to mitigate the part fit-up problem considering production shape variation.

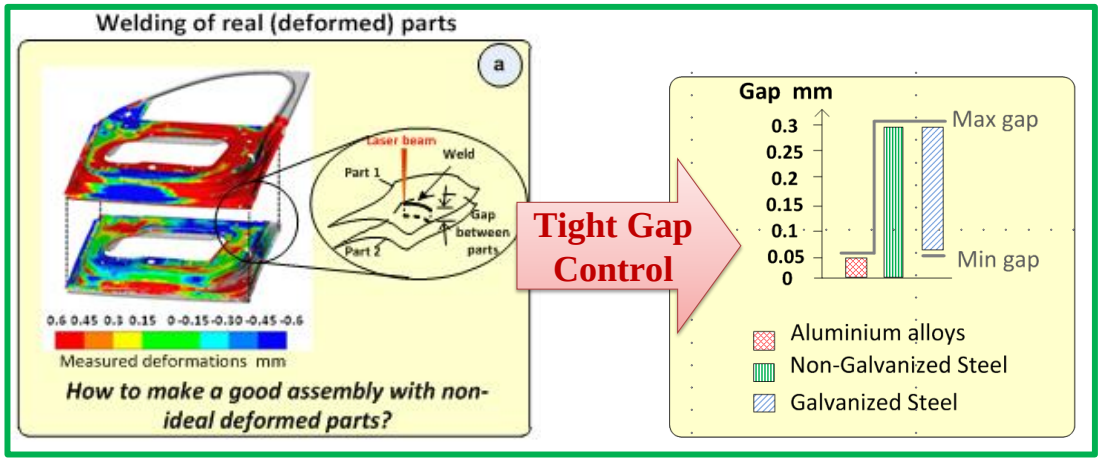

Figure 2.4 RLW requirements for tight part-to-part gap control (Ceglarek, 2011)

In this thesis, RLW joining process has been considered as case-in-point to demonstrate the developed methodologies and their applicability.

2.2 MEASUREMENT OF COMPLIANT PARTS

In manufacturing industry, the quality of a part is evaluated by Key Product Characteristics (KPCs) which are defined by the quality control engineers. The conventional way of defining the KPCs is the physical measurement of the dimensional and geometric features, such as dimensions or part feature locations. Similarly, KPCs related to a stamped sheet metal part are defined by the part deviations and part features like surface point deviations, trim edge points, hole and slot dimensions, hole and slot locations etc. These KPCs are the indicators of the part quality and monitoring of the quality is the prerequisite for a good assembly. Conventionally, the choice of KPCs is determined by the type of measuring technologies available. In current industrial practice, automotive or aerospace body parts measurement are largely restricted to point based measurement which are measured by Coordinate Measuring Machine (CMM). CMMs are most widely utilised dimensional measurement tool. Moreover, parts to be measured with CMM are taken to measurement room which is in separate location from the production line as well as they have limited capabilities of measuring KPCs. Therefore, this is time consuming, off-line and costly process for compliant part measurement. Due to recent advancement in the field of 3D metrology scanning system development, 3D non-contact sensors are emerging in the industrial practice. They can capture the entire surface of the part in the form of Cloud-of-Points (CoP), the digital representation of the actual part surface. The part surface scanning process is fast, in-line and less costly compared with CMM data. Figure 2.5 illustrates the measurement capability of CMM where few defined KPCs are measured vs. surface measurement using 3D non-contact scanners where entire surface information presented through CoP. It illustrates the advantage of having 3D non-contact

measurement where whole compliant part surface information has been captured against few captured points through CMM. Many defects remain undetected through point based measurement, especially when the defects do not influence the KPCs. Subsequently, use of 3D non-contact type of measurement helps to overcome this problem since they can capture the entire product geometry.

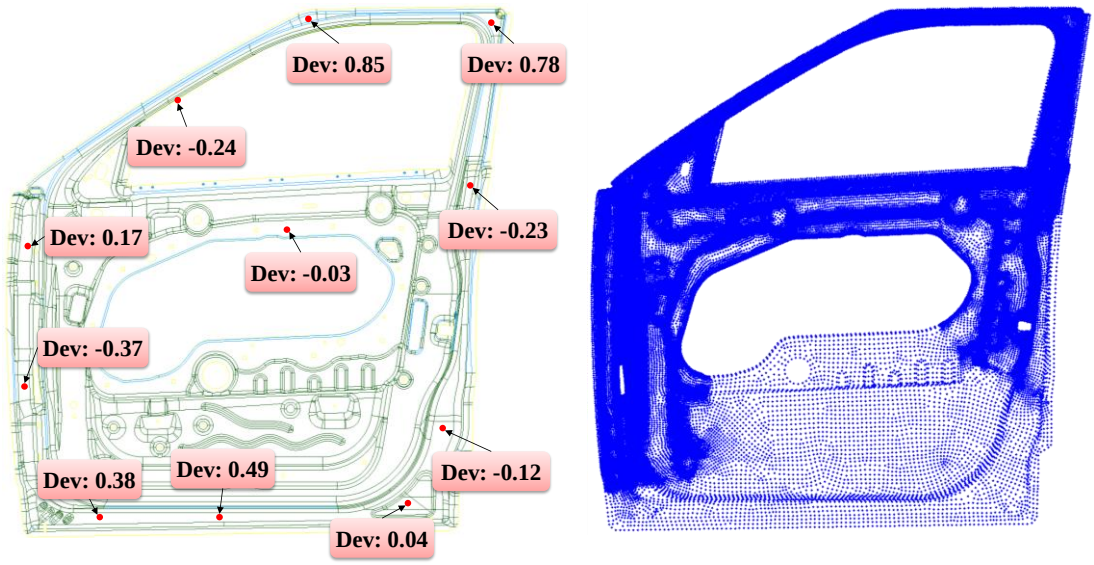

(a) (b)

Figure 2.5 Compliant part measurement (a) using CMM at few specific sampled points, and (b) using 3D non-contact optical scanners to capture entire product surface information (i.e. CoP data)

Relying on the application requirement, there are several 3D non-contact optical measurement systems available. Many researchers have used 3D laser scanners to capture surface data of part and compared the result for measurement systems improvements (Isheil *et al.*, 2011). Majeske and Hammett (2003) studied 3D non-contact measurement system, CogniTens Optigo 200, where the results have been compared with Coordinate Measuring Machine (CMM) and checked the suitability of the gauge towards meeting the typical requirement of industrial standards.

Further, Huang *et al.* (2008) studied the gauge repeatability and reproducibility of CogniTens Optigo 200 for specular machined components.

Further, current applications of these non-contact measurement gauges are limited to inspection or reverse engineering application in the context of sheet metal compliant parts. Figure 2.6 explains the research opportunities provided by 3D non-contact measurement scanners in the field of shape error or shape variation modelling as well as statistical monitoring of shape quality and shape variation reduction through assembly fixture design.

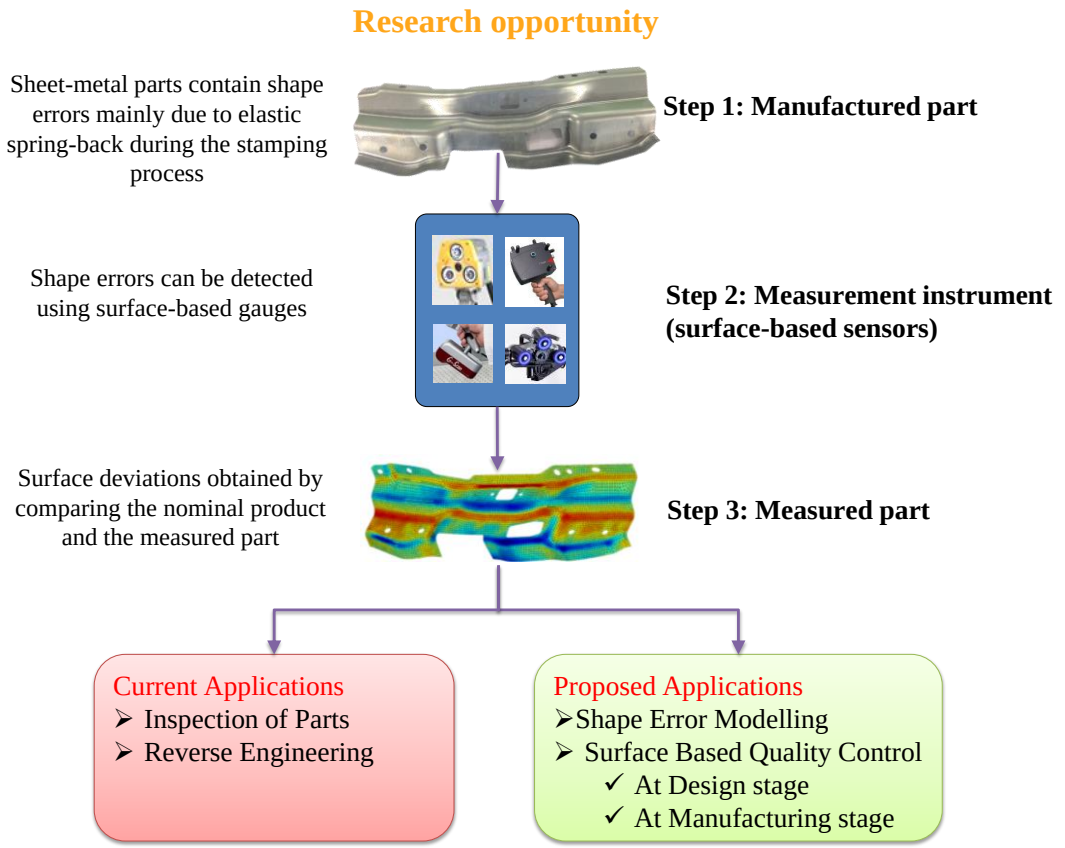

Figure 2.6 Current applications vs proposed applications of CoP measurement data

2.2.1 Measurement Data for Quality Inspection and Reverse Engineering of Compliant Parts

Part or feature inspection typically involves identifying the real part or feature deviation from the nominal geometry. Traditionally, it is assumed that each part should lies with the specification limit for ease of assembly and ideally, all the KPCs should be as close as the nominal target values (Montgomery, 2008). Therefore, part inspection plays a vital role in automotive and aerospace industries as the assembly composed of thousands of parts. Use of 3D non-contact scanners for part inspection is mainly conducted for eliminating the non-conforming parts as per the industrial standards. Typically, part inspection is conducted by obtaining the deviation map of the scanned part from the nominal geometry. Due to the advantage of quick data capturing through these 3D non-contact measurement scanners, a number of improvements have been reported in the field of inspection. Subsequently, the captured data can be utilised for inspecting parts for surface and feature abnormalities and numerous other KPCs that can reflect the product quality.

Wells *et al.* (2013b) classified the current use of 3D point clouds for part inspection into two main categories: (i) extracting geometrical and dimensional feature parameters, and (ii) an ad-hoc manual process where a visual representation of a point cloud (usually as deviations from nominal) is analysed.

Various works have been reported for inspecting manufactured parts or sheet metal parts using CoP data. Li and Gu (2004) carried out comprehensive review regarding the inspection techniques for free-form surface considering both contact and non-contact measurements. Martínez *et al.* (2010) inspected several canonical features as planes, spheres, cylinders, holes (outer and inner), and conical surfaces as part of

their non-contact measurement device goodness evaluation criteria. Further, Turley *et al.* (2014) inspected automotive body-in-white with CMM and laser based scanner to evaluate the measurement agreement of critical surface points using a multi-sensor horizontal dual arm CMM. Visual inspection is mainly related to entire surface deviation representation in the form of colour map to visually check the faults such as surface defects, dents, cracks, skin panel defects etc. Prieto *et al.* (1998) introduced a visual inspection system for manufactured parts to check visually the colour map to display the level of discrepancy between the measured CoP data and the nominal model.

Similarly, a comprehensive review on recent reverse engineering application based research using non-contact measurement systems can be found in the works of Várady *et al.* (1997) and Creehan and Bidanda (2006). Generally, in reverse engineering, the measured CoP data is used for generating CAD model. In order to accurately recreate the existing part, a CAD model of the part's geometry must be developed. Várady *et al.* (1997) mentioned the requirement of reverse engineering as to create geometric models of existing objects for which no such nominal model is available. Therefore, CoP data can be used to digitise the part in reverse engineering process. They divided the basic phases of reverse engineering into four major steps: (i) data accusation (i.e., CoP data), (ii) data pre-processing, (iii) segmentation and surface fitting, and (iv) CAD model creation. Hsiao and Chuang (2003) proposed a reverse engineering approach for designing product in shorter time using CoP data. Similarly, Mohaghegh *et al.* (2007) described a new approach to process the data points measured from turbine blade air-foils in order to make a valid shape via reverse engineering method.

Therefore, from the literature, it is clear that the current applications of non-contact measurement sensors/devices are mainly limited to inspection and reverse engineering. It should be noted that, inspection of part only provide information about defects or variation for single part which neglects the part-to-part variation. Consequently, it emphasises to develop new technique to explore the full potential of 3D non-contact scanners in the field of part shape monitoring.

2.2.2 Measurement Data for Monitoring and Control of Compliant Parts

Traditionally, few sampling surface points are picked by the quality engineers for monitoring purpose which are measured by CMM and then, point based SPC control charts are imposed to assess the out of control signal or variation from one part to another (Majeske and Hammett, 2003). Also, these discrete point based measurement methodologies which are used for inspection and process control have limited 6-sigma failure root cause identification. They seldom correct operational defects quickly. The point coordinates (x,y,z) are measured in area of interest of stamped or assembled parts to evaluate the specific KPCs. However, these few KPCs may not capture all the information related to possible patterns of variation or shape related form defects as it does not provide in-depth knowledge to understand the manufacturing defects related to a part or assembly. Further, capturing these KPCs are time consuming and costly off-line process which force manufacturers to reduce the number of points or KPCs to be measured for monitoring purpose. Subsequently, it doesn't provide compact information about the features, geometric properties or mating shape characteristics. Therefore, it is critical to develop better Statistical Process Control (SPC) method for monitoring the quality of complex part geometries where it can provide better understanding about the product shape. Further, the SPC

method should provide better indication about the quality deterioration which can avoid product failure or process downtime (Panagiotidou and Tagaras, 2010).

To overcome the aforementioned challenge of limited KPCs measurement, an advanced measurement technology will widen the opportunity where a surface based measurement device can capture millions of data points (i.e. CoP) related to the part geometries. This high volume of data overcomes the restriction of limited KPCs selection and fault detection is no longer narrowed by traditional measurement system capabilities like CMM. In the field of quality inspection, reverse engineering and remote sensing, 3D non-contact type of measurement devices are progressively being used (Mass, 2002; Son *et al.*, 2002). These measurement systems have the potential to be used for quality control, root cause analysis of faults, process monitoring and process parameter adjustment. Especially in automotive and aerospace industries, current use of CoP measurement is limited to inspection and reverse engineering. Son *et al.* (2002) explained that the current applications for those 3D scanners abide to inspection and reverse engineering applications which provide part mapping between as-build parts and their corresponding nominal representations. Therefore, it only provides crucial information about the individual part instead of process behaviours and part-to-part variation propagation. Especially for sheet metal production, capturing the process behaviours for within batch variation and batch-to-batch variation are very important. It has an urgent need in current manufacturing industries for accurate depiction of status of the process. Therefore, CoP measurement data can further be used for shape error modelling of individual compliant part, shape variation modelling of batch of compliant parts and statistical process control for compliant parts to detect shape related defects. Figure 2.7 depicts the use of CoP measurement data for shape error modelling, shape

variation modelling and statistical process control. Details of literature review regarding shape error modelling are explained in Section 3.2 and shape variation modelling in Section 3.2.

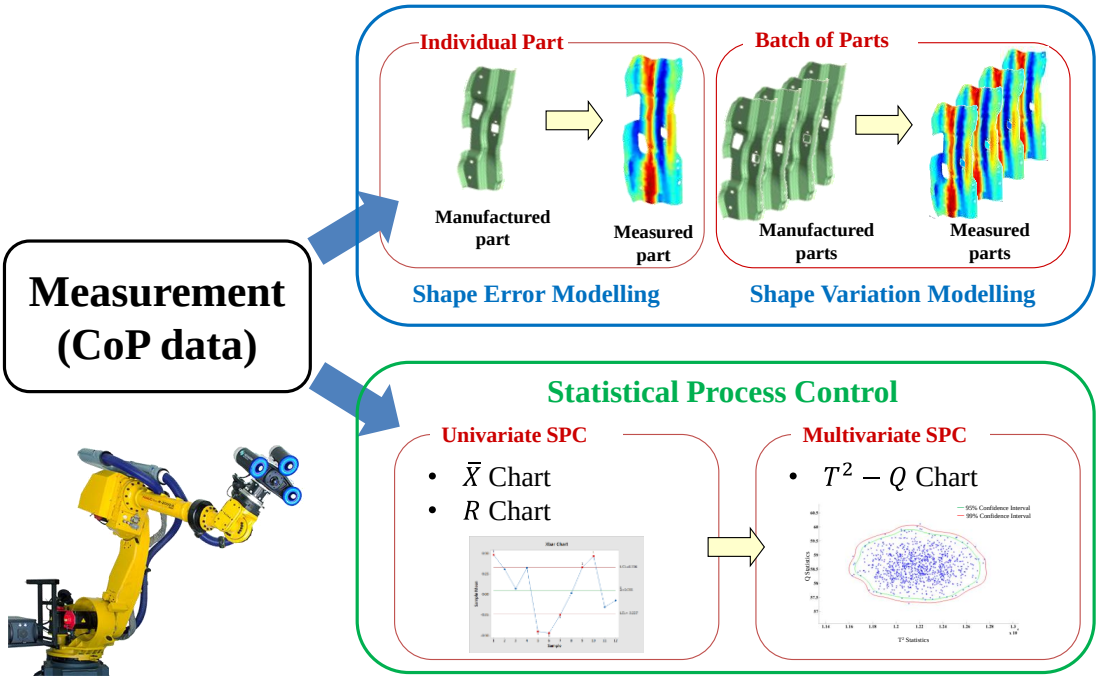

Figure 2.7 Use of CoPs measurement data for shape error modelling, shape variation modelling and statistical process control

The non-contact 3D measurement scanners have potential to collect off-line or in-line data directly from the production line. A shape related defects detection SPC chart is required which enables quality engineers to monitor the product quality by addressing the data rich but information poor problem as highlighted in Wang and McGreavy (1998) and Choudhary *et al.* (2009). As a result, shop-floor decision making and productivity can significantly be enhanced. The captured CoPs data can be categorised as highly data rich but extraction of useful information from the high volume data is still challenging. The research directions regarding the use of CoP data can be classified in two distinctive areas: (i) the research to develop the 3D non-contact type of measurement systems and enhance its ability by increasing accuracy,

calibration, repeatability and reproducibility issues (Aguilar *et al.*, 1996; Feng *et al.*, 2001; Isheil *et al.*, 2011; Xi *et al.*, 2001; Li *et al.*, 2008d). (ii) the use of the high density point clouds to extract critical information for different modelling and simulation validation along with the use of SPC apart from the inspection and reverse engineering applications (Creehan and Bidanda, 2006; Son *et al.*, 2002).

Several researchers have reported the extensive use of captured data for reverse engineering where the real part measurement data converted to CAD models (Hsiao and Chuang, 2003; Mohaghegh *et al.*, 2007). This reverse engineering conversion also detects the product failures by comparing with its CAD geometry and identifies the non-conforming areas as per the product specifications (Várady *et al.*, 1997).

Identifying the non-conforming areas of a part from the good part is typically based on the deviations of the scanned part from the nominal CAD geometry model (Shi and Xi, 2008; Mohib *et al.*, 2009). But, these inspection and reverse engineering approaches remain unsuccessful to capture the part-to-part variation or manufacturing process shifts during production. In case of sheet metal parts variation propagation behaviour analysis, capturing within batch variation and batch-to-batch process shift are very crucial. Though traditional statistical process control techniques based on few points remain important due to its simplicity and easy to interpret but not efficient to capture the geometric errors associated with the parts and its propagation within batch or batch-to-batch. These traditional SPC charts also fail to accommodate the increased volume and velocity data capturing process by 3D non-contact scanners. Therefore, more informative shape characteristics based statistical process control chart needs to be developed to explore the full potential of 3D non-contact measurement technologies as it can capture the entire surface information more efficiently.

2.2.3 Part and Assembly Measurement to Demonstrate Case Studies

Automotive door parts are used to demonstrate the developed methodologies in this thesis with RLW joining as an application. Part-to-part gaps between the joining parts are not constant due to part dimensional and shape variation. Usually the gap is changing over the area of interest and it depends largely on the part dimensional and shape errors. Moreover, the measurement must also be fast to benefit from the five times faster RLW technology compared to resistance spot welding (RSW). This leads to surface-based measurement systems as the most suitable option for RLW applications. The frequency of measurement depends on the variation of parts and type of shape errors in the assembly line. To identify and characterise the part shape error, surface based measurement is necessary which provides large data points in terms of 3D Cloud-of-Point (CoP).

In the context of this thesis, parts are measured with two commercial measurement systems: Optigo 200 (by Cognitens – Hexagon) and Romer (by Hexagon). Optigo 200 is an image acquisition, dimensional measurement gauge which is a non-contact, surface-based measurement system with capabilities to quickly capture data point of relatively large parts. However, sources of error of Optigo 200 are mapping of CoP data with CAD and external light. The Romer system is an arm-based (seven degrees of freedom) with an end-effector. The end-effector can be a touch probe or a laser scanner system. In this case, laser scanner is used to capture surface data of parts. The system automatically aligns point clouds using the inverse kinematics of the arm and source of error coming from the arm joints. PolyWorks (by InnovMatric Software) was chosen for data post-processing analysis which includes CoP data cleaning, uniform subsampling of highly dense CoP data and CoP data alignment with nominal CAD of the part.

2.3 SUMMARY

This chapter provides an overview of the modelling and technological aspects used for assembly station with compliant sheet metal parts. Further, it demonstrates the measurement requirement for compliant sheet metal parts with extended application towards statistical process control. The following items are explained:

(i) Assembly station with compliant parts: Assembly station with compliant parts involves variation as one of the major challenges reported in literature. The current approaches for compliant part modelling are evolving in stages: ideal rigid part model, ideal compliant part model and non-ideal compliant part model. Further, various attempts have been made to model assembly system with compliant parts at a single assembly station. The assembly process involves four major steps: (a) parts loading in the fixture; (b) parts clamping in the fixture; (c) joining operation; and (d) releasing clamps and springback. Further, the assembly process is evaluated based on key characteristics where process-oriented Key Control Characteristics (KCCs) have direct impact on product-oriented Key Product Characteristics (KPCs).

(ii) Assembly fixture design for compliant parts: Assembly fixture plays a significant role to achieve desired dimensional and joining qualities (KPCs) of assembled product where fixture design parameters act as KCCs. Therefore, proper design of assembly fixture is unavoidable when dealing with compliant sheet metal assembly. This chapter reviews the fixturing components, and N-2-1 part locating scheme to load the compliant sheet metal parts in the assembly fixture.

(iii) Assembly process joining: case-in-point application - Remote Laser Welding (RLW): The developed methodologies in this thesis are verified and validated with industrial case from remote laser welding process. In this chapter, the RLW advantages, current challenges, joining requirements are demonstrated for ease of understanding of the developed methods.

(iv) Measurement data for quality inspection and reverse engineering of compliant parts: It provides an overview of measurement data usage for quality inspection and reverse engineering of compliant parts. Further, it reports the advantages of 3D non-contact sensors based entire surface measurement against traditional Coordinate Measuring Machine (CMM). However, current applications of non-contact measurement devices are mainly limited to inspection and reverse engineering.

(v) Measurement data for monitoring and control of compliant parts: Quality control of compliant sheet metal parts is decisive to ensure increasing assembly functionality and reduce residual stress in the final assembly. Use of point-based CMM measurement data is well known for statistical process control for industrial application of compliant sheet metal part. However, few measurement points do not provide in-depth knowledge to understand the manufacturing defects related to a part or assembly. On contrary, surface based 3D measurement scanners have the potential to be used for statistical process control which considers entire surface information in terms of CoPs.

CHAPTER 3 **LITERATURE REVIEW**

3.1 INTRODUCTION

Generally, modelling of assembly system with compliant parts is not a trivial task due to necessary trade-offs between various sources of variations which need to be taken into consideration and required KPIs accuracy. The sources of variations are mainly related to parts, tooling and joining. To ensure quality of part shape as defined by GD&T, a key requirement is to model CoP data representing part shape variation in such a way that the model can be used for (i) process design (i.e. fixturing); and (ii) statistical process control to detect assignable causes of shape variation. To develop such model(s), the following issues needs to be addressed:

(i) Part shape error modelling: a generic model is required with capabilities to analyse CoP surface data of sheet metal parts or assemblies and providing information about *shape error* over a continuum of process parameters to reveal important aspects of the processes generating the data. For example, in the context of this thesis, the model should reveal important aspects of the process as related to SPC and also serve as a key enabler for process design (fixture layout optimisation for non-ideal parts). In particular, the shape error model should provide a parametric modal decomposition capability which can be further utilised in various application domains such as tolerance analysis and synthesis; assembly process design optimisation; shape error detection and process control; functional mapping of process parameters to correlate the root cause of the faults. As a consequence, this generic model,

also classified as functional data analysis in statistics, can play a crucial role in sheet metal parts shape error modelling and analysis.

(ii) Parts shape variation modelling: a functional data model of part shape error is a key enabler for representing and modelling parts *shape variation* of a batch of compliant sheet metal parts. The model of parts shape variation is based on the statistical characterisation of modal parameters coming not from a single part but also from a batch of parts. The model should help to quantify the shape variation incorporating all the significant shape error modes present in the production of a batch of parts. Therefore, the shape variation model can be used as enabler for process design which is robust not only to ideal (CAD) parts but also to a batch of non-ideal (real) parts.

(iii) Parts shape variation monitoring and detection (i.e. statistical process control to detect shape defects): efficient approaches for statistical process control of non-linear shapes are required to monitor the shape errors and detect the shape defects efficiently using high dimensional CoP data captured by in-process sensor networks. At present many industrial processes are capable of generating massive amount of CoP data which cannot be used for SPC and monitoring of shape variation.

(iv) Shape variation reduction at assembly process design (i.e. fixture layout optimisation): an efficient fixture modelling and optimisation method is required for assembly process simulation with compliant part considering the shape variation coming from the production parts. Fixture plays a dominant role in assembly system with compliant parts as it directly affects the dimensional and geometric quality of assembled product. Further, to mitigate the quality deterioration due to shape variation of compliant sheet metal

assembly, fixture must be modelled and optimised with shape variation. Therefore, it can predict the production yield of the assembly process and corrective actions can be taken to neutralise the high risk areas.

As evident from the aforementioned discussions, there are lack of modelling approaches to address the current challenges associated with shape variation modelling, analysis and statistical control. This chapter reviews past research on modelling of part shape error and parts shape variation, and further, application of these models in statistical process control and process design approaches.

The remaining part of this thesis is organised as follows: Section 3.2 reviews the approaches reported in literature to model part shape errors and identifies the research gap to model freeform shape errors. Section 3.3 reports the related work on shape variation modelling of a batch of compliant parts. Section 3.4 describes the current monitoring approaches and need of new control chart to detect shape defects. Section 3.5 reports the assembly fixture layout design and optimisation for compliant assemblies and current research gap of fixture optimisation considering production batch. Finally, Section 3.6 presents the summary.

3.2 RELATED WORK ON SHAPE ERROR MODELLING OF COMPLIANT PART

Most of the reported works in the field of shape error modelling are related to tolerance analysis, i.e. the variational feature modelling. The key principle behind the variational feature modelling is to model the functional features at design stage within the specified tolerance zone to meet the tolerance standards, such as ISO-1101 (2013) or ASME-Y14.5M (2009).

Initial studies were focused on modelling variational features as parametric models and then included them as part of CAD modellers (Requicha and Chan, 1986; Chase and Parkinson, 1991; Gupta and Turner, 1993). Then, these models are used for tolerance analysis. These approaches are also termed as parametric tolerancing and play a dominant role in current industrial design practice with application in tolerancing of rigid parts and assemblies. In these approaches tolerances for size, orientation and position are parameterised by few dimensions and modelled by offsetting the nominal geometry of a 3D solid model. Then, part variations are included into variational CAD modeller, for examples, Constructive Solid Geometry (CSG) with added feature-based approaches which parameterise the whole part geometry. In general, variations of key product features and dimensions are represented in statistical tolerancing as probability distribution functions.

A well-known approach to model variational features through rigid body motion is classified as Topologically and Technologically Related Surfaces (TTRS). It provides a methodology to divide complex part geometry into simple elementary components such as points, lines and planes (Clément *et al.*, 1998). The main idea is to represent the position and orientation of each feature by small rigid body movements. Moving forward from the TTRS theory, Whitney *et al.* (1994) introduced 4×4 variational matrix to simulate rigid body translation and rotational movements. These approaches are limited to small displacements and only deals with the representation and classification of functional features for rigid body, and cannot reapplied to model free-form shape errors. Therefore, products like sheet metal part with complex geometric features cannot be modelled by only using rigid body movements.

Pioneered research work on geometric tolerance representation can be found in Requicha (1983), Requicha (1984) and Requicha and Chan (1986). Few research works have been carried out to define the variation features for representation of geometric tolerances (Rossignac and Requicha, 1986; Requicha, 1984; Requicha and Chan, 1986; Requicha, 1983; Walker and Srinivasan, 1993). By offsetting the nominal surface of the product, the tolerance zone has been defined by two off-set bounded surfaces and all the functional features within these two bounded surfaces are being accepted as in-tolerance variation class. Walker and Srinivasan (1993) tried to define mathematical relation between the tolerance zone and variation class. Thereafter, several CAD modellers have adapted several approaches to compute the off-set surfaces in CAD models. In order to reach target accuracy, efforts have been made to increase the number of parameters to model the variational features (Turner and Wozny, 1987; Guiford and Turner, 1993). Subsequently, as the complexity of the geometric surface to be modelled increases, the number of parameters to be considered rapidly grows making the approach very difficult to use. To avoid this situation, Gupta and Turner (1993) proposed an alternative approach based on Bezier's triangle fitting and triangle patches to represent planar surface. Further, Li and Roy (2001) expanded Gupta and Turner's (1993) work by developing a sixteen-point bicubic surface interpolation method. These efforts can be classified as deterministic geometric tolerance (boundaries) representation with main focus on tolerancing of mechanical parts represented as solid models in CAD/CAM systems.

One of the critical problems in Geometric Statistical Tolerancing (G/ST) for a complex assembly is not only to represent and generate the tolerance zone (TZ), but also the variational classes of product instances (surface variations). Therefore, there is a strong need for modelling and characterisation of shape errors of part surface

feature which can be used for variation propagation modelling, as part of design optimisation of assembly process with compliant parts. To model and quantify shape errors within individual part, a unified and adaptive way is necessary. Additionally, the model should also provide a platform for batch of parts shape variation quantification, shape errors related defect detection, shape variation reduction through process design and enable storage of part shape error and variation information for future designs. To date only limited successes have been achieved in this aspect. The approaches for shape error modelling of compliant part can be broadly classified into two categories: (i) shape error representation; and, (ii) shape error decomposition. Table 3.1 summarises the research work carried out by different researchers to model part shape error under the category of shape error representation (see Section 3.2.1) and shape error decomposition (see Section 3.2.2).

Table 3.1 Literature review of part shape error modelling approaches with identified research gap

	Shape error representation (Reverse Engineering)	Shape error decomposition	
		Nominal Data Decomposition (CAD- Based)	Measured Data Decomposition (CoP- based)
1D	-	Merkley (1998)	Srinivasan and Wood (1997); Bihlmaier (1999)
2D	Capello and Semeraro (2000); Capello and Semeraro (2001); Duta *et al.* (2001); Srivastava and Jermyn (2009)	Tonks (2002)	Huang and Ceglarek (2002); Huang *et al.* (2014)
3D	Gupta and Turner (1993); Raffin *et al.* (2000); Sorkine (2006); Stoll *et al.* (2006); Franciosa *et al.* (2011); Wagersten *et al.* (2014)	Samper and Formosa (2006); Ungemach and Mantwill (2008)	**Proposed in this thesis**

3.2.1 Shape Error Representation

Shape error representation adapts reverse engineering approach where the manufactured part is measured and mapped into the CAD model to derive the shape errors associated with the manufactured part (Gupta and Turner, 1993; Raffin *et al.*, 2000; Stoll *et al.*, 2006; Franciosa *et al.*, 2011; Liang *et al.*, 2012). Reverse engineering approach is well-known in literature to represent the part deviation from design nominal. A number of efforts have been made to represent the variational features directly from the measured parts. Gupta and Turner (1993) used constructive solid geometry-based (CSG) modeller and surface-based variational modelling to embed shape errors with nominal geometry. B-spline and NURBS patches with few control points were used to model simple geometry which were then integrated to represent the whole part (Cubélès-Valade and Riviere, 1999; Raffin *et al.*, 2000; Pottmann and Leopoldseder, 2003). Raffin *et al.* (2000) presented a deformation model to represent part surface geometry based on the simple constrained deformation (scodef) model. This model is used for representing geometry modifications based on the magnitude of deformations for each point (also known as control point) on the part given by the user. These methods have limited applications in representing accurately the shape errors of the part which are composed of a set of patches due to large number of control point required for the constrained deformation.

A comprehensive method for representation of whole part surface geometry has been proposed by Sorkine *et al.* (2004) and Sorkine (2006) which is based on the Laplacian mesh deformation by relative movement of each vertex to its neighbourhood mesh nodes. The main application domain of Laplacian mesh deformation is in the field of computer graphics where the method furnishes a

variety of processing applications, such as shape approximation and compact representation, mesh editing, watermarking and morphing.

Sorkine's (2006) work has been extended by Stoll *et al.* (2006) where they tried to reconstruct the surface from the measured data. The CAD based template surface mesh has been deformed by using Laplacian mesh deformation to fit measured CoP data. Capello and Semeraro (2000; 2001) applied harmonic fitting model to fit the geometrical shape with discrete measurement points for inspecting machined components. However, harmonic fitting model is limited to planar, cylindrical or conical surfaces.

A similar approach of surface representation has been adapted where nodes of the mesh model are moved by morphing procedures (Franciosa *et al.*, 2011; Liang *et al.*, 2012; Wagersten *et al.*, 2014; Schleich *et al.*, 2014). They used few control points to parameterise the whole geometry and deform the template mesh through morphing mesh procedure. Therefore, by varying the control points a number of shape errors of part can be created. However, morphing approach with control points struggles to represent shape error of free-form 3D part geometry and the number of control points increases significantly with increase in geometric complexity.

The abovementioned approaches are mainly used to represent the shape error associated with a surface which has limited capability for statistical tolerance analysis by generating variational part instances. Further, in context of this thesis, the shape error representation is not sufficient to reveal important aspects of the process generating the shape error or to provide a parametric approach for tolerance analysis and synthesis; shape error detection and process control and assembly process design optimisation (fixture layout optimisation for non-ideal parts).

3.2.2 Shape Error Decomposition

To satisfy the need of a generic model with capabilities to extract underlying process information from measured CoP data, a functional data analysis based *shape error decomposition* can play a significant role in assembly process simulation with compliant sheet metal parts. Previous studies reports numerical and analytical attempts to establish the relationship between part shape errors and the source of variation by decomposing shape errors into *shape error modes*. However, shape error decomposition remains a challenging problem due to unavailability of functional data analysis based approach relying on CoP measurement data.

Many of the shape error models are based on geometric covariance based approaches. The geometric covariance defines the geometrical relation among the neighbouring points on the same surface to assure surface continuity and smoothness. Use of bounded random Bezier curves to model shape errors has been proposed by Merkley (1998) where the geometric covariance matrix within given the tolerance limit has been determined. Shape error has been parameterised by constraining the displacement of the control points of Bezier curves. The random Bezier curves provide a method of mapping profile tolerance of a curve to tolerance bands of the Bezier control points. The geometric covariance matrix (**Σ**) can be calculated as

$$\Sigma = \sigma^2 \cdot \left(A^T \cdot A \right)^{-1} \tag{3.1}$$

where, A is a rectangular matrix related to Bernstein polynomials, defining the Bezier curve and σ denotes the standard deviation associated to the tolerance band of Bezier control points.

Merkley's (1998) approach mainly focusing on one dimensional profile feature and potentially can be extended to rectangular Bezier patches. However, for free-form shapes, such as automotive sheet metal components, the parameterisation of the Bezier patches becomes non-trivial task and exhibits limitation for real implementation of variational feature modelling of real part.

Merkley's (1998) work has been extended by Bihlmaier (1999) to model profile as a finite summation of sinusoidal waves of varying magnitude and wavelength. Fourier transform has been used to transform the profile into frequency domain and the profile is decomposed into sinusoidal waves having different wavelengths and magnitudes.

As an extension of the methods proposed by Merkley (1998) and Bihlmaier (1999), a hybrid method has been proposed by Tonks (2002) to model the two dimensional surface errors by using decomposition of wavelengths. The hybbrid method uses two modelling technique: (i) Legendre polynomial to model the long wavelengths; and, (ii) frequency spectrum to model the shorter wavelengths. The hybbrid method was by validated using experimental data. However, this approach limited to two dimensional cases which is also inadequate to model 3D free-form shape errors.

Another approach has been reported in literature regarding the decomposition of shape errors based on the modal decomposition with main focus on geometric tolerancing. As per ANSI Y14.5M standard, geometric tolerances can be sub classified into form, orientation, location, and run-out tolerances (Walker and Srinivasan, 1993). Early studies related to shape error decomposition mainly focused on form tolerancing. One of the drawbacks of the ANSI Y14.5M standard is the lack of formal mathematical definition of form/shape errors. Therefore, Srinivasan and

Wood (1997) made an attempt to provide a mathematical representation of the form error tolerancing with the help of wavelet transform which is well known in the field of signal processing. They presented an enhanced shape error profile modelling method based on wavelet decomposition. The main idea is to decompose the free-form shape error profile using fractals and wavelets by establishing the relationship between fractals and wavelets in order to extract the principal deformation mode from the profile feature which is limited to one dimensional case. This approach is mostly suitable for localised and non-stationary error patterns instead of global error patterns whereas shape errors of compliant sheet metal parts can be considered as stationary and mainly composed of global errors. Further, wavelet decomposed error patterns are difficult to explain, especially in terms of GD&T tolerances.

Huang and Ceglarek (2002) and Huang *et al.* (2014) developed Statistical Modal Analysis (SMA) approach for 2D shape error decomposition into main deformation modes which are then characterised by manufacturing process parameters. The SMA method is based on Discrete Cosine Transform (DCT) technique and was applied to real measurement data. Further, the SMA method was used for quality monitoring, root cause diagnosis of shape errors, and process capability study in manufacturing. The main limitation of SMA approach is that shape error field is distributed as 2D rectangular space. Therefore, this approach cannot be applied to decompose real 3D sheet metal parts. Many sheet metal parts consist of several features such as holes, slots, edges which are not modelled by the SMA model. Therefore, a more generic approach is required to model and characterise 3D shape error associated with real sheet metal parts.

To model and characterise 3D shape error associated with real part, Samper and Formosa (2006) developed natural mode decomposition approach which is based on

free vibrational modal shapes of structural mechanics. Unlike SMA method where the decomposition was performed directly on the shape error field, the natural mode decomposition in based on the nominal CAD data, and then, the decomposed modes are compared with measured shape error field to obtain shape error modes.

The shape error decomposition by using natural mode decomposition approach is based on following steps: *firstly*, the nominal geometry is meshed to obtain mass and stiffness properties associated with the part. In linear dynamics, equations of conservative systems (e.g. a mass-spring system) can be written as follows

$$M \cdot \ddot{q} + K \cdot q = 0 \qquad \textbf{(3.2)}$$

where the dynamic equilibrium of the system is preserved. $M(N \times N)$ and $K(N \times N)$ represents the squared mass and stiffness matrices, respectively. The displacement vector for each node of the mesh is represented as $q(N \times 1)$. Solution to the equation (3.2) is determined by evaluating eigenvectors and eigenvalues related to the matrix $K^{-1} \cdot M$. The obtained eigenvectors are linearly independent to each other. Therefore, orthogonal modal matrix consist of main deformation modes is built (the column vector of the modal matrix). *Secondly*, the deformation modes are mapped with the original measurement to identify the individual shape error modes. The natural mode decomposition can be applied to decompose free-form shape errors; however, the method suffers from the accurate decomposition of global shape errors associated with sheet metal parts.

A similar nominal CAD data based decomposition approach proposed by Ungemach and Mantwill (2008) where the part is decomposed using the buckling principle instead of free vibrational modal shapes as in Samper and Formosa (2006). The first obtained eigenvector mode has been utilised to generate the initial variational

geometry in assembly process simulation. The buckling modes have no physical significance, especially in terms of GD&T applications.

As evident from the detail review of the reported work on shape error decomposition, current approaches can be classified into main two different categories:

(i) *Decomposition based on nominal CAD data*: Firstly, the nominal CAD model of the part is decomposed considering the material properties of the part, and then, the decomposed modes are compared with the measurement data to obtain shape error modes (Merkley, 1998; Tonks, 2002; Samper and Formosa, 2006; Ungemach and Mantwill, 2008).

(ii) *Decomposition based on measured CoP data*: Firstly, the part is measured as CoP to obtain the shape error field by computing deviation from nominal CAD Part, and then, the shape error field is decomposed into shape error modes (Srinivasan and Wood, 1997; Bihlmaier, 1999; Huang and Ceglarek, 2002; Huang *et al.*, 2014).

Extraction of all types of shape error modes, which are present in the real measurement data, might not be possible through decomposition based on nominal CAD data. Due to absence of few shape error modes obtained by nominal CAD data decomposition, limited accuracy is achieved during reconstruction of the measured shape error field. Therefore, there is a need to decompose the real measurement data (CoP) of 3D part into main shape error modes. Additionally, the shape error decomposition model should have the capabilities not to be affected by various part features such as slots, holes, curvatures or curved edges etc. As a consequence, functional data analysis based measured CoP data decomposition can play a crucial role in sheet metal parts shape error decomposition and analysis. This thesis attempts

to develop a generic functional data analysis approach named ***Geometric Modal Analysis (GMA)*** to decompose measured part shape error into shape error modes. The proposed GMA methodology with industrial case application is reported in Chapter 4. The most relevant shape error decomposition methods available in literature are listed in Table 3.2 with the underlying principle and main limitations.

Table 3.2 Major shape error decomposition approaches with applications and limitations

Researchers	Decomposition principle	Applications	Limitations
Merkley (1998); Bihlmaier (1999); Tonks (2002)	Geometric covariance with Legendre polynomials and frequency spectrum analysis	Statistical tolerancing, assembly process simulation, tolerance allocation	Decomposition of 1D profile or 2D surface but inadequate to decomposed 3D sheet metal part
Huang and Ceglarek (2002); Huang *et al.* (2014)	2D Discrete Cosine Transform (2D DCT)	Quality monitoring, root cause diagnosis, and process capability study	Decomposition of 2D rectangular part but insufficient for decomposing 3D sheet metal parts
Samper and Formosa (2006); Ungemach and Mantwill (2008)	Natural mode decomposition or buckling mode decomposition	Geometric Tolerancing, assembly process simulation, variation analysis	Decomposition of 3D part but limited accuracy due to nominal CAD based decomposition
Proposed in this thesis	Laplace interpolation of 3D voxel space; decomposition using generalised 3D DCT	Statistical process control, design optimisation (fixture layout)	Normal deviation assumption and ideal for global shape errors

3.3 RELATED WORK ON SHAPE VARIATION MODELLING OF COMPLIANT PARTS

A batch of sheet metal parts or machined components, produced by forming process or machining process, contains numerous shape errors. The *shape variation* can be defined as aggregation of all shape error modes with their magnitude associated with a batch of parts which in principle represents the *production shape variation*. These shape variations are mainly results of process parameters variation, tool wear or spring-back in case of sheet metal stamping process (de Souza and Rolfe, 2008). Therefore, modelling and prediction of shape errors associated with individual non-ideal part is not sufficient to meet industrial needs which emphasises to model and quantify the shape variation engraved within a batch of parts. Assembly system modelling which takes into consideration only one ideal or real compliant part does not represent the real scenario of production shape variation associated with production batch. Further, as production yield purely depends on the real production parts, part shape error model fails to depict the real shape variation of production parts and is not adequate for assembly system modelling. Therefore, efficient approach is required to model and quantify the shape variation of production batch.

As mentioned in Section 3.2, the *shape error modelling* approaches are categorised into *shape error representation* and *shape error decomposition*. Current shape error representation approaches represent the shape errors through reverse engineering for individual part (Gupta and Turner, 1993; Raffin *et al.*, 2000; Stoll *et al.*, 2006; Franciosa *et al.*, 2011; Liang *et al.*, 2012). These shape error representation approaches either limited to reconstruct the shape errors accurately or they are unable to control 3D part geometries, such as sheet metal part, as they are driven by few control points to deform the whole part surface. Therefore, current shape error

representation approaches do not have capability to be extended for modelling and quantification of shape variation for compliant parts of production batch.

On the other hand, *shape error decomposition* approaches have the potential to be extended for modelling and quantification of shape variation as the shape error decomposition extracts orthogonal shape error modes from the measured shape errors. These shape error modes can adapt varying modal magnitudes to fit measured shape errors associated with a batch of parts. Therefore, shape error decomposition provides a platform to obtain parametric shape error modes which can be used as building block for shape variation modelling. Therefore, shape error decomposition approaches have the potential to represent production shape variation. As mentioned Section 3.2.2, the shape error decomposition approaches can be classified into main two categories based on the types of data used for decomposition: (i) decomposition based on nominal CAD data; and, (ii) decomposition based on measured CoP data. A limited number of research works has been reported in literature addressing shape variation under the aforementioned two decomposition categories. Further, shape variation modelling involves two aspects: (i) virtual generation of shape variation, i.e. virtual representation of production part instances; and, (ii) quantification of shape variation, i.e. aggregation of the major shape error modes present within a batch of compliant parts. To address these two aspects of shape variation modelling, it is found that present research reported in literature is mainly focusing on virtual generation of production parts and no method can be found to address the quantification of shape variation. Subsequently, based on the decomposition category and shape variation modelling aspects, the reported methodologies are listed in Table 3.3 with the identified research gap.

Table 3.3 Literature review of shape variation modelling approaches with identified research gap

		Nominal data Decomposition (CAD-based)	Measured Data Decomposition (CoP-based)
Shape variation modelling	Virtual generation of shape variation	Samper *et al.* (2009)	Camelio *et al.* (2004b) Huang *et al.* (2014) **Proposed in this thesis**
	Quantification of shape variation		**Proposed in this thesis**

The following section describes the available methodologies in details under the decomposition category with their efforts to address the two aspects of shape variation modelling (as per Table 3.3):

(i) *Decomposition based on nominal CAD data*: The natural mode decomposition approach proposed by Samper and Formosa (2006) for a single part has been extended to shape variation model of batch of parts (Samper *et al.*, 2009). Samper *et al.* (2009) represent shape variation through identifying the modal parameters with their mean and standard deviation. The method assumes the normal distribution of the modal parameters and can be used for virtual generation of variational parts (i.e. representation of production part instances) using the estimated mean and standard deviation from the measurement data. For complex fabrication process, such as sheet metal stamping, normality assumption is far too simplified and not necessarily true that the process will follow normal distribution. Especially, sheet metal stamping exhibits variance shift or mean shift behaviour for within batch or batch-to-batch production where

normality assumption of shape error modes is not valid. Further, virtual generation of variational parts is not sufficient to quantify the shape variation. Therefore, an efficient shape variation model is required which can overcome the normal distribution assumption and also quantifies the production shape variation.

(ii) Decomposition based on measured CoP data: Currently, parts shape variation modelling approaches based on measured CoP data decomposition reported in literature are (a) geometric covariance decomposition based on Principal Component Analysis (PCA); and (b) Statistical Modal Analysis (SMA) based on 2D Discrete Cosine Transform (2D DCT). The *first* approach, geometric covariance decomposition has been developed by Camelio (Camelio, 2002; Camelio et al., 2004b) to model the assembly variation propagation with compliant parts. They extended Merkley's work (Merkley, 1998) on geometric covariance combined with Principal Component Analysis (PCA) to estimate the effect of parts shape variation at assembly level using Finite Element Analysis (FEA). To extract the main shape error modes from the measurement data, PCA decomposition has been used to decompose geometric covariance of parts into individual contributions of these shape error modes. However, PCA based decomposition is not suitable for shape error characterisation as it is incapable for detection of process shift in primary data set or presence of different shape errors in the data (Matuszyk *et al.*, 2010). As real process of part stamping clearly exhibit mean shift or variance shift of shape errors for within batch production and batch-to-batch production, PCA based shape variation is not suitable. As a consequence, the measured part errors need to

be decomposed independently to provide more accurate estimation of underlying shape errors. To decompose the shape errors into independent shape error modes, Huang and Ceglarek (2002) and Huang *et al.* (2014) develop the *second* approach named statistical modal analysis which is based on 2D Discrete Cosine Transform (2D DCT). The SMA method is mainly limited to 2D part and measurement data points are placed in regular rectangular grid. On the contrary, sheet metal parts used for automotive and aerospace body are 3D parts in nature. Therefore, SMA approach cannot be applied to model shape variation of 3D sheet metal parts.

As evident from the abovementioned discussion, current shape variation modelling techniques have limitations which are: (i) normality assumption of shape error modes; (ii) shape errors decomposition into independent shape error modes; and (ii) virtual generation of variational parts which is not sufficient in the context of assembly process modelling that requires shape variation quantification model. Currently, there is no approach found in literature to model and quantify the shape variation of a batch of compliant parts. Therefore, functional data analysis based parametric approach is required where the decomposed shape error modes can be used as elementary building blocks, and further, these building blocks can be parameterised with their magnitude to model shape variation. To address the generic model requirement for shape variation, this thesis extends the part shape error modelling approach (GMA) to model shape variation of a batch of compliant parts by characterising the statistical nature of decomposed modes. Further, the normality assumption of decomposed modes has been eliminated by using data driven Kernel Density Estimation (KDE). The shape variation model can be further utilised for statistical tolerancing and assembly performance evaluation.

Till date, the shape variation modelling approaches are limited to variational virtual part generation by randomly selecting shape error modes from the distribution without quantifying the shape variation associated with production parts. Therefore, the following challenges are associated with shape variation modelling:

(i) *Virtual generation of shape variation:* Accurate depiction of shape error modes is required based on measurement data to represent the real scenario of production parts. Further, the virtual generation of the variational parts will be representative of production parts.

(ii) *Quantification of shape variation:* Shape variation quantification for 3D production parts in not a trivial task as it involves identification of major shape error modes from production batch and aggregation technique of the major shape error modes. All the major shape error modes coming from the production parts are to be considered in an effective way to represent the quantified shape variation.

To address the aforementioned challenges, this thesis extends the previous functional data analysis approach Geometric Modal Analysis (developed in Chapter 4) to ***Statistical Geometric Modal Analysis (SGMA - proposed in Chapter 5)*** for modelling and characterisation of shape variation of a batch of compliant parts.

3.4 RELATED WORK ON SHAPE VARIATION MONITORING AND CONTROL OF COMPLIANT PARTS

In the field of statistical process control, traditionally, the point-based CMM measurements are being used which consequently led to point-based statistical control charts (Montgomery, 2008). For example, 15-25 measurement points are used for inspecting a single automotive stamped door during production (Wells *et al.*, 2012). Traditional SPC methods, such as $\bar{X}$ chart, R chart, Cumulative Sum (CUSUM) and/or Exponential Weighted Moving Average (EWMA) are widely implemented in industry. However, these charts have limited capability to handle high dimensional CoP data and extract useful shape error related information from the data. Therefore, more proactive technique is required to monitor the shape variation related defects. However, developing a single or two control charts is not trivial since the entire part surface information to be monitored which is captured as a high volume of CoP. Further, the captured CoP data can be classified as non-functional data as it cannot be used directly. To extract shape error information from the data, Ramsay and Silverman (2005) suggested functional data analysis based model development for non-functional data (e.g. CoP data).

Currently, multivariate statistical process control chart uses as *functional data analysis* model either Principal Component Analysis (PCA) or Partial Least Squares (PLS) to remove high degree of redundancy in the measured data (such as CoP data) by defining a reduced set of statistically uncorrelated variables (Chen *et al.*, 2004; Antory, 2007; Phaladiganon *et al.*, 2013). The T^2 and Q statistics are frequently used for multivariate statistical process control. Integrated T^2-Q monitoring chart has enhanced incipient faults detection capability when dealing with multivariate process (Chen *et al.*, 2004). It provides single control chart with improved sensitivity to

defects detection as compared to individual T^2 or Q statistics. However, the PCA-based T^2-Q control chart is not capable of detecting process shift in primary data sets; or indicates different shape errors variance change as compared to real manufacturing processes. For example, PCA-based or PLS based T^2-Q control charts present incorrect shape errors estimation for within-run production; or incorrect mean shift estimation for run-to-run production of stamped sheet metal parts. Similarly, classification or matching of shape-error faults (test images) to pre-defined template images such as CAD models with GD&T requirements is critical to ensure product quality. PCA-based T^2-Q control charts do not have the ability to distinguish between in-control process shift or variance change for shape measurement data which can be observed in real processes such as within-batch or batch-to-batch production (see case study Section 6.4). This is an important requirement when classifying parts based on the similar shape errors types or comparing image against template CAD. Therefore, the PCA based T^2-Q control chart is not effective for part shape error characterisation. To overcome the identified challenges, this thesis proposes a new direction of obtaining reduced set of statistically uncorrelated and independent process variables by decomposing the data set within a single sample (GMA method – details in Chapter 4) instead of PCA- or PLS-based decomposition which is done across the samples as illustrated in Figure 3.1. PCA- or PLS-based decomposition is done across the sample set to obtain the principal components (e.g. PC_1, PC_2, … PC_n) explaining the variance within the data set and T^2 statistic is determined based on the obtained principal components. On the contrary, functional data analysis based GMA method provides uncorrelated and independent modes (e.g. C_1, C_2, … C_p) by decomposing the correlated variables within a single sample and all samples are to be decomposed separately for

determining the T^2 statistic. This emphasises the enhanced granularity of decomposition which then leads towards enhanced shape fault detectability.

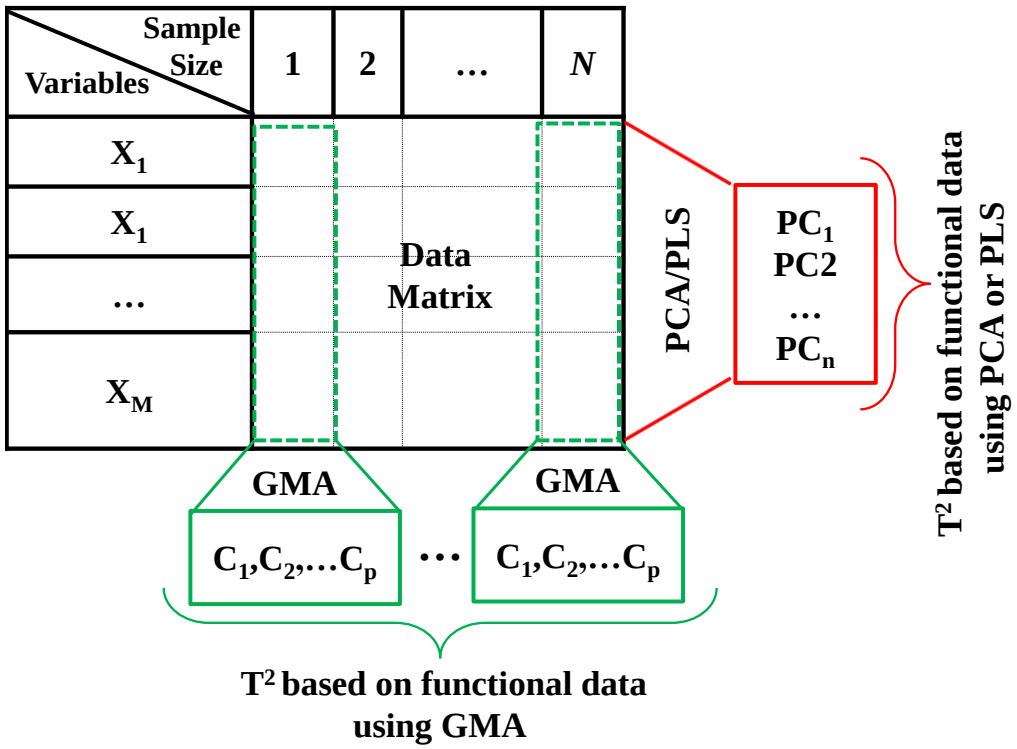

Figure 3.1 Current PCA- or PLS-based approaches vs. the proposed GMA-based decomposition approach

Current multivariate statistical process control techniques based on functional data analysis models can be categorised into (i) point features based control charts; (ii) profile features based control charts; and (ii) surface features based control charts. To date, very few attempts have been made to develop monitoring techniques for part form defects as defined by GD&T: (a) profile errors, and/or (b) surface errors. A review of literature focusing on control charts to monitor point features, profile features and surface features is summarised in Table 3.4. It underscores lack of current methods for control charts to monitor part shape errors and identifies the research gap.

Table 3.4 Multivariate statistical process monitoring approaches and research gap for shape error related defects monitoring

	Multivariate Statistical Process Control		
Functional Data Analysis based Control Charts	Point Monitoring and Control		Kourti and MacGregor (1995) Chen *et al.* (2004) Antory (2007) Phaladiganon *et al.* (2013)
	Profile Monitoring and Control		Jin and Shi (2001) Woodall *et al.* (2004) Woodall (2007) Colosimo *et al.* (2010) Huang *et al.* (2014)
	Surface Monitoring and Control	Localised Errors	Acciani *et al.* (2006) Du-Ming and Jie-Yu (2011) Du-Ming *et al.* (2012) Wang (2011)
		Shape Errors	**Proposed in this thesis**

The most popular control charts are to monitor *point* features. For example, the most popular are univariate control charts of point features monitoring which are also extended to multivariate control chart (Montgomery, 2008). Further, control charts based on variations, functional data analysis approaches such as PCA, PLS have been developed for multivariate data obtained from point feature measurement (Kourti and MacGregor, 1995; Phaladiganon *et al.*, 2013; Chen *et al.*, 2004).

Woodall *et al.* (2004) stated that little research has been done in the statistical monitoring of process or product *profiles* with control charts. Some of the methods developed for profile monitoring are based on Haar wavelet transform (Jin and Shi, 2001), Spatial Autoregressive Regression (SARX) model (Colosimo *et al.*, 2010),

PCA for profile data (Colosimo and Pacella, 2007) or quantile–quantile (Q–Q) plot (Wang and Tsung, 2005; Wells *et al.*, 2013a). However, profile monitoring techniques do not reveal all types of errors within a part as it is needed for surface or shape features (Woodall, 2007).

Part *surface* defects can be categorised into (i) localised errors, such as scratches, cracks, or wear (Du-Ming and Jie-Yu, 2011); and, (ii) shape errors such as part bending, twisting, or more complex shape defects such as complex form defects. Few functional data analysis based control chart techniques have been reported for *localised errors* detection in electronics assembly. Some of the methods developed for localised errors based surface monitoring and defects detection are based on mean shift technique (Du-Ming and Jie-Yu, 2011), wavelet transform of captured images (Acciani *et al.*, 2006), similarity measure (Du-Ming *et al.*, 2012), or PCA / PLS (Wang, 2011). These methods are mainly focused on localised surface defects detection and are not suitable for shape error detection. The challenges for shape error related defects detection and monitoring can be classified into three categories: (i) freeform shaped part geometry based shape errors are needed to be parameterised, (ii) efficient functional data model is required (bridged with CAD model) to emulate real part, and (iii) extracting most significant shape error modes (can be used as parameters) which can facilitate quality monitoring. Current approaches of shape error parameterisation are either inaccurate (Samper and Formosa, 2006) or not applicable to 3D sheet metal part (Huang *et al.*, 2014). Therefore, they cannot be used as functional model for shape error monitoring. To overcome these challenges, this thesis proposes a functional data analysis approach, named Geometric Modal Analysis (GMA), to quantify the shape errors within 3D sheet metal part. It decomposes the full spectrum of errors into main significant patterns.

In this thesis, GMA-based functional data analysis approach has been used to determine multivariate T^2 statistic. The measurement uncertainties in data are kept in Q statistic to improve the detectability of the control chart. Combining T^2 for the GMA modelled data and Q statistic for residual data (un-modelled) provides a bivariate scatter plot which is easier to monitor and also increases the sensitivity of the control chart towards fault detection than the individual T^2 and Q monitoring statistics. Integrated T^2-Q monitoring chart has enhanced incipient faults detection capability when dealing with multivariate process (Chen *et al.*, 2004). Further, as the measurement data of 3D shapes are non-normal, the shape monitoring chart is based on the joint probability density estimation of the integrated two statistics using non-parametric Kernel Density Estimator (KDE) which has enhanced sensitivity to detect part defects. The *GMA-based integrated T^2-Q bivariate monitoring chart* is proposed for statistical process monitoring of non-linear shapes (proposed in Chapter 6).

3.5 RELATED WORK ON ASSEMBLY FIXTURE LAYOUT OPTIMISATION CONSIDERING PRODUCTION BATCH

Jigs and fixtures are used to hold the parts to be assembled at correct position and orientation during the assembly/joining operation. The primary objective of any fixture is to satisfy dimensional quality requirements of the product by locating, supporting and providing the suitable orientation of the parts which are mainly restraining the rigid body motion. However, only restraining the rigid body motions is not sufficient when dealing with compliant sheet metal parts as shape variation needs to be taken into consideration to get to obtain uniform quality during assembly operation. To mitigate and reduce the shape variation in assembled product, proper fixture layout optimisation is a necessary step. For example, current emerging joining process like RLW requires to satisfy the requirements of tight Key Product Characteristics (KPCs are the quality indicators, such as part-to part gap) control. Failing to meet the requirement, it results in unsatisfactory weld quality. Therefore, to meet the part-to-part gap requirement, fixture layout optimisation is necessary as one of the fixture elements, i.e. clamps, control the KPCs requirement. Therefore, fixture plays a significant role to achieve desired dimensional and joining qualities (KPCs) of assembled product where fixture design parameters act as Key Control Characteristics (KCCs are the control parameters to satisfy the product quality, such as clamps, locators, support blocks). On the other hand, production quality depends on production parts which refer to shape variation reduction through fixture layout optimisation. To mitigate the quality deterioration due to shape variation of compliant sheet metal assembly, fixture must be modelled and optimised with shape variation considering production parts.

Several works have been reported in the field of assembly fixture design which can be classified into two categories based on the types of error considered during assembly: (a) individual part shape error based assembly – only single part instance (i.e. part shape error) has been considered during fixture design and optimisation; and, (ii) batch of parts shape variation based assembly – where the shape variation of the production parts has been considered during fixture design and optimisation. To address the shape error or shape variation of compliant sheet metal parts, researchers have mainly used 'N-2-1' locating scheme rather '3-2-1' for better product quality. State-of-the-art approaches available in literature for fixture layout optimisation considering error types are listed in Table 3.5 which exhibits the research gap this thesis focused on.

Table 3.5 Literature review of fixture layout optimisation approaches with identified research gap

	Fixturing Scheme	
	'3-2-1' Fixture	'N-2-1' Fixture
Individual part shape error based assembly	Rearick *et al.* (1993); Ceglarek (1998); Li *et al.* (2008c)	Cai et al. (1996); Li *et al.* (2001); Camelio *et al.* (2004a); Cai (2008); Li et al. (2008a); Yu *et al.* (2008); Li et al. (2010) ; Franciosa *et al.* (2011)
Batch of parts shape variation based assembly	-	**Proposed in this thesis**

The well-known locating principle ‘3-2-1’ is widely used in industries to locate rigid body parts without creating locator interferences (Lowell, 1982; Shirinzadeh, 2002). Fixture analysis for sheet metal part first proposed by Youcef-Toumi *et al.* (1988) where they used a single sheet metal plate for drilling operations in order to minimise deflection in the part. The fixture locations determination work has been extended to compliant sheet metal parts by Rearick *et al.* (1993) where they proposed a technique combining the nonlinear programming and finite element analysis for determining the best fixture locations. In case of flexible part assembly, Ceglarek (1998) mentioned a systematic method of flexible/adaptive assembly system evaluation, based on its ability to compensate for part dimensional variability caused by assembly process. Further, Li *et al.* (2008c) proposed integrated layout design for a 3-2-1 fixture scheme used in sheet metal assembly to reduce variation cost efficiently. Though 3-2-1 fixturing scheme is less complicated and easy to manufacture, unfortunately, this type of fixture is not able to mitigate the risk associated with the shape variation of compliant parts. Therefore, for compliant sheet metal joining process, 3-2-1 fixturing is not sufficient which emphasise on more locator in primary datum plane. Compliant parts like sheet metal parts cannot be controlled through ‘3-2-1’ scheme which require larger number of locators to ‘N-2-1’ to minimise geometric deviation (N>3).

For compliant part fixturing, Cai *et al.* (1996) proposed ‘*N*-2-1’ locating principle which allows to prevent excessive deformation of sheet metal parts and they developed an optimal fixture design method, which can reconfigure the *N* locators on the primary datum to minimize total part deformation. Lee *et al.* (1999) also mentioned that ‘3-2-1’ fixture mainly used to restrained 6 degree of freedom of a rigid part which is not sufficiently valid for a large stamped part due to its own

weight or welding forces. Therefore, they Lee *et al.* (1999) presented a system for fixture design for 'N-2-1' scheme to hold large flexible workpiece to minimise geometric deformation. For sheet metal assembly process, the error budgeting can be classified in three different categories, part error variation, fixture error variation and joining process variation (Liu and Hu, 1997; Rong *et al.*, 1999; Camelio *et al.*, 2004a). Camelio *et al.* (2004a) presented a new fixture design methodology for sheet metal assembly process focusing on the impact of fixture position on the dimensional quality of sheet metal parts after assembly considering the effect of part variation, tooling variation and assembly spring-back. A number of research articles focuses on the assembly joining process modelling considering resistance spot welding as joining process and parts are modelled as individual part errors (Cai, 2008; Li *et al.*, 2008a; Li *et al.*, 2010; Li *et al.*, 2008b).

In case of laser welding, fixture plays a vital role by providing the degree of metal fit-up required for joining the mating parts together. Li *et al.* (2001) proposed a predictive and corrective fixture design methodology incorporated with finite element analysis for laser welding where the objective function is to minimise the degree of Metal Fit-up (DMF as maximum distance between mating nodes) in weld joints. Several issues related to part fit-up are mentioned in literature where the part error is higher than the joining process requirement by laser and showed that 'N-2-1' locating scheme is required to meet the joint quality criteria (Li and Shiu, 2001; Li *et al.*, 2002b; Li *et al.*, 2002a; Li *et al.*, 2003). These existing methods for fixture layout optimisation are mainly based on individual ideal/non-ideal compliant assembly which are not sufficient to mitigate the shape variation associated with batch of assemblies. For example, one of the new emerging joining process Remote Laser Welding (RLW) specifically required very tight control of part-to-part gap of

the joining surfaces (Ceglarek, 2011). Failure to meet the part-to-part gap requirement, RLW results in welding defects, such as under-cut, porous weld, poor finishing and corrosion prone. As a consequence, a robust fixture layout optimisation methodology is required considering batch of parts for making the output results insensitive to shape variation and improving the product and process performance.

This thesis is to develop a novel robust methodology for fixture layout optimisation (proposed in Chapter 7) by addressing shape variation which has been modelled and quantified by using Statistical Geometric Modal Analysis (SGMA – also developed in this thesis - Chapter 5) method.

3.6 SUMMARY

The literature review and discussions reported in this chapter show the limitations of currently available state-of-art approaches and methodologies to meet the industrial needs for 'Shape Variation Modelling, Analysis and Statistical Control' in the context of assembly system modelling with compliant parts. Current modelling and simulation requirements for shape variation modelling, analysis and statistical control can be enumerated into *two* enabling models as (i) modelling and characterisation of *shape error* of compliant sheet metal part; and, (ii) modelling and characterisation of shape variation of a batch of compliant sheet metal parts. Subsequently, shape variation monitoring by using statistical process control and shape variation reduction at process design have been identified as *two* important applications in the context of assembly system quality improvement.

This chapter reviews the literature for shape variation modelling, analysis and statistical control requirements. Further, this chapter reports the research gaps as follows:

(i) *Modelling and characterisation of shape error of compliant sheet metal part*: There is a lack of modelling approach for shape error modelling of 3D compliant sheet metal part. The shape error modelling of compliant part can be broadly classified into two categories: (i) shape error representation; and, (ii) shape error decomposition. As shape error representation is not suitable for generic functional data analysis based shape error model development, shape error decomposition approaches have been identified as appropriate. However, current shape error decomposition methodologies are either suffering from accuracy as compared with measured part or limited to 2D applications. Therefore, a 3D part shape error decomposition methodology is required which can decompose the measured shape errors into shape error modes. To address this research gap, this thesis proposes a *functional data analysis* model, named Geometric Modal Analysis (GMA), to model and analyse the shape error of compliant part (proposed in Chapter 4).

(ii) *Modelling and characterisation of shape variation of a batch of compliant sheet metal parts*: Current shape variation modelling approaches are simplified either with the normality assumption of decomposed shape error modes or limited to virtual generation of variational part instances. There is no approach found in literature to quantify the shape variation of a batch of compliant parts. To overcome the limitation on normality assumption and quantify the shape variation of a batch of compliant sheet metal parts, Chapter 5 develops Statistical Geometric Modal Analysis (SGMA) model as an extension of GMA model.

(iii) *Shape variation monitoring and control to detect shape errors related defects:* Current non-contact metrology scanners can capture entire surface

information in terms of high density CoP data which has potential to be used for shape variation monitoring and defects detection. Current statistical process control techniques can be classified into (i) point monitoring and control; (ii) profile monitoring and control; and, (iii) surface monitoring and control. The available techniques for surface monitoring and control are mainly focused on localised errors, such as scratches, cracks, or wear which neglects the global shape errors such as part bending, twisting, mean shift or variance change. To address the requirements of shape monitoring, Chapter 6 develops GMA-*based integrated bivariate* T^2-*Q monitoring chart* where T^2 statistic is based on the GMA modelled reduced variable set and *Q* statistic is determined based on residual data.

(iv) Assembly fixture layout optimisation considering production shape variation: There are many reported work in literature to develop assembly fixture considering compliant nature of sheet metal parts which are mainly based on either ideal part or individual part shape error based assembly. The literature survey identifies the research gap as lack of efficient simulation and optimisation approach to obtain an optimised N-2-1 fixture layout considering a batch of non-ideal sheet metal parts. Chapter 7 develops an assembly fixture layout optimisation methodology considering the shape variation (quantified using SGMA method) coming from the production batch.

CHAPTER 4 SHAPE ERROR MODELLING OF COMPLIANT PART

4.1 INTRODUCTION

Prediction and modelling of shape error of compliant sheet metal parts are crucial for ensuring quality in assembly process. Sheet metal parts with freeform geometry and their assemblies play a dominant role for building car bodies, aerospace body parts and home appliances. Therefore, efficient modelling and analysis of shape error are crucial quality elements in compliant sheet metal assemblies. The shape error of the sheet metal part heavily influences the final quality of the assembly. Efficient control and reduction of shape error are important not only for increasing performance and functionality, but also for manufacturability and ease of assembly (Ceglarek and Shi, 1995; Shi and Ceglarek, 1996). Subsequently, to ensure quality in assembly process, shape error must be simulated to predict their impact on manufacturability and assembly performance. Therefore, there is need of modelling shape error of compliant sheet metal parts.

Further, strict quality requirements by *Geometric Dimensioning and Tolerancing* (GD&T) must also be fulfilled for 3D freeform shaped parts, such as sheet metal parts used for automotive and aerospace body parts. To facilitate one of the critical requirements of GD&T, freeform shape errors must be extracted from measured part data to simulate geometric tolerance requirements. Further, the 3D metrology sensors, such as 3D laser scanners or 3D white-light scanners represent part data by high dimensional Cloud-of-Points (CoP) which can be categorized as non-functional

data as it cannot be used directly for GD&T simulation. To extract useful information from the data, Ramsay and Silverman (2005) suggested functional model development for non-functional data (e.g. CoP data). This requirements lead to functional data analysis model development which can identify and characterise shape error of single 3D freeform shaped part. Additionally, the current advancement of surface based 3D metrology scanners emphasise on added requirements to functional data analysis model which can be used for (i) statistical process control to detect shape defects using CoP data (as current applications of 3D scanners are limited to quality inspection and reverse engineering (Son *et al.*, 2002), and (ii) efficient access and compact storage of real 3D parts shape information (as CoP data required high volume storage space for production parts) for future design requirements.

Currently, Computer-Aided Design (CAD) model represents the ideal/nominal part which does not take into account real part shape error. On the contrary, fabricated or manufactured part is inherently consisting of shape error. There is tremendous need for modelling and prediction of shape error of real part for many industrial applications. However, developing a unified shape error model that can link design (CAD model) with manufacturing (shape error) remains an obstacle due to major challenges involving part shape modelling. These challenges can be classified into three categories: (i) identification and characterisation of 3D freeform shaped real part shape error, (ii) functional data model (bridged with CAD model) to emulate real part, and (iii) extracting most significant shape error modes which can facilitate quality improvement during design and manufacturing.

The aforementioned challenges emphasise the development of a universal functional model to express shape error in a coherent manner by integrating design features

(ideal shape information) with manufacturing variability (real shape information). The proper understanding of shape error information engraved on a fabricated part (real part) is necessary to facilitate process improvement at design and manufacturing phases. The problem of shape error is especially unavoidable for various assembly applications involve compliant parts (Das *et al.*, 2014; Jing *et al.*, 2010; Franciosa *et al.*, 2014). For example, one of the emerging joining techniques, Remote Laser Welding (RLW) requires maintaining very tight control of part-to-part gaps and the inability to meet this requirement can result in non-conforming joints. Part shape error contributes significantly to part-to-part gap control. Therefore, shape error modelling is an unavoidable prerequisite to support the aforesaid critical tasks. As a consequence, a unified shape error model is required for efficient part management by quantifying the shape error through functional data analysis. One way to build a unified functional model is shape error decomposition from measured CoP data. However, shape error decomposition of 3D freeform shaped part is not trivial as it involves

(i) Transforming the 3D irregular freeform shape (such as 3D sheet metal parts with complex geometries, curvatures, holes and slots) to uniform 3D volumes structure to facilitate shape error decomposition into orthogonal shape error modes,

(ii) Truncation and selection of most significant shape error modes with engineering importance and GD&T relevance, and

(iii) Accurately emulate real part shape error with fewer modes such that the developed shape error decomposition model remains compact and tractable.

This chapter presents a novel and efficient *functional data analysis* approach named *Geometric Modal Analysis (GMA),* aiming to extract dominant shape error modes

from the fabricated part measurement data. GMA addresses the aforesaid challenges by proposing the following steps:

(i) To facilitate shape error modelling of 3D freeform shaped object (e.g. sheet metal part), the 3D object is enveloped in 3D volume with Laplace interpolation for uniform smooth voxel structure, and then, shape error field is decomposed into shape error modes by using 3D Discrete Cosine Transform (3D DCT);

(ii) To identify the significant shape error modes, mode truncation criteria have been introduced based on energy compaction and correlation criteria; and

(iii) To emulate real part more accurately with less number of modes, mode magnitude correction criteria have been proposed.

The proposed GMA model decomposes the engraved shape error into significant shape error modes to identify and characterise real part shape error. Due to orthogonal nature of the decomposed shape error modes, they are independent to each other which pose added advantage for statistical control or process design with compliant parts. Further, they can be used as parameters to link nominal data with manufacturing / fabrication process parameters to identify the correlation among them. Industrial case studies are conducted to demonstrate shape error decomposition of sheet metal part produced by stamping process and the obtained decomposition result has been compared with state-of-the-art methodologies available in literature.

In the next section 4.2 highlights the limitations of available shape error decomposition methods in literature. Section 4.3 describes the proposed GMA methodology through fundamental ideas of orthogonal decomposition of shape error;

and shape error modelling by taking into account only the dominant error modes. Section 4.4 describes the applicability of the proposed GMA method through industrial cases and compares the result with other available methods from literature, such as SMA decomposition or natural mode decomposition. Further, Section 4.5 summarises the chapter.

4.2 LIMITATIONS OF CURRENT DECOMPOSITION APPROACHES

The related literature and limitations of the available approaches to address shape error modelling are described in Section 3.2 with identified research gap. However, the most relevant state-of-the-art functional models available in literature are (i) *Statistical Modal Analysis (SMA)* (Huang and Ceglarek, 2002; Huang *et al.*, 2014) based on measured CoP data decomposition, and (ii) *Natural Mode Decomposition* (Samper and Formosa, 2006) based on nominal CAD data decomposition.

The functional model *Statistical Modal Analysis (SMA)* (Huang and Ceglarek, 2002; Huang *et al.*, 2014) has several limitations. A comparison between SMA model and proposed GMA model is summarized in Table 4.1. To overcome the limitations posed by the SMA model and expand the applicability to model 3D freeform shaped part, the present study proposes a novel functional data analysis based shape error decomposition method relying on part measurement data. Generalized 3D DCT is used as underlying decomposition principle to model the part shape error and identify the most significant shape error modes using mode truncation and mode magnitude correction criteria. 3D freeform shaped compliant part can be modelled using the proposed approach where most significant modes are used to predict and quantify the shape error of the part.

Further, comparison with *Natural Mode Decomposition* method is reported in details at Section 4.4.2.2 industrial case study where it compares the surface reconstruction using both *Geometric Modal Analysis* and *Natural Mode Decomposition* approaches.

Table 4.1 Comparison of SMA method and proposed GMA method

	SMA method (Huang and Ceglarek, 2002; Huang *et al.*, 2014)	Proposed GMA method
Problem Formulation	➢ The shape error space is defined in two dimensional space (2D space) ➢ The shape error fields are studied in equally spaced rectangular grid	➢ The shape error space is defined in three dimensional space (3D space) ➢ The shape error fields can be estimated in irregular sampled points
Error Estimation	➢ Shape error is considered as a function of height of the sampled data points, i.e. deviation = $f(x,y)$ defined in 2D domain	➢ Shape error is studied as a function of normal deviation of irregular sampled data points, i.e deviation = $f(x,y,z)$ defined in 3D domain
Applicability	➢ Limited to sampled error space in 2D domain ➢ Any irregularities in the rectangular grid will create unnecessary fitting models and main shape error modes are not distinguishable ➢ Modes are greatly affected by the features like holes, slots	➢ Extended to model freeform part in 3D domain ➢ Irregularities are taken care by Laplace interpolation to keep the main shape error modes unaffected ➢ Part features are taken care of and modes remain unaltered

Further, current 3D DCT cannot be applied directly to decomposed shape error of 3D freeform shaped part. The proposed GMA method introduces voxelisation and

Laplace interpolation to enable 3D DCT decomposition on the measured CoP data which is discussed in detail in the methodology section. At present, the application of 3D DCT is limited to image and video compression among the image processing communities. However, few applications can be found in 3D image data processing and face recognition. These applications can rather be classified as 2.5D DCT where time axis has been added with 2D DCT approach, e.g. in case of video compression, 2D images are stacked up to make video structure. Further, for the case of face recognition, 2.5D data application is well established where 2.5D is a simplified 3D (x, y, z) surface representation that contains at most one depth value (z direction) for every point in the (x, y) plane (Lu et al., 2006; Gökberk et al., 2009). Therefore, a unique projection along the z axis provides a unique depth image, sometimes called a range image, which can then be used to extract features by various researchers (Ekenel et al., 2007; Günlü and Bilge, 2010). Table 4.2 illustrates the applications of 2.5D DCT and the proposed application in the field of shape error characterisation.

Table 4.2 Diversified application of 2.5D DCT vs. proposed GMA (based on 3D DCT) application

Applications in literature	Proposed application
2.5D DCT applied mainly in the following domain ➢ Image compression (Ploix and Vigouroux, 1999; Manjón *et al.*, 2012) ➢ Video compression (Lee *et al.*, 1997; Božinović and Konrad, 2005) ➢ Face recognition (Günlü and Bilge, 2010)	Decomposition of part shape error of 3D freeform shaped geometry to address shape error modelling requirements of compliant sheet metal part for various applications, such as statistical process control, process design, and root cause identification based assembly process diagnosis.

4.3 GEOMETRIC MODAL ANALYSIS (GMA) METHODOLOGY

The present work focuses on the development of a functional data analysis model which will represent the part shape error and quantify the shape error. A part is composed of nominal features (represents design features - CAD) and deviation from the nominal (shape error) introduced during the part fabrication process. The proposed GMA method is an extension of the SMA method by Huang et al. (2014) where the limitations of SMA method have been eliminated and 3D freeform shaped part can be modelled. Two hypotheses are introduced to simplify the modelling process:

(i) Smoothness assumption: shape error field signal has sufficient smoothness such that the high spatial frequency components (short wavelength error such as surface roughness and waviness) are small and can be ignored. This assumption implies that shape error is highly spatially correlated.

(ii) Normal deviation assumption: the shape errors of a real part surface can be represented as a normal deviation function $f(x,y,z)$ defined in 3D domain. Normal deviation calculation has limitation around the curved features. Figure 4.1 illustrates the normal deviation calculation from nominal features to CoP. The deviations calculated in the flat region are providing accurate result but, in case of curved regions, the matching points are away from the normal deviation. Near the curved region at point 1, the normal deviation calculation does not match with the actual direction of deviation.

The shape error field is defined as the differences between the actual surfaces and nominal surfaces: $f(x,y,z) = F_{actual} - F_{nominal}$, where, $F_{nominal} = F_n\ (x,y,z)$ denotes the nominal position of the data point and $F_{actual} = F_a\ (x,y,z)$ denotes the actual position

of the data point. Shape error from a part population is defined as a random field process. The GMA methodology has been developed based on 3D DCT to model the random nature of the shape error. In general, part shape error field is sampled as discrete space signals. The sampled error data set $f(x,y,z) = f(l\Delta x, m\Delta y, n\Delta z)$ where, l, n and m represents the sample size of the in three dimensional axes. In general, for three-dimensional signal (sampled data), with number of sample points equals to N^3 (or $L \times M \times N$, if $L \neq M \neq N$), the forward and inverse transforms (models generation and reconstruction, respectively) are given as follows:

$$\left.\begin{aligned} T(u,v,w) &= \sum_{x=0}^{L-1}\sum_{y=0}^{M-1}\sum_{z=0}^{N-1} f(x,y,z)\, g(x,y,z,u,v,w) - \text{ forward transform} \\ f(x,y,z) &= \sum_{x=0}^{L-1}\sum_{y=0}^{M-1}\sum_{z=0}^{N-1} T(u,v,w)\, h(x,y,z,u,v,w) - \text{ inverse transform} \end{aligned}\right\} \quad \textbf{(4.1)}$$

where, $T(u,v,w)$ are independent transformation parameters representing contribution of the shape error modes with space frequency of u, v and w are in three axes x, y and z respectively. The $g(x,y,z,u,v,w)$ and $h(x,y,z,u,v,w)$ are called the forward and inverse transformation kernels.

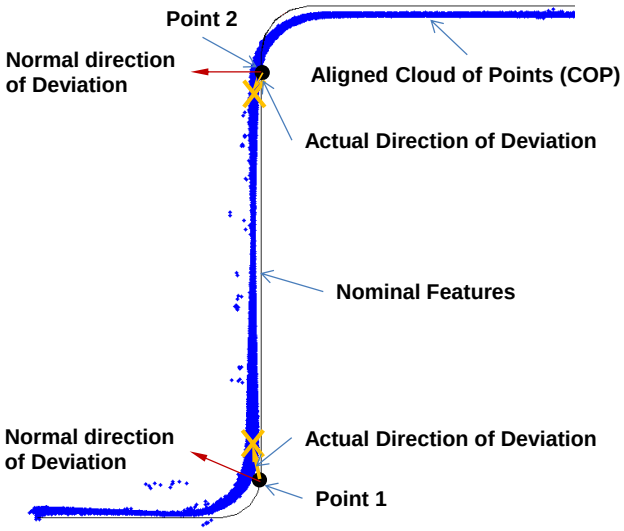

Figure 4.1 Normal deviation calculations from nominal features to CoP

The GMA method comprises of three major steps: (i) Data pre-processing which includes generation of mesh model from nominal CAD model and measured part data (CoP) post-processing to obtain shape error, (ii) GMA decomposition which involves voxelisation of mesh model, Laplace interpolation, and 3D DCT decomposition, and (iii) GMA mode identification which involves mode selection criteria and mode magnitude correction to achieve desired model accuracy. The overview of the proposed GMA method is depicted in Figure 4.2.

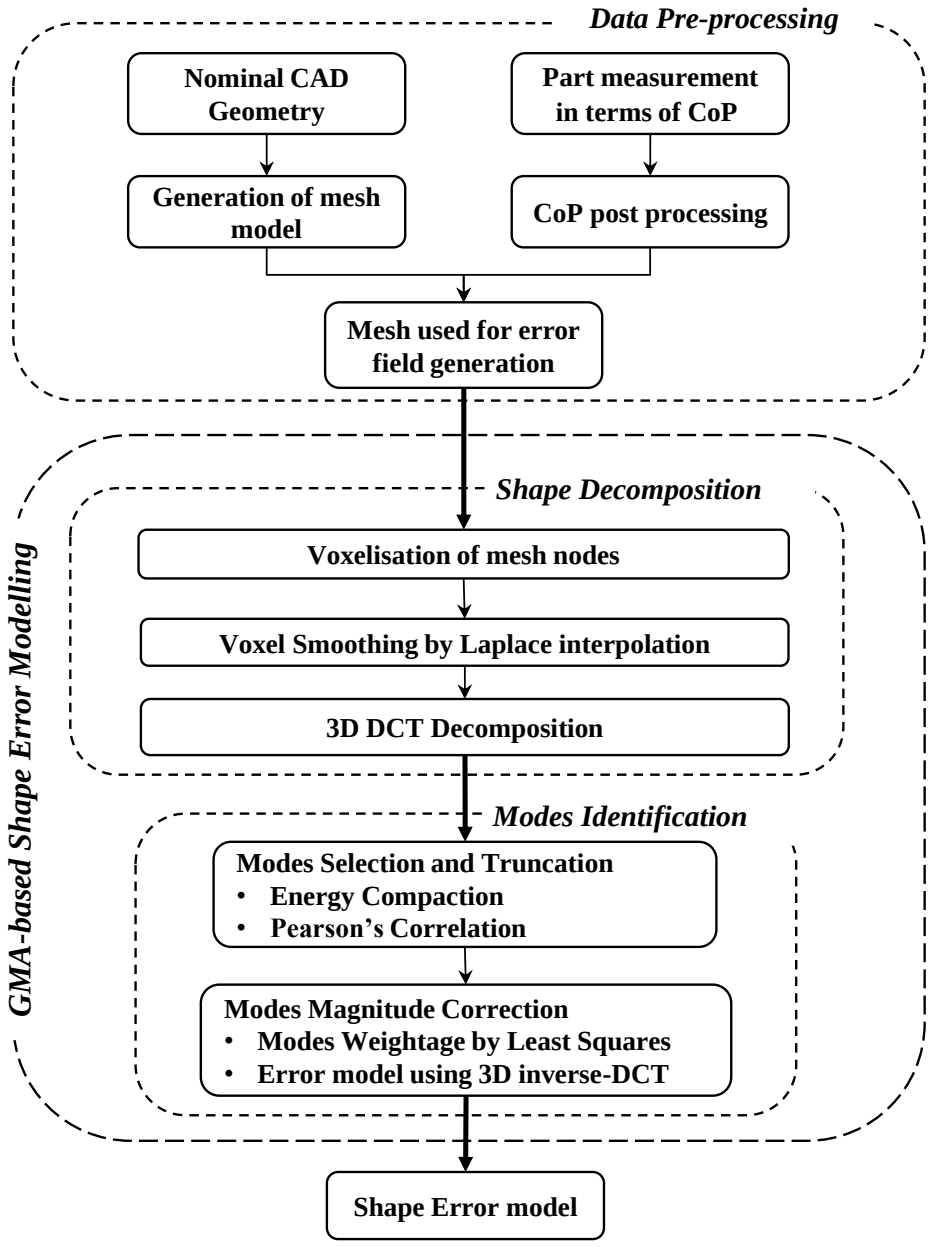

Figure 4.2 Overview of GMA based shape error decomposition methodology

4.3.1 Data Pre-processing

The nominal features of the part (CAD model) are composed of B-spline or NURBS surfaces which are not sufficient to embed the freeform shape errors. However, the mesh model of the nominal features helps to easily integrate part shape errors with the nominal part which leads to several benefits, such as normal vector of the mesh nodes can be utilised to compute the shape error field. The part measurement data captured through 3D non-contact scanner in terms of CoP is used to calculate shape error (i.e. deviation at each mesh node). In this proposed method, alignment of CoP with nominal CAD model is highly significant for model accuracy. Let N_n be the number of mesh node and D_n is set of calculated deviation at N_n. Therefore, D_n represents the calculated shape error field.

4.3.2 GMA-based Shape Error Decomposition

The GMA decomposition involves three major steps: (i) Voxelisation of mesh nodes to envelope 3D freeform shaped part which creates non-uniform scattered voxel structure, (ii) Laplace interpolation to smooth the non-uniform scattered voxel structure, and (iii) 3D DCT decomposition to obtain the shape error modes.

4.3.2.1 Voxelisation of Mesh Nodes

The shape error field decomposition using 3D DCT can be applied on the uniform grid data. Therefore, 3D freeform shaped part cannot be used directly for decomposition rather discretising it into 3D uniform grid points. A structure containing scattered deviation has been achieved through voxelisation of mesh nodes. For this purpose, $L \times M \times N$ voxel grid is used where each mesh node position of the nominal part is described as point coordinate,

$$N_k = \{x \quad y \quad z\}_k, \qquad k \forall [1,2,3,...,n] \tag{4.2}$$

where, k represents the node number and $\{x \quad y \quad z\}_k$ represents the Cartesian coordinates of a mesh node k.

For constant mapping of mesh node coordinate to voxel space, a bounding box has been computed enveloping the part mesh model. The voxels containing the mesh nodes have been identified by linear mapping of the node coordinates to voxel space. All the voxel elements are identified which are containing the mesh nodes and calculated deviations at mesh nodes are allocated to the corresponding voxel elements. Relying on the chosen $L \times M \times N$ voxel grid size, more than one mesh node may belong to same voxel in few cases and the allocated deviations of those voxels are computed as average of belonging node deviations. Therefore, shape error field in voxel space slightly differs from the original shape error field due to averaging. Optimal voxel grid size is chosen by minimising this difference. The basic voxelisation process has been depicted in Figure 4.3.

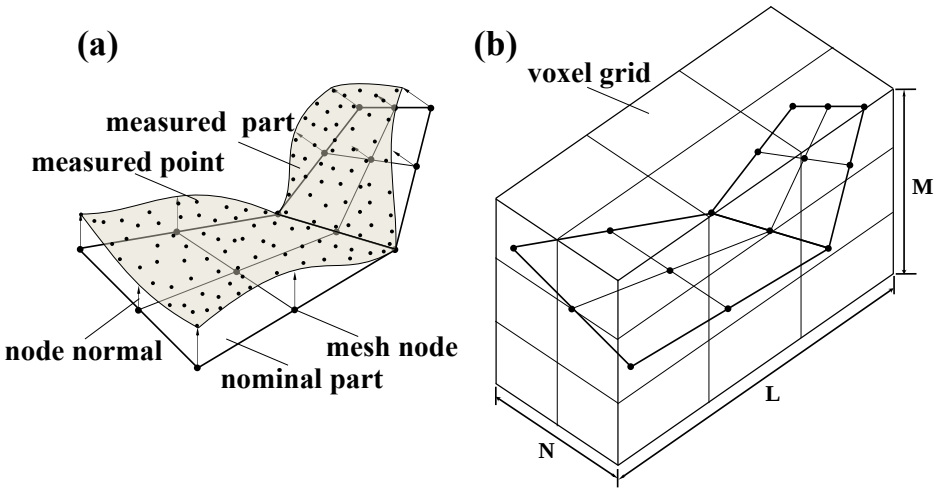

Figure 4.3 Voxelisation process: (a) nominal mesh model and deviation calculation at mesh node, and (b) bounding box computation and voxel grid mapping ($L \times M \times N$)

4.3.2.2 Voxel Smoothing by Laplace Interpolation

The nominal mesh nodes are enveloped with voxel grid to enable 3D DCT transformation on voxel structure. From the voxelisation process, it is evident that many voxel elements in the voxel grid do not contain mesh node deviation and remain as empty. This implies a non-continuous voxel deviation field, i.e. a non-uniform scattered voxel structure. Since DCT attempts to fit a set of continuous cosine function to the given data field, as soon as non-continuities are detected, a large number of undesired fitting modes are generated. This result is no longer acceptable because the main shape error modes cannot be distinguished from the other undesired fitting modes. Therefore, in order to smooth the voxel model and make a continuous data field, a Laplacian smoothing is applied to assign meaningful value in the empty voxel elements keeping the original deviation as internal boundary constraints.

In the voxel grid space of $L \times M \times N$, any voxel element deviation can be defined as $f(i,j,k)$, where, i=[1,2,…L], j=[1,2,…M], and k=[1,2,…N]. To transform non-uniform scattered voxel structure into uniform smooth voxel structure, 3D Laplace interpolation has been employed. 3D Laplace interpolation equation (4.3) can be written as generic equation (4.4) to calculate deviation at each empty voxel element.

$$\frac{\partial^2 f}{\partial x^2} + \frac{\partial^2 f}{\partial y^2} + \frac{\partial^2 f}{\partial z^2} = 0 \qquad \textbf{(4.3)}$$

$$\begin{aligned} &\frac{f(i-1,j,k) - 2f(i,j,k) + f(i+1,j,k)}{\Delta x^2} \\ &+ \frac{f(i,j-1,k) - 2f(i,j,k) + f(i,j+1,k)}{\Delta y^2} \\ &+ \frac{f(i,j,k-1) - 2f(i,j,k) + f(i,j,k)}{\Delta z^2} = 0 \end{aligned} \qquad \textbf{(4.4)}$$

where, $\Delta x, \Delta y$ and Δz represent the voxel element length in *L*, *M* and *N* voxel directions respectively.

4.3.2.3 3D DCT Decomposition

The 3D DCT transformation is applied on the Laplace interpolated voxel data (i.e. uniform smooth voxel structure) in order to decompose the shape error field into significant shape error modes. The 3D DCT decomposition is expressed as equation (4.5) where the transformed coefficients are decomposed shape error modes,

$$C(u,v,w) = \sqrt{\frac{2}{L}}\sqrt{\frac{2}{M}}\sqrt{\frac{2}{N}}\alpha(u)\alpha(v)\alpha(w)\sum_{u=0}^{L-1}\sum_{v=0}^{M-1}\sum_{w=0}^{N-1}\cos\left[\frac{\pi u(2i+1)}{2L}\right] \cos\left[\frac{\pi v(2j+1)}{2M}\right]\cos\left[\frac{\pi w(2k+1)}{2N}\right] f(i,j,k) \quad \textbf{(4.5)}$$

where, $\alpha(\xi) = \begin{cases} \frac{1}{\sqrt{2}} & if,\ \xi = 0 \\ 1 & if,\ \xi \neq 0 \end{cases}$

In the above equation (4.5), modes *C(u,v,w)* represent the 3D DCT coefficients which are class of orthogonal transformation. This transformation has high energy compaction property of the error signal which helps to store most of the error signal energy (in terms of information) of the error field using small number of significant transform coefficients or modes *C(u,v,w)* and *u,v,w* represent the modal position in voxel space.

4.3.3 GMA Modes Identification

It is important to include a few modes or transform coefficients in the model without losing much information on the shape error field to keep the shape error model tractable. However, the model should meet the desired accuracy of acceptable limit defined by the user. In order to keep dominant shape error modes which have

engineering importance and applicable to GD&T of sheet metal part, two criteria have been imposed which are mode truncation criteria and selected modes magnitude correction criteria.

4.3.3.1 Modes Selection or Truncation Criteria

To check mode significance, two criteria are proposed: (a) Energy compaction, and (b) Pearson's Linear Correlation.

(a) Energy Compaction Criterion (ECC)

Simplified shape error field expression can be given as:

$$C(u,v,w) = \sum_{u=0}^{L-1}\sum_{v=0}^{M-1}\sum_{w=0}^{N-1}\cos\left[\frac{\pi u(2i+1)}{2L}\right]\cos\left[\frac{\pi v(2j+1)}{2M}\right] \cos\left[\frac{\pi w(2k+1)}{2N}\right] f(i,j,k) \quad \textbf{(4.6)}$$

where, *u = 0, 1, 2, ...L-1*; *v = 0, 1, 2, ...M-1*; *w = 0, 1, 2, ...N-1*.

A criterion can also be developed from Parseval's theorem (energy preservation of DCT):

$$\sum_{u=0}^{L-1}\sum_{v=0}^{M-1}\sum_{w=0}^{N-1} C^2(u,v,w) = \sum_{i=0}^{L-1}\sum_{j=0}^{M-1}\sum_{k=0}^{N-1} f^2(i,j,k) \quad \textbf{(4.7)}$$

The ratio of the energy in a selected number of significant modes to the total energy of the signal (sampled data) can be used to characterise the energy compaction of the model. To achieve a given energy compaction (threshold) of $0 \leq E \leq 100\%$, the most significant modes/coefficients should be included in a coefficient index set Ω_e such that:

$$\frac{\sum_{u=0}^{L-1}\sum_{v=0}^{M-1}\sum_{w=0}^{N-1}C^2(u,v,w)}{\sum_{i=0}^{L-1}\sum_{j=0}^{M-1}\sum_{k=0}^{N-1}f^2(i,j,k)} \geq E \qquad (u,v,w) \in \Omega_e \tag{4.8}$$

The above truncation criterion is based on coefficients from sampled data of an individual part. The truncation is equivalent to selection of coefficients in case the magnitude of the coefficients is monotonically decaying.

(b) Pearson's Linear Correlation (PLC)

All the energy compacted modes (Ω_e) are selected to evaluate correlation coefficients by comparing to original shape deviation, D_n. Each energy compacted coefficient has unique pattern of shape error distribution over the mesh node and the mesh node deviations corresponding to each coefficients are kept as $T = [T_1 \quad T_2 \quad T_3 \quad . \quad . \quad T_{\Omega_e}]_{n\times\Omega_e}$. The mesh node deviations corresponding to each coefficient are compared with original deviation to evaluate the coefficients with higher correlation, ρ, which are calculated as

$$\rho_q = \frac{cov\left(T_q, D_n\right)}{\sigma_{T_q}^2 \sigma_{D_n}^2} \tag{4.9}$$

where, $q = (1,2,3,....\Omega_e)$ the set of indices of the energy compacted modes.

A threshold value, α, has been applied for further reduction in the number of modes. Only those modes are taken to model the shape error which have correlation coefficient higher than the given threshold, α. The truncated highly correlated modes are kept in the coefficients index set Ω_c ($\rho_q > \alpha$). In case where E reaches 100% and α to 0, all the decomposed modes are included in the model.

Higher energy compaction of a coefficient indicates the significance of this specific shape error mode which should be considered in the model. Therefore, the energy

compaction criterion should be used together with the Pearson's linear correlation criteria simultaneously for coefficient selection (truncation). For an energy compaction E and given correlation threshold α, the truncated shape error model must include the coefficients $C(u,v,w) \in \Omega$, where Ω is an index set in which all the indices of the intersection of Ω_e and Ω_c are included:

$$\Omega = \Omega_e \cap \Omega_c \tag{4.10}$$

where, Ω represents a set which includes those coefficients that are both energy and highly correlated.

4.3.3.2 Modes Magnitude Correction

The selected modes through the mode truncation criteria are mainly to recognise the main shape error modes which does not necessarily depict the correct magnitude associated with each mode. Therefore, as corrective measures, a least squares based mode magnitude correction method is proposed, and then, by applying 3D inverse-DCT (3D IDCT) shape error field can be recovered.

(a) Modes Weightage by Least squares

To overcome the challenge associated with the magnitude of shape error field, least squares based mode magnitude correction has been employed to obtain proper weightage of the selected coefficients. The coefficients are selected from the coefficient index set, Ω which will satisfy the following least squares equation

$$D_n = \sum_{q=1}^{\Omega} wt_q T_q \tag{4.11}$$

where, $q = 1,2,3,....\Omega$ the number of selected coefficients, $wt_q =$ weightage associated with each coefficient, and $T_q =$ mesh node deviations associated with each coefficients.

(b) Error model using 3D IDCT

Each truncated and magnitude corrected coefficient from set Ω is selected to represent the shape error model. 3D IDCT applied, as per equation (4.12) by reversing equation (4.5), on the selected set of truncated coefficients, Ω to recover the shape error deviation field.

$$\tilde{f}(i,j,k) = \sqrt{\frac{2}{L}}\sqrt{\frac{2}{M}}\sqrt{\frac{2}{N}}\sum_{u=0}^{L-1}\sum_{v=0}^{M-1}\sum_{w=0}^{N-1}\alpha(u)\alpha(v)\alpha(w)\cos\left[\frac{\pi u(2i+1)}{2L}\right]\cos\left[\frac{\pi v(2j+1)}{2M}\right] \cos\left[\frac{\pi w(2k+1)}{2N}\right]\tilde{C}(u,v,w) \quad \textbf{(4.12)}$$

The function $\tilde{f}(i,j,k)$ refers to the shape error field signals (deviation) which are generated by using the truncated and magnitude corrected coefficient set, Ω = $\tilde{C}(u,v,w)$. The inverse function has been applied to obtain voxel deviations which are applied to corresponding mesh nodes to model part shape errors with few modes.

Therefore, by obtaining the magnitude corrected truncated coefficients and using (4.12), the recovered shape error field, $\tilde{f}(i,j,k)$ deviates from the original deviation field as

$$f(i,j,k) = \tilde{f}(i,j,k) + \varepsilon(i,j,k) \quad \textbf{(4.13)}$$

where, $\varepsilon(i,j,k)$ is the residual term from the original shape error deviation to GMA modelled deviation.

Aiming to understand better the methodological steps involving GMA technique, Figure 4.4 uses simple top hat part for explaining main GMA steps. The GMA data pre-processing involves nominal CAD geometry, CoP data measurement, alignment of CoP with CAD, mesh model representation of nominal CAD to map shape error comparing with CoP data as illustrated in Figure 4.4(a). Further, the pictorial

representation including the basic steps of GMA is shown in Figure 4.4(b). The actual representation by using top hat part is demonstrated Figure 4.4(c). It involves original deviation computation at mesh nodes, thereafter, voxelisation of nominal mesh nodes (voxel elements containing deviation data are represented as red elements and others are kept as empty voxels). In order to facilitate voxel structure smoothing, Laplace interpolation is applied on voxel structure to assign meaningful data to empty voxels (represented as green voxel elements). 3D DCT based decomposition is applied on Laplace interpolated voxel structure to obtain GMA decomposed shape error modes. Furthermore, modes selection criteria applied on shape error modes to keep most significant shape error modes and they are used to reconstruct the shape error related to top hat part as in Figure 4.4(c).

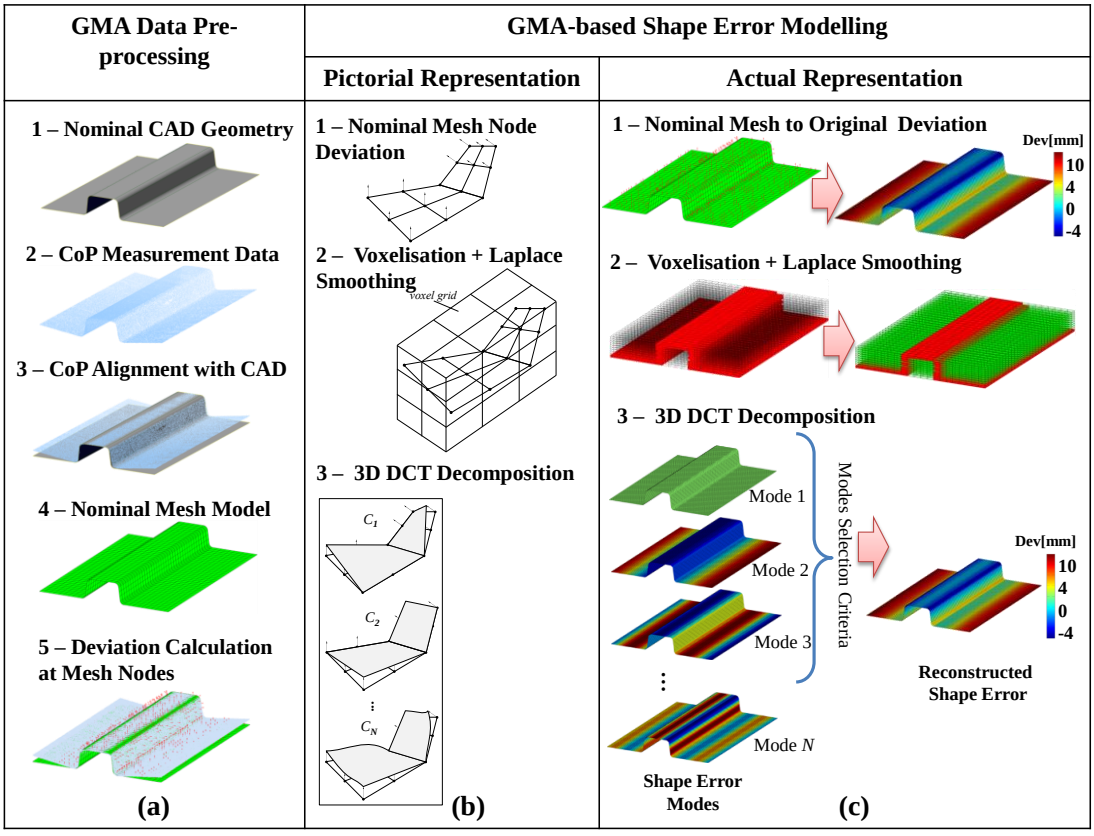

Figure 4.4 GMA-based shape error modelling steps using top hat part: (a) data pre-processing, (b) pictorial representation, and (c) actual representation

4.4 RESULTS OF GMA WITH INDUSTRIAL CASE STUDIES

Results of the developed GMA method is illustrated with two industrial case studies, i.e. (i) Hinge reinforcement part, and (ii) Door inner panel (refer to Figure 4.5). Both parts are crucial in terms of shape error to achieve good quality in assembly. These case studies explain the capability of the GMA to model 3D freeform shaped part.

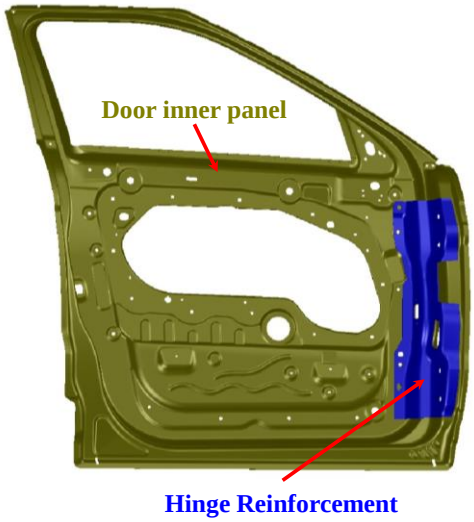

Figure 4.5 Automotive door components hinge reinforcement and door inner panel as in assembly configuration

4.4.1 GMA Based Mode Decomposition

The GMA methodology has been applied to decompose shape errors of hinge reinforcement and door inner panel of automotive door. The hinge reinforcement is generally joined through Resistance Spot Welding (RSW) process with door inner to provide sufficient strength to hold the door with the main automotive body frame. It avoids deformation of the door inner panel during opening/closing of the door. The hinge reinforcement part has many features and curvatures on the part where the shape error belongs to several different normal directions. It proves that the developed GMA methodology can be used for 3D part and it enables modelling the

part as a whole. For example, if this assembly is to be remote laser welded, the gap or clearance between the two parts is required to be 0.3 mm, i.e., the gap between the hinge reinforcement (1.8 mm thick) and door inner panel (0.75 mm thick) should be within 0.3 mm to ensure satisfactory joining quality. Therefore, part shape error modelling is crucial to ensure the gap and quality of the welding.

The captured CoP data is aligned with nominal CAD and deviations are calculated at nominal mesh nodes [nominal mesh model as represented in Figure 4.7(a)] to obtain the shape error field [as depicted in Figure 4.7(b)]. As per the voxelisation process, the mesh nodes and corresponding deviations are stored in the voxel structure with selected voxel grid size. The selection of voxel grid size has been made when Root Sum of Squares (RSS) error, between original calculated mesh node deviations and mesh node deviations after voxelisation, is minimum or constant with further increment of voxel grid. Figure 4.6 depicts that the voxelisation error is reducing with increment of voxel grid and becomes almost constant after grid size of 60×60×100 which has been used for our proposed model as shows in Figure 4.7(c). Thereafter, Laplace interpolation has been performed on the voxel data to fill the empty voxel elements with meaningful data and 3D DCT applied on the interpolated voxel grid data. The transform coefficients are truncated based on 90% signal energy compaction and Pearson's correlation test performed to identify the most significant coefficients related to original shape error field. Further, truncation on the coefficients has been performed using correlation threshold, α=0.25. A total of 12 coefficients are selected to model the part shape error and by using least squares proper weightage has been applied to those selected 12 coefficients (corresponding shape error modes are shown in Figure 4.8). 3D IDCT applied on the weighted coefficients to reconstruct the part shape error field. The original shape error field,

GMA reconstructed shape error field and model residue plot are shown in Figure 4.9. A residue surface can be determined as the difference between the measured shape error field and GMA reconstructed shape error field. Therefore, the proposed methodology identifies the main shape error modes associated to the part.

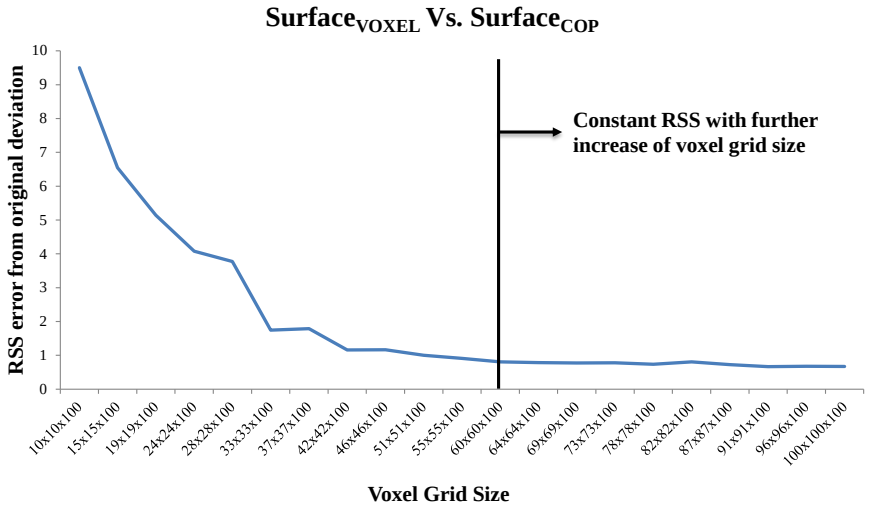

Figure 4.6 Voxel grid size selection

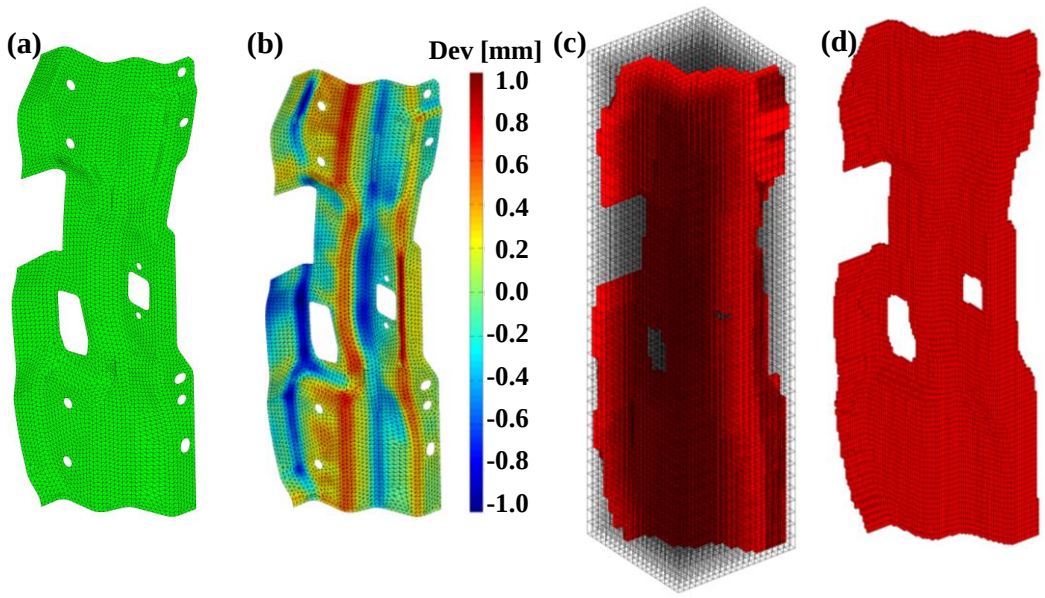

Figure 4.7 Hinge reinforcement part: (a) mesh model of hinge reinforcement (b) measured shape error from CoP, (c) voxelisation of error data (Voxel grid size = 20×20×40, used for visualization only), and (d) voxel elements containing error data only (Voxel grid size = 60×60×100)

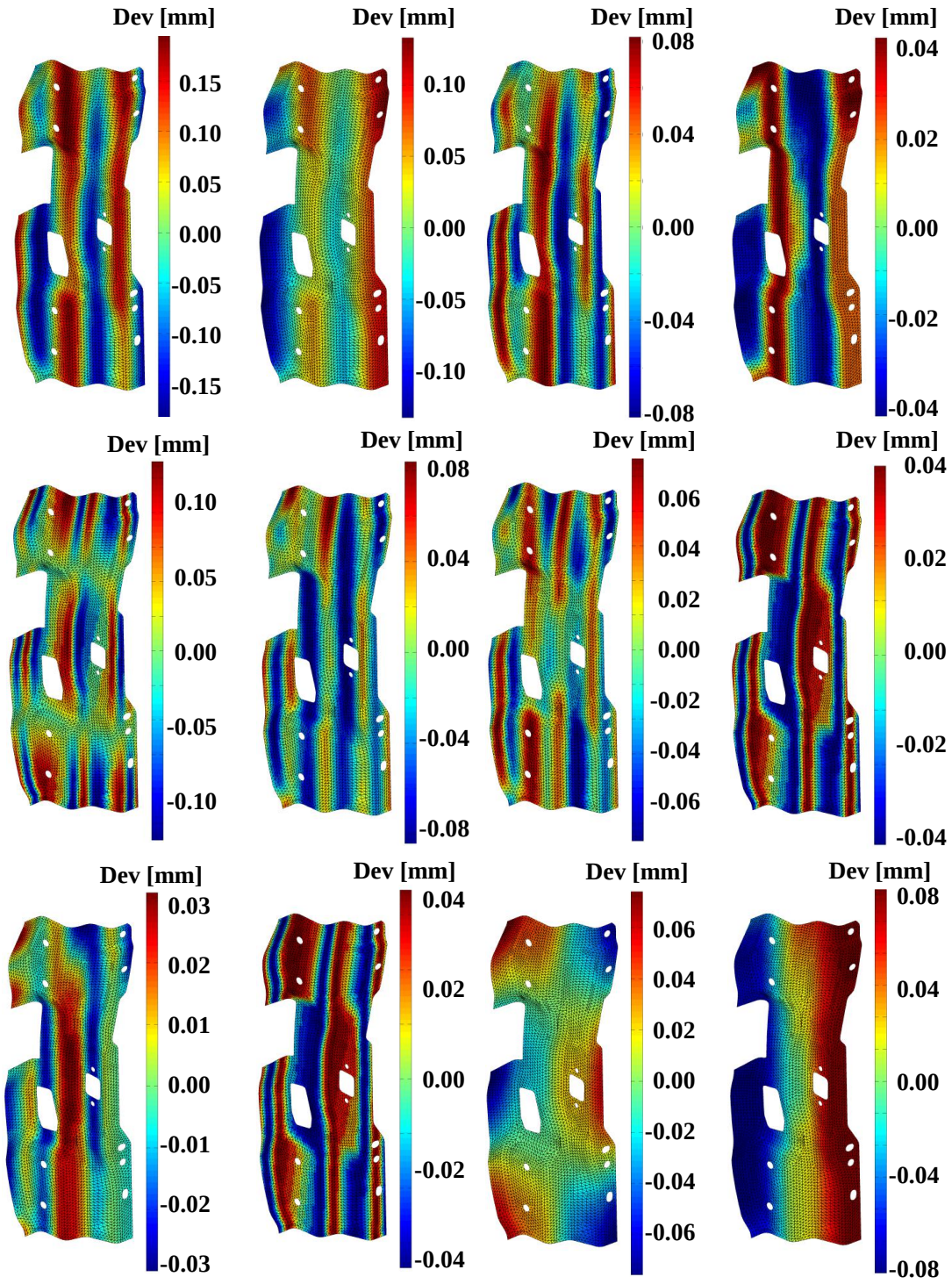

Figure 4.8 GMA decomposed major shape error modes of the hinge reinforcement part

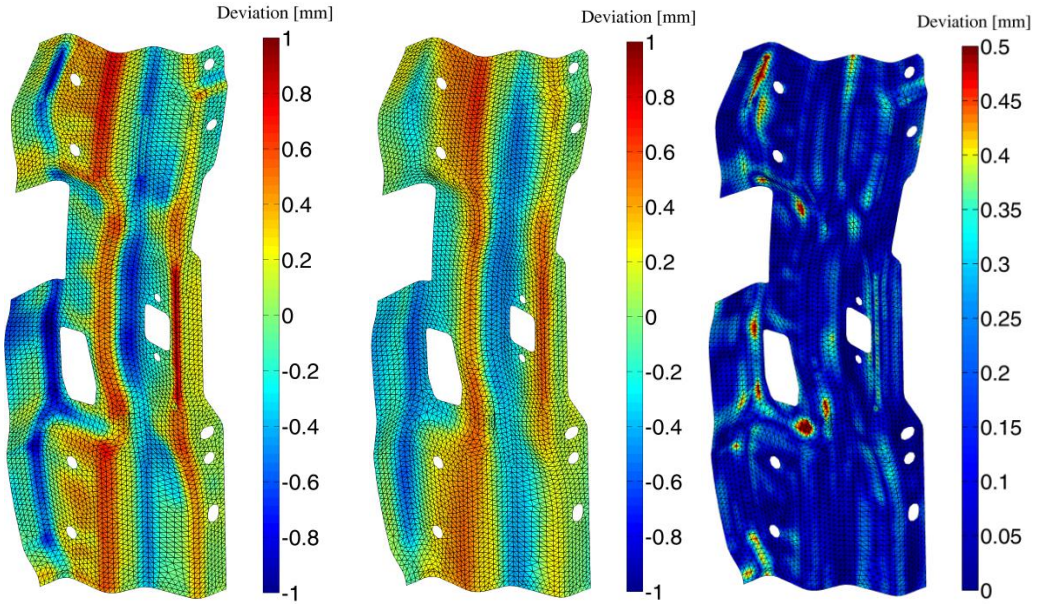

(a) (b) (c)

Figure 4.9 Shape error (i.e. deviation plot) of the hinge reinforcement: (a) original shape error plot, (b) GMA reconstructed shape error plot, and (c) error plot between original shape error and GMA reconstructed shape error.

Similarly, GMA method is also used to decompose door inner panel which is the main door frame which keeps dimensional and geometric quality of the final assembly. This part is relatively large size and composed of many features, curvatures and edges as depicted in Figure 4.10(a) as nominal CAD model. The corresponding mesh model is represented in Figure 4.10(b). A voxel grid size of 50x100x100 has been selected to store the computed mesh node deviations. GMA coefficients are truncated using coefficient truncation criteria which are based on the 90% energy compaction and significant coefficient selection has been achieved using Pearson's correlation test which facilitates to recognize the most significant modes represents the measured shape errors. A correlation threshold, α=0.10 has been implied to keep the decomposition model smooth. A total of 28 modes have been identified as main error modes and original deviation to decomposed modes have been presented in Figure 4.11.

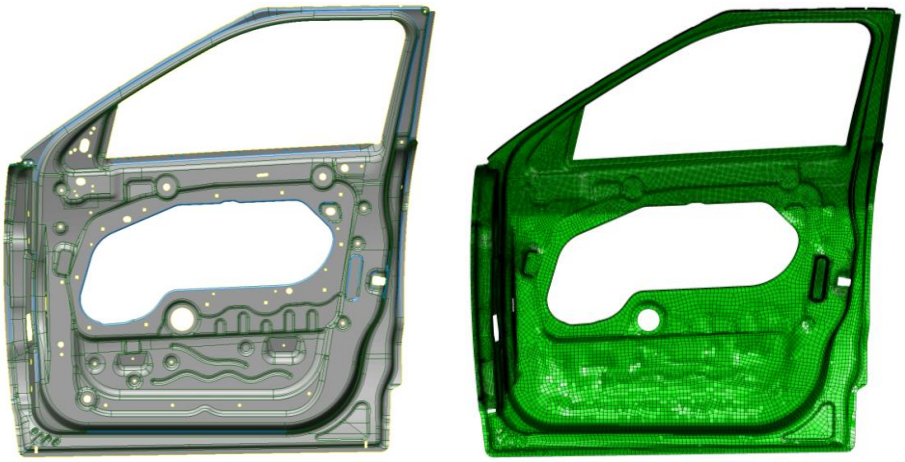

(a) (b)

Figure 4.10 Door inner panel of automotive door: (a) nominal door part, and (b) mesh model of the part

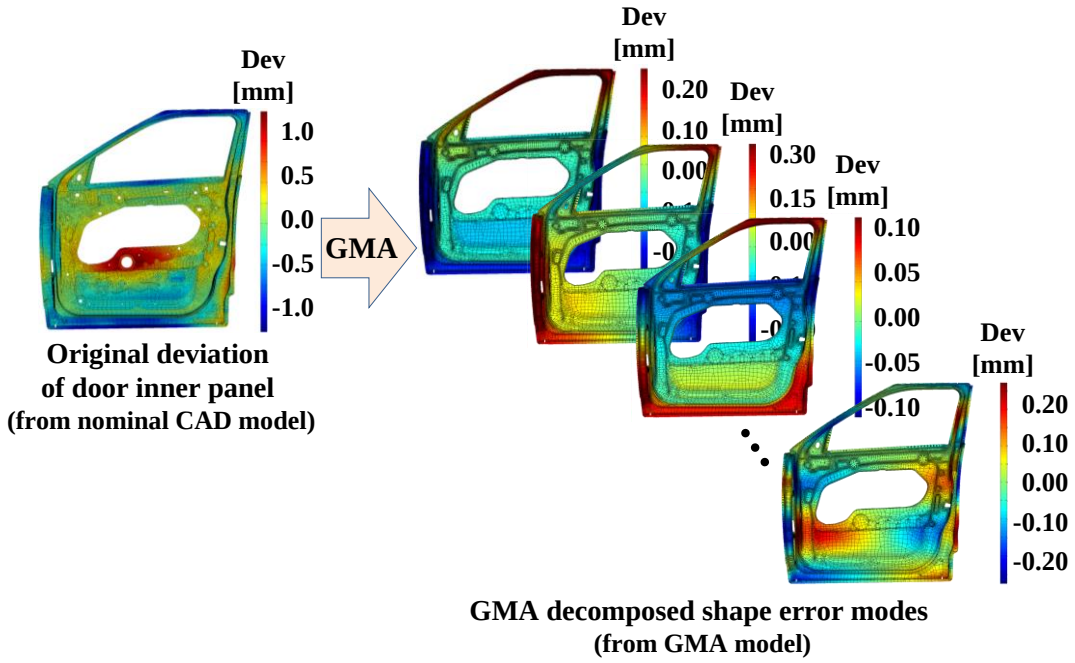

Figure 4.11 GMA decomposition of door inner panel into significant shape error modes

A doo inner panel has been selected for further diagnosis to identify the types of error modes associated with the part. Few significant shape error modes have been reported in Figure 4.12. It can be observed from the plots that the part is more

centrally bended and outward twisted which give more understanding of the physical phenomenon.

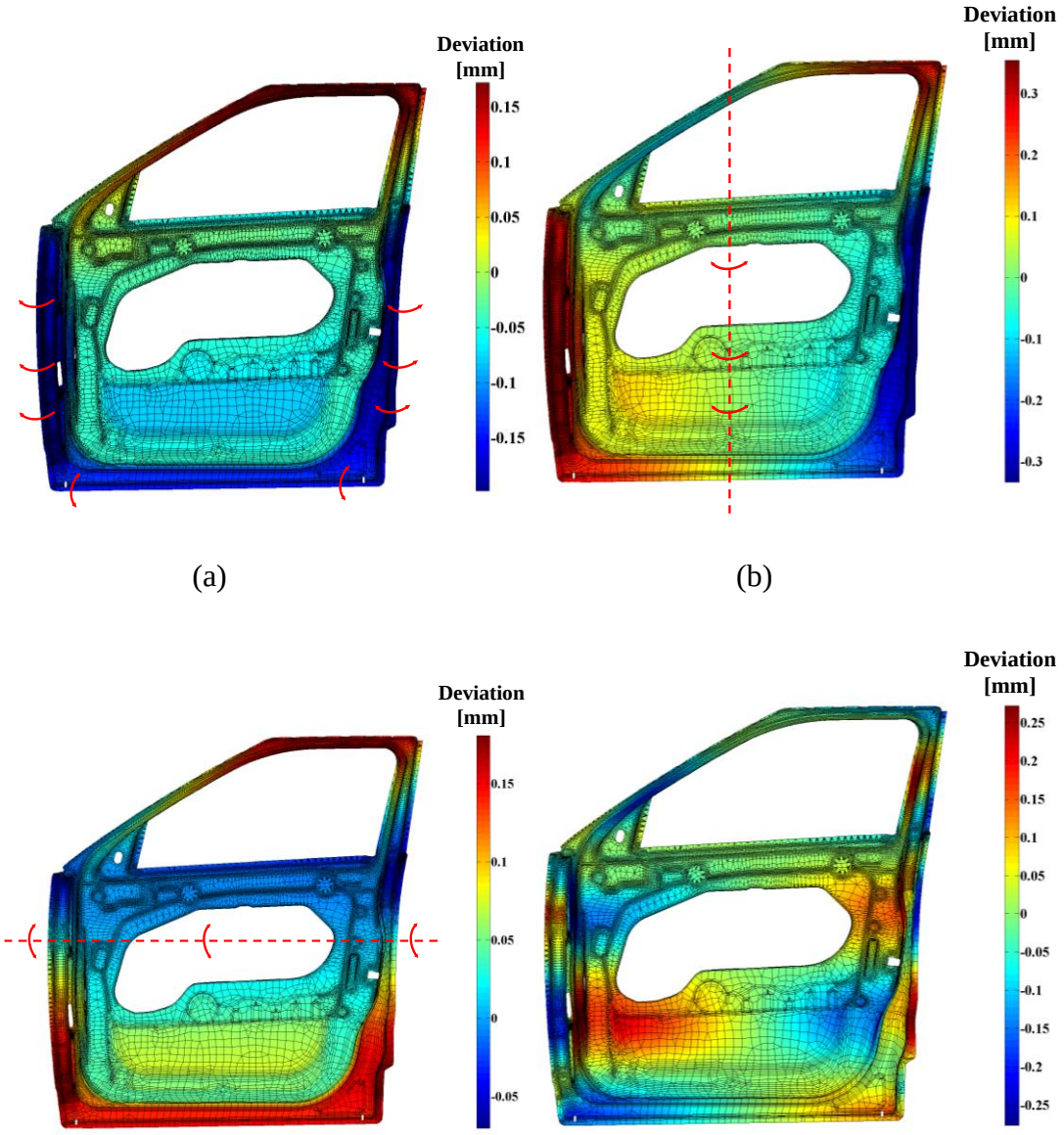

Figure 4.12 Few main shape error modes with their interpretation

For example, looking at the first four main shape error modes (see Figure 4.12), the following can be concluded:

- The first mode exhibits a predominant bending effect around the flange area [Figure 4.12(a)]

- The second mode shows a tendency to pure bending around the dotted line in vertical axis as represented in red dotted line [Figure 4.12(b)]
- The third mode presents the bending of the part around the horizontal axis [Figure 4.12(c)]
- The fourth mode presents freeform shape error defects on the part [Figure 4.12(d)]

These GMA decomposed shape error modes can be utilised for freeform shape error simulation as per the GD&T requirements. Further, the functional data analysis model, GMA, can be used for statistical monitoring of shape error related defects based on measured CoP data.

4.4.2 Comparison with Other Models

The current shape error decomposition techniques similar to GMA decomposition are SMA method (Huang and Ceglarek, 2002; Huang *et al.*, 2014) and natural mode decomposition (Samper and Formosa, 2006). The GMA method has been compared with both techniques to demonstrate its usefulness and applicability for shape error modelling.

4.4.2.1 Comparison with SMA Model

The SMA methodology has several limitations which are listed in Table 4.1. As the SMA technique fails to model shape error with complex topological structure, a numerical case study based on rectangular shape error field has been selected for comparison. The shape error field is defined by a grid of 1326 points where the part is bended and twisted as shown in Figure 4.13(a). The recovered shape error fields from SMA and GMA model using 8 modes are exactly the same as shown in Figure 4.13(b). It authenticates the ability of GMA to decompose part shape error into

dominant modes and the reconstructed shape error is evident of part shape error modelling which has been extended to model 3D freeform shaped part.

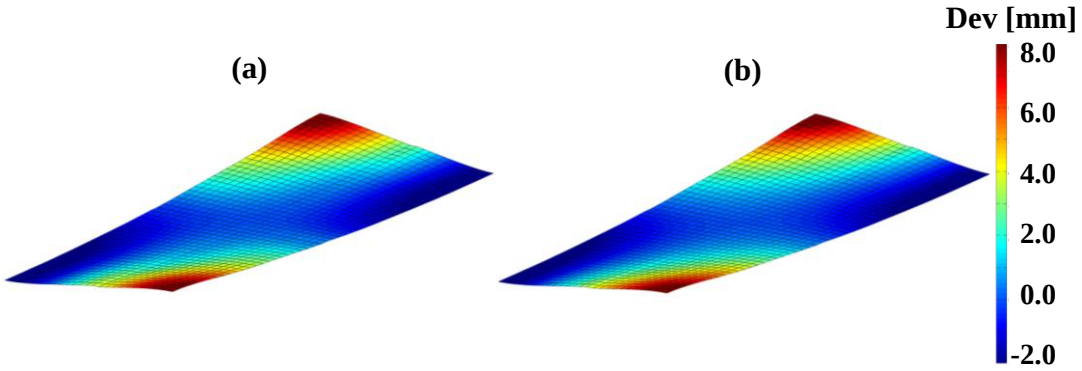

Figure 4.13 Numerically developed rectangular shape error: (a) original shape error, and (b) reconstructed shape error using SMA and GMA methods

4.4.2.2 Comparison with Natural Mode Decomposition

The GMA approach has also been compared with natural mode decomposition proposed by Samper and Formosa (2006). The hinge reinforcement case study has been selected for comparison with identical parameters chosen for both decomposition methods. Figure 4.14 shows the original measured shape error of hinge and reconstructed shape error using natural mode decomposition and GMA decomposition (200 modes selected to rebuild the shape error). Further, authors (Samper and Formosa, 2006) explicitly state that the residue surface does not decrease with the mode number. The possible reasons for their limitation may be due to predefined modes which are based on the stiffness and mass material properties. However, a manufacturing or forming process may not only depend on these two material properties but can also be influenced by a host of other factors such as, sliding friction, damping effect, creep effect, buckling effect, thermal distortion etc. The natural mode decomposition does not consider all those factors which might be associated with the manufacturing process; this implies that some error modes

cannot be modelled. Subsequently, results in higher residue surface. Due to the absence of these error modes, the residue surface cannot reach near zero. On the contrary, the developed GMA approach does not depend on the predefined modes and directly decomposes the measured shape error, hence, the residue surface can reach to near zero with addition of sufficient number of modes. It is essential to identify the minimum number of modes for accurate reconstruction when parametric modelling of shape error is important for many applications, such as prediction of shape error under new process conditions; GD&T analysis for shape deviations; or assignable cause identification through root cause analysis. Therefore, for ease of analysis and applicability of the shape error model, accurate shape error representation with reduced number of modes is essential and unavoidable.

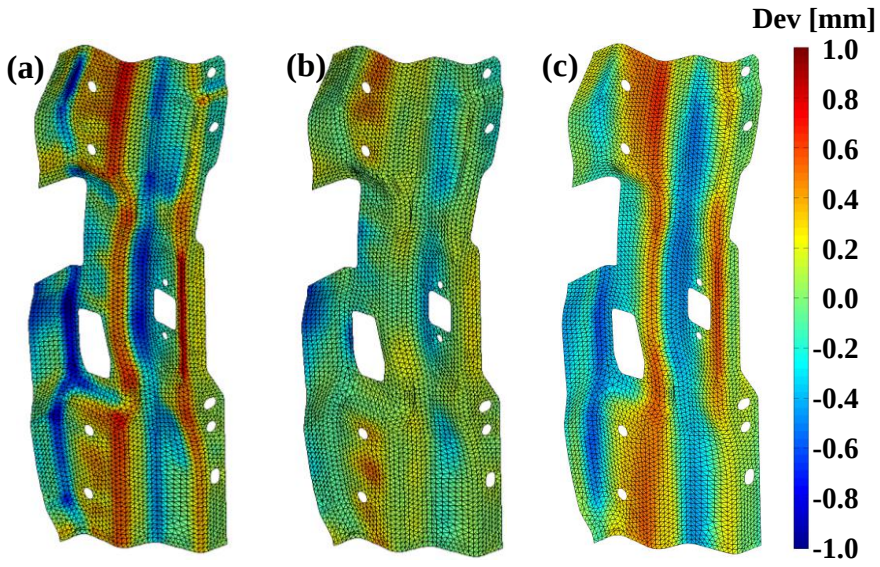

Figure 4.14 Hinge surface deviation: (a) Original shape error, (b) Rebuild shape error using natural mode decomposition (200 modes), and (c) Rebuild shape error using GMA decomposition (200 modes)

Root Sum of Squares (RSS) error has been selected to quantify the residue surface. RSS error of residue surface after surface reconstruction for same number of modes is typically higher for natural modes decomposition and also Standard Deviation

(SD) of residue surface for GMA decomposed modes are usually less in comparison with natural modes.

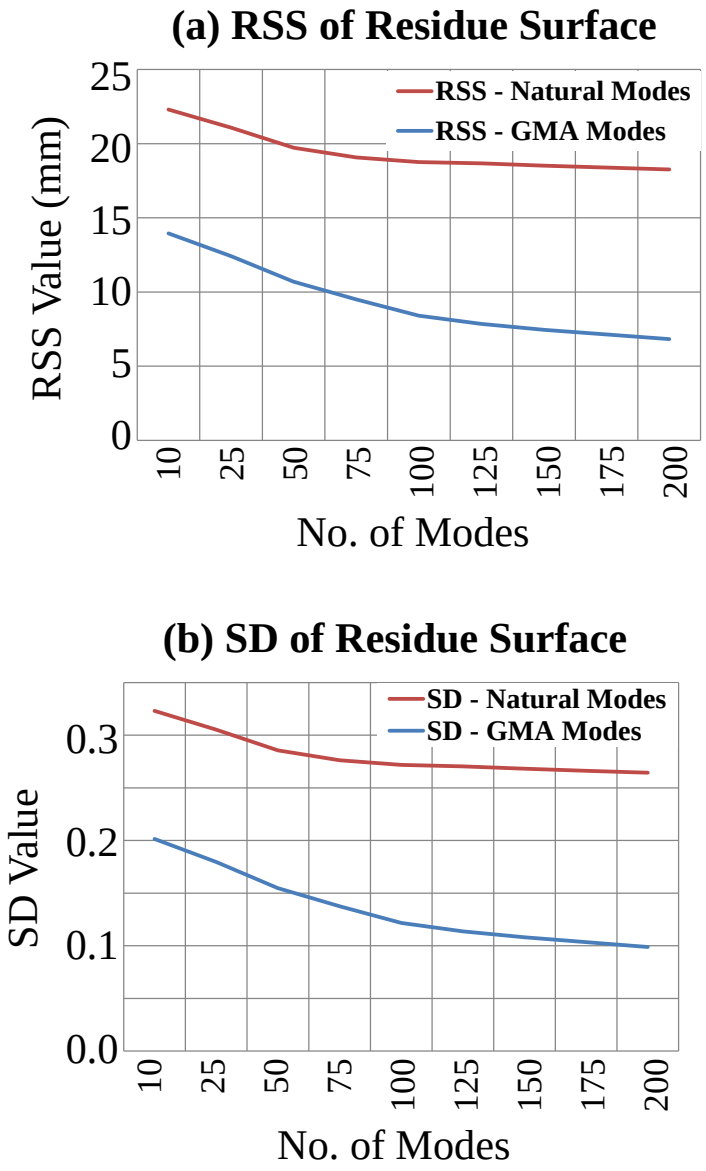

Figure 4.15 Comparison of natural modes and GMA modes: (a) root sum of squares of the shape error of residue surface, and (b) standard deviation of the shape errors of residue surface

This is the evident from Figure 4.15 where GMA is converging to the original surface deviation much faster than the natural mode decomposition. GMA can reconstruct the measured shape error by selecting all the modes where the RSS and

SD become zero. On the contrary, using natural mode decomposition the original shape error cannot be reconstructed even if all modes are selected.

4.5 SUMMARY

This chapter focuses on developing shape errors modelling approach for individual compliant part. Current industrial emphasis is on development of a universal functional model to express shape error in a coherent manner by integrating design features (ideal shape information) with manufacturing variability (real shape information). The major challenges to bridge design data (CAD model) with manufacturing are limited availability of appropriate shape errors modelling methodology which can identify and characterise shape errors to emulate real part. Currently existing shape error modelling approaches are mainly limited to 2D domain or limited accuracy in case of emulating 3D parts.

In order to address this problem, this chapter proposed a *functional data analysis* model, named *Geometric Modal Analysis (GMA),* has been developed to extract significant shape error patterns associated with non-ideal part. It mainly takes design information (CAD data) and manufacturing information (part surface measurement) as input to extract significant shape error patters. However, building a unified functional data analysis model is not trivial due to irregular surface of 3D shaped complex part, significant error mode identification, and correct depiction of error model to emulate real part shape errors.

The GMA method involves three main steps:

(i) Data pre-processing includes generation of mesh model from nominal CAD model and measured part data (CoP) post-processing to obtain shape error

deviation field. The CAD model using nominal mesh to obtain the original mapping of shape error field from CoP data.

(ii) *GMA decomposition* involves voxelisation of mesh model, Laplace interpolation, and 3D DCT decomposition. The mesh model is enveloped with 3D voxel grid in order to transform the 3D irregular surface model to uniform 3D volume structure. The calculated mesh node deviations are stored in the corresponding voxel element and Laplacian smoothing is applied to assign meaningful values in the empty voxel elements while keeping the original deviation as internal boundary constraints. Thereafter, 3D DCT decomposition performed on the Laplace interpolated uniform voxel grid data and main shape error modes are obtained.

(iii) *GMA mode identification* involves mode selection criteria and mode magnitude correction to achieve desired model accuracy. GMA mode truncation has been achieved through (a) Energy Compaction Criteria; and (b) Pearson's Linear Correlation Criteria to keep the shape error model controllable. The model accuracy is achieved through introducing least square based mode magnitude correction criteria.

The industrial case study shows that GMA method can be applied to decompose measurement data of 3D freeform shaped parts. Further, comparison with state-of-art available methods shows advantages of GMA method for modelling shape errors of individual compliant part.

CHAPTER 5 SHAPE VARIATION MODELLING OF BATCH OF COMPLIANT PARTS

5.1 INTRODUCTION

Quantification and prediction of shape variation of sheet metal parts as well as machined components are crucial for accurate analysis of assembly functionality and tolerancing. Due to inherit process variation, fabricated parts exhibit shape variation which is required to be quantified to predict and control the production quality. For example, a batch of sheet metal parts produced by metal forming process such as stamping consists of shape variation. Therefore, the fabricated parts are not identical in terms of engraved shape errors. This shape variation is mainly results of process parameters variation, tool wear or spring-back in case of sheet metal stamping (de Souza and Rolfe, 2008). The shape variation creates quality and assemblability issues in many sectors such as automotive body-in-white assembly, aerospace wing or fuselage assembly, home appliances or electronics assembly. Therefore, to predict the assembly quality or to understand the effect of shape variation at the end of assembly, part shape error model is not sufficient. Modelling of shape error associated with individual non-ideal part fails to quantify the *production shape variation*. Therefore, quantification of individual part errors is not sufficient enough to meet industrial needs which emphasise to quantify shape variation engraved within a batch of parts. End of line product quality variation (caused by part deformation due to fabrication process variation) or part fit-ups errors (caused by part-to-part interaction) are the result of shape variation. Further, quantification of these shape variation is important to generalise the type of shape errors associated

with batch of parts. Therefore, shape variation must be simulated upfront in order to predict assembly performance, product quality and production yield. As a result, there is a strong need for shape variation modelling of a batch of parts.

Major challenges involving batch of non-ideal parts' shape variation modelling and quantification can be categorised into

(i) Identification and characterisation of shape variation by developing functional data model, and

(ii) Quantification of shape variation by analysing the shape error modes from production parts.

To meet the functional requirement of shape variation modelling, the functional data analysis approach (developed in Chapter 4), named Geometric Modal Analysis (GMA), has been used to extract the shape error modes. However, the GMA approach is limited to extract shape error information from individual part which is not able to model and quantify the shape variation associated with a batch of production parts.

Therefore, the part shape error decomposition approach, GMA (proposed in Chapter 4), has been extended to model and quantify the shape variation of a batch of production parts. This chapter proposes a *Statistical Geometric Modal Analysis (SGMA)* method aiming to mitigate the obstacles towards shape variation modelling of production parts by addressing the following:

(i) statistical characterisation of the shape error modes (i.e. modal parameters) encrypted within a batch of parts, and

(ii) quantification of production shape variation by synthesising *composite parts*.

SGMA method uses the parametric nature of decomposed shape error modes to model batch of parts and quantifies the shape variation by synthesising *composite parts*. By changing the magnitude of shape error modes, a large number of production parts can be represented. On contrary, c*omposite part* can be defined as a part which is composed of all the major shape error modes present in the production parts. In reality, the composite part may not exist but it reduces the efforts required for assembly process simulation by avoiding Monte-Carlo type simulation. Manufacturing processes which are very sensitive to part shape variation, require in-depth understanding on the effect of shape variation to the end product quality. Especially in case of assembly process simulation with compliant parts, the shape variation modelling for production parts is unavoidable as it has direct impact on the achievable assembled product quality and process performance (Das *et al.*, 2014; Jing *et al.*, 2010; Franciosa *et al.*, 2014). For example, emerging new assembly joining process, such as Remote Laser Welding (RLW) cannot be simulated without taking into consideration of compliant production parts as it requires tight control of both minimum and maximum part-to-part gap (Ceglarek, 2011). Thus, simulation conducted for ideal part results in incorrect and unreliable output (100% of conforming assemblies) which does not depict the real production scenario (Das *et al.*, 2014). Therefore, to eliminate a large number of simulation runs with different shape error instances, the concept of composite part helps to (i) reduce number of simulation iterations without losing the performance of assembly process simulation; and, (ii) to predict the overall final assembly quality quickly. Therefore, the shape variation modelling is inevitable prerequisite as input for assembly process simulation with compliant parts and process performance evaluation.

The following sections of this chapter are arranged as follows: Section 5.2 summarises the limitations of current shape variation modelling methods available in literature. Section 5.3 describes the proposed SGMA methodology to model shape variation through mode selection and statistical characterisation of modes. Further, the subsections describe the virtual generation of variational parts and synthesis of composite parts. Section 5.4 describes SGMA method with industrial cases for generating variational virtual parts and synthesising of composite parts. The chapter is summarised in Section 5.5.

5.2 LIMITATIONS OF CURRENT APPROACHES

To decompose shape errors based on measurement data, few data-driven as well as analytical approaches have been reported in literature. To extract shape error modes from a batch of parts, Camelio *et al.* (2004b) and Matuszyk *et al.* (2010) proposed Principal Component Analysis (PCA) based pattern recognition approach. However, PCA based decomposition has limitations which are discussed in Chapter 3 (refer to Section 3.3) towards identifying the shape error of sheet metal part. Further, Samper *et al.* (2009) extended their natural mode decomposition approach (Samper and Formosa, 2006) to model shape variation where they reported virtual generation of variational parts using estimated mean and standard deviation under normality assumption which is far too simplified and not necessarily true for sheet metal stamping. Another decomposition approach, Statistical Modal Analysis (SMA) proposed by Huang and Ceglarek (2002) and Huang *et al.* (2014) assumes normal distribution of shape error modes during virtual generation of variational parts and is limited to 2D parts. Further, not only to generate variational virtual parts but also to quantify shape variation, this chapter extends the GMA approach to model batch of

parts (i) by characterising the statistical nature of decomposed modes to generate variational instances; and (ii) by synthesising composite parts (i.e. to quantify shape variation). Till date, the shape variation modelling approaches are limited to variational virtual part generation and there is no approach found in literature to quantify the shape variation of a batch of parts. Table 5.1 summarises shape variation modelling approaches reported in literature with their limitations.

Table 5.1 Current shape variation modelling approaches with their applications and limitations

Researchers	Decomposition principle	Applications	Limitations
Camelio *et al.* (2004b) Matuszyk *et al.* (2010)	Principal component analysis (PCA) based decomposition of batch of parts	Assembly process simulation	Normality assumption and shape error modes are not decomposed independently
Huang and Ceglarek (2002); Huang *et al.* (2014)	2D Discrete Cosine Transform (2D DCT) of measured data set.	Virtual generation of variational parts	Normality assumption and limited to virtual shape error generation of 2D part.
Samper and Formosa (2006) Samper *et al.* (2009)	Natural mode decomposition and then, compared with measured data (CoP)	Assembly process simulation, statistical tolerancing	Not accurate to model freeform shaped sheet metal parts and only limited to virtual generation
Proposed in this thesis	GMA based shape variation characterisation and quantification	Process design, statistical tolerancing	Sample size selection to develop the model

5.3 STATISTICAL GEOMETRIC MODAL ANALYSIS (SGMA) METHODOLOGY

The Statistical Geometric Modal Analysis (SGMA) method extends the GMA model to extract shape error modes from a batch of parts. The present methodology focuses on, *firstly*, the statistical characterisation of shape error modes at production level to represent variational virtual parts; and *secondly*, shape variation quantification of a batch of parts by synthesising composite parts. These variational virtual parts are representative of the production volume and composite parts are the quantification of production shape variation. The methodology identifies the GMA decomposed significant shape error modes associated with a batch of parts. Subsequently, it describes mode selection for batch of parts and modal matrix creation for statistical characterisation followed by virtual generation of variational parts. It also develops different criteria for creating composite parts which are mainly based on maximum energy compaction, minimum energy compaction; root sum of squares (RSS) error. Figure 5.1 depicts the overview of the SGMA method to generate variational virtual parts and composite parts relying on the modal characteristics of the measured batch.

The methodology is based upon the following two hypotheses to simplify the modelling process for a batch of parts:

(i) Sample size selection assumption: The shape error is not of deterministic type but random error field process. Therefore, the number of parts selected is the statistical representative of the production population. The shape error modes obtained through GMA decomposition are the representative of the shape variation obtained from the production process.

(ii) Production process stability assumption: The operating conditions under which the selected samples are produced remain almost same throughout the

production. Therefore, the shape error modes within the sample parts remain approximately same throughout the production without introducing completely different shape error modes.

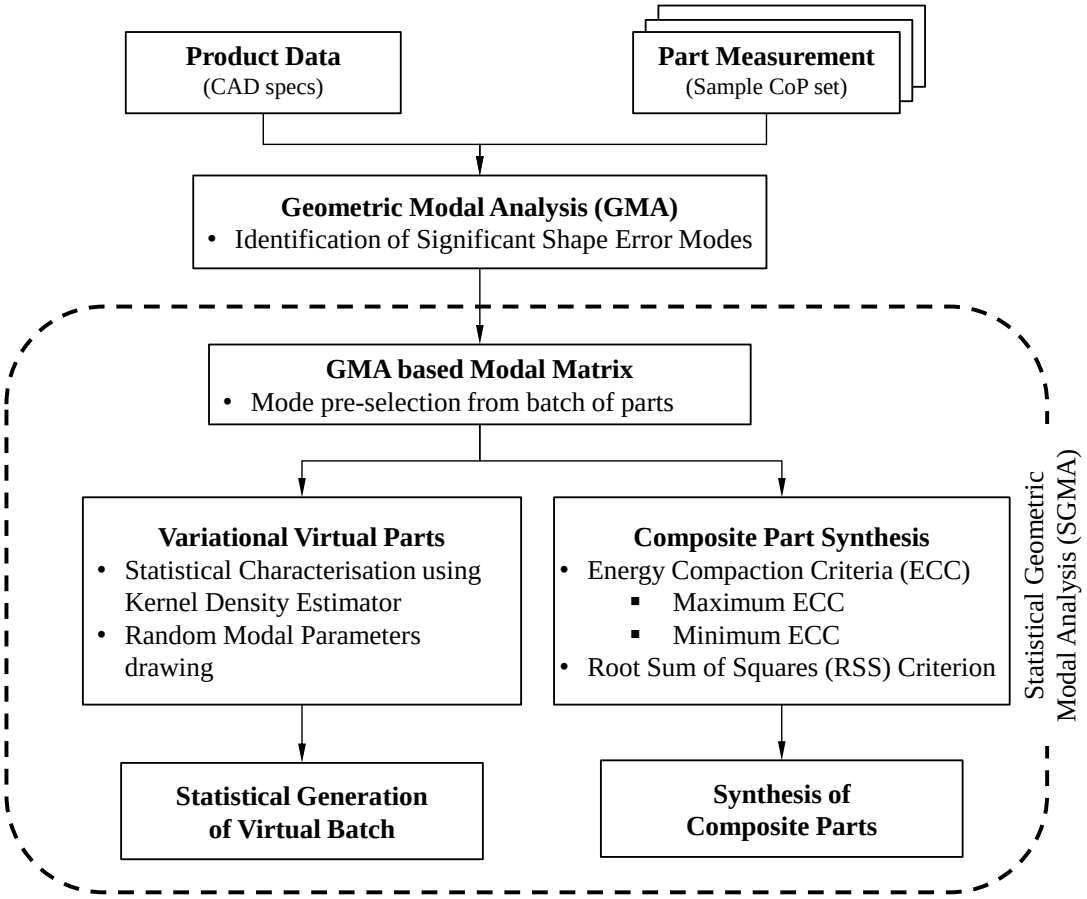

Figure 5.1 Overview of Statistical Geometric Modal Analysis (SGMA) method for shape variation modelling

5.3.1 GMA Based Modal Matrix

Utilising the GMA decomposition, a batch of parts (i.e. representative of production parts) is decomposed. The batch of parts carries the engraved process information in terms of shape variation. These GMA extracted modes will be further utilised for virtual part generation and synthesising composite parts. To identify the shape error modes responsible for main process variation, the energy compaction and correlation criteria have been employed. Therefore, the truncated shape error modes are reserved

for SGMA model development and the residual shape errors, occurring mainly due to uncertainly and noise in measurement data, are discarded. By reversing the equation (4.5), the original shape error field can be expressed as equation (5.1), where $\tilde{C}(u,v,w)$ contains the truncated or preserved modes and residual is expressed as ε. The preserved shape error modes can be further reduced to *Xb*, where *b* is the set of energy truncated and correlation truncated coefficient values and *X* is composed of orthogonal shape vectors.

$$\begin{aligned} f(i,j,k) &= \sqrt{\frac{2}{L}}\sqrt{\frac{2}{M}}\sqrt{\frac{2}{N}}\sum_{u=0}^{L-1}\sum_{v=0}^{M-1}\sum_{w=0}^{N-1}\alpha(u)\alpha(v)\alpha(w)\cos\left[\frac{\pi u(2i+1)}{2L}\right] \\ &\quad \cos\left[\frac{\pi v(2j+1)}{2M}\right]\cos\left[\frac{\pi w(2k+1)}{2N}\right]\tilde{C}(u,v,w)+\varepsilon \\ &= Xb+\varepsilon \end{aligned} \qquad \textbf{(5.1)}$$

where, $\alpha(\xi)=\begin{cases}\frac{1}{\sqrt[2]{2}} & if,\xi=0\\ 1 & if,\xi\neq 0\end{cases}$

Suppose, q number of modes $(\tilde{C}_1,\tilde{C}_2,...\tilde{C}_q)$ are preserved after energy and correlation truncation of individual part decomposition and represents as b_1 which can be expressed as

$$b_1=[\tilde{C}_1,\tilde{C}_2,...\tilde{C}_q] \qquad \textbf{(5.2)}$$

Further, considering the sample batch size *m*, the decomposed modal parameters can be expressed as

$$\beta=[b_1,b_2,...b_m]^T \qquad \textbf{(5.3)}$$

The set β composed of mainly two set of modal parameters: (i) Common modes: present in every part of the sample *m*, and (ii) Uncommon modes: appear only in few sample (<*m*) of the decomposed parts. Combining both common and uncommon modal set, *p* modal parameters have been preserved for shape variation modelling.

These p modal parameters are again extracted from m parts which forms the modal parameter set β, a $p \times 1$ vector, can be generalised as

$$\beta = [\tilde{C}_1, \tilde{C}_2, ... \tilde{C}_p]^T \quad \textbf{(5.4)}$$

Evaluation of proper magnitude of the modal parameters is necessary for accurate shape variation modelling. As described in GMA method, magnitude correction has been achieved through assigning proper weightage to p number of selected modal parameters using least squares where the truncated coefficients multiplied with associated weightage wt i.e., $\tilde{C} = C \times wt$. Therefore, modal parameter set β (selected based on m sampled parts) creates the modal matrix for the batch and can be expressed as $p \times m$ matrix.

$$\beta_{p \times m} = \begin{bmatrix} \tilde{C}_{11} & \tilde{C}_{12} & \cdots & \tilde{C}_{1m} \\ \tilde{C}_{21} & \tilde{C}_{22} & \cdots & \tilde{C}_{2m} \\ \vdots & \vdots & \ddots & \vdots \\ \tilde{C}_{p1} & \tilde{C}_{p2} & \cdots & \tilde{C}_{pm} \end{bmatrix} \quad \textbf{(5.5)}$$

The modal matrix $\beta_{p \times m}$ will be utilised for statistical characterisation to generate variational virtual parts and also for synthesising composite parts.

For example, a batch of top hat parts (sample size m) is decomposed into main orthogonal shape error modes by using GMA technique as explained in Figure 5.2. After applying the modes selection criteria, p number of modes is selected to generate the modal matrix. Therefore, each top hat part is decomposed and p set of modes is retained for shape variation modelling. Each mode has unique deformation pattern, however, the magnitudes of the deformation pattern is changing from part-to-part. Therefore, from the modal matrix created for top hat parts, it can be observed that each mode has varying magnitudes across the parts which pointing towards the statistical characterisation of modes.

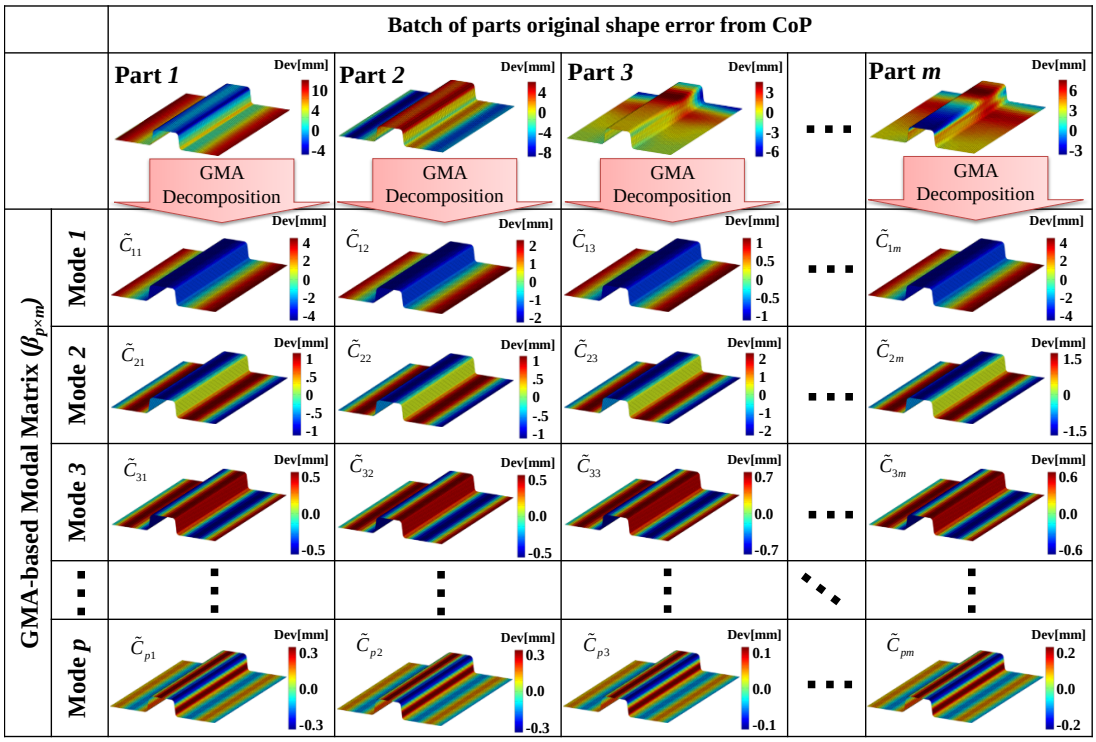

Figure 5.2 GMA based modal matrix creation by using a batch of top hat parts

5.3.2 Variational Virtual Parts

Generating virtual parts involves two major steps: *first*, the statistical characterisation of modal parameters which are identified through individual part decomposition of the sample set. One way to address the statistical characterisation is to fit proper statistical distribution to the each mode of modal matrix. *Second*, relying on the statistical distribution of the modes, a set of p modal parameters can be drawn for N_v times to create virtual batch of N_v parts.

5.3.2.1 Statistical Characterisation of Preserved Modes

The each modal parameter of modal matrix, $\beta_{p\times m}$, needs to be fitted with suitable statistical distribution. Typically, the modal parameters are characterised by mean modal vector and covariance matrix based on the assumption that the modal parameters are normally distributed (Huang *et al.*, 2014). Samper *et al.* (2009) demonstrated virtual batch production assuming normal distribution where the modal

parameters are obtained by decomposing nominal CAD model of the parts. Many real processes, the assumption of normal distribution may not be accurate as most of the processes do not conform to normal distribution. GMA decomposition technique is based on the real measurement data where the assumption of normal distribution may not be accurate as sheet metal stamping does not conform to it. Therefore, use of Kernel Density Estimation (KDE) to estimate the Probability Density Function (PDF) of the modal parameters may overcome the problem if the modal parameters are not normally distributed.

A parametric approach for determining the PDF assumes that the density function will take a particular form which needs to be specified upfront (Montgomery, 2008). For example, in case of normal density function, the mean value and standard deviation of the process variables are to be estimated first. In contrast, nonparametric density estimation does not require prior knowledge about form of the density function. KDE is a very powerful class of data driven techniques for non-parametric estimation of PDFs (Silverman, 1986; Wand and Jones, 1994) which fits an empirical distribution to a sample data set approximating the population. The density function is determined by summing up small bumps that are placed at the centre of the each observation. The shape of the bumps is defined by the kernel functions such as Gaussian, Triangular or Epanechnikov type (Silverman, 1986). Consider a kernel function $K(\tilde{C})$ and a sample set for modal parameters, $\beta = [\tilde{C}_1, \tilde{C}_2, ...\tilde{C}_m]$ from a population distribution density $F(\tilde{C})$, then the density estimate (Silverman, 1986) of the sample can be written as

$$\hat{F}(\tilde{C}, h) = \frac{1}{mh} \sum_{r=0}^{m} K\left(\frac{\tilde{C} - \tilde{C}_r}{h} \right) \qquad \textbf{(5.6)}$$

where, h is the window width also called as smoothing parameter or bandwidth parameter. In this work, the kernel function is a Gaussian kernel as the form of the kernel function is not important. On the contrary, the smoothing parameter or bandwidth determines the accuracy of the PDF. Therefore, each mode is fitted with PDF as per the modal matrix defined in equation (5.5) and p modal fitting distribution obtained as explained in Figure 5.3. Further, ranges and distributions are plotted in Figure 5.4.

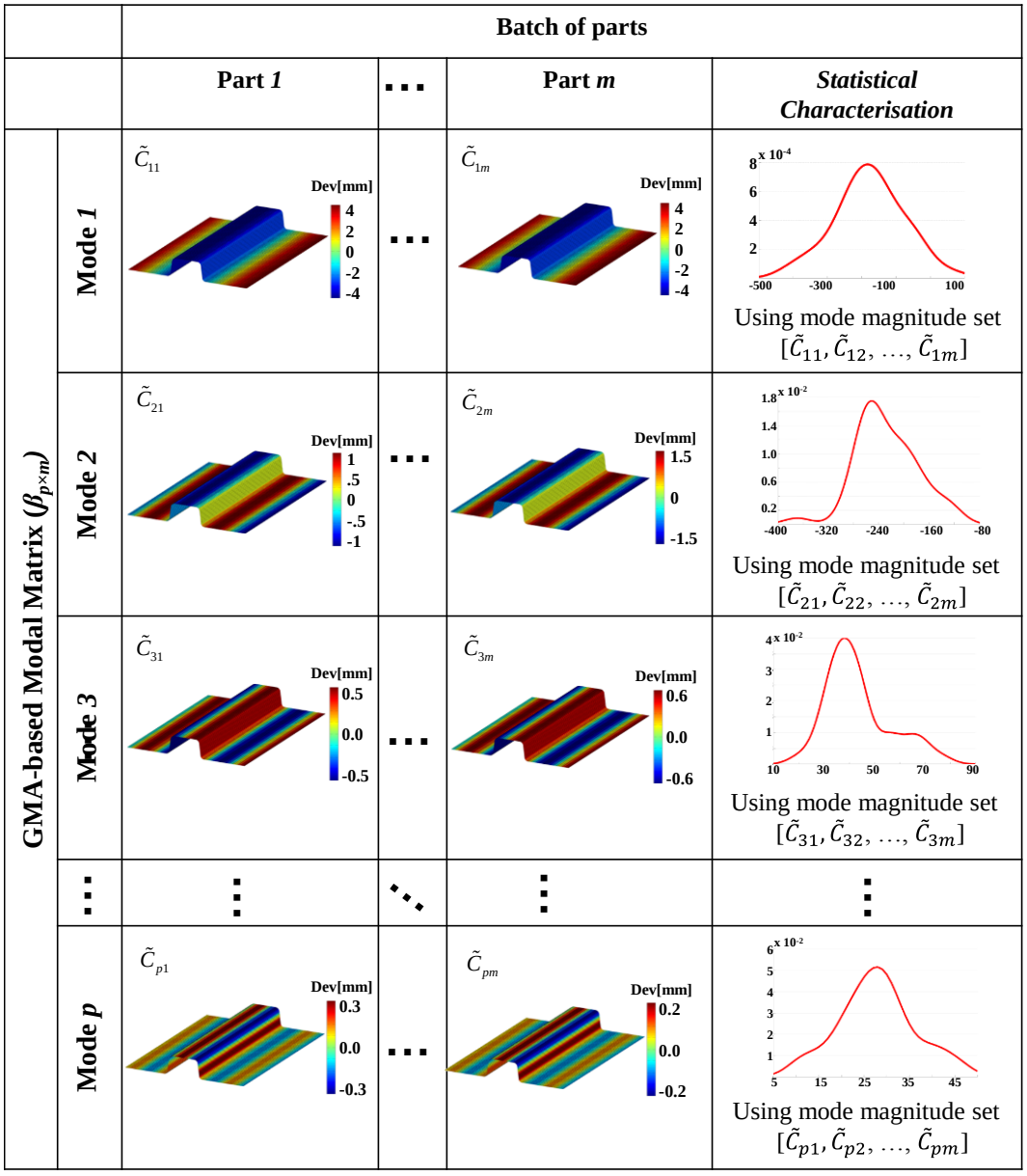

Figure 5.3 Statistical characterisation of modal parameters using top hat parts

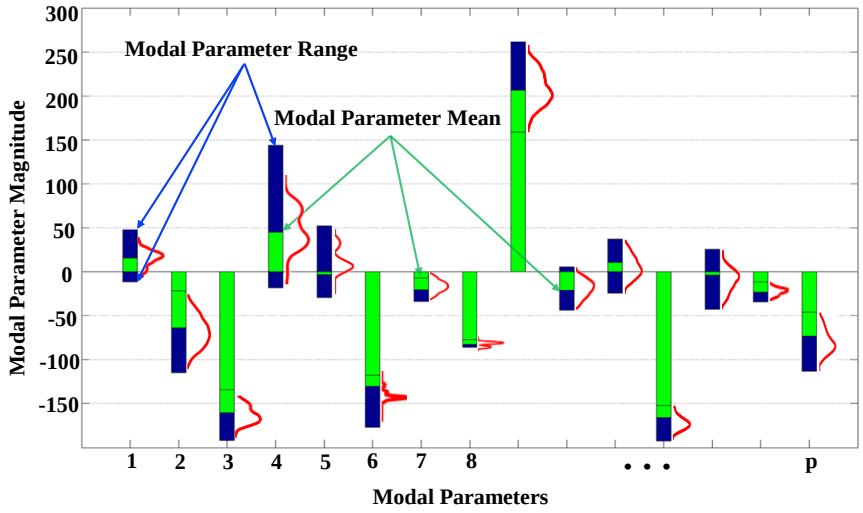

Figure 5.4 Statistical characterisation of modal parameters using KDE

5.3.2.2 Generation of Virtual Batch of Parts

The aim is to generate a batch of virtual parts based on the PDF of fitted kernel density to each modal parameter of $\beta_{p\times m}$. Utilising this statistical characterisation, a number of batches can be generated which may consist of different modal parameters or magnitudes relying on the batch measurement data. Magnitudes of the p preserved modal parameters are drawn to generate variational virtual part as presented in Figure 5.5 and following the same, a number of parts can be generated which represents the virtual batch.

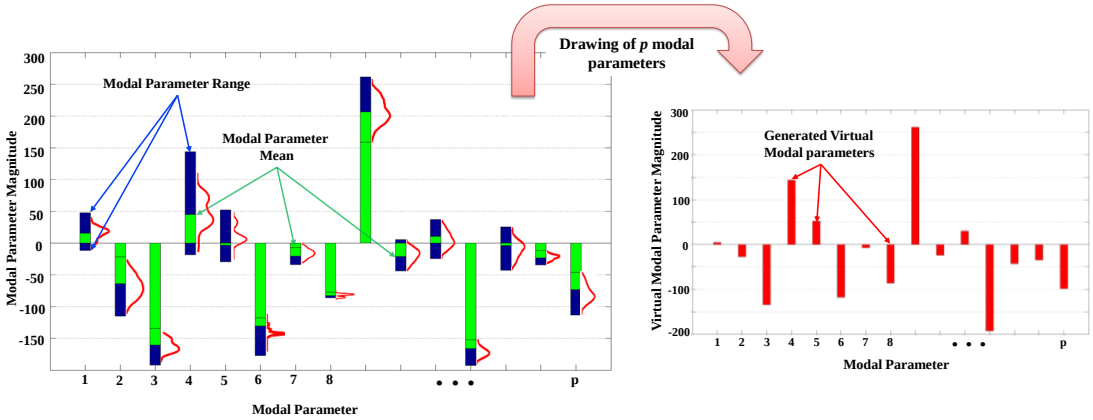

Figure 5.5 Generation of variational virtual parts based on statistical characterisation of modal parameters

The generation of virtual batch depending upon the modal parameter characteristics is made as follows:

- A set of p modal parameters is drawn for N_v times to make virtual batch of N_v parts. Each modal parameter follows the probability distribution obtained through KDE which form virtual modal matrix for N_v parts, $\beta_{p\times N_v}$ consisting of p modal parameters.

$$\beta_{p\times N_v}=\begin{bmatrix}\tilde{C}_{11} & \tilde{C}_{12} & \cdots & \tilde{C}_{1N_v}\\ \tilde{C}_{21} & \tilde{C}_{22} & \cdots & \tilde{C}_{2N_v}\\ \vdots & \vdots & \ddots & \vdots\\ \tilde{C}_{p1} & \tilde{C}_{p2} & \cdots & \tilde{C}_{pN_v}\end{bmatrix} \quad \Downarrow \quad \beta_{p\times\tau}=[\tilde{C}_{11},\tilde{C}_{12},\cdots,\tilde{C}_{p\tau}]^T \quad \text{where, } \forall\,\tau=(1,2,\cdots,N_v) \tag{5.7}$$

- From the obtained virtual modal matrix, $\beta_{p\times N_v}$, each virtual part coefficients $\beta_{p\times\tau}$, where $\tau\ \forall\ (1,2,\ldots,N_v)$ are applied with 3D Inverse-DCT (3D IDCT) as per the following equation (5.8) to obtain the shape error field.

$$\tilde{f}(i,j,k)=\sqrt{\frac{2}{L}}\sqrt{\frac{2}{M}}\sqrt{\frac{2}{N}}\sum_{u=0}^{L-1}\sum_{v=0}^{M-1}\sum_{w=0}^{N-1}\alpha(u)\alpha(v)\alpha(w)\cos\left[\frac{\pi u(2i+1)}{2L}\right]\cos\left[\frac{\pi v(2j+1)}{2M}\right]\cos\left[\frac{\pi w(2k+1)}{2N}\right]\beta_{p\times\tau} \tag{5.8}$$

where, $\alpha(\xi)=\begin{cases}\frac{1}{\sqrt[2]{2}} & if,\xi=0\\ 1 & if,\xi\neq 0\end{cases}$

The function $\tilde{f}(i,j,k)$ refers to the shape error field (i.e. mesh node deviations) which are generated by using the virtually generated modal coefficients set, $\beta_{p\times\tau}$. The obtained deviations are applied to corresponding mesh nodes to generate variational virtual parts.

5.3.3 Synthesis of Composite Parts

The composite part can be defined as a hypothetical part which is composed of all the major shape error modes present in the population. Depending on the nature of shape error present in the measured batch, composite part might be more than one to represent the whole population. To categorise the parts having similar type of shape error, shape error modes based clustering approach has been adapted. For clustering, k-means method has been applied to classify the parts with similar shape error. This clustering method helps to partition measured parts into mutually exclusive clusters and provides the index of the parts belong to each clusters. Ray and Turi (1999) explained intra-cluster distance and inter-cluster distance based approach which allows the number of clusters to be determined automatically. However, the graphical approach developed by Rousseeuw (1987) is very well known to check where the Silhouettes graph provides a measure of how close each point in one cluster is to points in the neighbouring clusters. This measure ranges from +1, indicating points that are very distant from neighbouring clusters, through 0, indicating points that are not distinctly in one cluster or another, to -1, indicating points that are probably assigned to the wrong cluster. A more quantitative way to compare the cluster solutions is to look at the average silhouette values.

Through the clustering process, R number of cluster has been obtained and corresponding cluster will consist of N_R number of parts. Therefore, the modal matrix for N_R number of parts which contains p modal parameters become

$$\beta_{p\times N_R} = \begin{bmatrix} \tilde{\tilde{C}}_{11} & \tilde{\tilde{C}}_{12} & \cdots & \tilde{\tilde{C}}_{1N_R} \\ \tilde{\tilde{C}}_{21} & \tilde{\tilde{C}}_{22} & \cdots & \tilde{\tilde{C}}_{2N_R} \\ \vdots & \vdots & \ddots & \vdots \\ \tilde{\tilde{C}}_{p1} & \tilde{\tilde{C}}_{p2} & \cdots & \tilde{\tilde{C}}_{pN_R} \end{bmatrix} \quad \textbf{(5.9)}$$

where, $\forall R = (1,2,..R)$ and $N_R \subseteq N_v$.

Composite part(s) can be synthesised from the $\beta_{p\times N_R}$ modal matrix using different selection criteria which are mainly based on energy compaction and root sum of squares.

5.3.3.1 Energy Compaction Criteria (ECC) for Composite Part

Energy compaction index of a mode is the ratio of the energy of the selected mode to the total energy of the modes (particular part) which can be used to select modes for energy compacted composite part generation. Therefore, energy compaction index can be obtained for every modal parameter of the $\beta_{p\times N_R}$ modal matrix which can be determined as

$$E_{\tilde{C}_{p\tau}} = \frac{\tilde{C}_{p\tau}^2}{\sum_{p=1}^{p} \tilde{C}_{p\tau}^2} \qquad \textbf{(5.10)}$$

$$\textit{where,} \quad \begin{cases} \forall p = 1,2,\cdots p \\ \forall\, \tau = 1,2,\cdots N_R \end{cases}$$

Further, relying on the maximum and minimum energy index criteria, maximum and minimum set of modal parameter values can be obtained which will create composite parts containing maximum and minimum variation of shape error respectively.

$$\begin{aligned} (E_{\tilde{C}_p})_{\max} &= \max\{E_{\tilde{C}_{p1}}, E_{\tilde{C}_{p2}}, \cdots E_{\tilde{C}_{pN_R}}\} \\ (E_{\tilde{C}_p})_{\min} &= \min\{E_{\tilde{C}_{p1}}, E_{\tilde{C}_{p2}}, \cdots E_{\tilde{C}_{pN_R}}\} \\ \text{where, } \forall p &= (1,2,\cdots, p) \end{aligned} \qquad \textbf{(5.11)}$$

Therefore, the maximum and minimum energy compaction part can be expressed as

$$\begin{aligned} \beta_{\max} &= [\tilde{C}_{(E_{\tilde{C}_1})_{\max}}, \tilde{C}_{(E_{\tilde{C}_2})_{\max}}, \cdots \tilde{C}_{(E_{\tilde{C}_p})_{\max}}]^T \\ \beta_{\min} &= [\tilde{C}_{(E_{\tilde{C}_1})_{\min}}, \tilde{C}_{(E_{\tilde{C}_2})_{\min}}, \cdots \tilde{C}_{(E_{\tilde{C}_p})_{\min}}]^T \end{aligned} \qquad \textbf{(5.12)}$$

Using equation (5.8) and equation (5.12), the composite parts can be created which are consisting of maximum and minimum energy coefficients. These composite parts

can be expressed as the maximum and minimum boundary of shape error. Furthermore, pictorial demonstration on synthesising top hat composite parts based on maximum and minimum energy compaction criteria is illustrated in Figure 5.6.

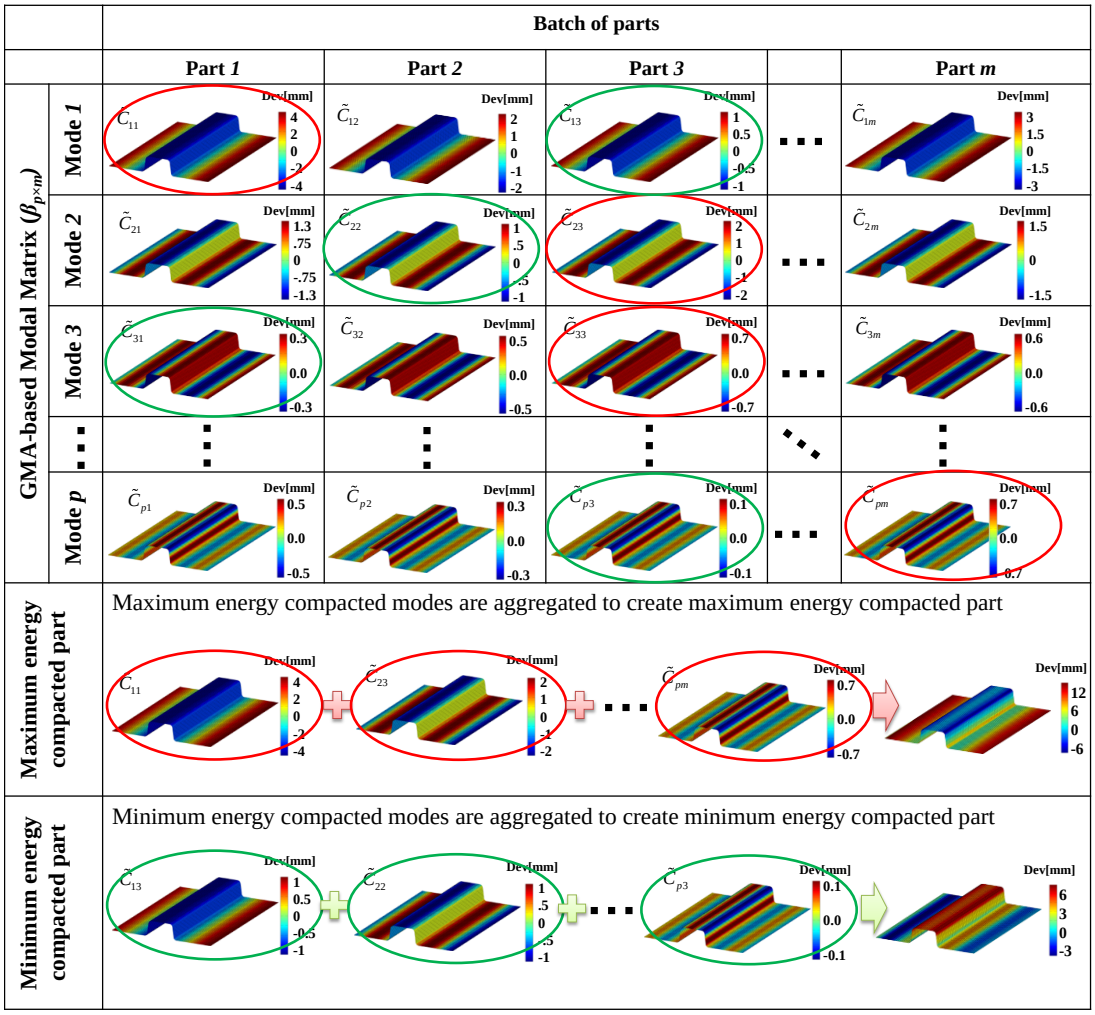

Figure 5.6 Synthesis of maximum and minimum energy compacted composite parts based on top hat parts

5.3.3.2 Root Sum of Squares (RSS) Criterion for Composite Part

A RSS based composite part can be defined as the part from which root sum of squares measure to original shape error of all the parts belong in the cluster is minimum. Therefore, by determining the proper weightage associated with each modal parameter, RSS based composite part can be created and the weightage vector are computed through least squares approach. The original shape errors (i.e. mesh

node deviations) of N_R parts are kept as $D = [D_1 \quad D_2 \quad \cdots \quad D_{N_R}]_{n \times N_R}$. The RSS based mesh node deviation $[D_{RSS}]_{n \times 1}$ can be obtained through the following minimisation problem as explained in equation (5.13).

$$min\left[\sqrt{\sum_{R=1}^{N_R}(D_{RSS} - D_R)^2}\right] \tag{5.13}$$

Each preserve modal parameter has unique orthogonal shape vector corresponding to unit value. Mesh node deviations of each parameter are stored as $T = [T_1 \quad T_2 \quad \cdots \quad T_p]_{n \times p}$. Therefore, using the least squares to solve the over determined systems which minimises the sum of squares corresponding to each part and provides the weighted coefficients, β_{LS}.

$$\begin{bmatrix} T_1 & T_2 & \cdots & T_p \end{bmatrix}_{n \times p} \times \begin{bmatrix} wt_1 \\ wt_2 \\ \vdots \\ wt_p \end{bmatrix}_{p \times 1} = \begin{bmatrix} D_{RSS} \end{bmatrix}_{n \times 1} \tag{5.14}$$

The least squares estimation for the weightage associated with each modal parameter is computes as $wt = (T^T T)^{-1} T^T D_{RSS}$. Therefore, the coefficient set for creating composite part using RSS criteria is given as

$$\begin{aligned} \beta_{LS} &= [C_1 \times wt_1, C_2 \times wt_2, \cdots C_p \times wt_p]^T \\ &\Downarrow \\ \beta_{LS} &= [C_{wt_1}, C_{wt_2}, \cdots C_{wt_p}]^T \end{aligned} \tag{5.15}$$

The coefficient set, β_{LS}, is applied in equation (5.8) to obtain the shape error field over the voxel grid and voxel deviation is applied to mesh nodes to get the composite part error field deviation.

5.4 RESULTS OF SGMA WITH INDUSTRIAL CASE STUDY

Results of the developed SGMA method is illustrated with an industrial case study of door inner panel. The case study demonstrates the two aspects of SGMA method: (i) generation of variational virtual parts, and (ii) synthesis of composite parts. Door inner panel is the main door frame on which all other reinforced components (such as reinforced door opening, hinge reinforcement, latch reinforcement) are welded. Therefore, the shape variation management of door inner panel is very crucial to achieve quality product. The door inner panel is of 0.75 mm thick and relatively large size with a number of features and curvatures on it as displays in Figure 5.7(a). The shape error field has been obtained by calculating the deviations at the nominal mesh nodes [refer to Figure 5.7(b)].

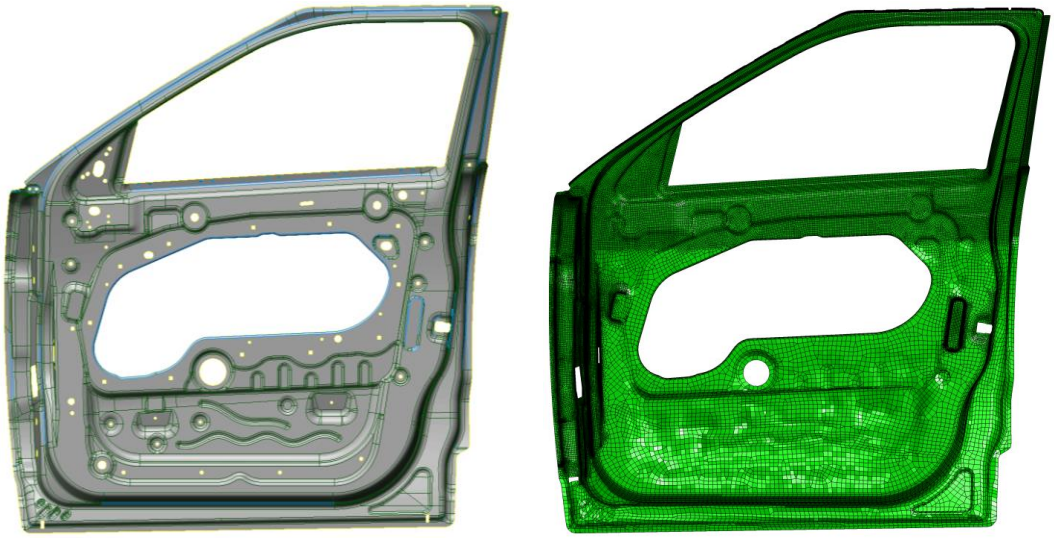

(a) (b)

Figure 5.7 Door inner panel of automotive door: (a) nominal CAD model, and (b) mesh model of the part

Initially, GMA method (developed in Chapter 4) has been applied to decompose original shape error of a batch of parts obtained from the measurement. To apply GMA methodology, a voxel grid size of 50×100×100 has been selected to store the

computed mesh node deviations. GMA decomposed modes are truncated using 90% energy compaction criterion. Further, selection of significant shape error modes has been achieved using Pearson's correlation criterion which facilitates to recognise the most significant modes to reconstruct the original shape error. A correlation threshold, α=0.10 has been implied to keep the decomposition model smooth. Total 53 modes have been identified as main error patterns, (*p=53*), from the batch of parts which are illustrated in Figure 5.8. These modal parameters are used as preserved modes.

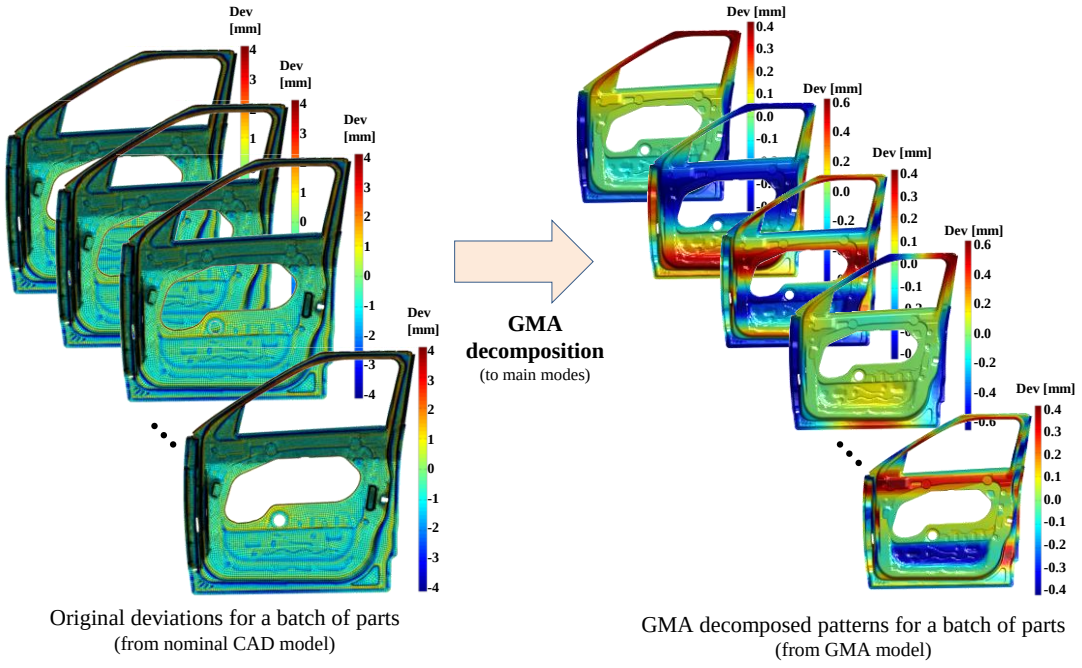

Original deviations for a batch of parts
(from nominal CAD model)

GMA decomposed patterns for a batch of parts
(from GMA model)

Figure 5.8 Main shape error modes identification of a batch of parts using GMA decomposition

After identifying the main modal parameters in terms of main modes, the associated magnitudes are corrected using least squares as explained in GMA method. The identified modal parameters are stored to form the modal matrix in order to characterise, further, for generating variational virtual parts and composite parts.

5.4.1 Variational Virtual Door Inner Panel Generation

Each modal parameter is fitted with distribution function using KDE to determine the PDF associated with each mode. A few significant modes with their distributions have been reported in Figure 5.9.

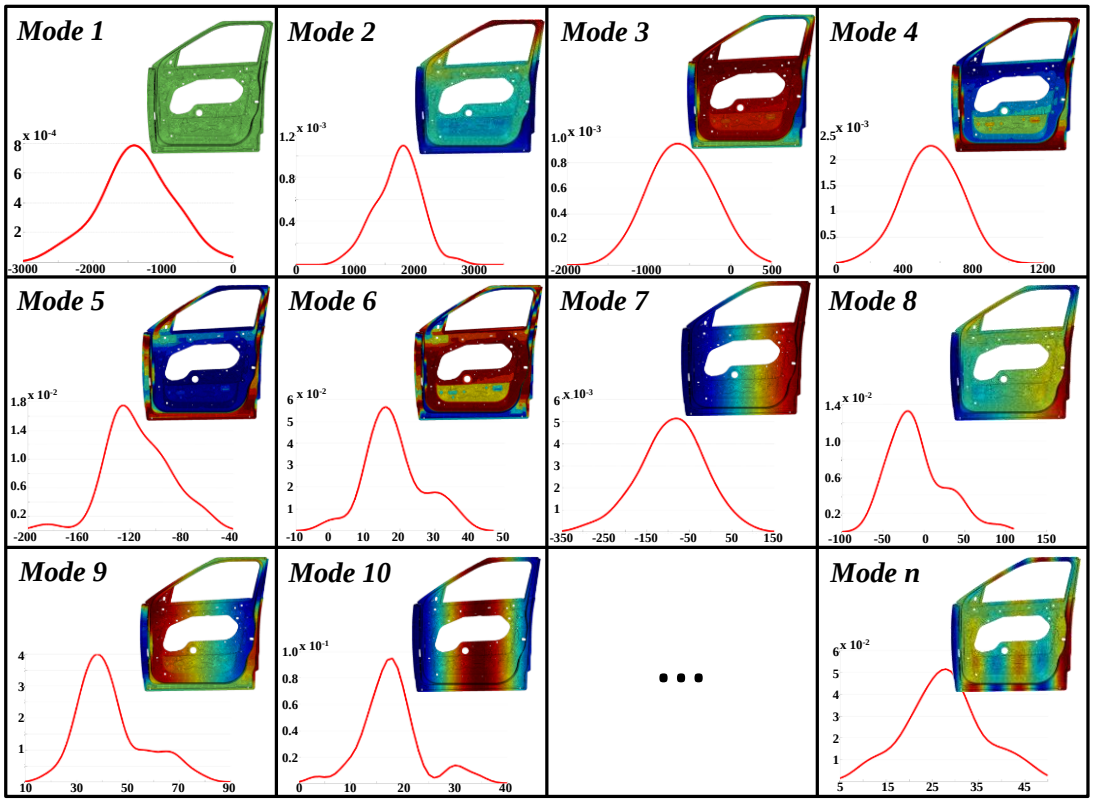

Figure 5.9 Statistical characterisation of modal parameters of door inner panel by determining the probability density function (PDF) using KDE

Based on the distribution obtained through decomposition of a batch of parts, a number of random modal parameters can be drawn from the distribution, and virtual modal matrix for N_v parts can be obtained, $\beta_{p\times N_v}$ consisting of p modal parameters. Each row of the virtually generated modal matrix represents a virtual variational part. Therefore, the virtual generation of parts has been generalised and random variational virtual parts can be generated based on the batch of measured parts data.

5.4.2 Synthesis of Composite Parts

Initially, clustering has been carried out to identify the number of clusters present in the batch using the k-means technique. The selection of correct number of clusters is not a trivial task. One of the widely accepted approaches is to examine the Silhouettes graph with their average values for deciding proper number of clusters. Figure 5.10 depicts the Silhouettes plot for different cluster combinations and average Silhouettes values are evaluated for each occurrence for proper selection of number of clusters.

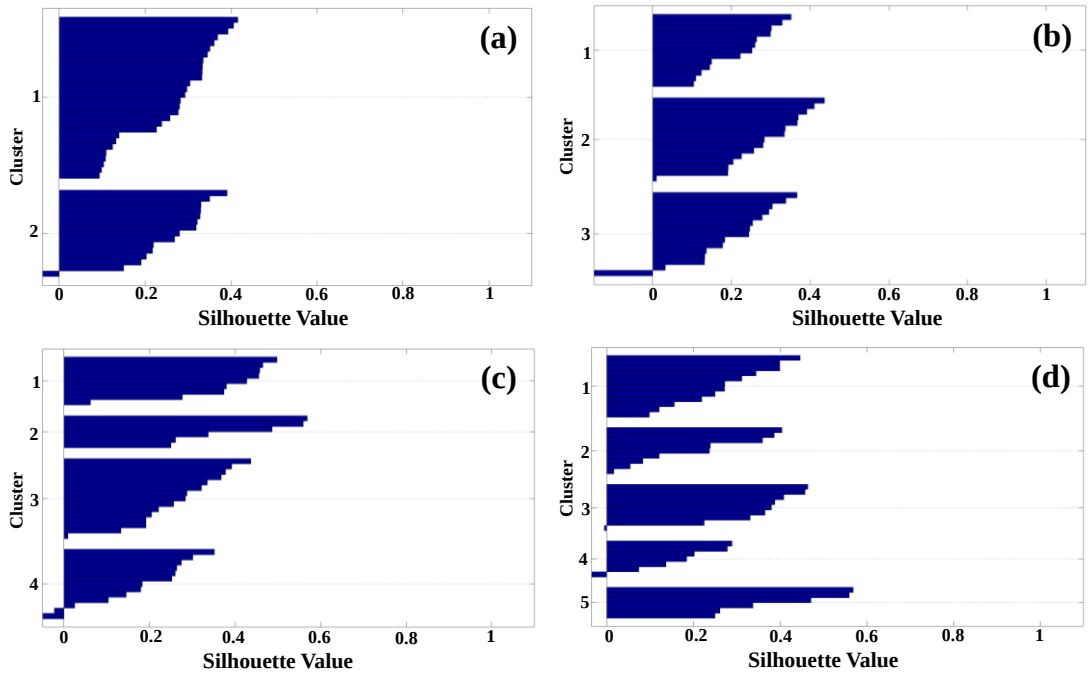

Figure 5.10 Silhouettes graph plot for (a) 2 clusters; (b) 3 clusters; (c) 4 clusters; and (d) 5 clusters

It is evident from the Silhouettes plots, the average Silhouettes values for the four different occurrences are below 0.3 which is an indication that the grouped parts are relatively close to each other. However, parts are divided into three clusters [Figure 5.10(b)] exhibit highest Silhouette value of 0.282 and decreases with increase of number of clusters. Therefore, reasonably the batch can be sub grouped into three

clusters which are consisting of similar shape error modes. For each cluster, three types of composite part can be obtained based on the maximum energy compaction criterion, minimum energy compaction criterion, and RSS criterion. These three types of composite part for three clusters are presented in Figure 5.11. Therefore, the shape variation coming from the production can be quantified through the composite parts where only few composite parts can represent the whole production. It is worth noticing that the root sum of squares error based composite parts are exhibiting almost similar shape error for all the clusters while maximum and minimum energy compacted composite parts differ from cluster to cluster.

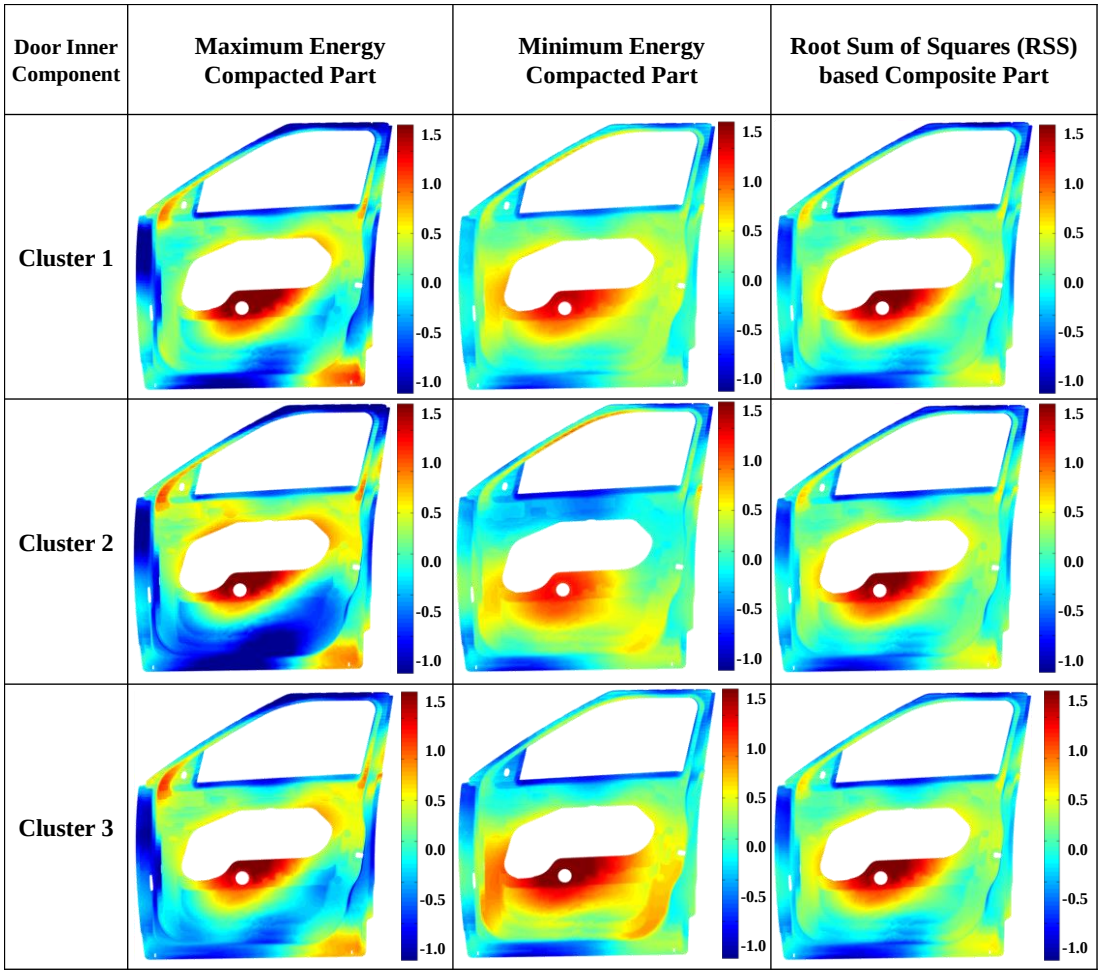

Figure 5.11 Synthesis of composite parts (deviation in mm) for three clusters based on (a) maximum energy compaction, (b) minimum energy compaction, and (c) root sum of squares criterion

The composite parts are compared with original part deviations in order to evaluate the quality of the synthesised composite parts. The representative error map of residue surface (i.e. the difference from composite part to original part deviation of corresponding cluster) is shown in Figure 5.12. It can be observed that residue surfaces from RSS based composite parts are similar as the RSS based composite parts are representative of original average part deviation. On contrary, residue surfaces generated from maximum and minimum energy compacted composite parts are showing the areas of shape variation occurring during production run. Further, the average root sum of squares (RSS), mean and standard deviation (SD) of residue error surfaces are reported in Table 5.2. It can be observed that RSS error of residue surface is higher for maximum energy compacted parts and lower for root sum of squares based composite parts.

	Average Residue Surface Plot (Difference between Composite Parts and Original Parts)		
Door Inner Component	**Maximum Energy Compacted Part**	**Minimum Energy Compacted Part**	**Root Sum of Squares (RSS) based Composite Part**
Cluster 1	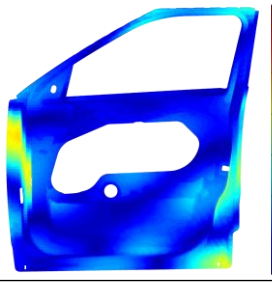	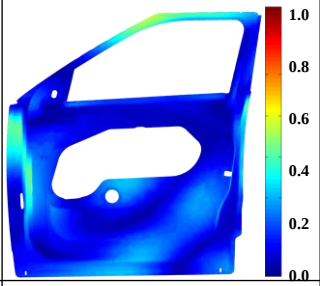	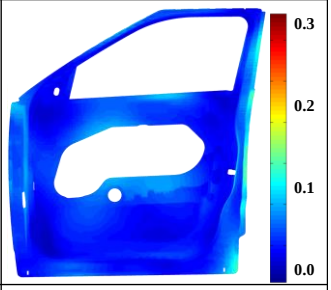
Cluster 2	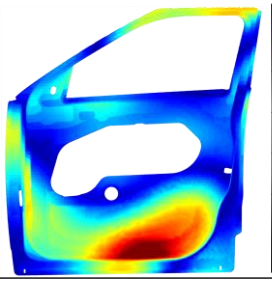	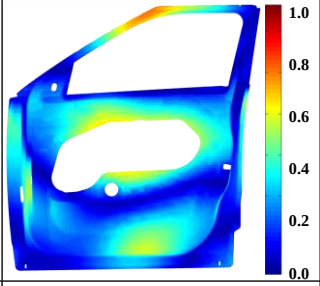	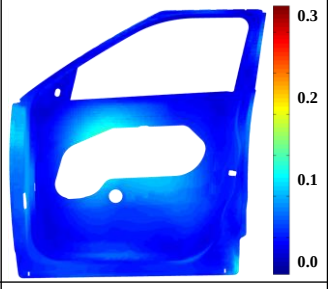
Cluster 3	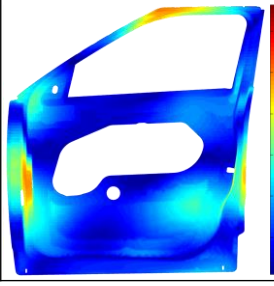	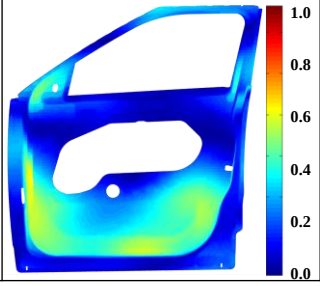	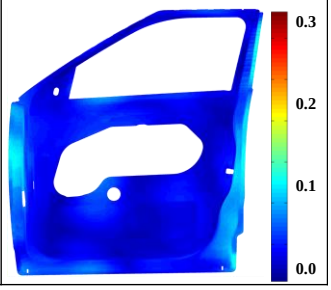

Figure 5.12 Average residue surface plot by using maximum, minimum and RSS based composite parts (deviation in mm)

Table 5.2 Comparative analysis between the generated composite parts and original part deviation by quantifying the average residue surface

Residue Surface Variation Quantification		Maximum Energy Compacted Part	Minimum Energy Compacted Part	Root Sum of Squares (RSS) based Composite Part
Cluster 1	RSS	72.01	65.32	19.61
	Mean	0.192	0.173	0.051
	SD	0.155	0.138	0.049
Cluster 2	RSS	101.97	93.299	18.15
	Mean	0.286	0.258	0.047
	SD	0.196	0.183	0.056
Cluster 3	RSS	92.553	79.234	16.014
	Mean	0.253	0.217	0.04
	SD	0.185	0.157	0.039

5.5 SUMMARY

This chapter develops shape variation modelling methodology to quantify the shape variation associated with a batch of parts which is representative of production population. As the product quality and production yield are determined based on the production volume of real parts, *production shape variation* modelling and quantification method is required for accurate depiction of production process. Individual part shape error quantification is not sufficient enough to meet industrial needs which emphasises on quantification of the shape variation engraved within a batch of parts. There are very few approaches available in literature and those are mainly focused on virtual generation of variational parts. However, no reported work

is available to quantify the shape variation associated with production parts. The challenges in the area of shape variation modelling are:

(i) Identification and characterisation of real part shape variation, and

(ii) Quantification of shape variation through analysing the production parts.

To address the aforementioned shape variation modelling challenges of production batch, this chapter proposed *Statistical Geometric Modal Analysis (SGMA)* method which is an extension of GMA method. The main steps involve:

(i) Identification of significant shape error modes: GMA decomposition has been used on a batch of parts (i.e. production parts) to identify the main shape error modes coming from the production volume. Further, it creates a GMA based modal matrix which is composed of main modal parameters with their varying magnitudes.

(ii) Statistical characterisation of each mode: Statistical behaviour of the identified significant shape error modes has been determined using data-driven Kernel Density Estimator (KDE). This helps to overcome the limitations associated with normal distribution assumption if the modal parameters are not normally distributed.

(iii) Quantification of shape variation: The composite parts are synthesised to quantify the shape variation of a batch of compliant parts. They are composed of major shape errors coming from production volume.

The SGMA method produces the following results:

(i) *Generation of variational virtual parts:* Relying on the statistical distribution of the modes, variational virtual parts can be generated by randomly drawing modal parameters from the distribution.

(ii) *Generation of composite parts:* Synthesis of composite parts has been achieved through selection of different composition criteria. It quantifies the shape variation of a batch of parts.

The industrial case study shows that SGMA method can be applied to generate variational virtual parts and composite parts. Depending on the type of shape errors present in the measured sample set, composite part might be more than one to represent the whole population.

CHAPTER 6 CONTROL CHARTS TO MONITOR PROCESS AND PRODUCT QUALITY SHAPES

6.1 INTRODUCTION

Many industrial processes are capable of generating massive amounts of data increasingly captured by in-process sensor networks. At present, some of these data cannot be used for statistical process control, defect detection or prediction of end-of-line product quality. For example, shapes of manufactured parts often represent an important aspect of quality, yet, there is lack of efficient approaches for statistical process monitoring of non-linear shapes. Similarly, assembly manufacturing processes with compliant (deformable) parts are one of the most common processes used in many industries such as automotive, aerospace, appliance, and electronics. Many of these processes are quite complex, for example, an automotive body assembly process includes 55-75 processing steps for around of 150-250 deformable sheet metal parts (Ceglarek and Shi, 1995; Shiu *et al.*, 1996). Additionally, there are strict quality requirements as described by the *Geometric Dimensioning and Tolerancing* (GD&T) which must be controlled as a part of the process quality monitoring system. This leads to the following requirements for process monitoring: (i) *types of defects detection*: *part errors* (part deformations caused by fabrication processes); *part fit-ups errors* (part-to-part interactions and interferences due to part errors, positioning errors or/and joining errors); and, (ii) *speed of detection*: delay from defect occurrence to detection and correction due to high volume production (cycle time can be between 50-70 vehicle per hour) which can help to reduce high

cost of scrap, repair, vehicle warranty and service. As a result, the above requirements have led to key advances in the development of modern metrology systems such as: (i) *metrology system types*: point-based measurement gauges (Coordinate Measuring Machines [CMM]) and the more frequently used surface-based measurement gauges (3D laser scanners or 3D white-light scanners) which allow to detect part errors (deformations) by capturing high dimensional Cloud-of-Points (CoP); and, (ii) *metrology system distribution:* due to process complexity, metrology sensors are used from off-line system (CMM gauges; 3D scanners placed in the metrology rooms) to rapidly increasing applications of in-process systems (end-of-line location and/or distributed metrology systems connected within a single network; for example 2D point-based scanners or emerging 3D surface-based white light scanners which capture CoP data directly during production).

The aforementioned advances in metrology systems development expanded opportunities for their applications in: (i) reverse engineering (generating CAD models from measured CoP data); and, (ii) quality inspection (template matching – referential approach that compares similarity between a template image and a test image; or comparing test image against CAD with GD&T requirements) (Son *et al.*, 2002). While the capability of 3D scanner metrology systems to capture massive amounts of in-process data (CoP of 3D object shape images) provides a unique opportunity for control of assembly process with compliant parts, however, currently 3D scanners cannot be used for statistical process control, defect detection or prediction of end-of-line or intermediate part errors or product shape quality.

This chapter presents a novel approach for shape-monitoring using high dimensional data (cloud-of-points) captured by in-process or off-line sensors or sensor networks. The proposed shape-monitoring methodology is based on a *functional data analysis*

model which is then used to develop integrated bivariate T^2-Q monitoring chart. The used *functional data analysis* model, called Geometric Modal Analysis (GMA) proposed in Chapter 4, aims to remove high redundancy in the data by defining reduced set of statistically uncorrelated and independent variables.

The *GMA-based integrated bivariate T^2-Q monitoring chart* uses both reduced variable sets as modelled by the GMA (T^2-statistic) and their residuals (Q-statistic) as a single bivariate scatter diagram. It is based on the joint probability density estimation using non-parametric Kernel Density Estimator (KDE) which has enhanced sensitivity to detect part defects. The resulting *GMA-based integrated bivariate T^2-Q monitoring chart* can be used for high dimensional non-normal data (cloud-of-points) captured by in-process or off-line sensors or sensor networks with the ability to: (i) detect global part shape failures such as unwanted variance change or mean shift, a common occurrence for batch-to-batch variation of stamped sheet metal parts; (ii) detect local part shape failures such as local shift or variance change; and, (iii) classify the shape faults to predict manufacturing quality and yield. Experimental and simulated cloud-of-points data from automotive manufacturing are used to determine the effectiveness of the proposed control chart under different defect conditions.

6.2 PROBLEM IDENTIFICATION

Due to increasing product and process complexity, 3D shape variations have critical impact on the final quality of the assembled product (Das *et al.*, 2014; Hu *et al.*, 2011). As a result, quality control of these deformable 3D shapes is key to ensure increasing assembly functionality and reduced residual stress in the final assembly. The monitored 3D shapes need to be evaluated and compared to the CAD model and

linked to the GD&T requirements. Modern 3D scanner metrology systems provide the opportunity to capture 3D shapes efficiently in-process or off-line using high dimensional data (CoP). Traditionally, the commonly used multivariate control charts involve monitoring small numbers of individual or composite variables. However, these are not sufficient for many industrial processes (Bersimis *et al.*, 2007), including 3D shape monitoring of compliant objects. For example, it is not uncommon to have hundreds of process variables most of which cannot be monitored simultaneously and are often correlated. Therefore, novel process control techniques are required which can fully utilize the potential of CoP data and provide a small number of effective process control chart(s) (ideally one).

Developing a single effective control chart is not trivial since the entire part shape information is to be monitored. In such a scenario, multivariate control chart plays a significant role to remove high redundancy in the data by defining reduced set of statistically uncorrelated and independent composite variables. For continuous feedback about the process in real time, these composite process variables (also termed latent variables) can provide a framework for continuous monitoring and highlight potential problems. Therefore, to obtain the relevant and effective set of latent variables, there is a tremendous need for 3D shape error modelling using high dimensional (CoP) measurement data. This model must represent the shape error in ways that can support further engineering analysis of 3D shape error patterns. Such shape error modelling can also be viewed as falling into the general area of functional data analysis (Ramsay and Silverman, 2005). This work involves a novel functional data analysis model, Geometric Modal Analysis (GMA) which aims to remove high redundancy in the data by defining reduced set of statistically uncorrelated and independent variables. The utilization of the functional data

analysis such as the GMA model provide significantly reduced set of latent variables (LVs) to represent 3D shape error. However, the GMA model of 3D shape error does not include residual errors caused by truncating the model, and measurement noise or error which might significantly affect the process control results. Additionally, the reduced set of LVs is often still too large (often more than 10-15 LVs; the presented case study of relatively complex hinge reinforcement part shape includes p>150 LVs) which gives rise to the problem of monitoring multiple control charts.

To avoid the aforementioned problem, *GMA-based functional data analysis* approach has been used to determine multivariate T^2 statistic. The measurement uncertainties in data are kept in Q statistic to improve the detectability of the control chart. Combining T^2 for the GMA modelled data and Q statistic for residual data (un-modelled) provides a bivariate scatter plot which is easier to monitor and also increases the sensitivity of the control chart towards fault detection. Further, as the measurement data of 3D shapes are non-normal, the shape monitoring chart is based on the joint probability density estimation of the integrated two statistics using non-parametric Kernel Density Estimator (KDE) which has enhanced sensitivity to detect part defects. The objective is to develop a statistical process control chart to detect shape errors using CoP data at single measurement station.

6.3 SHAPE MONITORING METHODOLOGY

The proposed GMA-based integrated T^2-Q shape monitoring control chart approach uses 3D scanner part shape data represented as CoP with millions of measurement points on a single part. Extraction of Latent Variables (LVs) is necessary to capture significant and essential information that is being encapsulated within the high dimensional recorded data (Kruger and Xie, 2012). The GMA approach is used to

extract Latent Variables (LVs) with key part shape information which is represented in the form of multiple orthogonal shape error modes. These shape error modes are then used to determine T^2 of the modelled shape information and Q which includes residual information. This gives a bivariate control chart for shape error monitoring. The overall shape error based monitoring methodology is depicted in Figure 6.1.

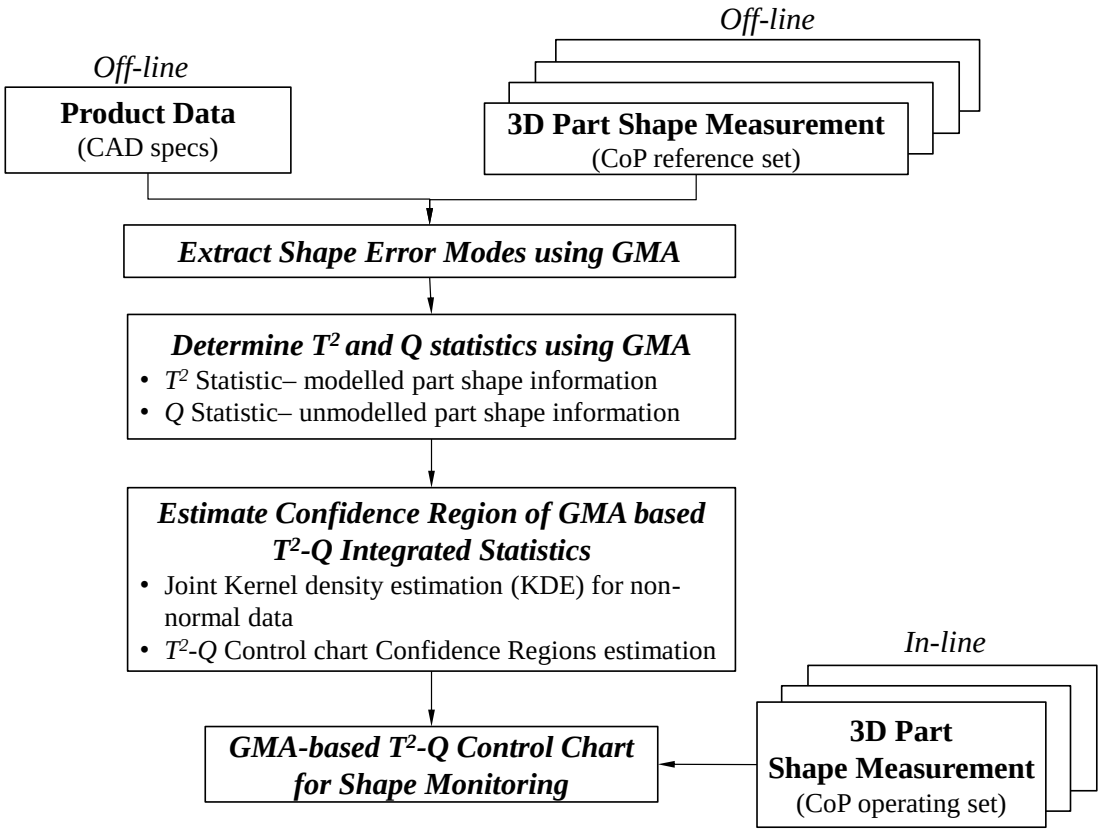

Figure 6.1 Overview of shape monitoring methodology driven by GMA method

6.3.1 Determine T^2 and Q Statistics using GMA

Compliant parts produced by fabrication processes contain shape errors which are required to be monitored. Geometric Modal Analysis (GMA) methodology has been developed in Chapter 4 which is used to characterise the inherent design features or patterns of shape errors within a part. A set of sample parts can be decomposed using GMA to obtain the significant modes which carry the engraved process information

in terms of shape errors. These modes will be further utilized for process monitoring and diagnosis where the modes can be used to represent root cause of the problem. Huang *et al.* (2014) found that lower frequency modes are caused by locator or datum induced part position or orientation errors whereas higher frequency patterns are due to manufacturing process variations such as spring back, part twisting, material handling, die or fixture misalignment etc. Therefore, efficient controlling method is a prerequisite to track whether the process is in control or out of control. The GMA transformed modes, i.e., equation (4.5) can be rewritten as

$$C(u,v,w) = f\left(i,j,k\right) \times_L C_L \times_M C_M \times_N C_N \tag{6.1}$$

Where, $\times_L, \times_M$ and $\times_N$ are the product operator and C_L, C_M and C_N are cosine basis transform matrices whose entries are given by

$$\left.\begin{aligned} C_L &= \left[\sqrt{\frac{2}{L}}\alpha(\varsigma)\cos\left(\frac{\pi u(2i+1)}{2L}\right)\right]_{L\times L} \\ C_M &= \left[\sqrt{\frac{2}{M}}\alpha(\varsigma)\cos\left(\frac{\pi v(2j+1)}{2M}\right)\right]_{M\times M} \\ C_N &= \left[\sqrt{\frac{2}{N}}\alpha(\varsigma)\cos\left(\frac{\pi w(2k+1)}{2N}\right)\right]_{N\times N} \end{aligned}\right\} \tag{6.2}$$

where, $\alpha\left(\varsigma\right) = \begin{cases} \frac{1}{\sqrt{2}} & \text{if, } \varsigma = 0 \\ 1 & \text{if, } \varsigma = 0 \end{cases}$

In equation (6.1), modes *C(u,v,w)* represent the transformed coefficients/modes (LVs) which is the class of orthogonal transformation where *(u,v,w)* defines the transformed coefficient elements in voxel space.

The GMA transformed modes can be classified into two categories: (i) dominant shape error modes which explain most of the shape error; and, (ii) residual error components which are mainly noise in the data, i.e., the measurement uncertainly. By reversing equation (6.1), the original shape error field deviation can be expressed

as (6.3), where $\tilde{C}(u,v,w)$ contains the truncated or preserved modes and residuals are expressed as ε. The significant error components can be further reduced to *Xb*, where *b* is the set of energy truncated coefficient values and *X* is composed of orthogonal shape vectors.

$$\begin{aligned} f(i,j,k) &= \tilde{C}(u,v,w) \times_N C_N^{-1} \times_M C_M^{-1} \times_L C_L^{-1} + \varepsilon \\ &= Xb + \varepsilon \end{aligned} \quad \textbf{(6.3)}$$

Using energy compaction criteria as per GMA, *p* modal parameters are preserved after decomposing *m* sampled parts. Therefore, the modal parameters set or LVs set (β), a $p \times 1$ vector, can be generalised as

$$\beta = [\tilde{C}_1, \tilde{C}_2, \ldots \tilde{C}_p]^T \quad \textbf{(6.4)}$$

where, $\tilde{C}_1, \tilde{C}_2, \ldots \tilde{C}_p$ are the truncated modal parameters used as LVs.

The residual coefficients are obtained for each part by considering all the remaining coefficients after deducting the β set from the original transform coefficient set *C(u,v,w)*. The residual vector is estimated as

$$\varepsilon = C(u,v,\mathrm{w}) - \beta \quad \textbf{(6.5)}$$

Synthesis of two statistics: (i) T^2 statistic has been determined by considering the LVs set β; and, (ii) *Q* statistic has been computed using the residual modal component, ε. Combining the T^2 and *Q* statistics together (Chen *et al.*, 2004) provides single bivariate scatter plot which is easier to monitor. Further, joint Probability Density Function (PDF) calculation becomes much easier as it depends only on two variables, additionally from a quality perspective, engineers need only use one single control chart for process monitoring.

6.3.1.1 T^2 Statistic

T^2 statistic gives a measure of significant variations of the process. Simply, it is the summation of squared coefficient values divided by their variance. T^2 statistic has been calculated as in equation (6.6) based on the modal parameters or LVs set (β), which are mainly result of common causes in the process.

$$T_k^2 = \sum_{i=1}^{p} \frac{\beta_{ki}^2}{\sigma_i} \tag{6.6}$$

where, $\forall k = 1,2,...,m$ represents the k^{th} part in the sample. β_{ki} and σ_i denote the i^{th} LV for k^{th} part and the estimated variance of i^{th} LV respectively.

6.3.1.2 Q Statistic

The residual variation is computed in Q statistic where the insignificant variations, caused mainly by measurement uncertainty are stored. The insignificant trends in the process are computed as

$$Q_k = \sum_{i=p+1}^{L\times M\times N} \varepsilon_{ki}^2 \tag{6.7}$$

where, $\forall k = 1,2,...,m$ represents the k^{th} part in the sample set and ε_{ki} denotes the insignificant i^{th} LV.

6.3.1.3 Orthogonality of T^2 and Q Statistics

The aforementioned T^2 and Q statistics depends upon the orthogonality property of GMA modes. Basically, the GMA modes are the transformed coefficients from voxel data using 3D DCT. The 3D DCT transformation equation (4.5) can be simplified and written in matrix form (Li *et al.*, 2013) as expressed in equation (6.1) and (6.2). It has been proven that each cosine bases transform matrix is an

orthogonal matrix (Rao and Yip, 1990; Strang, 1999), i.e. $C_Z^T = C_Z^{-1}$, where *Z = L or M or N*. Accordingly, 3D IDCT can be formulated as

$$\begin{aligned} f(i,j,k) &= C(u,v,w) \times_N C_N^{-1} \times_M C_M^{-1} \times_L C_L^{-1} \\ &\downarrow \\ f(i,j,k) &= C(u,v,w) \times_N C_N^{T} \times_M C_M^{T} \times_L C_L^{T} \end{aligned} \tag{6.8}$$

Further, the transformation matrix may be converted into a vector by concatenating the rows, columns and pages. The 3D DCT and 3D IDCT shown in equation (6.1) and (6.8) may convert into the following vector form:

$$\begin{aligned} \hat{C} &= G^T \hat{f} \\ \hat{f} &= H^T \hat{C} \end{aligned} \tag{6.9}$$

where $\hat{C}$ and $\hat{f}$ are *LMN* dimensional vectors, and *G* and *H* are $LMN \times LMN$ transformation matrices. The $\hat{C}$ and $\hat{f}$ are obtained by concatenating the columns and pages of *C* and *f* respectively, i.e.

$$\begin{aligned} \hat{C} &= [C_{0,0,0},...,C_{L-1,0,0},...,C_{L-1,M-1,0},...,C_{L-1,M-1,N-1}]^T \\ \hat{f} &= [f_{0,0,0},..., f_{L-1,0,0},..., f_{L-1,M-1,0},..., f_{L-1,M-1,N-1}]^T \end{aligned} \tag{6.10}$$

It can also be derived from equation (6.1) and (6.8) that the inverse transformation matrix *H* is the transpose of *G*, i.e. $G = H^T$. Thus, combining with equation (6.9), the obtained result

$$G^{-1} = G^T \tag{6.11}$$

The equation (6.11) proves that the transformation matrix *G* is orthogonal. Therefore, the transform coefficients are also orthogonal.

Further, it has been proved that the DCT transformed coefficients are equivalent to cosine based least square regression (Huang *et al.*, 2014; Huang and Ceglarek,

2002). The least square estimation for the *f(i,j,k)* is as follows for estimated regression coefficients *B*:

$$\begin{aligned} &\hat{f}_{LS} = XB \\ &where, B = \left(X^T X\right)^{-1} X^T f \end{aligned} \tag{6.12}$$

The orthogonal cosine base yields,

$$\begin{aligned} &\left(X^T X\right)^{-1} = \left[I\right] \\ &\Downarrow \\ &B = X^T f \end{aligned} \tag{6.13}$$

The least square estimation with error for DCT transformation is presented in equation (6.3) and combining with (6.13), it gives,

$$B = \beta \tag{6.14}$$

The T^2 and Q statistics are based on the aforementioned orthogonally transformed coefficients which imply that they are also orthogonal to each other, since the residuals of the GMA model are orthogonal to the modal plane. The correlation between the residual of the transformation and the preserved variables are analysed for GMA as:

$$\begin{aligned} \varepsilon^T X &= \left[f - \hat{f}_{LS} \right]^T X \\ &= \left[f - XB \right]^T X \\ &= \left[f - X \left[X^T X \right]^{-1} X^T f \right]^T X \\ &= f^T X - f^T X = 0 \end{aligned} \tag{6.15}$$

Therefore, it is proved that T^2 and Q statistics determined in the GMA domain are orthogonal to each other.

6.3.1.4 Estimate Confidence Region of GMA based T^2-Q Integrated Statistics

In the field of multivariate SPC (MSPC) application, few frequently concerning issues are related to normal distribution assumption and size of the reduced process variables or LVs (Kruger *et al.*, 2001). The likelihood of occurrence of a data point in a sampled data set is described by PDF. A parametric approach for determining the PDF assumes that the density function will take a particular form which needs to be specified upfront (Montgomery, 2008). For example, in case of normal density function, the mean value and standard deviation of the process variables to be estimated first. In contrast, nonparametric density estimation does not require prior knowledge about form of the density function. In the practical case of industrial applications, the process variables may not be normally distributed. To overcome this challenge, joint PDF is estimated using Kernel Density Estimator (KDE) which allows more accurate results when the reduced variable set is not normally distributed (Chen *et al.*, 2004). The aforementioned T^2 and Q statistics require the orthogonal property of *functional data analysis* model which need to be orthogonal to each other which has been proved in the previous subsection. KDE is a very powerful class of data driven techniques for non-parametric estimation of PDFs (Silverman, 1986; Wand and Jones, 1994) which fits an empirical distribution to a sample data sets approximating the population. The density function is determined by summing up small bumps that are placed at the centre of the each observation. The shape of the bumps is defined by the kernel functions such as Gaussian, Triangular or Epanechnikov type (Silverman, 1986).

In order to estimate the joint density function of T^2 and Q statistics, a data driven technique has been adapted, where the multivariate kernel density estimator can be written as

$$\hat{F}(X,H) = \frac{1}{z}\sum_{r=1}^{z} K\left(\frac{X - X_r}{H}\right) \quad \textbf{(6.16)}$$

where $X = \left\{\frac{T^2}{Q}\right\}$, $X_r = \left\{\frac{T_r^2}{Q_r}\right\}$, the X_r denotes the r^{th} instance of measurement, K = kernel function, and H= the rescaling factor so the data are in the same scale in all dimensions.

The confidence region of the control chart is drawn using numerical integration of the joint KDE function (6.16) as follows:

$$Vol_\alpha = \int_{-\infty}^{1-\alpha} \hat{F}\left(x,H\right)dx \quad \textbf{(6.17)}$$

The graph obtained from T^2 and Q joint PDF is a 3D graph. However, the 2D plot of the confidence region is more useful for identifying whether the incoming part is within the desired confidence region or not. Therefore, it is important to identify the confidence regions with (1-α)% confidence level. Using equation (6.17), it estimates the volume (Vol_α) equivalent to (1-α) under the 3D graph and the corresponding projection of the volume in the 2D space determines the confidence region.

6.3.1.5 GMA based T^2-Q Control Chart for Shape Monitoring

The use of multivariate statistics has added advantage over the univariate statistics when it comes to extracting complete information of the data. Therefore, the joint statistics of T^2 and Q could extract more information to enhance the detectability of the control chart by increasing sensitivity. Assuming the associated sensitivity of T^2

and Q statistics are S_{T^2} and S_Q, respectively, and the T^2-Q, joint sensitivity could be expressed as

$$S_{T^2-Q} = \theta_1 S_{T^2} + \theta_2 S_Q + \varphi \tag{6.18}$$

where, θ_1 and θ_2 are the weightage associated with T^2 and Q statistics to the joint sensitivity, φ is the increased sensitivity.

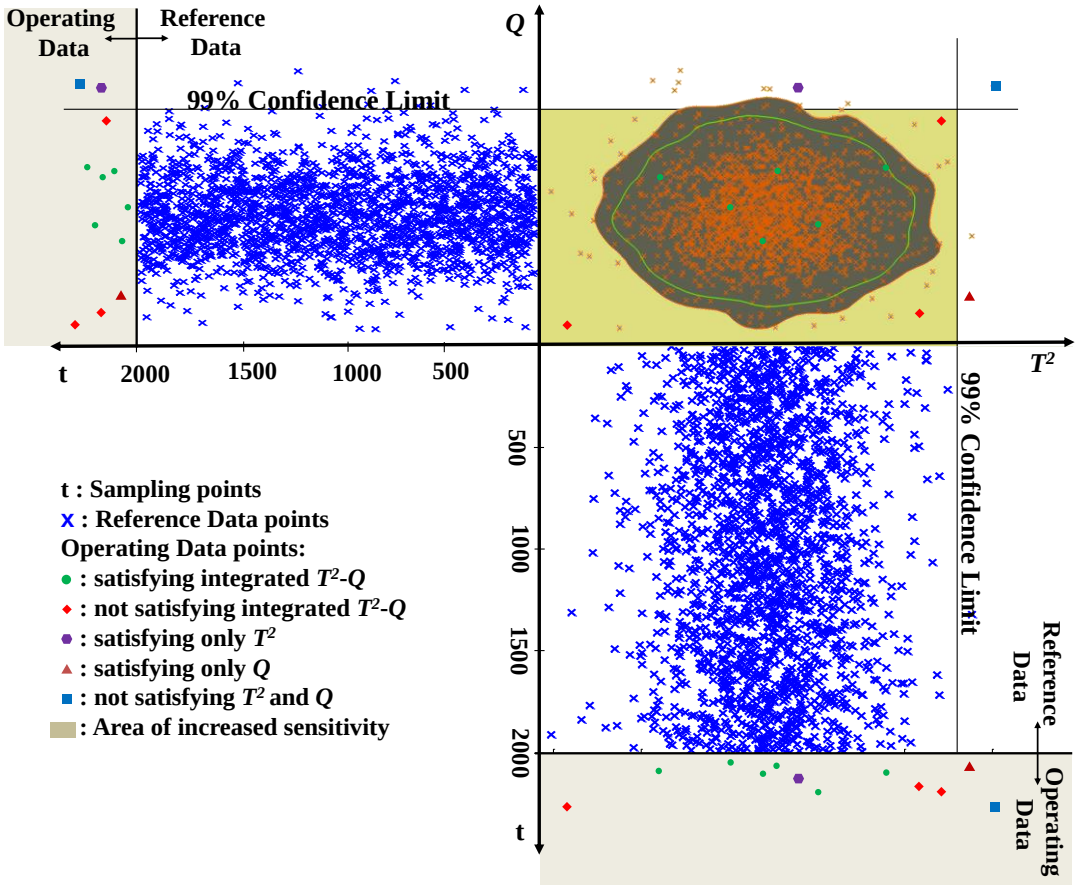

Figure 6.2 Increased sensitivity of control chart by joint T^2- Q statistics

Figure 6.2 illustrates the enhanced detectability of the control chart by increased sensitivity of the joint T^2-Q statistics. The green dots represent the conditions that are satisfied by integrated T^2-Q statistics in the operating data. Further, red diamonds are not satisfied by integrated T^2-Q joint statistics. Similarly, purple hexagon, brown triangle and blue square in the operating data points represent points satisfied by T^2 only, satisfied by Q only and not satisfied by T^2 and Q respectively. The control

chart is developed in two phases: (i) Phase I which involves a preliminary charting procedure to discard the outliers from the initial set; and, (ii) Phase II involving the development of control limits based on the discarded data set.

After constructing the control chart, a new operating part data is decomposed into GMA modes and the corresponding T_r^2, Q_r statistics is plotted in the control chart. Under normal operating condition, a good part (T_r^2, Q_r) should lie within the defined confidence regions with 95% and 99% confidence levels with occasional outliers. Abnormal process or product changes may cause the shift of data points from its confidence regions to outside. Selection of confidence regions is determined by quality practitioners based on their control requirements.

6.4 INDUSTRIAL CASE STUDY

This case study is conducted on hinge reinforcement part of an automotive door. The original shape error deviation and a sample set of decomposed dominant error patterns (LVs) are shown in Figure 6.3. The hinge reinforcement is normally assembled with main door frame (i.e., door inner panel) to provide sufficient strength to hold the door with the side frame assembly of the automotive body. The hinge reinforcement part consists of several features and curvatures on the nominal part which raises the requirements that the parts be produced within the tight tolerance limits in order to minimize variations of the final door assembly. Consequently, developing a control chart considering the shape errors is crucial for quality of the part by ensuring whether it is within or outside of tolerance. Additionally, if any part is out of the control region (limits), the proposed control chart is also able to detect the type of dominant modes of the fault which is a crucial step in identifying fault root causes.

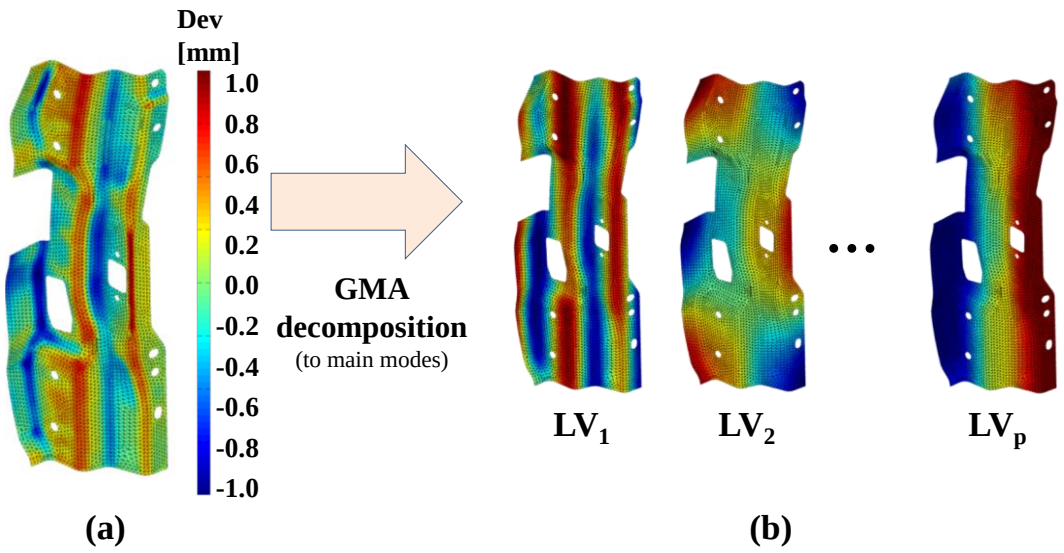

Figure 6.3 Hinge reinforcement part of automotive door: (a) original shape error computed from CoP, and (b) decomposed shape error modes (LVs)

6.4.1 GMA-based T^2-Q Control Chart Development

A set of hinge reinforcement parts is measured, and then the parts are categorized as good parts by the quality engineer. Based on these good parts, a set of CoPs is generated through simulation. These combined set of CoPs are used to develop the control chart. The reported control chart is based on sample of 1000 parts data and computation of joint PDF for T^2 and Q joint statistics using KDE. The estimated joint PDF is presented as 3D plot in Figure 6.4. However, for process monitoring purposes, 2D plot with control limits is more useful for faults detection which has been represented as 2D plot with 95% and 99% control regions in Figure 6.5. The confidence interval explains that only 5% and 1% data points should scatter outside the control regions, respectively, if the process is in normal operation conditions. If any process change occurs, then the process will migrate from in-control region to outside of the control region.

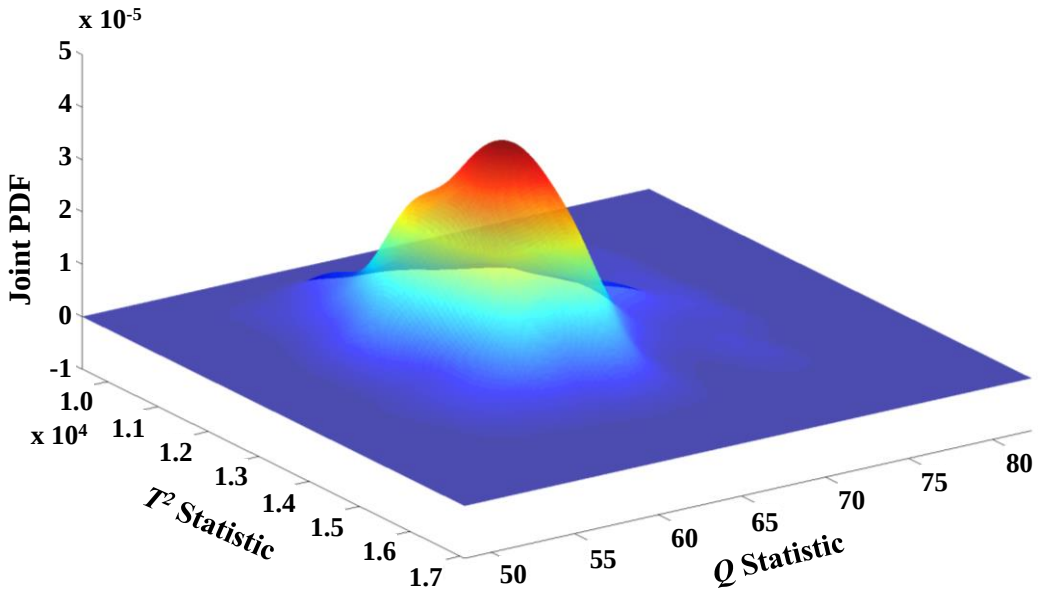

Figure 6.4 Joint probability density function (PDF) of integrated T^2-Q statistics for hinge reinforcement part

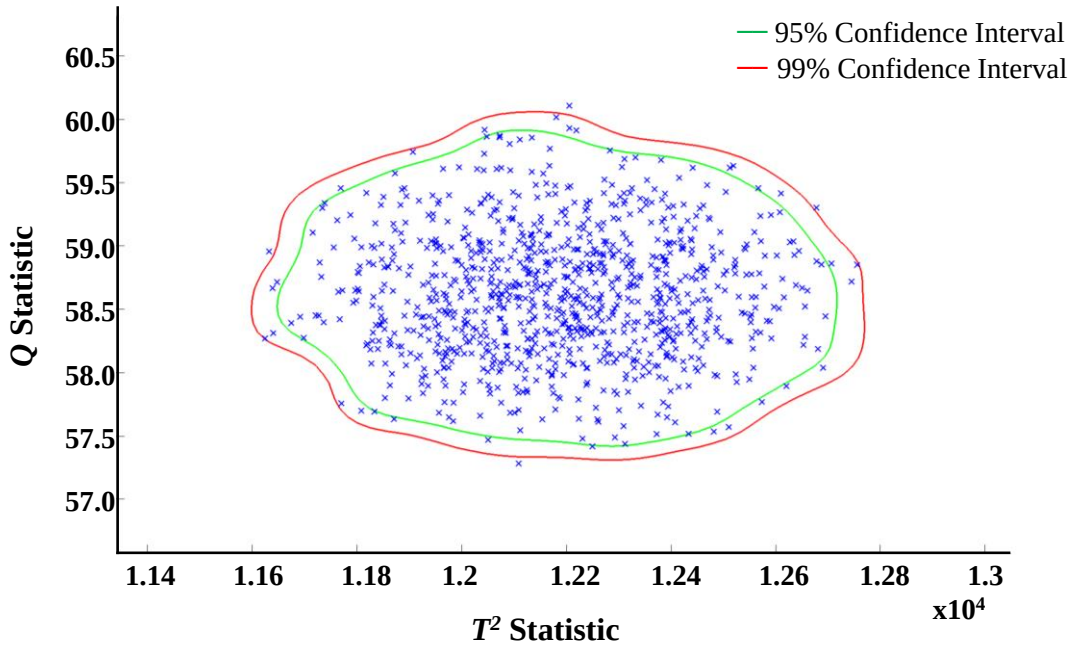

Figure 6.5 2D plot of confidence regions estimation with 95% and 99% confidence intervals of integrated T^2-Q statistics

6.4.2 Detection of Faulty Conditions

The developed T^2-Q control chart is used to detect defects or faulty conditions which are caused by manufacturing process parameter variations or parameter shifts. These fabrication process variation leads to part shape errors which may cause by sample mean shift or variance change. A global deformation mean shift is caused mainly due to fixture or die worn out whereas a local deformation mean shift can be due to part misalignment, or localized die worn out. Part bending and twisting which may cause by sample variance change are mainly results of the material spring-back, material handling etc. Subsequently, the part errors caused by mean shift or variance change can cause part fit-ups errors during assembly due to part-to-part interactions. The control chart also has the capability to detect the part fit-ups problem when they are deviating from in-control region to outside of the control region. The operating characteristics (OC) curve provides measure on control chart performance by showing that the probability of an observation will fall within the control region for a given state of the process. Figure 6.6 shows the probability of being within control region with respect to changing global mean shift. In case of part with 0.05mm global mean shift, the probability of accepting the part is 0.977 (green line in Figure 6.6) whereas , the probability of accepting the part is 0.036 when mean shift reaches 0.15 mm (red dotted line in Figure 6.6).

The result of a global mean shift of 0.1 mm and 0.15 mm is showing that almost half and all of the parts are outside the confidence regions, respectively as depicted in Figure 6.7. Further calculations also indicate that the average run length (ARL) for the in-control part is 278.57 which is significantly reduced to 3.23 and 1.023 after introducing the 0.1 mm and 0.15 mm mean shift. This demonstrates the control chart capability for the purpose of fast detection of defects for high volume production.

Further, the GMA-based T^2-Q control chart can efficiently process the capture CoP data during production. It opens the opportunity for 3D optical scanners to be used for statistical process control purpose by extracting abnormal process behaviour.

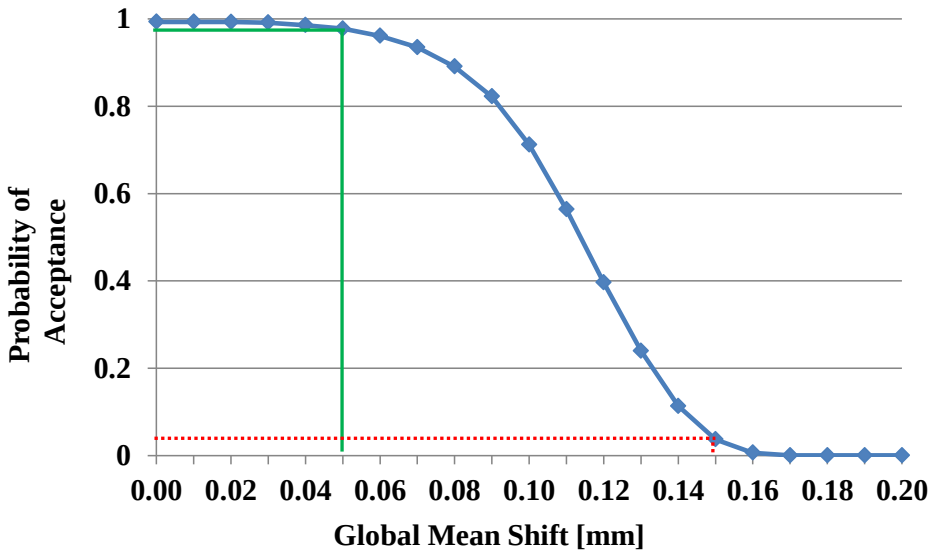

Figure 6.6 Control chart operating characteristics behaviour with changing global mean shift

A univariate statistic can be deducted based on the probability distribution function from the joint statistics of T^2 and Q, which indicates the behaviour of the process with time. The parts are plotted as univariate statistic against the time as abscissa which is depicted in Figure 6.8. It is shown that the first 1000 parts are in-control parts which exhibit the normal process behaviour whereas subsequent 2000 parts are mean shifted by 0.1 mm and 0.15 mm respectively.

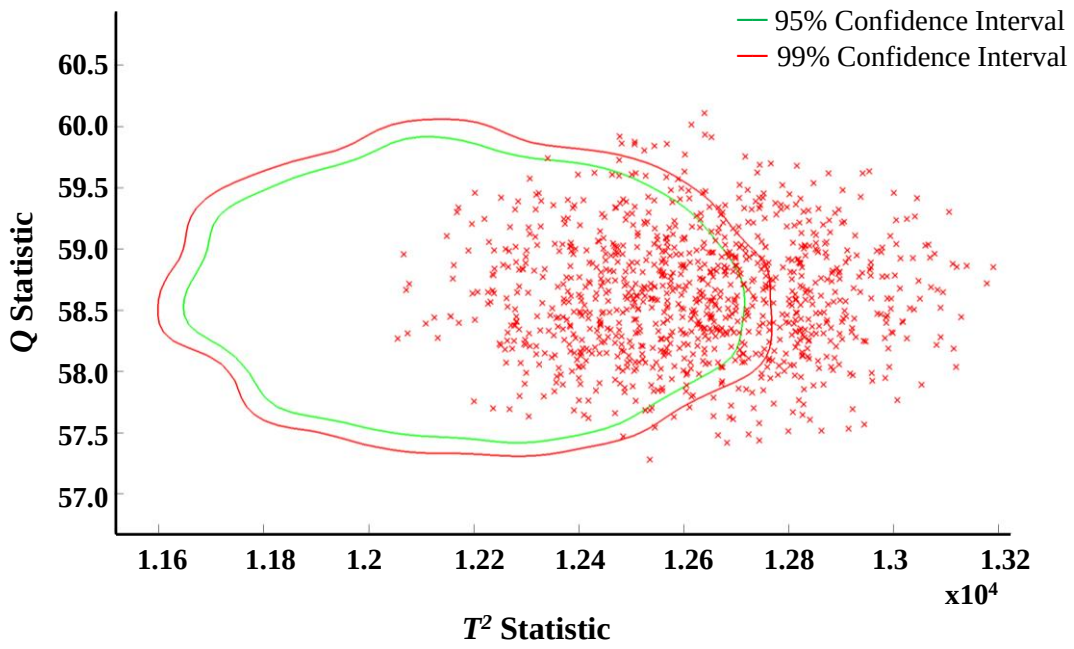

(a)

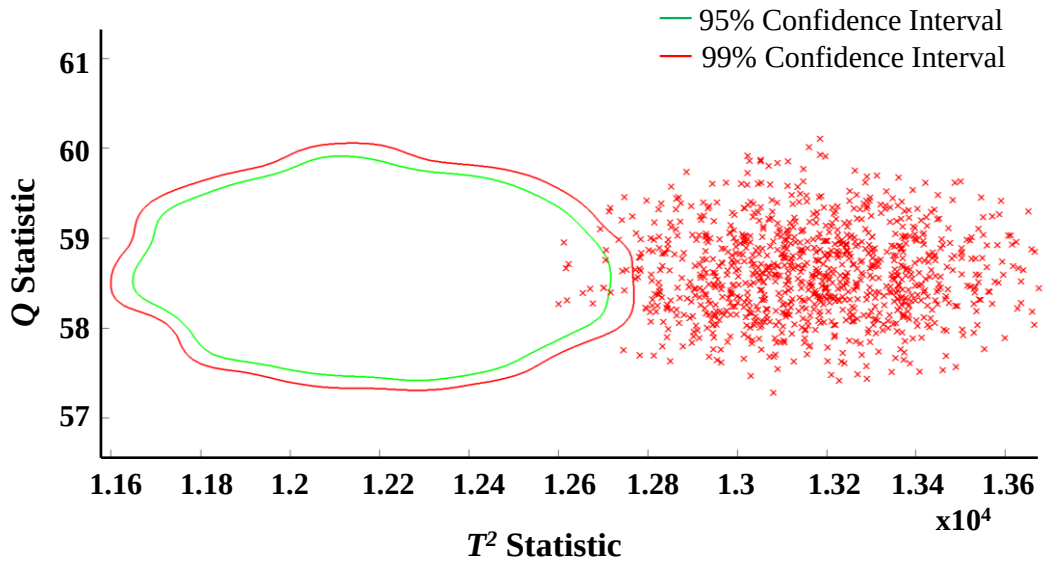

(b)

Figure 6.7 Product data with global mean shifts of (a) 0.1 mm, and (b) 0.15 mm at 95% and 99% confidence interval

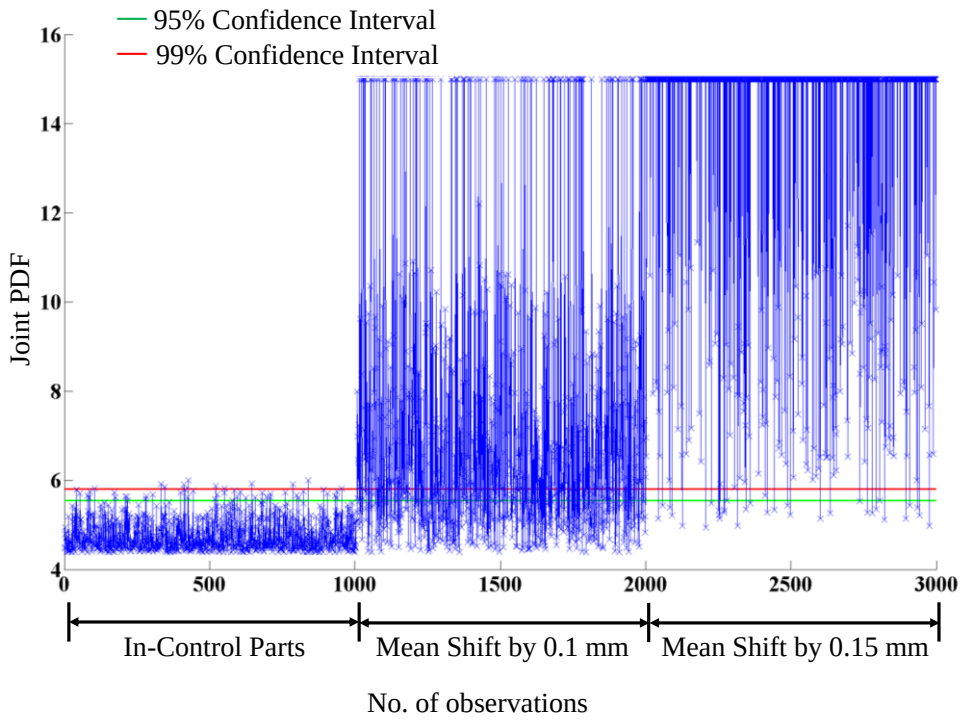

Figure 6.8 Univariate chart (log scale) on joint analysis of T^2 and Q statistics for global mean shift of hinge reinforcement parts

Similarly, hinge reinforcement parts are simulated with local deformation (e.g. a dent type fault) by gradually increasing to 1.0 mm as depicted in Figure 6.9. Results indicate that the parts are scattering closer to outside of the control regions when the average dent deviation value reaches to about 0.5 mm as reported in Figure 6.10. A univariate statistic can be deducted based on the probability distribution function from the joint statistics of T^2 and Q, which indicates the behaviour of the process with time. The univariate statistic, based on the probability density values of the joint PDF, has been plotted with a time-base as shown in Figure 6.11. The joint PDF values are plotted in logarithmic scale (inverse of original values) for visualization purpose. It is observed that there is a change of around 0.5 mm local deformation on the parts resulting in the migration of the parts out of the confidence interval. The localised part deformation may cause part fit-ups problem when they are mating with other parts due to interference with the part surfaces.

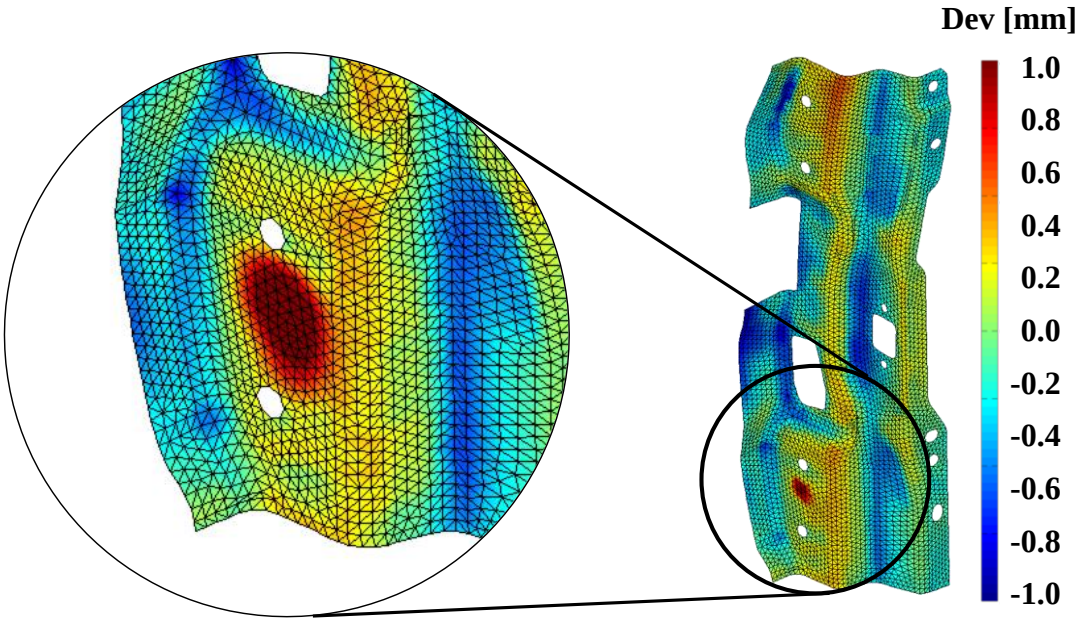

Figure 6.9 Product shape error with localised part deformation by 1.0 mm

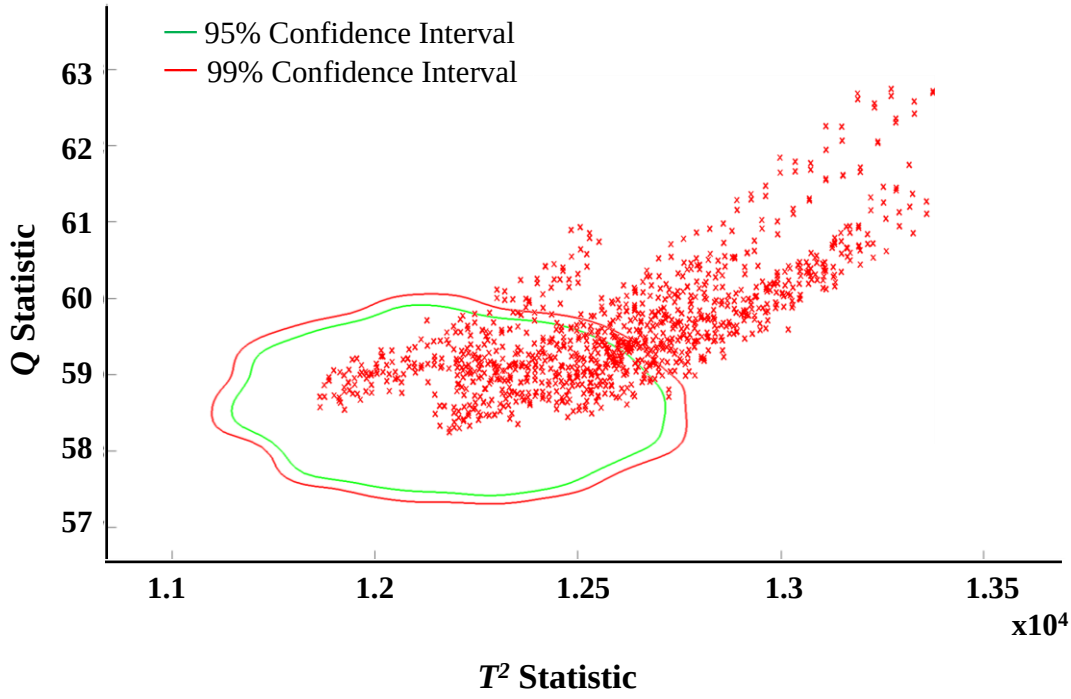

Figure 6.10 T^2-Q control chart for locally deformed hinge reinforcement parts

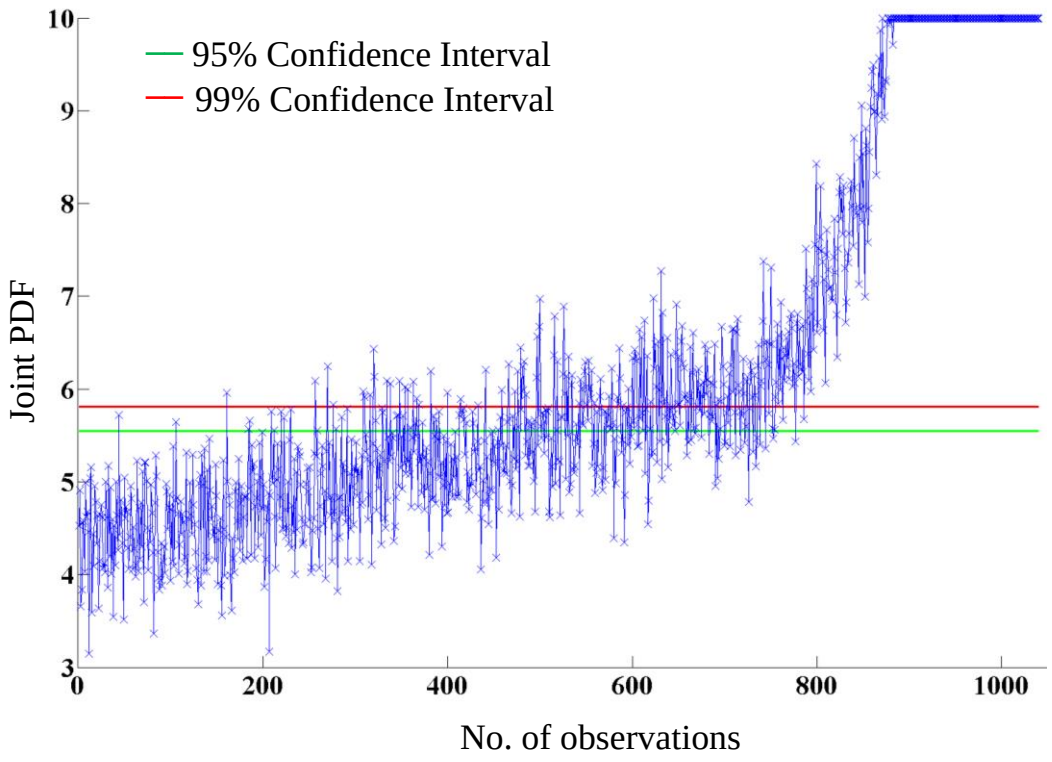

Figure 6.11 Univariate chart (log scale) on joint analysis of T^2 - Q statistics for locally deformed hinge reinforcement parts

6.4.3 Comparative Analysis of GMA-Based T^2-Q Control Chart vs. PCA-Based T^2-Q Control Chart

The comparative analysis of the developed GMA-based T^2-Q control chart with the current state-of-the-art is conducted using PCA-based T^2-Q control chart. Classical multivariate statistical monitoring methods based on PCA (Ku *et al.*, 1995; Bakshi, 1998; Phaladiganon *et al.*, 2013) implicitly assume that the observations at one point of time are statistically independent of observations to another point of time and that latent variables follow a Gaussian distribution (Lee *et al.*, 2004b; Lee *et al.*, 2004a). However, in real industrial processes, these assumptions are invalid due to their dynamic and nonlinear characteristics. Moreover, PCA decomposition is incapable for detecting shift in data which can lead to incorrect principle component of part

data (Matuszyk *et al.*, 2010). Therefore, monitoring charts based on conventional PCA tends to show many false alarms and poor detectability.

The proposed approach of process monitoring with PCA-based monitoring have been compared. Firstly, a set of in-control parts is considered for the PCA decomposition which is applied on the nominal mesh node deviation of each part in order to evaluate the shape error field. The obtained eigenvectors and eigenvalues are selected relying on the explaining variance of the data set in descending order. Secondly, the principle components explain 90% of the total variance is considered for T^2 statistic and rest are computed in the Q statistic. Therefore, T^2 and Q statistics are extracted based on the retained principal components of the data set and discarded principle components, respectively. To obtain T^2 and Q statistics on new part data, the observed deviation on the mesh nodes are projected onto the plane defined by the PCA retained principal components. The Q statistic gives the residual between the PCA model and observed deviations.

6.4.3.1 In-Control Mean Shift and Variance Change Detection

During real production of stamped sheet metal parts, variance change can be observed for within-run production; or mean shift may present for run-to-run production. The GMA-based T^2-Q control chart has the capability to decompose the part shape errors independently, and it can detect in-control mean shift or variance change present in the primary data set. Therefore, the GMA-based T^2-Q control chart clearly exhibit whether the mean shift or variance change present in the primary data set. On the contrary, PCA-based T^2-Q control chart fails to identify the variance change or mean shift present in the data set. Figure 6.12 shows that GMA-based T^2-Q control chart has the capability to identify if there is any variance change or mean shift present in the part data set when the mean shift and variance induced data sets

are plotted together. In contrast, PCA-based T^2-Q control chart fails to detect in-control mean shift or variance change present in the data set as it can be seen in Figure 6.13 where the 'blue cross' and 'red dots' are mixed.

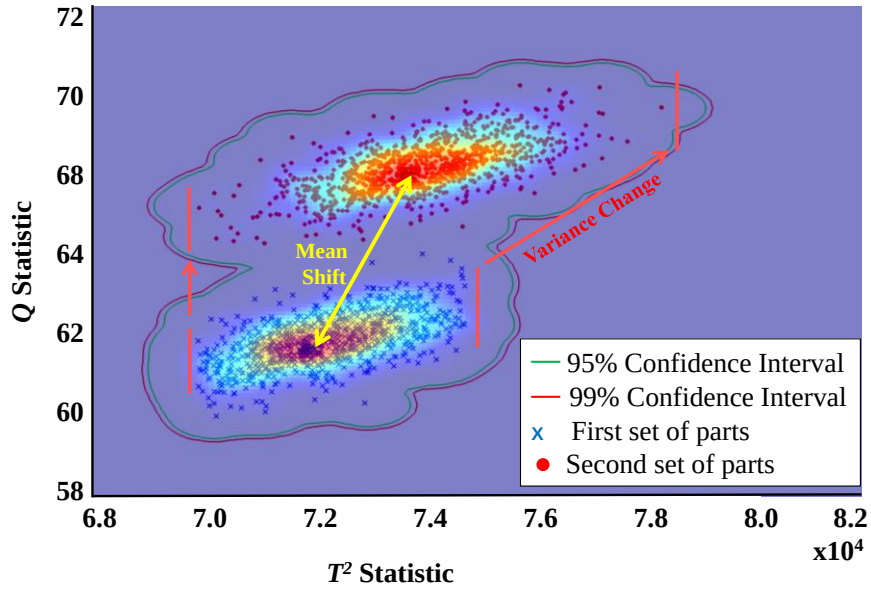

Figure 6.12 GMA-based T^2-Q control chart plot considering mean shift and variance induced data sets

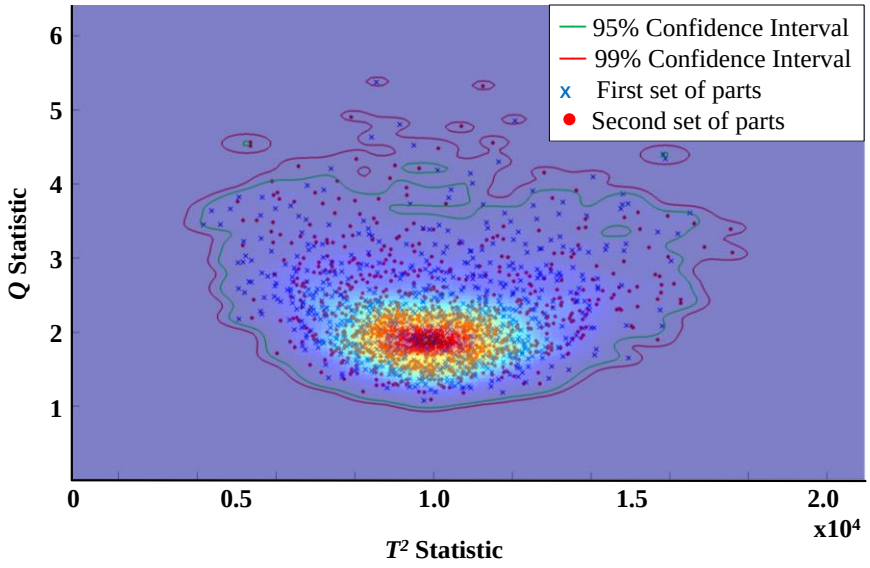

Figure 6.13 PCA-based T^2-Q control chart plot considering mean shift and variance induced data sets

6.4.3.2 Average Run Length (ARL) Comparison

The developed approach of process monitoring is compared with PCA-based T^2-Q control chart. For this, first, PCA decomposition is applied on the mesh node deviation and eigenvalues are selected based on 90% of the variation. Second, T^2-Q control chart developed with KDE and confidence regions are identified. ARL for both charts is compared with in-control data. In this study, a total of 10,000 parts have been simulated to estimate the average run length for PCA decomposed and GMA decomposed control chart. ARL is compared for increasing global mean shift and local deformation with PCA-based T^2-Q control chart and GMA-based T^2-Q control chart (Figure 6.14).

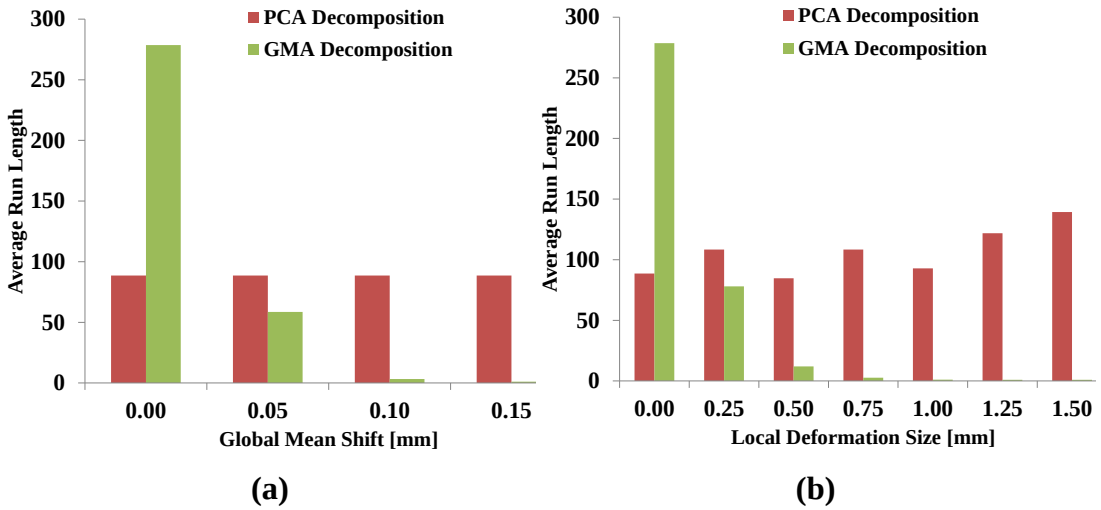

Figure 6.14 ARL comparison between PCA-based and GMA-based T^2-Q control chart: (a) global mean shift, and (b) local deformation

PCA-based T^2-Q control chart is unable to detect the global mean shift and ARL remains constant, whereas GMA-based T^2-Q control chart detects the global mean shift by rapidly decreasing ARL with increasing mean shift [as depicted in Figure 6.14(a)]. Similarly, in the case of local deformation detection, GMA-based T^2-Q control chart respond quickly with rapidly decreasing out-of-control ARL as shown in Figure 6.14(b). In-control ARL (at 0.0 mm) is always preferred to be higher side

as it reduces the false alarm. It can be observed that GMA-based T^2-Q control chart ARL at 0.0 mm is approximately three times higher than the PCA-based T^2-Q control chart. Therefore, massive amounts of in-process CoP data captured by 3D scanner metrology systems can be plotted simultaneously using the control chart to detect the defects quickly. It demonstrates that the control chart has the capability to fully utilise 3D metrology scanners for in-line process control and speedy defects detection.

The aforementioned three criteria: (a) in-control mean shift and variance change detection, (b) out-of control ARL for global, and, (c) localised mean shift detection have been used to compare the *GMA-based* and *PCA-based* T^2-Q control charts. The obtained results demonstrate that the *GMA-based* T^2-Q control chart has better detection power in comparison with PCA decomposed control chart.

6.5 SUMMARY

This chapter presents multivariate statistical process control chart for non-linear shape errors monitoring using high dimensional data (cloud-of-points) captured by in-process or off-line sensor at single station. The state-of-the-art control charts are not able to utilise modern 3D non-contact metrology scanners as they capture high dimensional and high volume data. Further, CMM based point data at key features is not able to reveal all shape related defects, especially if the fault does not influence the key feature. On the contrary, surface based measurement data can capture entire part surface, however, extracting useful information is not trivial. Moreover, current market requirements are more focused on the type of faults detection and speed of detection. To overcome the aforementioned limitations and meet the current market

demand, a more proactive control chart is required which can use high dimensional CoP data for fast shape related faults detection.

This chapter developed a *GMA-based integrated bivariate T^2-Q monitoring chart* which uses reduced variable sets as modelled by the GMA (Proposed in Chapter 4). The major steps to generate the control chart involve:

(i) *Part shape error decomposition:* GMA aims to remove high redundancy in the data by defining reduced set of statistically uncorrelated and independent variables. The utilisation of the functional data analysis such as the GMA model provides significantly reduced set of latent variables (LVs) to represent 3D shape error.

(ii) *Determination of T^2/Q statistics:* Often the reduced variables are still in large number which arises the problem of monitoring multiple control charts. To overcome this problem, two multivariate statistics have been computed. Significant variations of the process are captured through T^2 statistic which is computed based on the GMA modelled LVs. The insignificant variations/trends, caused mainly by measurement uncertainty, are stored Q statistic which is determined through residual mode set.

(iii) *T^2-Q Integration:* T^2 and Q statistics are integration with joint PDF estimation. Joint PDF of T^2 and Q statistics have been evaluated through KDE which allows more accurate results when the reduced variable set is not normally distributed. The joint statistics of T^2 and Q can extract more information to enhance the detectability of the control chart by increasing the sensitivity. This results in *GMA-based integrated bivariate T^2-Q monitoring chart* which can be used for high dimensional non-normal data (cloud-of-points).

The proposed control chart exhibits following advantages to detect faulty conditions:

(i) *Global or local shape defects detection:* It detects global part shape defects such as unwanted variance change or mean shift, a common occurrence for within batch or batch-to-batch variation of stamped sheet metal parts.

(ii) *In-control mean shift or variance change detection:* During real production of stamped sheet metal parts, variance change can be observed for within-run production; or mean shift may present for run-to-run production. The GMA-based T^2-Q control chart has the capability to handle the part shape errors independently and it can detect in-control mean shift or variance change present in the primary data sets.

(iii) *Speedy detection of defects:* Average run length drops significantly when the process starts migrating from its normal working conditions. This demonstrates speedy detection of faults.

The proposed control chart has been demonstrated with industrial case study and different faulty conditions. This demonstrates the ability of the control chart to use Cop data from 3D metrology scanners for in-line process control and speedy defects detection.

CHAPTER 7 FIXTURE LAYOUT OPTIMISATION CONSIDERING PRODUCTION BATCH

7.1 INTRODUCTION

Assembly fixture plays a significant role to achieve desired dimensional and joining qualities (Key Product Characteristics - KPCs) of assembled product where fixture design parameters act as Key Control Characteristics (KCCs). It has been demonstrated that the assembly fixtures have significant impact on product dimensional and geometric / shape variation and, subsequently, on product yield (Phoomboplab and Ceglarek, 2008; Das *et al.*, 2014). This is especially true for assembly process with sheet metal parts which lead to significant shape variation due to mainly spring-back, forming process parameter variations, tooling errors etc. Additionally, due to the compliance of sheet metal, parts can get deformed and cause variation in assembly process (Li et al., 2001). As a consequence, excessive variation in automotive closure panels may cause fundamental problems, such as, unnecessary closing effort, improper fit causing vibration and noise, air leakage as well as poor aesthetic appearance due to misalignment (Ceglarek et al., 2004; Camelio et al., 2004a; Huang et al., 2014). Therefore, the shape variation management is a key issue in current industrial assembly process as it has direct impact on the product quality, cost and time-to-market. Shape variation management through robust fixture design is inevitable prerequisite to minimise the defects caused by variation during manufacturing and product usage.

Additionally, new assembly joining processes require proper part-to-part interaction management in order to eliminate assembly shape variation and satisfy joining

requirements. For example, Remote Laser Welding (RLW) joining process requires tight control of both minimum and maximum part-to-part gap (Ceglarek, 2011) which emphasises proper design of fixture locators and clamps to mitigate the part-to-part gap (i.e. KPCs) requirement. Unable to satisfy the part-to-part gap requirements result in unsatisfactory joint quality and low process yield. Subsequently, the fixturing elements such as locators and clamps are to be optimally configured on the part surface such that part-to-part fit-up/gap remains within the specified limit. Few attempts were made to optimise fixture layout considering the metal fit-up problem of sheet metal assembly (Li *et al.*, 2001; Li and Shiu, 2001). However, research on fixture layout optimisation is limited to single compliant assembly due to lack of proper methodology to include shape variation associated with a batch of compliant assemblies. Undoubtedly, a batch of sheet metal parts, produced by metal forming process, contains shape variation. Consequently, fixture layout optimised for single assembly is not sufficient to provide optimum results for batch of assemblies. Therefore, fixture design optimisation of single non-ideal compliant assembly is not sufficient to mitigate the shape variation associated with batch of assemblies. Absence of proper method to optimise fixture layout considering batch of assemblies poses critical challenges on performance of the assembly fixture during production and results in poor production yield. The challenges in developing an optimum fixture layout considering shape variation of production batch can be summarised into three categories as follows:

(1) *Shape variation quantification for production batch:* The part shape error results in part-to-part fit-ups problem during assembly. Further, the production yield and product quality are based on the real production parts. Thus, the shape variation related to production volume is required to be quantified in order to obtain

optimum fixture layout aiming towards increased production yield and product quality.

(2) *High-dimensional design space:* The design space for fixture layout optimisation can be classified into two categories: *(i) The types of part to be assembled in the assembly station* – The design space is expanded with the types of part (e.g. door inner panel, hinge reinforcement and reinforces door opening) being assembled in a station and to represent the production shape variation of each type, number of parts are to be modelled. *(ii) Large number of locators* - The locating scheme for compliant sheet metal parts involves large number of locators (N-2-1 fixture layout where N>>3) to satisfy the dimensional and shape quality of the assembly. Further, number of locator increases proportionally to the types of part to be assembled, size of the part and complex nature of part-to-part interaction. The design space for each locator further increases depending upon the allowed position of the locator on the corresponding part surface.

(3) *Highly nonlinear relationship between KPCs and KCCs:* The locations of the KCCs (such as clamps) have nonlinear effects on KPC variations. Further, single KCC might have influence on the multiple KPCs or single KPC might have effected by multiple KCCs. Therefore, explicit understanding of the relation between KCCs and KPCs is unavoidable prerequisite for sheet metal assembly process simulation with fixture.

This chapter addresses the aforementioned challenges by proposing a novel robust fixture layout optimisation methodology considering production batch of non-ideal compliant assemblies. This chapter has been disseminated in a conference paper (Das *et al.*, 2015). To address the *first challenge*, this chapter adapts the shape variation quantification methodology, namely, Statistical Geometric Modal Analysis

(SGMA) (proposed in Chapter 5) which aims to identify the main shape error modes from a batch of parts and quantifies the shape variation into few composite parts. Composite part can be defined as a part composed of all the major significant shape error modes present in the production population. In reality, the composite part may not exist but it reduces the efforts required for assembly process simulation as it composed of all major shape error modes. These composite parts carry the shape variation information associated with batch of production parts and they are utilised for fixture layout optimisation. Further, the design space for optimisation increases with (a) the number of composite parts required to explain the shape variation of each part type, and (b) types of part to be assembled. To reduce the number of composite parts required for optimisation, i.e. to reduce design space, this chapter proposes composite assemblies selection based on correlation and entropy based selection criteria. Subsequently, the locators are varied within the allowed design space to map the KCCs to the KPCs which addresses the aforementioned *second challenge* of high dimensional design space reduction. Thereafter, the *third challenge* of nonlinear relationship between KPCs and KCCs are identified through parameterisation of fixture locators and calculation of analytical surrogate model by linking composite assembly model and fixture locators. The optimisation is focused on maximising the probability of joining feasibility index which represents the likelihood of obtaining satisfactory joint quality.

The following sections are arranged as follows: Section 7.2 describes the problem formulation for fixture layout optimisation considering production batch of sheet metal parts. Section 7.3 provides an overview of fixture layout optimisation methodology by synthesising composite parts, high dimensional design space reduction by composite assembly selection, and identification of analytical relation

between KPCs and KCCs. Section 7.4 demonstrates the applicability of the proposed method through industrial cases and compares with Monte-Carlo based simulation. Further, Section 7.5 presents the summary of this chapter.

7.2 PROBLEM FORMULATION

Let denote that an assembly consists of L number of KCCs, i.e. the number of locators. The position of a locator is denoted as

$$KCC_l = \{x, y, z\}_l, \quad \forall l = 1, 2, \cdots L \tag{7.1}$$

where, $\{x, y, z\}_l$ represents the Cartesian coordinate of the KCC location, KCC_l. The KCCs are allowed to move within its lower and upper limit on the defined part surface, i.e. the KCCs are controlled within the design space from start location to end location. Therefore, the KCCs can take any location within the defined design space and each KCC has its impact on the KPCs (e.g. part-to-part fit-ups). Therefore, the positions of KCCs are defined as

$$\begin{aligned} & KCC_l \in \left[KCC_l^{\min} \quad KCC_l^{\max} \right], \quad \forall l = 1, 2, \cdots L \\ & \textit{where,} \\ & KCC_l^{\min} = \{x_i, y_i, z_i\}_l \\ & KCC_l^{\max} = \{x_e, y_e, z_e\}_l \end{aligned} \tag{7.2}$$

The $KCC_l^{\min} = \{x_i, y_i, z_i\}_l$ denotes the initial start location of the KCC, $KCC_l^{\max} = \{x_e, y_e, z_e\}_l$ denotes the initial end location of the KCC and it can take any value in between $KCC_l^{\min}$ and $KCC_l^{\max}$.

Further, the KPCs can be defined as part-to-part interaction based fit-ups requirement at joining location. For example, the assembly consists of N_{st} number of KPCs which can be written as

$$KPCs: \{KPC_i\}, \quad \forall i = 1,2,\cdots N_{st} \tag{7.3}$$

where, *i* represents the i^{th} KPC in the assembly.

In the assembly station, all the locators (KCCs) are required to be placed optimally which will conform to the KPC specification such as part-to-part gap should be below the upper specification limit defined by the process requirements. In addition, the KPC's conforming specification is effected by the shape variation of mating surfaces as excessive variation may result in higher part-to-part gap. The optimisation problem is formulated as satisfying the KPC requirement by defining the probability of joining feasibility index *(p)*. The probability of satisfying the KPC requirement is defined as

$$p = \frac{\text{No.of points satisfying the requirement at } KPC}{\text{Total number of points defined at } KPC} \tag{7.4}$$

The optimisation is formulated as maximisation of the probability of joining feasibility index, as

$$\begin{aligned} &maximise\left(\sum_{i=1}^{N_{st}} p\right) \\ &sub\ to\ KCC_l \in \left[KCC_l^{\min}, KCC_l^{\max}\right],\ where\ \forall l = 1,2,\cdots L \end{aligned} \tag{7.5}$$

where, KCCs are controlled within the design space ($KCC_l^{\min}$ = starting clamp position and $KCC_l^{\max}$ = end clamp position) as per the product design guidelines and constraints. Figure 7.1 illustrates the KCC movement with respect to KPC (e.g.

clamp movement along the remote laser welded joint stitch) and also demonstrates the corresponding part-to-part gap distribution to calculate probability of joining feasibility index.

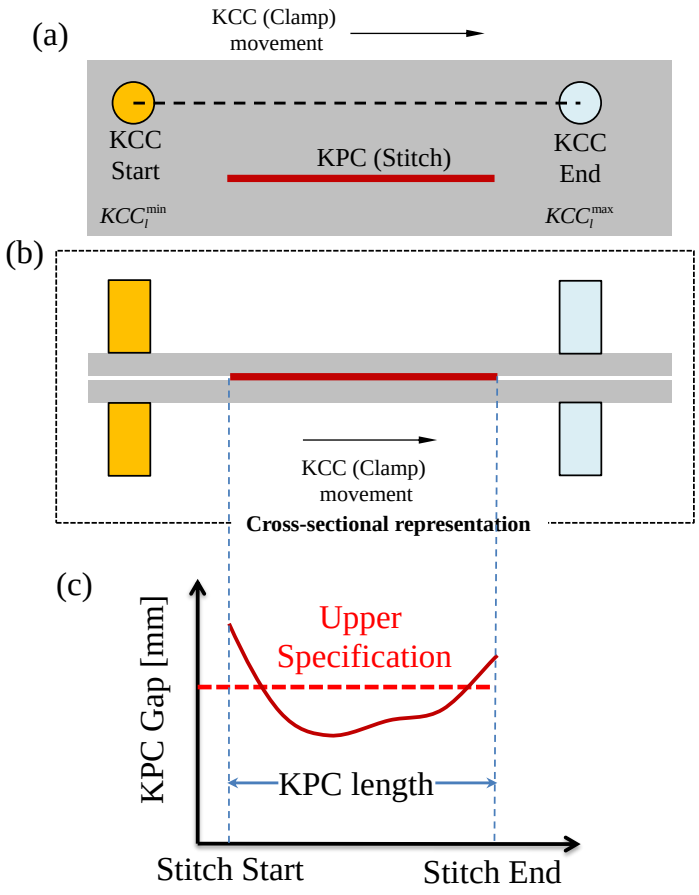

Figure 7.1 Schematic representation of the KPC and KCC locations: (a) the KCC (clamp) movement from start to end point in the design space, (b) cross sectional view of part-to-part interactions along with KPC and KCC, and (c) KPC lengthwise part-to-part gap distribution with upper specification limit to satisfy the KPC quality criteria

7.3 FIXTURE LAYOUT OPTIMISATION METHODOLOGY

The proposed fixture layout optimisation methodology is composed of three stages. *Firstly*, a batch of parts is measured and shape variation is quantified by synthesising composite parts; and initial process configurations such as joint locations, initial

fixture locations (clamps, support blocks and locators etc.) are considered as initial process input. Thereafter, the finite element modelling for fixture simulation is performed considering composite parts, fixture elements (KCCs) and contact pairs using Variation Response Method (VRM) software which is a MatLab™ based finite element modelling software toolkit with capabilities of fast modelling specific features required by assembly process (Franciosa *et al.*, 2015). VRM is a new comprehensive methodology for dimensional management of assembly processes with compliant non-ideal parts which allows to model the product-to-process interaction. At this stage, fewer composite assemblies have been selected based on developed composite assembly selection criteria which quantify the batch variation of assembled parts. This helps to reduce design space as fewer composite assemblies are selected for optimisation. Finally, analytical surrogate model is developed by identifying the relation between the defined KPCs (e.g. RLW stitch requirements) and KCCs (e.g. clamp locations) to address the nonlinear relationship between KPCs and KCCs. The optimisation is carried out to obtain the optimised fixture layout considering the KPCs by varying the KCCs (clamp locations) based on the obtained surrogate model. Optimiser updates the variables (i.e. KCCs) of the process to maximise the joining feasibility index as defined in equation (7.5). Figure 7.2 illustrates the fixture design optimisation methodology considering the batch of parts shape variation modelling, composite assembly selection to reduce design space, and optimisation performed on the developed surrogate model under the VRM modelling environment.

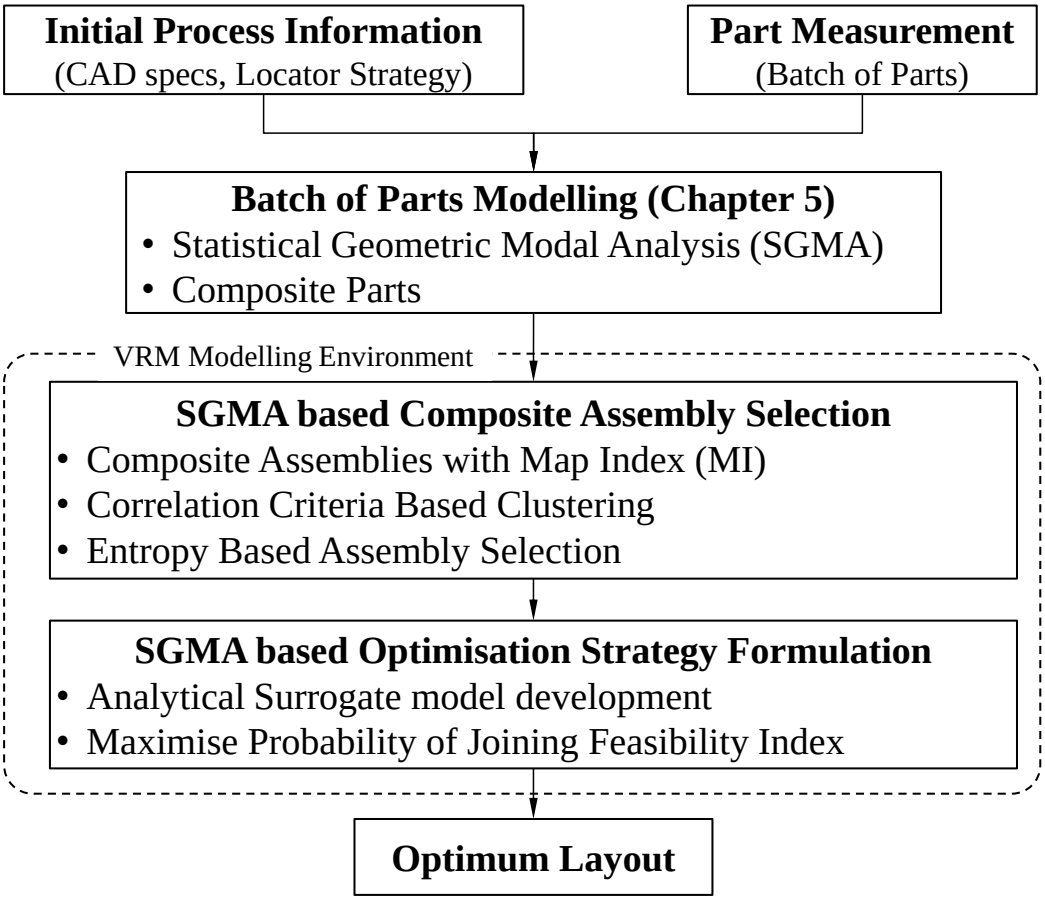

Figure 7.2 Overview of fixture design optimisation considering production batch of sheet metal parts

As the sheet metal parts are compliant in nature, *'N-2-1'* fixture locating scheme has been adapted in this thesis to satisfy the quality criteria at KPCs. As the number of clamps increases with the number of KPCs and number of composite assemblies, the optimisation problem turns into high dimensional design space. Therefore, the KPCs (part-to-part gaps) are controlled with KCCs (clamps) in this high dimensional design space. The KPCs are evaluated by using Finite Element Analysis (FEA) in Variation Response Method (VRM) simulation platform which is developed by Franciosa *et al.* (2015). The proposed methodology is based on the following assumptions:

- Single station assembly process is considered with multiple sheet metal parts, i.e. all parts are loaded into same fixture.
- Part thickness is constant and parts are considered as shell element for the FEA simulation.
- The locators such as pins are represented as frictionless point contacts to position the parts with respect to fixture and mating parts.
- Clamps and part support blocks (i.e. NC blocks) are frictionless surface contacts and they are considered as rigid bodies.

The fixture simulation involves locating the parts using the pins at hole and slot locations and contact pair is defined between the mating surfaces in order to avoid part-to-part penetration. Fixture modelling using VRM aims to model the elastic deformation of parts or assembly when the parts are loaded and clamped in the fixture.

7.3.1 SGMA based Composite Assembly Selection

Relying on the composite parts and number of parts present in an assembly, several composite assemblies can be created by considering the exhaustive combination of all types of composite parts. Therefore, the design space is expanded with the increased number of part types (e.g. door inner panel, hinge reinforcement, reinforced door opening, hinge plates) in an assembly and number of composite parts are to be considered to quantify the batch variation of each part type. Therefore, to reduce the high dimensional design space, efficient selection criteria are required to choose the most influential composite assemblies for the optimisation. For example, in an assembly operation, M number of parts ($PT_m, \forall m = 1,2, \cdots M$) are to be joined which consists of N_{st} number of KPCs ($KPC_i, \forall i = 1,2, \cdots N_{st}$), where m represents

the part id and i represents the i^{th} KPC in the assembly. The assembly consists of L number of KCCs. Therefore, relying on the types of shape error present in a batch, each part type may be grouped into N_m number of clusters. For each cluster, a total of three composite parts can be created depending on maximum, minimum and average energy compaction criteria, i.e. $CPT_{m,max}, CPT_{m,min}, CPT_{m,avg}$. Therefore, the assembly system can be written as

$$\begin{aligned}
&KPCs: \{KPC_i\}, \forall i = 1,2,\cdots N_{st} \\
&Parts: \{PT_m\}, \forall m = 1,2,\cdots M \\
&KCCs: \{KCC_l\}, \forall l = 1,2,\cdots L \\
&CompositeParts: \{CPT_{m,\max}, CPT_{m,\min}, CPT_{m,avg}\} \\
&MaximumCompositeParts: CPT_{MAX} = \{CPT_{m,\max,g}\} \\
&MinimumCompositeParts: CPT_{MIN} = \{CPT_{m,\min,g}\} \\
&AverageCompositeParts: CPT_{AVG} = \{CPT_{m,avg,g}\} \\
&where, \forall m = 1,2,\cdots M; g = 1,2,\cdots N_m
\end{aligned} \quad \textbf{(7.6)}$$

Therefore, relying on the number of clusters to be modelled for each part type, the combination of composite assemblies also increases. The number of obtained composite assemblies, by taking exhaustive combination of all parts, can be formulated as

$$CompositeAssembly: CA = \{CPT_{MAX} \cup CPT_{MIN} \cup CPT_{AVG}\} \quad \textbf{(7.7)}$$

Therefore, equation (7.7) indicates that even though the part shape variations are quantified in few composite parts, still the combination of the composite parts of one part type (e.g. composite parts of door inner panel) with composite parts of other part types (e.g. hinge reinforcement or reinforced door opening) becomes larger design space. As each simulation is computationally expensive, optimisation based on all combinations of composite assemblies become computationally inefficient. Therefore, aiming to reduce the design space for optimisation, it emphasises the

selection of fewer composite assemblies which are representative of all other assemblies (i.e. batch variation). In order to achieve fewer composite assemblies' selection, two criteria are proposed: (i) Correlation Criteria Based Clustering and (ii) Entropy Based Assembly Selection.

7.3.1.1 Correlation Criteria Based Clustering

All combinations of composite parts are determined as per equation (7.7) to create complete set of composite assemblies. In order to achieve reduced number of composite assemblies for optimisation, a correlation threshold based clustering criteria is introduced. It involves clustering of composite assemblies based on similar KPC Map Index (*MI*). MI depends on the selected KPCs such as point deviation, part-to-part gap distribution, or surface area deformation etc. Considering the initial locator strategy (KCCs), such as given clamp layout and NC blocks, an initial fixture simulation provides part-to-part KPC map index for all the composite assemblies, *CA*. A map index of a given i^{ih} KPC (KPC_i) of j^{th} composite assembly is defined as a function,

$$MI_{i,j} = f(CA_{i,j}, KCC) \quad \textbf{(7.8)}$$

where, the function *'f'* denotes the fixture simulation process which is composed of part-to-part interaction, boundary constraints, contact pair detection and part/assembly flexibility under FEA simulation. Therefore, equation (7.8) represents the fixture simulation process with map index as an outcome.

Subsequently, considering all the defined KPCs in the assembly, a total MI (*TMI*) for the j^{th} composite assembly of the composite assembly set *CA*, is evaluated as,

$$TMI_j = \bigcup_{i=1}^{N_{st}} MI_{i,j} \quad \textbf{(7.9)}$$

Similar shape error contained assemblies will exhibit similar MI as all other parameters are kept constant. The correlation coefficient ($\rho_{j,k}$) between two composite assemblies (*j* and *k*) is estimated as,

$$\rho_{j,k} = \frac{\mathrm{cov}\left(TMI_j, TMI_k\right)}{\sigma_j^2 \sigma_k^2} \quad \textbf{(7.10)}$$

where, $j \neq k$ and σ_j, σ_k represent the standard deviations of the total map index of j^{th} and k^{th} assembly respectively.

Therefore, the correlation matrix has been determined for all composite assemblies and a user defined correlation threshold, α, has been applied to group the assemblies having the similar KPC map index. By applying the correlation based clustering, the composite assemblies can be clustered into fewer groups consist of similar type of map index distribution. For example, total number of clusters created after applying the map index based correlation criteria is N_{cl} and all the composite assemblies (i.e. *CA*) are grouped into N_{cl} number of groups. This implies that one assembly from the specific cluster can be chosen for the optimisation and the obtained result should be optimum for all the assemblies belong to that cluster.

7.3.1.2 Entropy Based Assembly Selection

To select one representative assembly from each cluster for optimisation, entropy based selection criterion is introduced. The analysis of the MI's content can be performed by borrowing tools that have been developed in the field of information

theory. In particular, it is proposed first to determine the Information (*I*) contained on a MI. This is calculated for the i^{th} MI of j^{th} assembly ($MI_{i,j}$) as (Suh, 2005),

$$I_{i,j} = -\log_2 p_{i,j} \quad \textbf{(7.11)}$$

where, $p_{i,j}$ represents the probability of satisfying the joining requirements of $MI_{i,j}$. This is estimated as a ratio between the numbers of points in a MI satisfying the joining requirements over the total number of points of the MI. The *I* closer to zero indicates that the parts are more likely to be joined, i.e. the assembly will satisfy the upper specification.

The entropy (*H*) of whole assembly having N_{st} number of KPCs is calculated, following the Shannon's definition involving the quantification of information by measuring the uncertainty in a MI, as (Cover and Thomas, 2006),

$$H_j = \sum_{i=1}^{N_{st}} p_{i,j} \cdot I_{i,j} \quad \textbf{(7.12)}$$

The entropy of an assembly reflects the probability level of satisfying the KPC criteria. One the other hand, higher entropy value implies greater difficulty to satisfy the KPC. Therefore, to select the representative assembly from each cluster, the assembly with highest entropy value has been selected for optimisation. The Selected Composite Assembly (*SCA*) for optimisation for a^{th} cluster can be written as $SCA_a = \max\left\{H_{a,p}\right\}$, where, p represents the p^{th} assembly in that cluster. Subsequently, the total number of selected composite assembly for optimisation can be estimated as

$$SCA = \left\{SCA_a\right\}; \forall a = 1, 2, \cdots N_{cl} \quad \textbf{(7.13)}$$

where, a represents the a^{th} cluster and N_{cl} represents the number of cluster after the correlation based clustering process.

7.3.2 SGMA Based Optimisation Strategy Formulation

The optimisation strategy is developed relying on the KPC MI satisfying criteria. All KPCs are to be satisfied to achieve good quality assembly, i.e. the KPCs should satisfy the specification limit defined by the process. Additionally, the design space for each KCC (e.g. clamps) is large and KCC positions have nonlinear behaviour with the KPCs. In order to address this challenge, three step optimisation approach is adapted.

Firstly, the design space of each KCC is discretised with sampled KCC locations. Thereafter, finite element based fixture simulation is performed considering the selected composite assemblies with respect to sampled KCCs locations in the design space. The probability of joining feasibility index for each selected composite assembly has been determined.

Secondly, the nonlinear relationship between the KPCs and KCCs has been identified by developing analytical surrogate model to satisfy the KPCs index, i.e. the probability of joining feasibility index as per equations (7.4) and (7.5).

Lastly, genetic algorithm based optimisation has been performed to find the optimum KCC location by maximising the joining feasibility index (p) on the analytical surrogate model. Figure 7.3 illustrates the optimisation methodology based on the selected composite assembly by quantifying the shape variation of a batch of parts.

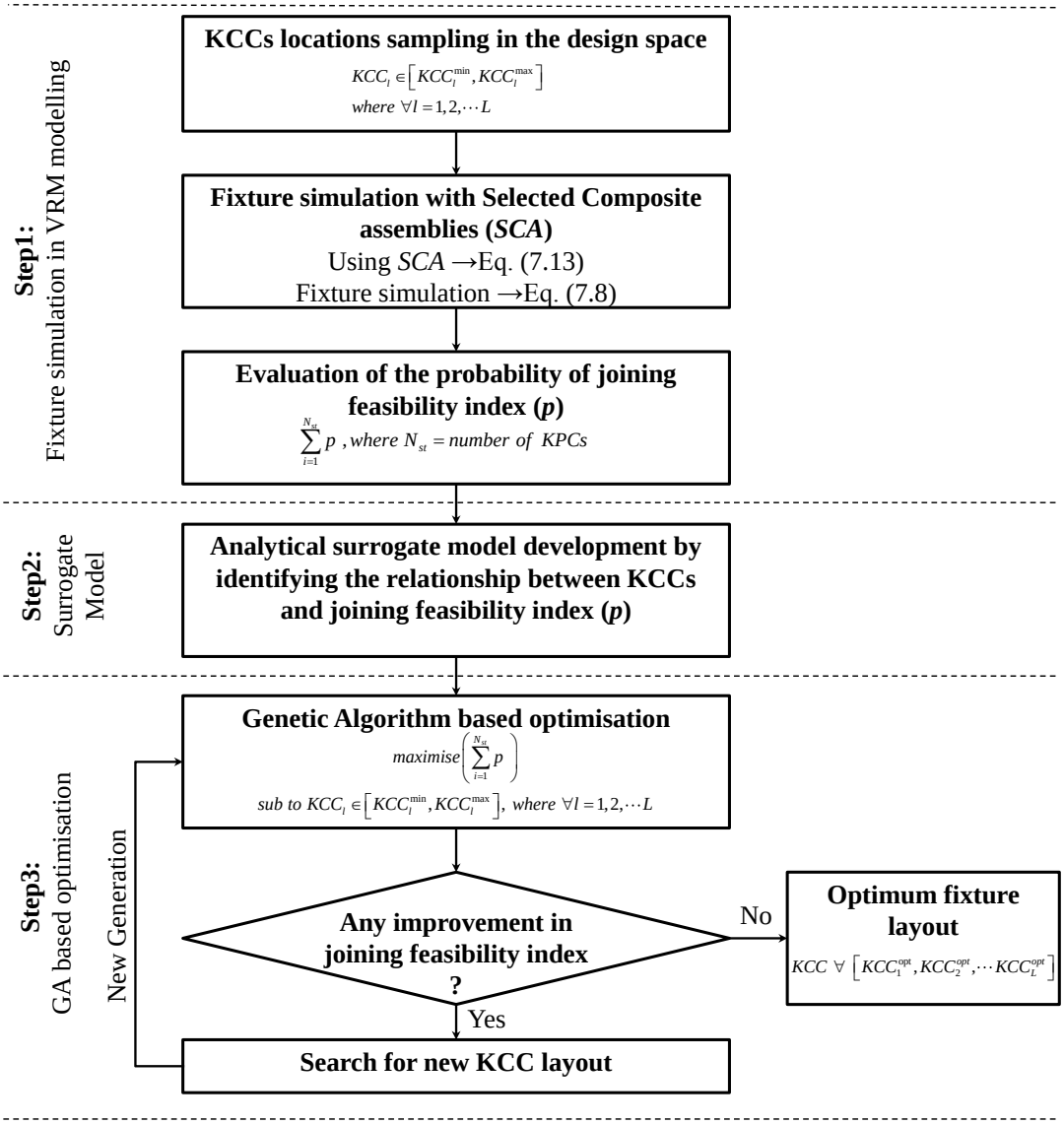

Figure 7.3 Overview of optimisation framework with objective function

7.4 RESULTS OF FIXTURE LAYOUT OPTIMISATION WITH INDUSTRIAL CASE STUDY

The proposed fixture layout optimisation methodology has been validated with industrial case study from automotive assembly. The hinge reinforcement part is assembled with main door inner frame providing sufficient strength to hold the door with main automotive body frame and further resists deformation of the door inner panel during opening/closing of the door. The assembly configuration of hinge

reinforcement part (1.8 mm nominal thickness) and door inner panel (0.75 mm nominal thickness) is shown in Figure 7.4. To enable remote laser welding (RLW) joining process, the required gap or clearance between the two parts is required to be 0.35 mm, i.e. the gap between the hinge reinforcement and door inner panel should be within 0.35 mm to ensure the joining quality standards. As per the product design specification, the assembly is composed of total 13 RLW stitches with an initial fixture layout of 16 clamps and 14 NC blocks to support the assembly joining process. The part-to-part gap map (GM) along the stitch length is used as map index (MI).

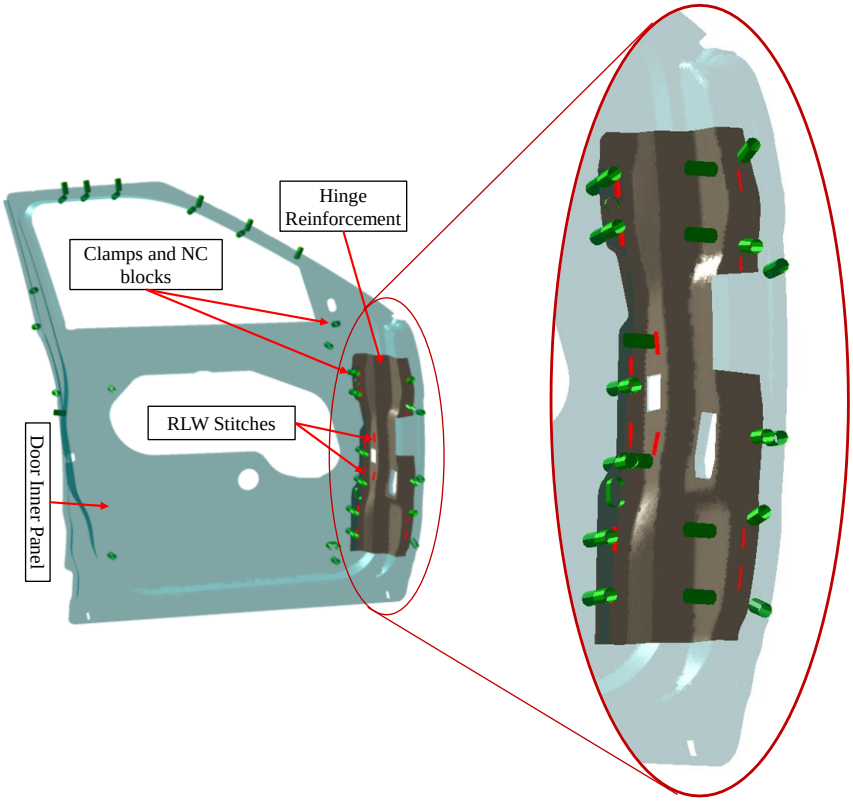

Figure 7.4 Door inner panel and hinge reinforcement assembly configuration

7.4.1 SGMA based Composite Assembly Selection

Composite parts are created by utilising SGMA technique for hinge reinforcement and door inner panel parts. The hinge component is grouped into two clusters based on the shape errors contained within the measured batch of parts and composite parts

are created for these two clusters using maximum, minimum and average energy compaction criteria as shown in Figure 7.5. The hinge part measurement data mainly has two groups of shape errors and composite parts from these groups can be utilised for optimisation instead of individual parts. The obtained map index (MI) for 13 RLW stitches considering hinge composite parts of cluster 2 and individual hinge parts belong to cluster 2 assembled with nominal inner panel are plotted in Figure 7.6. The upper boundary limit shows that every gap map distribution should be under 0.35 mm to ensure good quality joint or to maximize the probability of joining feasibility index. It shows that the map index of maximum and minimum energy compacted composite parts create a boundary for the individual hinge parts where the average energy compacted composite part behaves more likely average gap map.

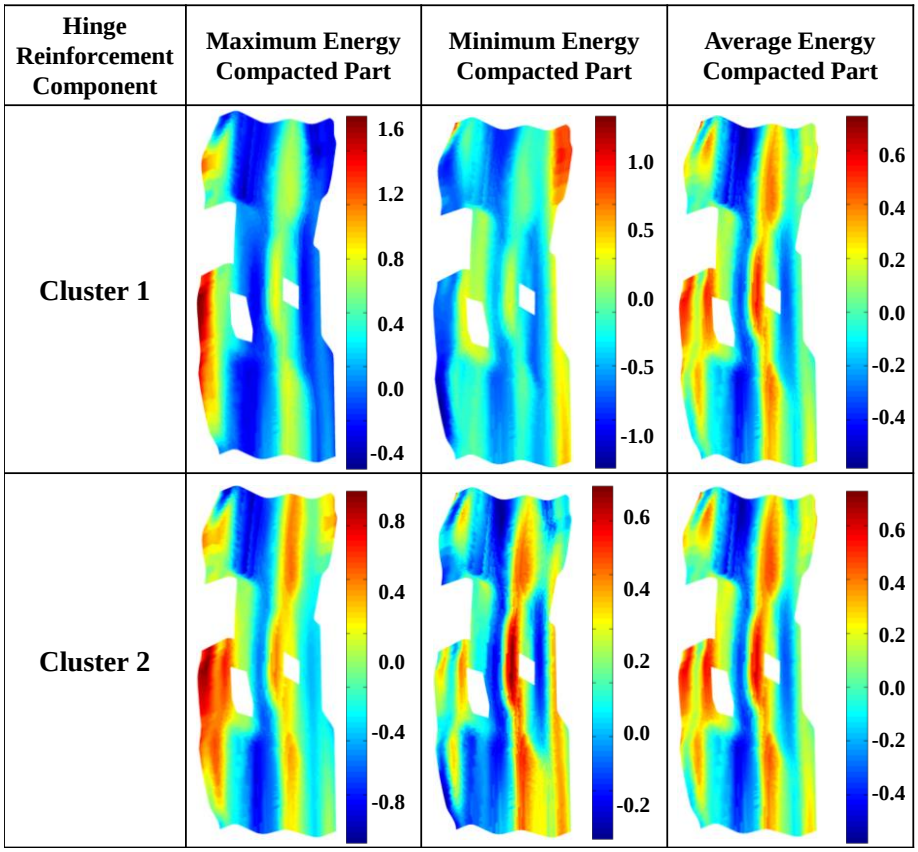

Figure 7.5 Synthesis of composite parts (deviation in mm) for hinge reinforcement component using SGMA methodology

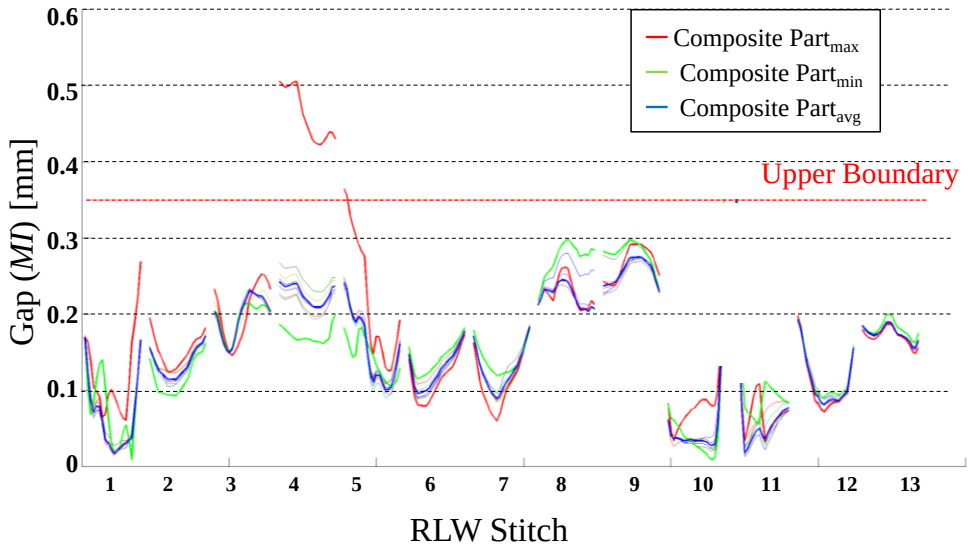

Figure 7.6 Map Index (*MI*) for composite parts of hinge cluster 2 and individual hinge parts belong to the cluster assembled with nominal door inner component

Similarly, the door inner panel exhibits three clusters and each cluster consists of maximum, minimum and average energy compacted composite parts as reported in Figure 7.7. The obtained map index (*MI*) for all 13 RLW stitches considering inner panel composite parts of cluster 1 and individual door inner parts belong to cluster 1 assembled with nominal hinge reinforcement are plotted in Figure 7.8. Similar to hinge reinforcement composite parts, door inner panel composite parts also exhibit alike behaviour towards the map index distribution. It can also be observed from Figure 7.8 that the map index for maximum or minimum energy compacted composite parts creates a boundary for the individual door inner panel parts where the average energy compacted composite part behaves more likely average gap distribution. Therefore, optimisation based on the composite parts will be sufficient enough to optimise the all individual belongs to the same cluster. Further, maximum and minimum energy compacted composite parts may be selected for the optimisation as they satisfy the boundary gap map distribution enclosing the gap distribution of individual parts.

Door Inner Component	Maximum Energy Compacted Part	Minimum Energy Compacted Part	Average Energy Compacted Part
Cluster 1	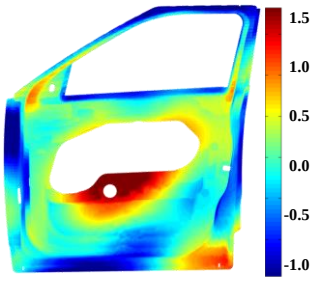	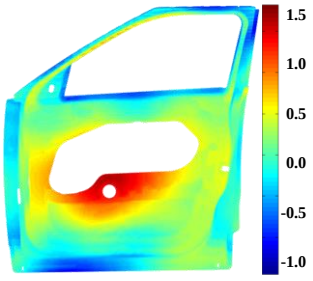	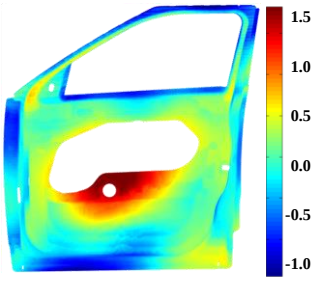
Cluster 2	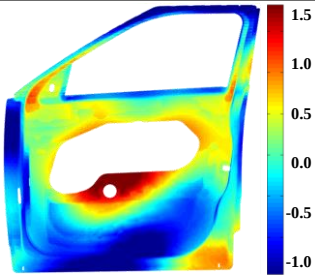	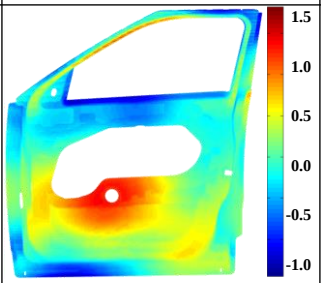	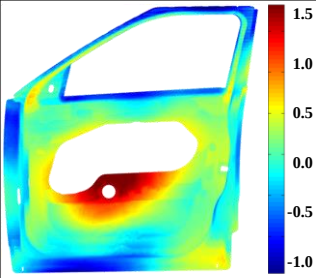
Cluster 3	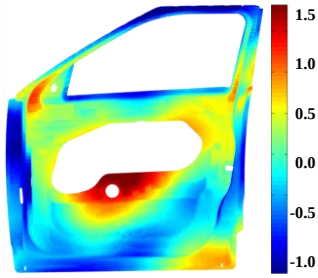	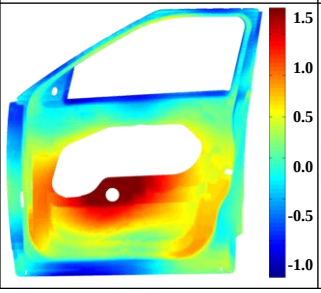	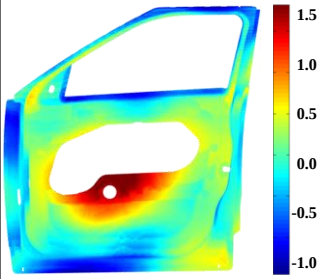

Figure 7.7 Synthesis of composite parts (deviation in mm) for door inner component using SGMA methodology

Further, map index is generated considering assembly of variational hinge belongs to cluster 2 and variational inner belongs to cluster 1. A total of 30 assemblies have been created through randomly selecting individual variational hinge and door inner panel from the respective cluster and the gap map distributions are plotted with composite assemblies in Figure 7.9. Composites assemblies have been created by combining the composite parts from the cluster of hinge and door inner panel respectively. Therefore, these composite parts are used to create composite assemblies.

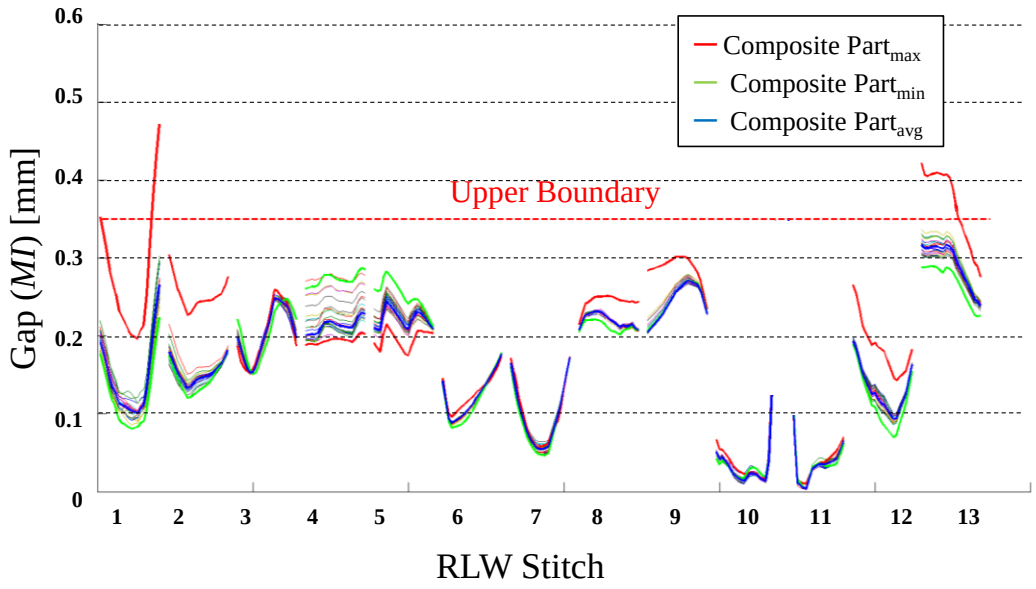

Figure 7.8 Map Index (*MI*) for composite parts of door inner cluster 1 and individual door inner parts belong to the cluster assembled with nominal hinge component

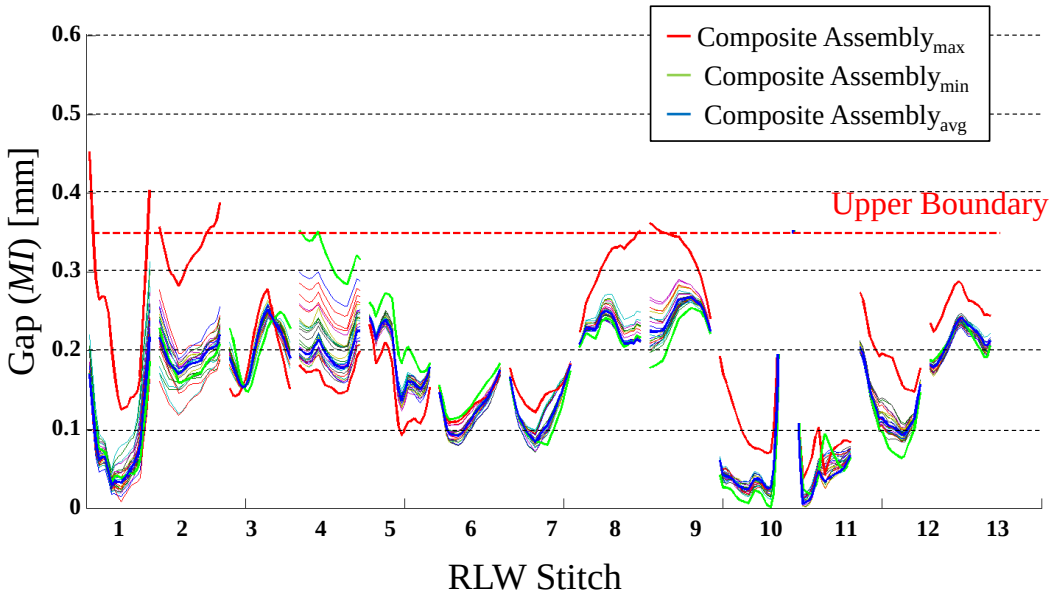

Figure 7.9 Map Index (*MI*) for composite assemblies of inner cluster 1 and hinge cluster 2 with 30 randomly generated variation hinge-inner assemblies

In Figure 7.9, map index for maximum, minimum and average composite assemblies is also plotted considering maximum-maximum, minimum-minimum and average-average combination of hinge and inner composite parts respectively. The results again confirm that composite parts may be used instead of using every composition

of variational hinge or inner part for optimisation and optimisation based on these composite assemblies is eventually optimising all combination. Further, maximum and minimum energy compaction based composite parts may be used for composite assembly creation. In total 4 composite parts for the hinge reinforcement component and 6 composite parts from the door inner panel (only maximum and minimum energy compaction based criteria used) can be utilised for composite assembly creation. Therefore, total of 24 composite assemblies can be obtained which can be utilised for optimisation. The number of composite assemblies depends on the number of types of part belong to the assembly and also the number of clusters for each part type.

7.4.1.1 Correlation Criteria Based Clustering

Relying on the number of part types belong to an assembly as well as the number of clusters present in each part type, the number of composite assemblies for optimisation also increases which is not again computationally efficient. This results in expanded design space for optimisation. Aiming to reduce the design space, fewer representative composite assemblies must be selected for optimisation. To overcome this challenge, correlation criteria based composite assembly grouping technique has been adapted and assembly entropy based selection has been introduced to select representative assembly from each cluster.

For the hinge reinforcement and door inner panel assembly optimisation, in total of 24 assemblies have been created considering maximum and minimum energy compaction criteria. Applying the initial clamp configuration, map index has been determined for all the 24 assemblies. Subsequently, the gap map based correlation matrix has been developed to identify the similarity among assemblies and cluster them according to correlation coefficient based threshold value (α). For this case

study, the correlation threshold, $\alpha = 0.93$, has been applied to identify the similar gap map based assemblies and group them into clusters. The higher correlation threshold will increase the number of selected composite assemblies for optimisation which may be unnecessary as similar type of multiple composite assemblies will be included resulting in higher computation time. On the other hand, lower threshold will eliminate few assemblies from the optimisation process resulting in same assembly present in multiple cluster, i.e., clusters are not mutually exclusive to each other. Therefore, the correlation threshold has been chosen such that the composite assemblies are become mutually exclusive to each cluster.

7.4.1.2 Entropy Based Assembly Selection

Based on the correlation cut-off, a total of 7 clusters are obtained and they are tabulated in Table 7.1. The highest entropy base assembly of each cluster has been selected for optimisation.

Table 7.1 Composite assembly clustering and entropy based assembly selection

Cluster	Assembly No	Selected highest entropy (H_j)
1	1, 5, 9	Assembly 5: 2.14
2	2, 6, 10	Assembly 2: 0.86
3	3, 7, 11, 21	Assembly 3: 0.21
4	4, 8, 12, 14, 18, 22	Assembly 4: 0.21
5	13, 17	Assembly 13: 1.02
6	15, 19, 23	Assembly 15: 0.21
7	16, 20, 24	Assembly 24: 0.50

Moreover, it can be observed that assemblies selected for cluster 3, 4 and 6 exhibit same entropy level. Consequently, further reduction in assembly selection for optimisation may possible when only one assembly is selected from the assemblies

having same entropy value. Therefore, instead of selecting total 7 composite assemblies, only 5 composite assemblies can be selected for optimisation which eventually consider batch of parts or production variation in principle.

For this case study, relying on highest entropy, a total of 7 composite assemblies have been considered for optimisation with given layout to obtain optimal clamp location aiming to satisfy the gap requirements. Therefore, the selected composite assemblies can be listed as

$$SCA = \begin{Bmatrix} Assembly\ 5, Assembly\ 2, Assembly\ 3, \dots \\ Assembly\ 4, Assembly\ 13, Assembly\ 15, Assembly\ 24 \end{Bmatrix}$$

7.4.2 SGMA Based Optimisation

The optimisation strategy for this case study has been illustrated in two stages, firstly, selection of stitches which are going out of the upper boundary specification. From the initial clamp simulation, it has been observed that 6 out of total 13 stitches are violating the upper specification limit. Therefore, for demonstrating the case study, those 6 stitches, $KPC = \{RLW1, RLW2, RLW4, RLW5, RLW8, RLW9\}$ are selected for optimisation as the other stitches are already satisfying the joining feasibility index.

Thereafter, initial clamp sensitivity analysis has been performed to identify the effect of clamp movement (KCCs movement) on the stitches (KPCs). Subsequently, the clamps (KCCs) related to those out-of-bound stitches have been identified and they are made as movable clamps and rest of the clamps are kept in their original position as fixed clamps. For this case study, there are 5 movable clamps and 11 fixed clamps, summing total 16 clamps (KCCs) to ensure gap map criteria. The movable clamps are responsible to mitigate the risk associated with out-of-bound stitches. The other clamps are kept as fixed as they have already satisfied the upper specification

criteria for all composite assemblies. Therefore, by obtaining the optimal position of *KCCs* will satisfy the global joining feasibility index. A pictorial view of the stitches as well as the initial clamp location is depicted in Figure 7.11(a). The clamps are made to move along the flange side and parameterised in between start position ($KCC_l^{\min}$) as '0' and end position ($KCC_l^{\max}$) as '1' ($KCC \in [0, 1]$) as depicted in Figure 7.11(c).

As the design space for each KCC (e.g. clamp) is large and KCC positions have nonlinear behaviour with the KPCs, analytical surrogate model has been developed identifying the relationship between KPCs and KCCs. In order to avoid long computation time, the design space has been sampled with initial sampling points, i.e. a sample of clamp locations have been utilised to evaluate the probability of joining feasibility index. Based on the initial results, an analytical function based fitting model has been developed using surrogate modelling technique (Forrester *et al.*, 2008) and optimisation has been carried out based on the analytical model. As explained by Das *et al.* (2014), individual response function for each assembly has been developed initially based on the sampled points. This step is mainly to avoid high computation time of simulation during optimisation as optimisation on analytical based function is much faster.

The optimisation has been performed based on maximisation of probability of joining feasibility index as per the equation (7.5). The analytical function based surrogate models are plotted in Figure 7.10 where the responses are quite complex in nature. It depicts the relationship of clamps (KCCs) to probability of joining feasibility index.

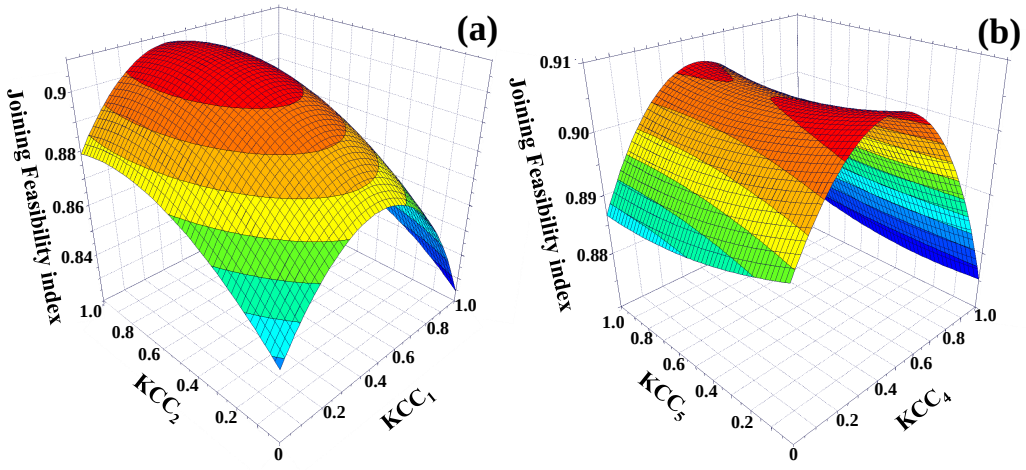

Figure 7.10 Probability of joining feasibility index plot (surrogate model) for selected composite assemblies (a) with respect to KCC_1 and KCC_2, and (b) with respect to KCC_4 and KCC_5

Genetic algorithm has been selected as optimiser to maximise the probability of each RLW stitch for all selected composite assemblies. The clamp locations (KCCs) have been optimised to maximise the total joining probability considering all the selected composite assemblies (SCA). Single point crossover has been used and the crossover probability is considered as 0.5. The mutation probability is considered as 0.10. The population size has been considered as 50. The number of generation is considered as 1000. The total number of generations is considered as optimisation termination criterion i.e., optimisation terminated after 1000 generations. Figure 7.11(b) shows the optimised clamp layout with optimised position of clamps with the gap colour map of selected composite assembly 1 (SCA_1). Figure 7.11(c) depicts the pictorial clamp movement and Figure 7.11(d) reports the optimised movable clamp location.

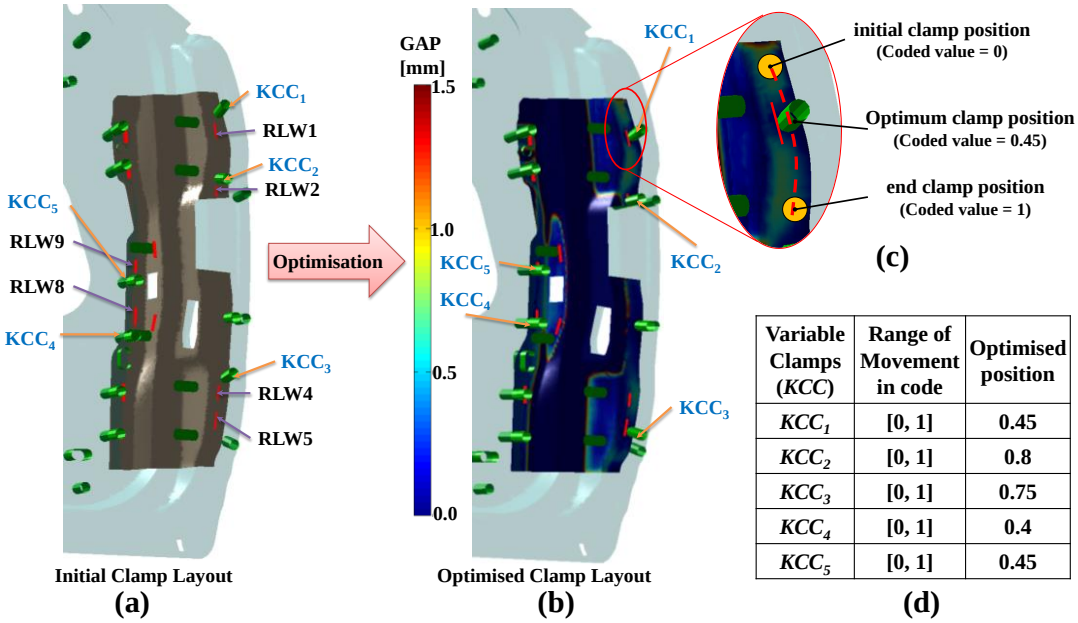

Variable Clamps (*KCC*)	Range of Movement in code	Optimised position
KCC_1	[0, 1]	0.45
KCC_2	[0, 1]	0.8
KCC_3	[0, 1]	0.75
KCC_4	[0, 1]	0.4
KCC_5	[0, 1]	0.45

Figure 7.11 Hinge reinforcement and door inner panel composite assembly: (a) initial clamp layout, (b) optimised clamp layout, (c) clamp movement, and (d) optimised clamp location values

The optimal clamp layout has been applied on all the selected composite assemblies and gap distribution of critical stitches have been plotted in Figure 7.12. The clamp layout results in probability of joining feasibility index as 0.949 for all stitches. From the gap distribution plotted in Figure 7.12, it can be observed that few gaps mainly for $RLW1$, $RLW4$ and $RLW5$ for few composite assemblies are not conforming to the maximum gap specification. The following corrective actions may be taken to mitigate the risk associated with non-conforming stitches

- Based on the gap distribution of the neighbouring area of $RLW1$, the stitch location can be moved from its present location by which the stitch will satisfy the gap criteria. A small violation of $RLW2$ stitch is observed where it tends to out of upper boundary limit.

- $RLW4$ and $RLW5$ both stitches are controlled with single clamp, KCC_3. It might be possible to add another clamp in this region to mitigate the risk of going out of the tolerance zone.
- $RLW8$ and $RLW9$ are controlled by clamps KCC_4 and KCC_5. Both the stitches conforming to the upper boundary gap requirement for satisfactory weld quality.

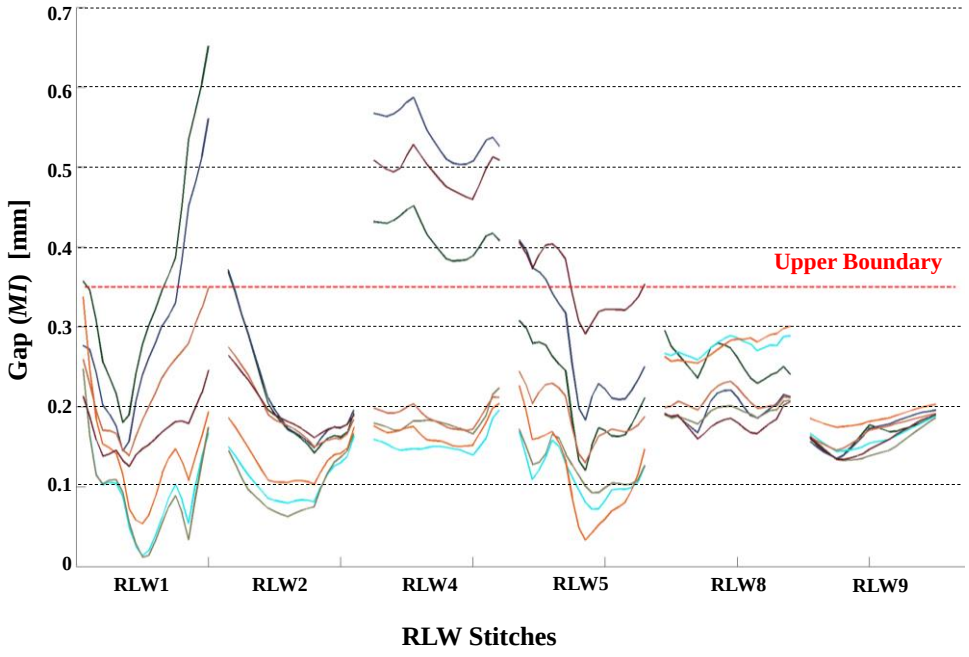

Figure 7.12 Map Index (*MI*) at optimised clamp location for selected composite assemblies (*SCA*)

The state-of-the-art modelling approach for batch of parts optimisation, such as Monte-Carlo based optimisation requires thousands of variational assembly instances. This large number of assemblies implies very high dimensional design space and time consuming simulation process. Subsequently, the simulation time increases with the increase in number of clamp layouts to be evaluated for each variational assembly. To compare the Monte-Carlo based simulation with proposed methodology based simulation, the optimal clamp locations have been used with all other identical parameters to obtain the map index. The map index of selected

stitches has been plotted for 50 Monte-Carlo based assemblies in Figure 7.13 and it shows that the gap behaviour is same as composite assemblies. The probability of joining feasibility index for Monte-Carlo simulation is 0.977 based on 1000 assemblies generation which is slightly higher than the composite assembly based optimisation result, i.e, 0.949. This means composite assembly based solution is giving higher probability to obtain satisfactory joints when applied on Monte-Carlo based assemblies. Therefore, the obtained result implies that composite assembly based optimisation provides more robust solution and it can substitute the Monte-Carlo based simulation for sheet metal assembly fixture design optimisation considering batch of parts.

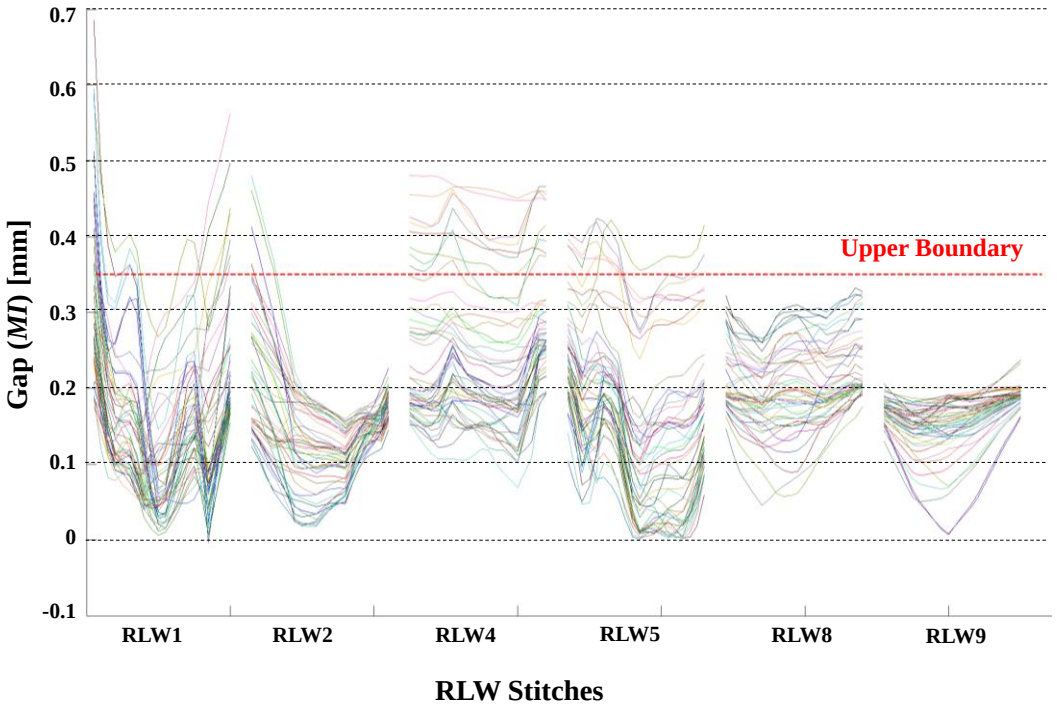

Figure 7.13 Map index (*MI*) for 50 Monte-Carlo based assemblies at optimised clamp location

7.5 SUMMARY

This chapter presents a new approach to improve the probability of joining feasibility index by determining an N-2-1 fixture layout optimised for a production batch of non-ideal sheet metal parts. Fixtures control the position and orientation of parts in an assembly process and thus significantly contribute to process capability that determines production yield and product quality. As a result, a number of approaches were developed to optimise a single- and multi-fixture assembly system with rigid (3-2-1 fixture layout) to deformable parts (N-2-1 fixture layout). These approaches aim at fixture layout optimisation of single ideal parts (as define by CAD model). Thus, major challenges involving the design of a fixture layout for assembly of sheet metal parts can be enumerated into three categories:

(i) Shape variation quantification for production batch: The production yield and product quality are determined based on a production volume of real (non-ideal) parts. Therefore, shape variation quantification model is required to depict the real production scenario.

(ii) High-dimensional design space: The dimensionality of design space increases with the number of parts to be assembled in the assembly station and large number of locators (‘N-2-1’ locating scheme) due to compliant nature of sheet metal parts.

(iii) Highly nonlinear relationship between KPCs and KCCs: The locations of the KCCs (such as clamps) have nonlinear effects on KPC variations.

To address the aforementioned challenges, this chapter proposed fixture layout optimisation methodology utilising the shape variation model, SGMA which is developed in Chapter 5. The methodology is based on: (i) generation of composite

parts to model shape variation within given production batch; (ii) selection of composite assembly representing production batch and parameterisation of fixture locators; and (iii) calculation of analytical surrogate model linking composite assembly model and fixture locators to probability of joining feasibility index. The analytical surrogate model is, then, utilised to maximise the probability of joining feasibility index starting from initial fixture locator layout. An industrial case study involving assembly process of remote laser welded door assembly illustrates and validates the proposed methodology.

CHAPTER 8 CONCLUSIONS, CRITICAL REVIEW AND FUTURE SCOPE

This chapter provides conclusions and overall research findings which are derived from the research presented in the previous chapters in the context of Shape Variation Modelling, Analysis and Statistical Control with compliant sheet metal parts. Thereafter, the advantages and limitations of the proposed methodologies are summarised as critical review. Broader impact of the research shows the applicability and significance of the proposed methods in the domain of assembly simulation with sheet metal parts. Furthermore, future scope based on the current research is proposed.

8.1 CONCLUSIONS

In assembly system modelling, there are industrial needs to simulate assembly system with compliant parts in order to improve product and process quality by addressing shape variation modelling, analysis and statistical control. In the context of shape variation modelling, analysis and statistical control, this thesis, *firstly*, develops the *shape error* and *shape variation* models to represent non-ideal part(s), *thereafter*, statistical process control and fixture analysis are carried out to monitor and reduce shape variation from the assembly process. The major research findings of the developed methodologies are listed as follows:

(i) *Shape error modelling of compliant part:* A functional data analysis based GMA method is proposed for modelling part shape error by decomposing the shape error field into a series of independent shape error modes. This

functional data analysis approach is based on the underlying principle of the shape error characterisation which identifies and quantifies the shape error of 3D freeform shaped part by decomposing the measured deviation into significant shape error modes. The kernel used for the decomposition is three dimensional Discrete Cosine Transform (3D DCT) which has ability to decompose the measured shape error data into various orthogonal error modes. Currently, 3D DCT is used for (i) video compression or image compression - these applications require 2.5D capability (2D pictures presented sequentially as frames per sec); or (ii) 3D volumes with "*uniform non-scattered voxel structure*" such as used in MRI or CT data (solid with no voids). However, the application of 3D DCT approaches cannot be used directly to model 3D volumes with "*non-uniform scattered voxel structure*" such as sheet metal parts used in automotive, aerospace, appliance and ship building industries; or other 3D solids with genuses (holes that penetrate the solid) or shells (internal void of a solid). Therefore, to apply 3D DCT on "*non-uniform scattered voxel structure*", the data structure has been generalised with Laplace interpolation. To extract the main significant error modes, Pearson Correlation test and Least Squares correction criteria have been employed. Therefore, in short, to apply 3D DCT effectively on 3D freeform shaped geometry, total three criteria have been introduced

- Generalisation of 3D DCT to model 3D volumes with "*non-uniform scattered voxel structure*"
- Generalisation of 3D DCT interpretability criteria to identify significant shape error modes

- Generalisation of 3D DCT accuracy criterion to model correct magnitude of shape error modes of individual part

The aforementioned three criteria have been achieved with the following:

- *Uniform smooth voxel structure:* 3D sheet metal parts are in the category of 3D freeform shaped parts where 3D decomposition cannot be applied directly as they are based on 3D volume model. In order to convert the 3D freeform shaped model to 3D volume model, voxelisation method has been adapted which creates non-uniform scattered voxel structure. Further, Laplace interpolation has been applied to this non-continuous voxel deviation field to smooth the voxel structure enabling the 3D decomposition to be applied on the smooth volume structure.

- *Mode interpretation criterion:* The shape error decomposition into significant modes and identification of most relevant shape error modes, Pearson's correlation coefficient based mode interpretation criterion has been introduced. This helps to reduce the number of modes for model development keeping the GMA model tractable.

- *Model accuracy criterion:* To achieve the accuracy of the selected modes for compact model development, least squares based modes magnitude correction has been implied. This enhances the overall model accuracy to depicts the original part deviation field with fewer selected modes.

The main advantage of GMA method is that it can be applied to characterise shape errors of 3D freeform shaped part. Voxelisation of the mesh model plays a dominant role in modelling and achieving accuracy of shape error

decomposition. Further, compactness of the shape error model is achieved by using mode truncation and selection criteria. Energy compaction criterion selects the coefficients/modes according to their global energy contribution (i.e. it provides a global control to model shape error), whereas the correlation test emphasises the important shape error modes related to original part shape error. Therefore, the proposed GMA methodology plays significant roles when exploring the following areas: 1) part shape error identification of freeform shaped part by using functional data model without application of any Finite Element Analysis (FEA); 2) identification of main shape error modes from real part which will allow the variation simulation in statistical tolerance analysis; 3) the modal decomposition pointing towards the characterisation of fabrication process at design stage and manufacturing stage; and, 4) from part shape error model to batch of parts shape variation model, where, the mode magnitudes can be parameterised by means of its values to quantify the variation associated with a batch of parts.

(ii) Shape variation modelling of batch of compliant parts: The functional data analysis approach, Geometric Modal Analysis (Chapter 4) has been extended to shape variation characterisation and quantification method, named Statistical Geometric Modal Analysis (SGMA). The GMA decomposed shape error modes have been used as parameters to represent shape variation of a batch of parts, eventually the *production shape variation.* SGMA method characterises the shape variation associated with a batch of parts by generalising the statistical behaviour of shape error modes, and quantifies the shape variation of production parts by synthesising composite parts.

The shape variation modelling of a batch of parts is achieved by generalising the statistical behaviour of shape error modes and synthesising composite part(s). However, statistical characterisation of shape error modes and creation of composite parts are not trivial tasks as they involve the following: (a) identification of important shape error modes not only from individual part but also from batch of parts, (b) the identified shape error modes might not be normally distributed, or (c) composition rule to synthesise composite part(s) considering all the major shape error modes with their magnitudes. Therefore, to model shape variation effectively, the following issues have been addressed

- *Identification of major shape error modes from a batch of parts:* The decomposed shape error modes can be classified as common modes (i.e. modes are obtained from every part decomposition of the batch) and uncommon modes (i.e. modes are obtained only from few parts decomposition). To characterise shape variation, both common and uncommon modes are considered.

- *Non-normal distribution of shape error modes:* For statistical characterisation of identified major shape error modes, normal distribution based fitting might not be accurate enough to depict real shape error modes distributions. Many real processes, the assumption of normal distribution may not be accurate as most of the processes do not conform to normal distribution. Therefore, non-parametric density estimation, such as, Kernel Density Estimation (KDE) to estimate the Probability Density Function (PDF) of modes, has been employed to overcome the problem if the modes are not normally distributed.

- *Number of composite parts required to quantify shape variation:* The composite part is a hypothetical part composed of all the major significant shape error modes from the batch. Depending on the types of shape error present in the measured batch, composite part might be more than one to represent the whole population. To classify parts into few groups, having similar shape error modes, k-means clustering method has been applied. Each cluster has been represented with composite parts based on energy compaction criteria and root sum of squares criteria.

The SGMA method fulfils the following two objectives:

- *Generation of variational virtual parts:* The statistical characterisation of extracted shape error modes helps to generate virtual parts. The statistical characterisation is based on batch of parts measurement data. The main assumption of normality distribution of modes has been overcome by using Kernel Density Estimation (KDE). The probability density function of each modes helps to generate variational virtual parts which represent the virtual production parts. Therefore, the virtual generation of shape error field can be extended to synthesise the statistical tolerance zone for freeform shaped parts.

- *Synthesis of composite parts:* The SGMA method develops a novel technique to quantify the shape variation into single or few *composite part(s)* which is composed of major shape error modes present in a batch of parts. The SGMA method based composite parts act as an enabler to optimise the fixture design process considering not only the individual part but also a batch of parts.

Furthermore, the GMA and SGMA methods can be extended to model shape variation at early design phase. Current, Computer Aided Tolerancing (CAT) tools are mainly capable of modelling orientation and position tolerance specifications, where part shape errors are omitted. The developed Geometric Modal Analysis (GMA) and Statistical Geometric Modal Analysis (SGMA) methods provide a simulation platform where shape errors can be modelled and included for statistical tolerance analysis. However, GMA and SGMA methods are based on the measurement data which might not be available at early design phase. To overcome the limited or no measurement data availability at early design phase, a physics-driven simulation framework to model shape errors of compliant sheet metal parts can be proposed.

This implementation can be carried out at three stages: (i) initial shape error prediction by using physic-based simulation, such as, stamping process simulation based on nonlinear finite element analysis (e.g. using commercial tools - AutoForm, HyperForm, or, DYNAFORM) to predict the initial shape error at early design stage; (ii) decomposition of initial shape error into orthogonal shape error modes by utilising GMA; and, (iii) simulation of shape error variation classes by assigning distribution to each orthogonal shape error modes by using SGMA. At this stage, the distributions may be assumed based on historical data or keeping the mean (decomposed mode magnitude) to variance ratio as constant. This proposed approach enables to generate shape errors at early design stage of assembly process which can be utilised to optimize the assembly process, including fixture design and joining process parameters.

(iii) *Control charts to monitor process and product quality shapes:* A GMA-based integrated bivariate T^2-Q control chart for monitoring and detection of shape defects has been developed. The shape defects may involve global and local mean shift or variance change. They are caused by manufacturing process variation. These mean shift or variance change lead to part error during fabrication or part fit-ups error in assembly. The current approaches for synthesising these two statistics (T^2 and Q) are not sufficient to identify the shape error modes. The proposed multivariate control chart adapts a new direction of obtaining statistically uncorrelated and independent latent variables set by decomposing the data set within a single sample using GMA decomposition method (proposed in Chapter 4). This helps to achieve enhanced granularity of information extraction from the measured data set and increase the shape defects detectability. The latent variables (GMA modelled data) are used to determine multivariate T^2 statistic, and residual data (un-modelled) gives the Q statistic. Integrating the T^2 and Q statistics using non-parametric Kernel Density Estimator (KDE) provides a bivariate scatter plot which has enhanced sensitivity to detect shape defects. The proposed methodology is demonstrated with automotive sheet metal parts which fulfil the following critical requirements for stamped sheet metal part monitoring:

- *Mean shift detection:* Sheet metal parts, produced with different runs/batches, exhibit mean shift. The obtained results successfully demonstrate that GMA based T^2-Q control chart is able to detect mean shift effectively.

- *Local shift detection:* Local shift in stamped parts is mainly caused by stamping tool worn out locally, tools not bottoming out as well as uneven material flow during stamping. The power of detectability for local deformation is demonstrated with GMA based control chart and compared with PCA based control chart. It results in increased detectability for GMA decomposed T^2-Q control chart.
- *Identification of in-control mean shift or variance change detection:* The control chart has the ability to detect in-control mean shift or variance change which can be observed for within-run production or for run-to-run production.

Currently, the parts can be measured using fast, in-line 3D metrology scanners which can capture high volume CoP data. The measured part CoP data, then, can be used for statistical process monitoring and shape defects detection using the proposed GMA-based T^2-Q control chart. Industrial case study based results show the capabilities of the GMA-based T^2-Q control chart for monitoring and detecting the shape defects caused by variance change or mean shift. It also demonstrates advantages of the proposed GMA-based T^2-Q control chart for detecting in-control mean shift, variance change or ARL over currently used PCA-based T^2-Q control chart. Therefore, the control chart has the following capabilities:

- *New direction to obtain the reduced variable set to synthesise T^2 and Q statistics:* a new direction of obtaining reduced set of statistically uncorrelated and independent process variables by decomposing the data set within a single sample (GMA decomposition) instead of PCA- or

PLS-based decomposition which is done across the samples. This emphasises the enhanced granularity of decomposition which enhances the shape fault detectability.

- *Use of high dimensional and high volume CoP data:* The control chart has the ability to process the high dimensional and high volume CoP data captured using modern 3D non-contact scanners. As these scanners have potential to be used for in-line to capture whole part surface information (CoP data) very quickly, the proposed control chart can use the CoP data for in-line process/product monitoring and defects detection.
- *Detection of shape based faults:* The control chart has the ability to detect the mean shift or variance change which can cause part fit-ups errors during assembly due to part-to-part interactions. The localised mean shift or variance change can also be detected using the proposed control chart. During real production of stamped sheet metal parts, variance change can be observed for within-run production, or mean shift may present for run-to-run production. Further, the proposed GMA-based T^2-Q control chart has the ability to detect in-control mean shift, variance change and ARL change over state-of-the-art PCA-based T^2-Q control chart.

(iv) Fixture layout optimisation considering production batch: A new fixture layout optimisation methodology for non-ideal compliant assembly has been proposed considering the shape variation associated with a batch of parts. This research objective is motivated by the industrial need of fixture design with compliant sheet metal parts to achieve better product quality. It is an application based extension of batch of parts shape variation quantification method, i.e., SGMA method (Chapter 5) which quantifies the shape variation

by creating composite parts. Subsequently, fixture layout optimisation methodology utilises the composite parts for creating composite assemblies which can be used for optimisation. The proposed fixture layout optimisation methodology can be applied on production fixture development which involves non-ideal deformable sheet metal parts, applicable in various sectors such as automobile, aerospace, rail and home appliances. The fixture layout optimisation significantly goes beyond the current state-of-the-art and practice as the fixture can be designed and optimised not only for part shape error but for production shape variation. Fixturing design optimised only for part shape error provides significant limitations which are reflected in (a) large number of fixture tuning quality loops and adjustments; (b) longer product development time; and (c) lower product quality.

To address the aforementioned limitations, a new fixture layout optimisation methodology has been developed considering the shape variation of a batch of production parts. By extending SGMA method, this fixture layout optimisation methodology proposes a novel way for selecting fewer composite assemblies which will represent the production shape variation. The fixture layout optimisation method involves: (i) composite part model of production batch to create composite assemblies, (ii) selection of composite assembly by correlation and entropy criteria, and (iii) maximisation of the probability of the joining feasibility index.

The developed fixture layout optimisation methodology addresses the following:

- *Consideration of shape variation of production batch:* As the production yield or product quality depends on the real shape variation of production

parts, the developed fixture layout optimisation methodology addresses this challenge by using composite parts which represent the production shape variation.

- *Reduction of high dimensional design space:* The design space for fixture layout optimisation increases with number of parts to be assembled as well as large number of locators. The fixture layout optimisation methodology addresses this challenge by selecting fewer composite assemblies which are representative of the production shape variation and by restricting locator's movement.
- *Highly nonlinear relationship between KPCs and KCCs:* The nonlinear behaviour of KPCs and KCCs is identified through developing the analytical surrogate model by linking the selected composite assemblies and fixture locators (i.e. clamp locations) with an aim to increase the joining feasibility index.

The proposed fixture layout optimisation methodology significantly explores the following areas: (1) Fixture layout optimisation, by addressing shape variation of a batch of non-ideal compliant assemblies, considers the production parts and identifies robust fixture layout parameters through optimisation; and (2) Replacement of time expensive Monte-Carlo based simulation by eliminating thousands of variational assembly instances based simulation. The industrial case study shows that the results obtained through the use of selected composite assemblies can replace the time consuming Monte-Carlo simulation with same level of joining feasibility index.

8.2 CRITICAL REVIEW

The research aims to develop models for shape variation modelling, analysis and statistical control with compliant sheet metal parts where these models can be used for product and process development. This thesis discusses two new enablers for shape variation monitoring and reduction: (i) *modelling and characterisation of shape errors of compliant part-GMA method;* and (ii) *modelling and characterisation of shape variation of a batch of compliant parts-SGMA method.* These two methods provide in-depth understanding of shape errors and shape variation of non-ideal compliant parts. Further, these two enablers have been used to develop (iii) *Control charts to monitor process and product quality shapes* of compliant parts and detects the shape related faults; and (iv) *optimisation of fixture layout considering production batch* for assembly process design to reduce shape variation.

This section provides a critical review of the methodologies developed in this thesis. Firstly, the advantages of proposed methodologies for shape variation modelling, analysis and statistical control in the context of assembly system with compliant sheet metal parts are highlighted in Section 8.2.1. Thereafter, limitations of the adapted approaches are listed in Section 8.2.2.

8.2.1 Advantages of Proposed Methodologies

The advantages of the four methods developed in this thesis for shape variation modelling, analysis and statistical control are summarised as follows:

(i) Accurate shape error modelling of 3D freeform shaped compliant part which provides a simplified parametric functional model to achieve quality solutions for assembly process simulation and process diagnosis –

The developed GMA methodology has been compared with available state-of-the-art decomposition approaches which fail to accurately extract shape error modes from measurement data. The proposed GMA method (in Chapter 4) efficiently extracts significant shape error modes which can be further used for GD&T simulation and process diagnostics due to the parametric nature of the decomposed shape error modes. Industrial case studies show improvements between results obtained via proposed GMA decomposition and those obtained by state-of-the-art methods.

(ii) Quantification of shape variation of a batch of 3D freeform shaped compliant parts which provides a novel approach to quantify production errors to achieve quality solutions when assembly process involves production parts –

Due to unavailability of production shape variation quantification model, intrinsic variation of the production process cannot be considered during assembly process simulation which leads to significant limitation to predict production quality. The proposed SGMA method (developed in Chapter 5) characterises the statistical nature of product and quantifies shape variation to support assembly process simulation by depicting real scenario of production parts.

(iii) Identification of shape related faults of 3D freeform shaped compliant part/product utilising high dimensional CoP data captured by using fast, in-line non-contact optical measurement scanners –

Current control charts are not able to handle high dimensional data for detecting shape related faults. There is a lack of efficient approach for statistical process monitoring of non-linear shapes. The proposed *GMA-based*

integrated bivariate T^2-Q monitoring chart (developed in Chapter 6) can be used for high dimensional non-normal data (cloud-of-points) captured by in-process or off-line sensors with the ability to: (i) detect global part shape failures such as unwanted variance change or mean shift, a common occurrence for within batch or batch-to-batch variation of stamped sheet metal parts; (ii) detect local part shape failures such as local shift or variance change; and, (iii) classify the shape faults to predict manufacturing quality and yield.

(iv) Improvement of production yield and product quality of assembly process with compliant parts considering production shape variation to optimise assembly fixture layout –

Current approaches for assembly systems modelling with compliant parts are mainly limited to case-by-case which is based on individual part shape error instead of production shape variation. The production shape variation significantly affects the assembled product quality and production yield. Therefore, the proposed *SGMA based fixture layout optimisation* (demonstrated in Chapter 7) is focused on maximising the probability of joining feasibility index which represents the likelihood of any assembly will have satisfied quality.

Overall benefits of assembly system modelling with compliant parts

Current industrial practice is to develop assembly system based on the trial-and-error approach by experienced product and process engineers which is time consuming, expensive and repetitive in nature. To support product and process engineers, efficient and effective modelling approaches are required for early detection of

faults, subsequently, to take preventive actions. This thesis discusses the industrial needs for shape variation modelling, analysis and statistical control. Further, the developed methodologies provide an engineering platform for accurate depiction of assembly system to achieve improved product quality, early stage optimisation and reduced quality loops during assembly system development.

8.2.2 Limitations of Proposed Methodologies

Driven by industrial needs and to simulate assembly process with compliant parts, the proposed methodologies in this thesis address the following four critical modelling areas: (i) *modelling and characterisation of shape error of compliant part;* (ii) *modelling and characterisation of shape variation of a batch of compliant parts;* (iii) *shape variation monitoring and detection of shape defects*; and (iv) *optimisation of assembly fixture layout considering production batch*. However, there might be other enhancements required to support assembly process in addition to the proposed methodologies in this thesis.

The limitations of the proposed techniques (developed in Chapter 4, 5, 6 and 7) are

- As the GMA decomposition methods based on the underlying principle of 3D DCT which is very efficient to characterise the global errors or repetitive local errors. In case of non-repetitive local errors with low magnitude, the shape error modes might not be accurate. Further, special attention must be required during voxelisation (voxel size selection) of mesh model to accurate representation of shape error modes.
- For SGMA method, the main assumption is the production process stability and selected sample parts are representative of the production population.

- The developed control chart can detect the shape related faults efficiently for global errors whereas for local errors, it fails to identify the location of the fault. Further, the control chart is able to process data captured from single measurement station. Captured data from multiple sensors at multi-station poses additional challenges due to further increase in data dimensionality and data dependency.
- The fixture layout optimisation is based on single station which might not be applicable to multi-station fixture layout optimisation for batch of parts as the variation propagation between stations needs to be considered as well.

Under the abovementioned conditions, there are requirement to extend the proposed modelling techniques to address multi-station interaction related issues. The following Future Scope (Section 8.3) analyses the potential extension of the proposed methodologies.

8.3 FUTURE SCOPE

The thesis has proposed a new direction of shape error and shape variation modelling using real measurement data. Further, both models have been applied for shape defects detection and robust assembly fixture layout optimisation. The proposed methodologies can be applied in various sectors of design and manufacturing with compliant sheet metal parts. The future research can be summarised as follows:

- Geometric dimensioning and tolerancing (GD&T) together with process capability analysis plays a significant role in quality assurance. Tolerance synthesis for compliant non-ideal parts is a challenging task due to complex shapes and geometries. The complexity of shape errors increases with the increase in geometrical complexity. The developed GMA decomposition method

can be used for tolerance synthesis of individual part as well as assembly tolerancing. The GMA transform coefficients can be used for tolerance allocation of individual component to meet the assembly requirement. Further, their distribution through SGMA can help to quantify the process capability.

- In sheet metal stamping, die tryout is an important yet iterative task to perform in order to make the die and punch with correct geometry. Die manufacturers are keen to reduce this iterative die construction process and total time required for die tryout. Further, the die tryout solely depends on the experience of stamping process engineer and the process is very time consuming. Therefore, the GMA transformed modes or shape error patterns can be used to reduce the number of iteration required for the die tryout. To reduce the rework on die tuning, the shape error decomposition methods can be used by identifying what to reduce and by how much to meet the part acceptance requirements.

- Currently, all the design is based on the nominal geometry expressed as CAD model. However, there is no model available to embed the shape error patterns with CAD model. Therefore, it is real challenge to represent real part model with CAD by developing standard for variational parts. The developed GMA and SGMA models can be further integrated with CAD model in order to represent real part variation, i.e. non-ideal geometry.

- The proposed GMA-based integrated T^2-Q control chart (proposed in Chapter 6) is related to the detection of shape error based on the measurement from single measurement station. Captured data from multiple sensors at multi-station poses additional challenges to handle due to further increase in data dimensionality and data dependency. Therefore, there is future scope for distributed sensors based

multi-station process monitoring. Further, shape error detection can be linked with the root cause analysis to identify the cause of the defects. For example, stamping process parameters can be mapped with shape error modes to minimise the variation, to identify the cause of variation, and to adjust the process to its original operating state. These mode based approach can be utilised to take corrective actions and preventive actions related to process stabilisation.

- Current, SGMA-based fixture layout optimisation (proposed in Chapter 7) is focused on single assembly station. Therefore, the work on the fixture layout optimisation can be further extended to multi-station considering batch of parts' shape variation. Future focus will be multi-fixture optimisation at multi-station level where variation propagation through stations is to be considered.

8.4 BROADER IMPACT

The methodologies developed in this thesis for 'shape variation modelling, analysis and statistical control' with compliant parts can be considered as basic building blocks for carrying out engineering tasks related to assembly process considering the variation associated with it. They can be utilised to achieve near zero defect production with improved quality and reduced time-to-launch. These systematic approaches are especially unavoidable when increasing market requirements are to be met and Right First Time (RFT) is to be achieved. They are the key enablers for facilitating cost and time-to-launch (or time-to-market) reduction during new product introduction. In global market scenario, the manufacturers are in tremendous need of effective methods and models to simulate assembly system to achieve Right First Time in cost-effective way. The developed methodologies have the capabilities to reach near zero defects by (i) reducing the number of engineering changes during the

product launch stage; (ii) identifying upfront the risk regions during prototype building stage; and (iii) improving in-process quality during manufacturing stage. These aforementioned capabilities will result in increased productivity and quality (reduced maintenance time and scrap) to place manufacturers at the forefront of a rapidly developing market.

The developed methodologies provide a systematic analysis and synthesis framework when the assembly process is affected by variations, especially it holds true for emerging remote laser welding joining technology. Integrating RLW joining process with existing production system triggers new requirements of key enablers which can optimise and monitor assembly system aiming to achieve near zero defect and reduced time-to-market. Current, computer-aided engineering (CAE) tools fail to provide sufficient flexibility and capability to model assembly system with new requirements imposed by RLW joining technology. The developed methodologies in this thesis provide the much needed platform to meet the requirements of RLW joining process and overcome the modelling limitations of current CAE techniques. Further, current industrial practice to eliminate faults occurring at product ramp-up stage and/or production stage is based on trial-and-error method. As a result, it becomes a repetitive, time consuming and expensive process. To overcome the trial-and-error based limitations, the methodologies developed in this thesis contribute to reduce development lead time (i.e. reduction in engineering changes and quality checks), early detection of risk regions which might occur during production, and monitoring of assembly quality for pre- and post- production stages.

REFERENCES

Acciani, G., Brunetti, G. & Fornarelli, G. 2006. Application of neural networks in optical inspection and classification of solder joints in surface mount technology. *IEEE Transactions on Industrial Informatics,* 2**,** 200-209.

Aguilar, J. J., Torres, F. & Lope, M. A. 1996. Stereo vision for 3D measurement: accuracy analysis, calibration and industrial applications. *Measurement,* 18**,** 193-200.

Antory, D. 2007. Application of a data-driven monitoring technique to diagnose air leaks in an automotive diesel engine: A case study. *Mechanical Systems and Signal Processing,* 21**,** 795-808.

ASME-Y14.5m 2009. Dimensioning and tolerancing. New York: American Society of Mechanical Engineers.

ASME 2004. Mathematical definition of dimensioning and tolerancing principles : an American national standard; ASME Y14.5.1M, New York, American Society of Mechanical Engineers.

Bakshi, B. R. 1998. Multiscale PCA with application to multivariate statistical process monitoring. *AIChE Journal,* 44**,** 1596-1610.

Bersimis, S., Psarakis, S. & Panaretos, J. 2007. Multivariate statistical process control charts: an overview. *Quality and Reliability Engineering International,* 23**,** 517-543.

Bihlmaier, B. F. 1999. *Tolerance analysis of flexible assemblies using finite element and spectral analysis.* M.S. Thesis, Brigham Young University, Utah.

Božinović, N. & Konrad, J. 2005. Motion analysis in 3D DCT domain and its application to video coding. *Signal Processing: Image Communication,* 20**,** 510-528.

Cai, W. 2008. Fixture optimization for sheet panel assembly considering welding gun variations. *Proceedings of the Institution of Mechanical Engineers, Part C: Journal of Mechanical Engineering Science,* 222**,** 235-246.

Cai, W., Hu, S. J. & Yuan, J. X. 1996. Deformable sheet metal fixturing: principles, algorithms, and simulations. *Journal of Manufacturing Science and Engineering,* 118**,** 318-324.

Cai, W. W., Hsieh, C.-C., Long, Y., Marin, S. P. & Oh, K. P. 2005. Digital panel assembly methodologies and applications for compliant sheet components. *Journal of Manufacturing Science and Engineering,* 128**,** 270-279.

Camelio, J., Ceglarek, D. & Hu, S. J. 2003. Modeling variation propagation of multi-station assembly systems with compliant parts. *Journal of Mechanical Design,* 125**,** 673-681.

Camelio, J. A. 2002. *Modeling and diagnosis of dimensional variation for assembly systems with compliant parts.* Ph.D. Thesis, University of Michigan.

Camelio, J. A. & Hu, S. J. 2004. Multiple fault diagnosis for sheet metal fixtures using designated component analysis. *Journal of Manufacturing Science and Engineering,* 126**,** 91-97.

Camelio, J. A., Hu, S. J. & Ceglarek, D. 2004a. Impact of fixture design on sheet metal assembly variation. *Journal of Manufacturing Systems,* 23**,** 182-193.

Camelio, J. A., Marin, S. P. & Hu, S. J. 2004b. Compliant assembly variation analysis using component geometric covariance. *Journal of Manufacturing Science and Engineering,* 126**,** 355-360.

Capello, E. & Semeraro, Q. 2000. Harmonic fitting approach for plane geometry measurements. *The International Journal of Advanced Manufacturing Technology,* 16**,** 250-258.

Capello, E. & Semeraro, Q. 2001. The harmonic fitting method for the assessment of the substitute geometry estimate error. Part I: 2D and 3D theory. *International Journal of Machine Tools and Manufacture,* 41**,** 1071-1102.

Ceglarek, D. 2011. Remote Laser Welding (RLW) system navigator for eco and resilient automotive factories. Digital Factories Theme. WMG, University of Warwick.

Ceglarek, D., Huang, W., Zhou, S., Ding, Y., Kumar, R. & Zhou, Y. 2004. Time-based competition in multistage manufacturing: stream-of-variation analysis (SOVA) methodology—review. *International Journal of Flexible Manufacturing Systems,* 16**,** 11-44.

Ceglarek, D., Li, H. F. & Tang, Y. 2001. Modeling and optimization of end effector layout for handling compliant sheet metal parts. *Journal of Manufacturing Science and Engineering,* 123**,** 473-480.

Ceglarek, D. & Shi, J. 1995. Dimensional variation reduction for automotive body assembly. *Manufacturing Review,* 8**,** 139-154.

Ceglarek, D. J. 1998. Multivariate analysis and evaluation of adaptive sheet metal assembly systems. *CIRP Annals - Manufacturing Technology,* 47**,** 17-22.

Chase, K. & Parkinson, A. 1991. A survey of research in the application of tolerance analysis to the design of mechanical assemblies. *Research in Engineering Design,* 3**,** 23-37.

Chen, Q., Kruger, U., Meronk, M. & Leung, A. Y. T. 2004. Synthesis of T2 and Q statistics for process monitoring. *Control Engineering Practice,* 12**,** 745-755.

Choudhary, A. K., Harding, J. A. & Tiwari, M. K. 2009. Data mining in manufacturing: a review based on the kind of knowledge. *Journal of Intelligent Manufacturing,* 20**,** 501-521.

Clement, A. & Bourdet, P. 1988. A study of optimal-criteria identification based on the small-displacement screw model. *CIRP Annals - Manufacturing Technology,* 37**,** 503-506.

Clément, A., Rivière, A., Serré, P. & Valade, C. 1998. The TTRSs : 13 constraints for dimensioning and tolerancing. *Geometric Design Tolerancing: Theories, Standards and Applications.* Springer US.

Colosimo, B., Mammarella, F. & Petrò, S. 2010. Quality control of manufactured surfaces. *Frontiers in Statistical Quality Control 9.* Physica-Verlag HD.

Colosimo, B. M. & Pacella, M. 2007. On the use of principal component analysis to identify systematic patterns in roundness profiles. *Quality and Reliability Engineering International,* 23**,** 707-725.

Cover, T. M. & Thomas, J. A. 2006. Elements of information theory, Wiley.

Creehan, K. & Bidanda, B. 2006. Reverse engineering: a review & evaluation of non-contact based systems. *Rapid Prototyping.* Springer US.

Cubélès-Valade, C. & Riviere, A. 1999. Nominal and actual geometry explicit declaration. *Integrated Design and Manufacturing in Mechanical Engineering '98.* Springer Netherlands.

Das, A., Franciosa, P. & Ceglarek, D. 2015. Fixture design optimisation considering production batch of compliant non-ideal sheet metal parts. *Procedia Manufacturing,* 1**,** 157-168.

Das, A., Franciosa, P., Prakash, P. K. S. & Ceglarek, D. 2014. Transfer function of assembly process with compliant non-ideal parts. *Procedia CIRP,* 21**,** 177-182.

De Souza, T. & Rolfe, B. 2008. Multivariate modelling of variability in sheet metal forming. *Journal of Materials Processing Technology,* 203**,** 1-12.

Ding, Y., Ceglarek, D. & Shi, J. 2002. Design evaluation of multi-station assembly processes by using state space approach. *Journal of Mechanical Design,* 124**,** 408-418.

Du-Ming, T., Chiang, I. Y. & Ya-Hui, T. 2012. A shift-tolerant dissimilarity measure for surface defect detection. *IEEE Transactions on Industrial Informatics* 8**,** 128-137.

Du-Ming, T. & Jie-Yu, L. 2011. Mean shift-based defect detection in multicrystalline solar wafer surfaces. *IEEE Transactions on Industrial Informatics,* 7**,** 125-135.

Duta, N., Jain, A. K. & Dubuisson-Jolly, M. P. 2001. Automatic construction of 2D shape models. *IEEE Transactions on Pattern Analysis and Machine Intelligence,* 23**,** 433-446.

Ekenel, H. K., Hua, G. & Stiefelhagen, R. 2007. 3-D face recognition using local appearance-based models. *IEEE Transactions on Information Forensics and Security,* 2**,** 630-636.

Feng, H.-Y., Liu, Y. & Xi, F. 2001. Analysis of digitizing errors of a laser scanning system. *Precision Engineering,* 25**,** 185-191.

Forrester, A., Sobester, A. & Keane, A. 2008. Engineering design via surrogate modelling: a practical guide, Wiley.

Franciosa, P., Das, A., Ceglarek, D., Bolognese, L., Marine, C. & Mistry, A. 2014. Design synthesis methodology for dimensional management of assembly process with compliant non-ideal parts. *Proceedings of Joint Conference on Mechanical, Design Engineering & Advanced Manufacturing.* Toulouse, France.

Franciosa, P., Das, A., Yilmazer, S., Gerbino, S. & Ceglarek, D. 2015. Variation Response Method (VRM): a kernel for dimensional management simulation of non-ideal compliant parts.

Franciosa, P., Gerbino, S. & Patalano, S. 2011. Simulation of variational compliant assemblies with shape errors based on morphing mesh approach. *The International Journal of Advanced Manufacturing Technology,* 53**,** 47-61.

Gökberk, B., Salah, A., Alyüz, N. & Akarun, L. 2009. 3D Face Recognition: Technology and Applications. *Handbook of Remote Biometrics.* Springer London.

Guiford, J. & Turner, J. 1993. Advanced analysis and synthesis for geometric tolerances. *Manufacturing Review,* 6**,** 305-313.

Günlü, G. & Bilge, H. S. 2010. Face recognition with discriminating 3D DCT coefficients. *The Computer Journal,* 53**,** 1324-1337.

Gupta, S. & Turner, J. U. 1993. Variational solid modeling for tolerance analysis. *IEEE Computer Graphics and Applications,* 13**,** 64-74.

Hsiao, S.-W. & Chuang, J.-C. 2003. A reverse engineering based approach for product form design. *Design Studies,* 24**,** 155-171.

Hu, M., Lin, Z., Lai, X. & Ni, J. 2001. Simulation and analysis of assembly processes considering compliant, non-ideal parts and tooling variations. *International Journal of Machine Tools and Manufacture,* 41**,** 2233-2243.

Hu, S. J., Ko, J., Weyand, L., Elmaraghy, H. A., Lien, T. K., Koren, Y., Bley, H., Chryssolouris, G., Nasr, N. & Shpitalni, M. 2011. Assembly system design and operations for product variety. *CIRP Annals - Manufacturing Technology,* 60**,** 715-733.

Huang, W. & Ceglarek, D. 2002. Mode-based decomposition of part form error by discrete-cosine-transform with implementation to assembly and stamping

system with compliant parts. *CIRP Annals - Manufacturing Technology,* 51**,** 21-26.

Huang, W., Liu, J., Chalivendra, V., Ceglarek, D., Kong, Z. & Zhou, Y. 2014. Statistical modal analysis for variation characterization and application in manufacturing quality control. *IIE Transactions,* 46**,** 497-511.

Huang, Z., Ni, J. & Shih, A. J. 2008. Quantitative evaluation of powder spray effects on stereovision measurements. *Measurement Science and Technology,* 19**,** 025502.

Isheil, A., Gonnet, J. P., Joannic, D. & Fontaine, J. F. 2011. Systematic error correction of a 3D laser scanning measurement device. *Optics and Lasers in Engineering,* 49**,** 16-24.

ISO-1101 2013. Geometrical product specifications (GPS) — geometrical tolerancing — tolerances of form, orientation, location and run-out. *BSI Standards Publication.*

ISO-17450-1 2011. BSI standards publication geometrical product specifications (GPS) — general concepts part 1 : Model for geometrical specification.

Jin, J. & Shi, J. 2001. Automatic feature extraction of waveform signals for in-process diagnostic performance improvement. *Journal of Intelligent Manufacturing,* 12**,** 257-268.

Jing, Z., Jian, L. & Jianjun, S. 2010. Predictive control considering model uncertainty for variation reduction in multistage assembly processes. *IEEE Transactions on Automation Science and Engineering,* 7**,** 724-735.

Kourti, T. & Macgregor, J. F. 1995. Process analysis, monitoring and diagnosis, using multivariate projection methods. *Chemometrics and Intelligent Laboratory Systems,* 28**,** 3-21.

Kruger, U., Chen, Q., Sandoz, D. J. & Mcfarlane, R. C. 2001. Extended PLS approach for enhanced condition monitoring of industrial processes. *AIChE Journal,* 47**,** 2076-2091.

Kruger, U. & Xie, L. 2012. Multivariate data modeling methods. *Statistical Monitoring of Complex Multivariate Processes.* John Wiley & Sons.

Ku, W., Storer, R. H. & Georgakis, C. 1995. Disturbance detection and isolation by dynamic principal component analysis. *Chemometrics and Intelligent Laboratory Systems,* 30**,** 179-196.

Lee, J.-M., Yoo, C. & Lee, I.-B. 2004a. Statistical monitoring of dynamic processes based on dynamic independent component analysis. *Chemical Engineering Science,* 59**,** 2995-3006.

Lee, J.-M., Yoo, C. & Lee, I.-B. 2004b. Statistical process monitoring with independent component analysis. *Journal of Process Control,* 14**,** 467-485.

Lee, J., Hu, S. J. & Ward, A. C. 1999. Workspace synthesis for flexible fixturing of stampings. *Journal of Manufacturing Science and Engineering,* 121**,** 478-484.

Lee, M. C., Chan, R. K. W. & Adjeroh, D. A. 1997. Quantization of 3D-DCT coefficients and scan order for video compression. *Journal of Visual Communication and Image Representation,* 8**,** 405-422.

Li, B., Hu, Y., Tang, H., Yu, H. & Hu, H. 2008a. A comparative study on quality design of fixture planning for sheet metal assembly. *Journal of Engineering Design,* 19**,** 1-13.

Li, B. & Roy, U. 2001. Relative positioning of toleranced polyhedral parts in an assembly. *IIE Transactions,* 33**,** 323-336.

Li, B. & Shiu, B. W. 2001. Principle and simulation of fixture configuration design for sheet metal assembly with laser welding, part 2: optimal configuration design with genetic algorithm. *The International Journal of Advanced Manufacturing Technology,* 18**,** 276-284.

Li, B., Shiu, B. W. & Lau, K. J. 2001. Principle and simulation of fixture configuration design for sheet metal assembly with laser welding, part 1: finite-element modelling and a prediction and correction method. *The International Journal of Advanced Manufacturing Technology,* 18**,** 266-275.

Li, B., Shiu, B. W. & Lau, K. J. 2002a. Weld pattern design for sheet metal laser welding considering fixturing quality. *The International Journal of Advanced Manufacturing Technology,* 19**,** 418-425.

Li, B., Shiu, B. W. & Lau, K. J. 2003. Robust fixture configuration design for sheet metal assembly with laser welding. *Journal of Manufacturing Science and Engineering,* 125**,** 120-127.

Li, B., Shui, B. W. & Lau, K. J. 2002b. Fixture configuration design for sheet metal assembly with laser welding: a case study. *The International Journal of Advanced Manufacturing Technology,* 19**,** 501-509.

Li, B., Yang, X., Hu, Y. & Zhang, D. 2008b. Quality design of tolerance allocation for sheet metal assembly with resistance spot weld. *International Journal of Production Research,* 47**,** 1695-1711.

Li, B., Yu, H., Yang, X. & Hu, Y. 2010. Variation analysis and robust fixture design of a flexible fixturing system for sheet metal assembly. *Journal of Manufacturing Science and Engineering,* 132**,** 041014-041014.

Li, X., Dick, A., Chunhua, S., Van Den Hengel, A. & Hanzi, W. 2013. Incremental learning of 3D-DCT compact representations for robust visual tracking. *IEEE Transactions on Pattern Analysis and Machine Intelligence,* 35**,** 863-881.

Li, Y. & Gu, P. 2004. Free-form surface inspection techniques state of the art review. *Computer-Aided Design,* 36**,** 1395-1417.

Li, Z., Izquierdo, L. E., Kokkolaras, M., Hu, S. J. & Papalambros, P. Y. 2008c. Multiobjective Optimization for Integrated Tolerance Allocation and Fixture Layout Design in Multistation Assembly. *Journal of Manufacturing Science and Engineering,* 130**,** 044501-044501.

Li, Z., Shi, Y., Wang, C. & Wang, Y. 2008d. Accurate calibration method for a structured light system. *Optical Engineering,* 47**,** 053604-9.

Liang, Z., Hui, W., Berry, C., Xin, W. & Hu, S. J. 2012. Functional morphing in multistage manufacturing and its applications in high-definition metrology-based process control. *IEEE Transactions on Automation Science and Engineering,* 9**,** 124-136.

Liu, S. C. & Hu, S. J. 1997. Variation simulation for deformable sheet metal assemblies using finite element methods. *Journal of Manufacturing Science and Engineering,* 119**,** 368-374.

Liu, S. C., Hu, S. J. & Woo, T. C. 1996. Tolerance analysis for sheet metal assemblies. *Journal of Mechanical Design,* 118**,** 62-67.

Long, Y. & Hu, S. J. 1998. A unified model for variation simulation of sheet metal sssemblies. *Geometric Design Tolerancing: Theories, Standards and Applications.* Springer US.

Lowell, W. F. 1982. Geometrics II: dimensioning and tolerancing. *ANSI/ASME Standard, Y13.5M***,** 35-52.

Lu, X., Jain, A. K. & Colbry, D. 2006. Matching 2.5D face scans to 3D models. *IEEE Transactions on Pattern Analysis and Machine Intelligence,* 28**,** 31-43.

Majeske, K. & Hammett, P. 2003. Identifying sources of variation in sheet metal stamping. *International Journal of Flexible Manufacturing Systems,* 15**,** 5-18.

Manjón, J. V., Coupé, P., Buades, A., Louis Collins, D. & Robles, M. 2012. New methods for MRI denoising based on sparseness and self-similarity. *Medical Image Analysis,* 16**,** 18-27.

Martínez, S., Cuesta, E., Barreiro, J. & Álvarez, B. 2010. Analysis of laser scanning and strategies for dimensional and geometrical control. *The International Journal of Advanced Manufacturing Technology,* 46**,** 621-629.

Mass, H.-G. 2002. Methods for measuring height and planimetry discrepancies in airborne laser scanner data. *Photogrammetric Engineering & Remote Sensing,* 68**,** 933-940.

Matuszyk, T. I., Cardew-Hall, M. J. & Rolfe, B. F. 2010. The kernel density estimate/point distribution model (KDE-PDM) for statistical shape modeling of automotive stampings and assemblies. *Robotics and Computer-Integrated Manufacturing,* 26**,** 370-380.

Merkley, K. 1998. *Tolerance analysis of complaint assemblies.* Ph.D. Dissertation Ph.D. Dissertation, Brigham Young University, Utah.

Mohaghegh, K., Sadeghi, M. H. & Abdullah, A. 2007. Reverse engineering of turbine blades based on design intent. *The International Journal of Advanced Manufacturing Technology,* 32**,** 1009-1020.

Mohib, A., Azab, A. & Elmaraghy, H. 2009. Feature-based hybrid inspection planning: A mathematical programming approach. *International Journal of Computer Integrated Manufacturing,* 22**,** 13-29.

Montgomery, D. C. 2008. Introduction to statistical quality control, Hoboken, NJ, John Wiley & Sons.

Mori, K., Tarui, T., Hasegawa, T. & Yoshikawa, N. 2010. Remote laser welding applications for car bodies. *Welding International,* 24**,** 758-763.

Nee, A. Y. C., Tao, Z. J. & Kumar, A. S. 2004. An advanced treatise on fixture design and planning, World Scientific.

Panagiotidou, S. & Tagaras, G. 2010. Statistical process control and condition-based maintenance: a meaningful relationship through data sharing. *Production and Operations Management,* 19**,** 156-171.

Phaladiganon, P., Kim, S. B., Chen, V. C. P. & Jiang, W. 2013. Principal component analysis-based control charts for multivariate nonnormal distributions. *Expert Systems with Applications,* 40**,** 3044-3054.

Phoomboplab, T. & Ceglarek, D. 2008. Process yield improvement through optimum design of fixture layouts in 3D multistation assembly systems. *Journal of Manufacturing Science and Engineering,* 130**,** 061005-061005.

Ploix, A. & Vigouroux, B. 1999. Image sequence compression using adapted three-dimensional transform: Application to scintigraphic images. *Signal Processing: Image Communication,* 15**,** 255-263.

Pottmann, H. & Leopoldseder, S. 2003. A concept for parametric surface fitting which avoids the parametrization problem. *Computer Aided Geometric Design,* 20**,** 343-362.

Prieto, F., Redarce, T., Lepage, R. & Boulanger, P. 1998. Visual system for fast and automated inspection of 3D parts. *International Journal of CAD/CAM and Computer Graphics,* 13**,** 211-227.

Raffin, R., Neveu, M. & Jaar, F. 2000. Curvilinear displacement of free-form-based deformation. *The Visual Computer,* 16**,** 38-46.

Ramsay, J. & Silverman, B. W. 2005. Functional data analysis, Springer.

Rao, K. R. & Yip, P. 1990. Discrete cosine transform: algorithms, advantages, applications, Academic Press Professional, Inc.

Ray, S. & Turi, R. H. Determination of number of clusters in k-means clustering and application in colour image segmentation. Proceedings of the 4th

International Conference on Advances in Pattern Recognition and Digital Techniques, 1999. 137-143.

Rearick, M. R., Hu, J. S. & Wu, S. M. Optimal fixture design for deformable sheet metal workpieces. Transactions of NARMI/SME, 1993. 407-412.

Reinhart, G., Munzert, U. & Vogl, W. 2008. A programming system for robot-based remote-laser-welding with conventional optics. *CIRP Annals - Manufacturing Technology,* 57**,** 37-40.

Reinhart, G. & Tekouo, W. 2009. Automatic programming of robot-mounted 3D optical scanning devices to easily measure parts in high-variant assembly. *CIRP Annals - Manufacturing Technology,* 58**,** 25-28.

Requicha, A. a. G. 1983. Toward a theory of geometric tolerancing. *The International Journal of Robotics Research,* 2**,** 45-60.

Requicha, A. a. G. & Chan, S. 1986. Representation of geometric features, tolerances, and attributes in solid modelers based on constructive geometry. *IEEE Journal of Robotics and Automation,* 2**,** 156-166.

Requicha, A. G. 1984. Representation of tolerances in solid modeling: issues and alternative approaches. *Solid Modeling by Computers.* Springer US.

Rong, Q., Ceglarek, D. & Shi, J. 1999. Dimensional fault diagnosis for compliant beam structure assemblies. *Journal of Manufacturing Science and Engineering,* 122**,** 773-780.

Rossignac, J. R. & Requicha, A. a. G. 1986. Offsetting operations in solid modelling. *Computer Aided Geometric Design,* 3**,** 129-148.

Rousseeuw, P. J. 1987. Silhouettes: A graphical aid to the interpretation and validation of cluster analysis. *Journal of Computational and Applied Mathematics,* 20**,** 53-65.

Samper, S., Adragna, P.-A., Favreliere, H. & Pillet, M. 2009. Modeling of 2D and 3D assemblies taking into account form errors of plane surfaces. *Journal of Computing and Information Science in Engineering,* 9**,** 041005-041005.

Samper, S. & Formosa, F. 2006. Form defects tolerancing by natural modes analysis. *Journal of Computing and Information Science in Engineering,* 7**,** 44-51.

Savio, E., De Chiffre, L. & Schmitt, R. 2007. Metrology of freeform shaped parts. *CIRP Annals - Manufacturing Technology,* 56**,** 810-835.

Schleich, B., Anwer, N., Mathieu, L. & Wartzack, S. 2014. Skin model shapes: A new paradigm shift for geometric variations modelling in mechanical engineering. *Computer-Aided Design,* 50**,** 1-15.

Shalon, D., Gossard, D., Ulrich, K. & Firzpatrick, D. Representing geometric variations in complex structural assemblies on CAD systems. Proceedings of

the 19th Annual ASME Advances in Design Automation Conference, 1992. 121-132.

Shen, Z., Ameta, G., Shah, J. J. & Davidson, J. K. 2005. A comparative study of tolerance analysis methods. *Journal of Computing and Information Science in Engineering,* 5**,** 247-256.

Shi, J. & Ceglarek, D. 1996. Fixture failure diagnosis for autobody assembly using pattern recognition. *Journal of Engineering for Industry,* 118**,** 55.

Shi, Q. & Xi, N. Automated data processing for a rapid 3D surface inspection system. IEEE International Conference on Robotics and Automation, 19-23 May 2008 2008. 3939-3944.

Shibata, K. 2008. Recent automotive applications of laser processing in Japan. *The Review of Laser Engineering,* 36**,** 1188-1191.

Shirinzadeh, B. 2002. Flexible fixturing for workpiece positioning and constraining. *Assembly Automation,* 22**,** 112-120.

Shiu, B., Ceglarek, D. & Shi, J. Flexible beam-based modeling of sheet metal assembly for dimensional control. Trans. of NAMRI, 1997. 49-54.

Shiu, B. W., Ceglarek, D. & Shi, J. 1996. Multi-stations sheet metal assembly modeling and diagnostics. *Trans-NAMRI of SME***,** 199-204.

Silverman, B. W. 1986. Density estimation for statistics and data analysis. *Biometrical Journal*.

Son, S., Park, H. & Lee, K. H. 2002. Automated laser scanning system for reverse engineering and inspection. *International Journal of Machine Tools and Manufacture,* 42**,** 889-897.

Sorkine, O. 2006. *Laplacian mesh processing.* Doctoral dissertation, Tel Aviv University.

Sorkine, O., Cohen-Or, D., Lipman, Y., Alexa, M., Roessl, C. & Seidel, H.-P. 2004. Laplacian surface editing. *Proceedings of the 2004 Eurographics/ACM SIGGRAPH symposium on Geometry processing.* Nice, France: ACM.

Srinivasan, R. S. & Wood, K. L. 1997. A form tolerancing theory using fractals and wavelets. *Journal of Mechanical Design,* 119**,** 185-193.

Srivastava, A. & Jermyn, I. H. 2009. Looking for shapes in two-dimensional cluttered point clouds. *IEEE Transactions on Pattern Analysis and Machine Intelligence,* 31**,** 1616-1629.

Stoll, C., Karni, Z., Rössl, C., Yamauchi, H. & Seidel, H. P. 2006. Template deformation for point cloud fitting. *Proceedings of the 3rd Eurographics / IEEE VGTC conference on Point-Based Graphics.* Boston, Massachusetts: Eurographics Association.

Strang, G. 1999. The discrete cosine transform. *SIAM Review,* 41**,** 135-147.

Suh, N. P. 2005. Complexity: theory and applications, Oxford University Press.

Thornton, C. A. 1999. A mathematical framework for the key characteristic process. *Research in Engineering Design,* 11**,** 145-157.

Tonks, M. 2002. *A robust geometric covariance method for flexible assembly tolerance analysis.* M.S. Thesis, Brigham Young University, Utah.

Turley, G., Kiraci, E., Olifent, A., Attridge, A., Tiwari, M. & Williams, M. 2014. Evaluation of a multi-sensor horizontal dual arm Coordinate Measuring Machine for automotive dimensional inspection. *The International Journal of Advanced Manufacturing Technology,* 72**,** 1665-1675.

Turner, J. & Wozny, M. 1987. Tolerances in computer-aided geometric design. *The Visual Computer,* 3**,** 214-226.

Ungemach, G. & Mantwill, F. 2008. Efficient consideration of contact in compliant assembly variation analysis. *Journal of Manufacturing Science and Engineering,* 131**,** 011005-011005.

Vaamonde Couso, E. & Vázquez Gómez, J. 2012. Laser beam welding and automotive engineering. *Structural Connections for Lightweight Metallic Structures.* Springer Berlin Heidelberg.

Várady, T., Martin, R. R. & Cox, J. 1997. Reverse engineering of geometric models—an introduction. *Computer-Aided Design,* 29**,** 255-268.

Wagersten, O., Lindau, B., Lindkvist, L. & Söderberg, R. 2014. Using morphing techniques in early variation analysis. *Journal of Computing and Information Science in Engineering,* 14**,** 011007-011007.

Walker, R. K. & Srinivasan, V. Creation and evolution of the ASME Y14.5.1M standard. In: Proceedings of the international forum on dimensioning tolerancing and Metrology, 1993. 19-30.

Wand, M. P. & Jones, M. C. 1994. Multivariate plug-in bandwidth selection. *Computational Statistics,* 9**,** 97-116.

Wang, D. 2011. Robust data-driven modeling approach for real-time final product quality prediction in batch process operation. *IEEE Transactions on Industrial Informatics,* 7**,** 371-377.

Wang, K. & Tsung, F. 2005. Using profile monitoring techniques for a data-rich environment with huge sample size. *Quality and Reliability Engineering International,* 21**,** 677-688.

Wang, X. Z. & Mcgreavy, C. 1998. Automatic classification for mining process operational data. *Industrial & Engineering Chemistry Research,* 37**,** 2215-2222.

Wells, L., Megahed, F., Camelio, J. & Woodall, W. 2012. A framework for variation visualization and understanding in complex manufacturing systems. *Journal of Intelligent Manufacturing,* 23**,** 2025-2036.

Wells, L. J., Megahed, F. M., Niziolek, C. B., Camelio, J. A. & Woodall, W. H. 2013a. Statistical process monitoring approach for high-density point clouds. *Journal of Intelligent Manufacturing,* 24**,** 1267-1279.

Wells, L. J., Shafae, M. S. & Camelio, J. A. 2013b. Automated part inspection using 3D point clouds. *International Manufacturing Science and Engineering Conference.* Madison, Wisconsin, USA: ASME.

Whitney, D. E. 2004. Mechanical assemblies: their design, manufacture, and role in product development, Oxford University Press.

Whitney, D. E., Gilbert, O. L. & Jastrzebski, M. 1994. Representation of geometric variations using matrix transforms for statistical tolerance analysis in assemblies. *Research in Engineering Design,* 6**,** 191-210.

Woodall, W. H. 2007. Current research on profile monitoring. *Production,* 17**,** 420-425.

Woodall, W. H., Spitzner, D. J., Montgomery, D. C. & Gupta, S. 2004. Using control charts to monitor process and product quality profiles. *Journal of Quality Technology,* 36**,** 309-320.

Xi, F., Liu, Y. & Feng, H. Y. 2001. Error compensation for three-dimensional line laser scanning data. *The International Journal of Advanced Manufacturing Technology,* 18**,** 211-216.

Youcef-Toumi, K., Liu, W. S. & Asada, H. 1988. Computer-aided analysis of reconfigurable fixtures and sheet metal parts for robotic drilling. *Robotics and Computer-Integrated Manufacturing,* 4**,** 387-393.

Yu, K., Jin, S., Lai, X. & Xing, Y. 2008. Modeling and analysis of compliant sheet metal assembly variation. *Assembly Automation,* 28**,** 225-234.

Zhou, Z. & Cao, X.-R. 1994. Optimal process control in stamping operation. *Quality Engineering,* 6**,** 621-631.